Applying Artificial Neural Networks and Evolutionary Algorithms to Architectural and Building Acoustics

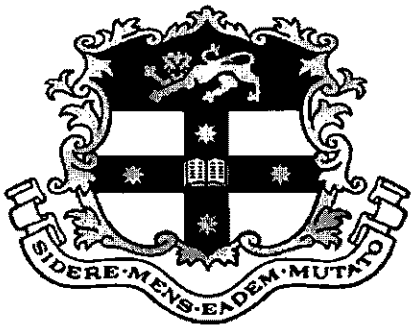

Jingfeng Xu

BE, MEngSc

A thesis submitted in fulfilment of the requirements for the degree of

Doctor of Philosophy

Faculty of Architecture

The University of Sydney

January 2006

ABSTRACT

The present work is concerned with the application of artificial neural networks and evolutionary algorithms to build a methodological framework for design and research in architectural and building acoustics in situations that are frustrated by issues such as multiple parameters, multiple criteria, discontinuous decision spaces and a large quantity of measured data. Efforts have been concentrated into the following specific topics: 1) predicting architectural speech intelligibility and security that involve multiple decision parameters; 2) optimising the design of flat-walled multi-layered anechoic linings that features multiple criteria decision making, multiple decision parameters and discontinuous decision spaces; 3) developing a new method for deriving the bulk acoustic properties of a rigid porous medium from a single impedance test, which needs to deal with a large quantity of measured data; and 4) predicting and optimising the airborne sound transmission of floor-ceiling constructions that involves multiple decision parameters.

Results of the present work show that 1) the artificial neural network approach provides a direct and accurate method for the prediction of architectural speech intelligibility scores and security thresholds; 2) a multi-objective evolutionary algorithm can be successfully employed as an optimiser to aid and speed up the design of flat-walled multi-layered anechoic linings; 3) a new method, requiring only a single surface impedance measurement and an optimisation process of the function coefficients, can be successfully applied for deriving the bulk acoustic properties of a rigid porous medium. (Both the traditional calculus-based optimisation technique and the evolutionary algorithm can be applied - nonetheless, the evolutionary algorithm is a more robust technique); and 4) the artificial neural network can be used to numerically describe the input-output relationship of airborne sound transmission of floor-ceiling constructions, and then the multi-dimensional space created by the artificial neural network can be searched by an evolutionary algorithm to find a particular solution that meets the architect's requirements.

ACKNOWLEDGEMENTS

I would like to express my deepest thanks to Honorary Professor Fergus R. Fricke for his invaluable advice, tremendous support and profound guidance throughout the entire period of this work.

I am grateful to Dr. John S. Bradley, Dr. Bradford N. Gover, Professor Alan Cummings, Dr. Ho-Chul Shin and Dr. John Davy who contributed invaluable data and generous comments. I am also grateful to Dr. Jörg M. Buchholz for the opportunity to cooperate on the design and evaluation of the anechoic room in MARCS Auditory Laboratories at the University of Western Sydney.

Special thanks are due to Dr. Chris Field who first aroused my interest in acoustics, and to Dr. Joseph Nannariello for many valuable and interesting discussions and his comments. Many thanks go to Dr. Densil Cabrera and John Bassett for their advice and support and to Phil Granger, Rick Moss and Ken Stewart for their technical support on all experiments involved in this work.

I wish to thank Gillian Delbridge for her proficient proofreading.

I am very much indebted to my wife, Haihong, for her patience and devoted support. Also this work would not have been possible without the unlimited love and encouragement of my parents.

This work was conducted under an Australian Postgraduate Award and a supplementary scholarship from the Faculty of Architecture, the University of Sydney.

TABLE OF CONTENTS

TABLES

FIGURES

GLOSSARY OF SYMBOLS

a_1	the depth of air cavity 1
a_2	the depth of air cavity 2
A#*H*	resulting value after the activation at each hidden neuron
AI	Articulation Index
ANN(s)	Artificial Neural Network(s)
AQI	Acoustic Quality Index
A_W	side wall angle of a room
b	unequal constraints
B#H	bias to the hidden neuron layer of the neural network
B#OP	bias to the output layer of the neural network
BR	Bass Ratio
c	velocity of sound in air
c_1-c_8	function coefficients of Delany and Bazley type formulae
C_{80}	clarity factor, assuming that the energy within the first 80 milliseconds is the early energy
CI	Computational Intelligence
CNRC	Canadian National Research Council
d	number of the objective values that do not meet the goals (Chapter 3)
d	thickness of test material sample (Chapter 6)
d_1	thickness of test material sample 1
d_2	thickness of test material sample 2
DiffMaxChange	maximum change in variables for finite difference derivatives
DiffMinChange	minimum change in variables for finite difference derivatives
DM	Decision Maker
D_{mean}	mean depth of a room
ΔE	difference of energy density
E	energy density
EA(s)	Evolutionary Algorithms

EDT	Early Decay Time
En	entire data set
$f()$	function
f	frequency
f_c	cut-off frequency
$f(\boldsymbol{x})$	objective function
$\boldsymbol{f}(\boldsymbol{x})$	objective function vector
FCMass	floor and ceiling layer surface density
FEM	Finite Element Model
FL	Fuzzy Logic
g	individual goal
$\boldsymbol{g}$	goal vector
g_{100}, g_{125}, g_{1000}	respective goal value at 100, 125 and 1000 Hz
$g_{L_{overall}}$	goal value for the overall thickness of the lining system
G	strength factor
GA(s)	Genetic Algorithms
GEATbx	Genetic and Evolutionary Algorithm Toolbox for Use with Matlab
G_{mid}	strength factor at low frequencies: average of the values of G in the 500 and 1000 Hz bands
h	equal constraints
H	hidden neuron of the neural network
H_{mean}	mean height of a room
H/W	ratio of height to width
i	index for orthogonal parameters (Chapter 1)
i	index for the first-layer neurons of the neural network (Chapter 2)
i	index for constraints (Section 3.2.2)
i	index for objective values (Section 3.2.9)
i	index for goals (Section 3.3.4.1)
i	index for layers of linings (Chapter 5)
I	imaginary part of the normal incidence acoustic impedance
IACC	Interaural Cross-correlation Coefficient

$IACC_{E3}$	early Interaural Cross-correlation Coefficient averaged over three frequency bands (500, 1000 and 2000 Hz)
IIC	Impact Insulation Class
Im	imaginary part of the difference
InsDensity	sound absorbing material density
InsThick	sound absorbing material thickness
IP	input neuron of the neural network
IP'	pre-processed input neuron of the neural network
IRC	Institute for Research in Construction
j	index for the hidden-layer neurons of the neural network (Chapter 2)
j	index for decision variables (Section 3.2.1)
j	index for goals (Section 3.3.4.1)
j	$\sqrt{-1}$ (Chapter 5 and Chapter 6)
JstDepth	joist depth
JstSpace	joist spacing
k	number of objective functions
lb	lower bounds
L	thickness
L_1, L_2, L_3	respective thicknesses of layer 1, layer 2 and layer 3 of the lining composite
LevenbergMarquardt	preference for Levenberg-Marquardt over Gauss-Newton algorithm
LF	Lateral Energy Fraction
LineSearchType	Line search algorithm choice
LL	Listening Level
L_{MX}	maximum length
$L_{overall}$	overall thickness of the multi-layered lining system
$L_{overall\_fixed}$	fixed value of $L_{overall}$
L/W	ratio of length to width
m	number of neural network inputs (Chapter 2)

m	number of unequal constraints (Chapter 3)
m	number of layers of linings (Chapter 5)
MaxFunEvals	maximum number of function evaluations allowed
MaxIter	Maximum number of iterations allowed
MLP	Multilayer Perceptrons
MOMGA	Multi-Objective Messy Genetic Algorithm
MOGA	Multi-Objective Genetic Algorithm
MOP(s)	Multi-Objective Optimisation Problem(s)
n	number of neural network hidden neurons (Chapter 2)
n	number of decision variables (Chapter 3)
n	number of the half wave length
N	number of seats
NPGA	Niched-Pareto Genetic Algorithm
NSGA	Nondominated Sorting Genetic Algorithm
OP	post-processed output neuron of the neural network
OP'	output neuron of the neural network
p	number of equal constraints
PAES	Pareto Archived Evolution Strategy
q	number of goals
r	pressure reflection factor at normal incidence
r_{100}, r_{125}, r_{1000}	respective reflection factor at 100, 125 and 1000 Hz
$r_u^{(t)}$	number of individuals in the current population that are preferable to $\boldsymbol{x}_u$
R	real part of the normal incidence acoustic impedance
R^2	coefficient of determination (correlation coefficient)
R^n	Euclidean n-space
RCSpace	resilient metal channel spacing
Re	the real part of the difference
RMS	Root Mean Square
RT	Reverberation Time
$RT_{125\text{-}250}$	Reverberation Time averaged over 125 and 250 Hz bands

$RT_{500\text{-}1000}$	Reverberation Time averaged over 500 and 1000 Hz bands
RT_{mid}	mid-band Reverberation Time (=$RT_{500\text{-}1000}$)
Rw	weighted sound reduction index.
S	scale value
S	search space
SC#IP	input scale factor of the neural network
SC#OP	output scale factor of the neural network
SD	Standard Deviation
SDR	Standard Deviation Ratio
SDI	Surface Diffusion Index
SH#IP	input shift factor of the neural network
SH#OP	output shift factor of the neural network
SII	Speech Intelligibility Index
S/N	signal-to-noise
SP	Sound Propagation
SPEA	Strength Pareto Evolutionary Algorithm
S_T	total acoustical floor area
STC	Sound Transmission Class
SU#H	resulting value after the summation at the each hidden neuron
SUS	Stochastic Universal Sampling
t	number of a generation
t_o	overall time taken for the sound wave to pass the multi-layered lining composite
Te	test data set
T_I	initial time-delay gap
TL	Transmission Loss
TolCon	termination tolerance on the constraint violation
TolFun	termination tolerance on the function value
TolX	termination tolerance on x
Tr	training data set
T_{sub}	subsequent reverberation time

$\boldsymbol{u}$	objective function vector corresponding to the decision variable vector $\boldsymbol{x}_u$
ub	upper bounds
UBC	University of British Columbia
v	acoustic wave velocity in the material
$\boldsymbol{v}$	objective function vector corresponding to the decision variable vector $\boldsymbol{x}_v$
v_a	average sound wave velocity in the multi-layered lining composite
V	Volume
Ve	verification data set
VEGA	Vector Evaluated Genetic Algorithm
W	characteristic impedance
W#H	weights connecting the pre-processed input neurons and the hidden-layer neurons of the neural network
W_{mean}	mean width of a room
W_{MX}	maximum width
W#OP	weights connecting the hidden-layer neurons and the output neuron of the neural network
x	decision variable
$\boldsymbol{x}$	decision variable vector
x^*	individual variable value in the global minimum solution vector
$\boldsymbol{x}^*$	global minimum solution vector
$\boldsymbol{x}_u$	decision variable vector corresponding to the objective function vector $\boldsymbol{u}$
$\boldsymbol{x}_v$	decision variable vector corresponding to the objective function vector $\boldsymbol{v}$
X	parameter space or the feasible region
y	objective value
y_a	individual objective value in the objective vector $\boldsymbol{y}_a$
y_b	individual objective value in the objective vector $\boldsymbol{y}_b$
$\boldsymbol{y}_a$	objective vector

y_b	objective vector
Y	objective space
Z	normal incidence acoustic impedance
Z_0	normal incidence acoustic impedance of the solid backing
Z_{0S}	surface impedance to an acoustic line terminated with zero air cavity between the line and the rigid wall
Z_a	surface impedance of an arbitrary depth of air cavity between the test material sample and the rigid wall
Z_{a1}	surface impedance of air cavity depth a_1 between the test material sample and the rigid wall
Z_{a2}	surface impedance of air cavity depth a_2 between the test material sample and the rigid wall
Z_{aS}	surface impedance of the test material sample with an arbitrary depth of air cavity between the test material sample and the rigid wall
Z_{aS1}	surface impedance of the test material sample with air cavity depth a_1 between the test material sample and the rigid wall
Z_{aS2}	surface impedance of the test material sample with air cavity depth a_2 between the test material sample and the rigid wall
Z_{aSFoam}	surface impedance of the foam applied in Chapter 6
Z_{d1}	surface impedance corresponding to the test sample thickness d_1
Z_{d2}	surface impedance corresponding to the test sample thickness d_2
Z_{qS}	surface impedance to an acoustic line terminated with an air cavity having a depth equal to a quarter-wavelength between the line and the rigid wall
α	attenuation constant
α_n	normal incidence sound absorption coefficient
β	wave number
β_{air}	wave number of air
γ	propagation constant

δ	flow resistivity
δ_1, δ_2, δ_3	respective flow resistivity of layer 1, layer 2 and layer 3 of the lining composite
κ	scalar factor used to tighten or loosen the constraint
λ_a	average quarter wavelength
ρ	air density

CHAPTER 1

INTRODUCTION

1.1 BACKGROUND TO THE STUDY

In architectural and building acoustics there are at least two factors that make design and research difficult: 1) the aspects such as multiple parameters, multiple criteria and discontinuous decision spaces involved and 2) a large quantity of measured data (which blur the inherent acoustic phenomena). These complex situations are not easily reconcilable and therefore remain difficult to resolve using conventional methods. On the other hand Computational Intelligence (CI) is one of the approaches to programming computers that make them behave more like they were human, that is, having the ability to understand and tackle highly complex problems. Two of the major domains of CI are Artificial Neural Networks (ANNs) and Evolutionary Algorithms (EAs).

In connectionist models of computation attempts are made to simulate the powerful cognitive and sensory functions of the human brain and to use this capability to represent and manipulate knowledge in the form of patterns. Based on these patterns, ANNs model input–output functional relationships and can make predictions about other combinations of unseen inputs (inputs not used in the training process). ANNs have the potential for making better, quicker and more practical predictions than any of the traditional methods such as physical and analytical modelling and numerical methods. ANNs can automatically learn to recognise patterns in data from real systems or from physical models, computer programs, or other sources. They can handle multiple inputs and produce answers that are in a form suitable for designers. ANNs are based on precedents and are therefore likely to be better understood and appreciated by designers than other theoretical and empirical methods. ANNs will allow designers to get an almost instantaneous expert opinion on the effect of a proposed change in a design (Nannariello *et al.*, 2001a).

In general, the accomplishment of any abstract task can be thought of as problem-solving, which, in turn, can be perceived as a search through a space of potential solutions. Since we are after the "best" solution, we can view this task as an optimisation process. Traditional search methods (for instance, the enumerative and calculus-based methods) are suitable only for small spaces or for the simple unimodal optimisation problems with smooth decision spaces. During the last forty years there has been a growing interest in computational algorithms for large continuous or discontinuous space searching and/or highly constrained and/or multi-objective complex problems based on principles of evolution and heredity. EAs are search procedures based on the mechanics of natural selection. With the ability to search a large-scale population (potential solutions), the EA can overcome the problem of local fitness optima to obtain the optima that are almost always close to global (Baker, 1981). Moreover, following biological evolution, it treats many individual genotypes (candidate solutions) in parallel, searching along many paths of similar genotypes simultaneously, with a higher density of paths in regions (of the space of all possible solutions) where fitness is improving: the "best" individual improves in fitness and so does the average fitness of the population (the set of candidate solutions) (Marks, 1992). This characteristic makes EAs very attractive for solving multi-objective problems (MOP).

It is an enticing challenge to a theoretician to develop a new method suitable for solving the given problem. However, from the application point of view, the time for developing the technique has to be added to the computer time invested. In that respect, utilising a non-specialised and robust procedure, to which ANNs and EAs belong, may be worthwhile. With the inherent power of CI, it is promising to use ANNs and EAs to solve architectural and building acoustics problems that feature high dimensionality, multiple criteria, discontinuous decision spaces and a large amount of data collection. In the present work, the application of ANNs to architectural acoustic issues has been extended to those not considered previously; and, perhaps more importantly, EA techniques have been applied to optimise acoustic designs, which has been difficult in the past.

1.2 LITERATURE REVIEW

ANNs and EAs have been applied to some of the complex architectural and building acoustic problems, such as the prediction of acoustical parameters of concert halls, the prediction of acoustical quality of concert halls and small music rooms, the prediction of sound propagation in university classrooms, the prediction of the sound insulation of walls and the optimisation of the design of classical shoebox-type concert halls.

1.2.1 Predicting Acoustical Parameters of Concert Halls Using ANNs

Sabine's work led to the widespread use of reverberation time (RT) and for many years this was the only acoustical parameter used in the design of auditoria. However, the many anomalies inherent in Sabine's equation and other related formulae are responsible for the often inaccurate prediction of reverberation times. These predictions are often not within 5% (the subjective difference limen for reverberation time). This and the absence of simple and accurate rules of thumb suitable for use at the early conceptual design stage led to the investigation of an alternative method of predicting reverberation time (Nannariello and Fricke, 1999). Neural networks were trained using constructional and acoustical data of auditoria as input variables. Importantly, the input variables associated with the absorption coefficients were replaced by simple rating coefficients in terms of the absorptiveness of materials.

On the basis of the results drawn from the above work (Nannariello and Fricke, 1999), networks with a reduced number of input variables (a network "dimensionality" reduction) have been developed to predict ($RT_{125\text{-}250}$) and ($RT_{500\text{-}1000}$) for auditoria (Nannariello and Fricke, 2002a). The concept was further extended to developing some basic relationships and rules of thumb on how simple geometric parameters affect reverberation time. The result of this work provided evidence that neural networks can be used to make predictions of reverberation times at low and mid frequencies for auditoria, and that these predictions are as good as, or better than, existing methods. Furthermore, and more importantly, the results showed excellent strength of association and high

percentage agreement between measured and predicted reverberation times. The results were also repeatable and within the range of the subjective difference limen of 5%.

It has long been realised that there is more to auditorium acoustics than reverberation time. Over the last 30 years or so, a number of objective acoustical parameters (related to the subjective assessment of the acoustical characteristics of auditoria) have emerged to aid the design of auditoria. Consequently, a number of methods have been developed (Baron and Lee, 1988; Gade, 1991; Bradley, 1994; Volander, 1995) to predict parameters such as the strength factor (G), the clarity factor (C_{80}), lateral energy fraction (LF), and the interaural cross-correlation coefficient ($IACC$); but these methods have their limitations. A method of predicting the values of G, C_{80}, LF and $IACC_{E3}$ (the early interaural cross-correlation coefficient, averaged over frequency bands 500 Hz, 1000 Hz and 2000 Hz) in auditoria using neural networks, was therefore investigated and developed by Nannariello and Fricke (2001b). As a trial of this concept, and because well-documented measured data from halls is a rarity, neural networks were trained using ODEON room acoustics program (Lynge, 1998) predictions (Nannariello and Fricke, 2001a). One of the important outcomes of this work was that there was a good basis for carrying out further investigations using "noisy" and poorly distributed measured data to train neural networks to predict G values and possibly values of other acoustical parameters.

Subsequent work (Nannariello and Fricke, 2001b) provided evidence that non-linear models, such as neural networks trained with geometrical and measured acoustical data, could make predictions of the G, C_{80}, and LF values in concert halls. These simple predictions were as accurate as those calculated using existing, more complex, models (Gade, 1991). The study demonstrated that neural networks could be trained with a handful of simple and available input variables such as the volume, maximum length, total floor area, reverberation time and tube ratio. Between five and eight input variables were used to train networks to predict seat-averaged G, C_{80}, and LF. Six input variables were used to train networks to predict position-dependent G values. It was demonstrated that the exact positions of seats in a hall were not required to accurately predict the

average parameters. For the 126 receiver positions, in the 8 auditoria tested, the neural network analysis produced excellent results. The absolute average errors and root mean squared errors for G, C_{80}, and LF were, in most cases, within the subjective limen of ±1 dB, ±0.5 dB, and ±0.05 respectively.

The idea of using neural networks to make predictions of auditorium attributes was further extended to using neural networks to develop some basic knowledge and rules of thumb on how simple geometric parameters affect the attributes of an auditorium, such as G (Nannariello and Fricke, 2001c). The use of acoustical parameters, such as reverberation time, as an input variable, was deliberately avoided. The results showed that neural networks trained with 4 simple geometric input variables – the hall volume, V; the maximum length, L_{MX}; maximum width, W_{MX}; the total acoustical floor area, S_T (Beranek, 1996); and the tube ratio, $D_{mean}/(W_{mean}xH_{mean})$ – where D_{mean} is the mean depth of the hall (distance from front of platform to rearmost wall) and W_{mean} and H_{mean} are the mean width and height respectively – gave accurate predictions of G. The prediction errors were well below the subjective difference limen for G. The other attendant benefit was that the neural network models produced relationships which, in most cases, agreed with the published literature (Gade, 1991; Gade, 1996; Beranek, 1996).

A neural-computation approach for predicting $IACC_{E3}$ in unoccupied auditoria was also investigated (Nannariello and Fricke, 2002b). Thirty-six auditoria were used in the neural network analysis. A multilayer perceptron, fully connected, three layer feedforward network architecture, based on the supervised learning procedure, was used to build the neural networks. Seven input variables were used in the first layer. The set-up function for the neural network analyses was: $(1\text{-}IACC_{E3}) = f(V, L_{MX}, W_{MX}, D_{mean}/W_{mean}xH_{mean}, S_T, A_w, RT_{mid})$, where the symbols specify quantities previously defined and A_w is the side wall angle of hall, and RT_{mid} is the mid frequency reverberation time. Results of the investigations showed that the neural network model could predict $IACC_{E3}$ values within the subjective difference limen, which is 0.075 ± 0.008. Five auditoria were used to validate the neural network analysis method and the errors between measured and predicted $(1\text{-}IACC_{E3})$ ranged from –0.05 to 0.02. The neural network model used to make

(1-$IACC_{E3}$) predictions was imbedded in an Excel spreadsheet so that designers and researchers, without access to specialized neural network software, could use the results of the work.

1.2.2 Predicting Acoustical Quality of Concert Halls Using ANNs

In designing concert halls architects and designers still make use of precedents, especially at the sketch design stage. This technique, in most cases, has not guaranteed good acoustics. A neural network analysis was undertaken to relate the acoustic quality of halls (*AQI*) (as judged by conductors and musicians) to hall parameters. In the first of these (Fricke and Haan, 1995), the ten input parameters used were hall volume, surface area, number of seats, length, width, height, mean rake angle of the seats, SDI (surface diffusion index, visually assessed), A_w and hall shape. This was an important study in that it was the first to gather data on the opinions of musicians about the acoustic qualities of many different halls. It was also the first study in which ANN analysis was applied to an architectural acoustics problem. However, the study was flawed in that the network used was over-trained, the ANN software could not be used to produce any statistical data on the reliability of the results, and the hall shape could not be adequately described in the four categories involved (rectangular, horse-shoe, fan and geometrical).

Thus a second study (Fricke and Han, 1999) was undertaken in an attempt to rectify the limitations of the first study. Two inputs were discarded (A_w and hall shape) and were replaced by the stage height and the degree of stage enclosure (visually assessed). The work demonstrated that neural networks offered the opportunity to study the non-linear interactions of the many variables involved in the acoustic performance of concert halls though the standard deviation ratio (the ratio of the standard deviation of the prediction error to that of the original output data) achieved was approximately 0.90, which left a lot to be desired. A standard deviation ratio (SDR) of 0.1 is considered an excellent fit of the data and an SDR of 1.0 is a poor fit. However, with a modified network using five inputs (number of seats, ratio of length to width, ratio of height to the cube root of volume, mean rake angle, and the ratio of surface diffusivity index to stage enclosure), one hidden

layer with four neurons and two classifications of acoustic quality ("good" and "poor") as the output, a 90% success rate was achieved.

In a related study (Fricke, 2000a), found that subjective assessments of SDI were not reliable and so one of the objectives of further work was to produce an ANN model which was independent of the subjectively assessed SDI factor that had been shown to be questionable. Other objects were to provide some statistical basis for Beranek's model (Beranek, 1996) of preferred values of acoustic quantities in good concert halls and to produce a simpler (less inputs) ANN model with a better prediction record using both "acoustical" and "architectural" inputs.

As indicated in Section 1.2.1 above, many measures of the acoustics of concert halls have been proposed. None of these measures is now considered sufficient in itself for the successful design or evaluation of a hall. Unfortunately multi-criteria issues are difficult to deal with and there does not seem to be a consensus on what combination of acoustic parameters creates good acoustics in a concert hall. Beranek opts for six orthogonal parameters: *SDI*, $IACC_{E3}$, the time delay between the direct and first reflected sound at the centre of the main seating area (T_1), the early decay time (*EDT*), the measure of the average sound level in a hall at mid-frequency (G_{mid}), and the bass ratio (*BR*) (Beranek, 1996). He shows how each parameter contributes to the overall acoustic quality of a hall and gives each a preferred value. However, he does not give the details of how he determined these relationships. Beranek's method also assumes a linear relationship between the *AQI* (Fricke and Haan, 1995) and each of the six parameters, which are given weightings to obtain the *AQI*. However, the basis for these weightings is not given.

Using Beranek's six parameters as input variables, a neural network was trained to predict the *AQI* of halls (Fricke, 2000a). The results of the neural network analysis were used firstly to investigate the importance of surface diffusion (Fricke, 2000a) and then the veracity of Beranek's assessment method. Modified networks with acoustical, as well as architectural inputs, were then used to see whether better fits could be obtained to existing concert hall data than could be obtained using Beranek's six inputs (Fricke,

2000b). From the results of the neural network analysis, it was postulated that Beranek's approach to the prediction of the acoustic performance of concert halls is reasonable. However, a better way of predicting the acoustic performance may be to use a trained neural network because ANNs have the ability to model the non-linear relationship between the inputs and outputs and to optimise the use of available information.

Because of the difficulty in obtaining reliable subjective acoustic quality ratings and acoustic data relating to concert halls, it is more realistic and practical to use three acoustic quality categories (best, middle and worst) rather than a finer scale or rank ordering of preferences. It is also more practical and useful, especially at the initial design stage, to use geometrical inputs rather than acoustic ones, or acoustic inputs that Nannariello (see section 1.2.1) has shown can be accurately obtained using a limited number of room geometrical inputs. Using five inputs: the ratio of length to width (L/W), the ratio of height to width (H/W), the number of seats (N), the volume (V), the shape (rectangular or non-rectangular), artificial neural networks were developed to predict the acoustic quality category of concert halls (Choi, 2004) and a prediction accuracy of 80% - 90% was achieved. This work also demonstrated that ANNs are capable of handling a problem that involves categorisation, which is impossible for some traditional analysis methods, such as multivariate regression analysis. It also indicated that ANNs with "geometrical" inputs only (which are much more useful for design purposes than "acoustic" inputs) could be developed.

1.2.3 Predicting Acoustical Quality of Small Music Rooms Using ANNs

Much research has been undertaken on acoustics of auditoria for the performance of live music and speech, but very little on the acoustics of smaller rooms used for music practice and music teaching. There are several reasons for this, the main ones being: that small rooms are rarely prestigious; that poor acoustics would not result in financial disaster; and that classical acoustical prediction methods are not applicable to small rooms because of the errors in ignoring diffraction effects in such spaces. With data collected and measured using binaural recordings made in small music rooms, a method of predicting the acoustic quality of small music rooms, using a neural network, was

developed (Osman and Fricke, 1996). The 36 rooms used in the investigations were parallelepipedic with volumes ranging from 24 to 427 cubic metres. A combination of simple input variables for four musical instruments (cello, saxophone, trumpet and guitar) was used to build a number of neural networks. The neural network models were used to predict the acoustic quality of six small music rooms. From the results of the investigations it was postulated that neural network models can be used to predict acoustic performance of small music rooms and that specific acoustic and architectural parameters are required to predict the acoustic quality of rooms for specific musical instruments.

1.2.4 Predicting Sound Propagation in University Classrooms Using ANNs

Classrooms are primarily auditory-verbal learning environments in which students must have access to acoustic signals (speech) in order to understand and learn. University classrooms are designed and purpose-built for this reason alone, that is, for speech communication from a source to a number of listeners. It would be very useful at the schematic design stage of a classroom to have an expeditious and accurate method of predicting the distribution of speech sound levels.

There are a number of theoretical models that can be used to calculate sound levels in rooms. The most widely used is the Hopkins-Stryker equation (Davis and Davis, 1991). Using this equation, the sound level at a receiver can be predicted from the source sound level and the characteristics of the room. Unfortunately, this equation is only suitable for predicting the sound level from a steady sound source in a fully diffuse field, and research and listening experiences have shown that the results from the traditional equation can be very inaccurate and usually produce predictions which are larger than measured values (Hodgson, 1996). The sound level in the room can also be predicted based on the statistical theory of room acoustics, such as Barron's revised theory (Barron and Lee, 1988). However, it requires further validation to use statistical models for predicting speech levels at the schematic design stage of a classroom. Other work (Hodgson, Rempel and Kennedy, 1999) showed that the statistical models for predicting speech level and student-activity noise level explains only less than 70% of the variation in data,

therefore, when these models are used predictions may be poor. It is for these and other reasons, such as the lack of success in applying traditional techniques, and the extended time required to conduct calculations, that a method of using ANNs to predict the Sound Propagation (*SP*) in university classrooms was investigated and developed (Nannariello *et al.*, 2001b).

The *SP* is the variation of sound pressure level, normalized to the source power level, with distance from an omnidirectional source. Constructional and acoustical data for 34 randomly chosen unoccupied University of British Columbia (UBC) classrooms were used as inputs for the neural network analyses. The results of this work showed that neural networks trained with variables that have a causal relationship to the acoustical quality of the UBC classrooms produce reliable and accurate predictions. *RMS* errors for *SP* in each of the frequency bands were within the subjective difference limen for steady-state sound pressure levels, which is about 1 dB (i.e. $\Delta E/E = 0.26$ where E is the energy density). Furthermore, results showed that the *SP* predictions obtained using ANNs for classrooms were closer to the measured values than were the predictions obtained using Barron's revised theory or the Hopkins-Stryker equation.

1.2.5 Predicting the Sound Insulation of Walls Using ANNs

Using the results from acoustic laboratory tests of known steel and timber stud drywall constructions, an investigation of the application of ANNs for predicting the transmission loss (TL) at specific frequencies and the sound transmission class (STC) was carried out (Coomes and Fricke, 2001). Basic parameters (stud frame type and size, mass of wall construction, type and thickness of any cavity absorption, overall partition width, minimum sheet lining thickness, and the difference in sheet lining from one side to the other, as well as the inclusion of lining vibration isolation) were used as inputs for the neural network analysis.

The results obtained were highly encouraging with neural network designs achieving predictions for STC values within a similar range to those determined by a number of acoustic laboratories for comparable wall constructions. For instance, using data from the

National Research Council of Canada on all types of dry wall construction, the prediction of STC using ANNs achieved an RMS error of 2.01, which is less than the error obtained when a given wall construction is tested in different laboratories complying with the same standard. It was also suggested that neural networks analysis would potentially overcome the problem of obvious different test results in different "standard" laboratories (Coomes and Fricke, 2001). In particular, the neural network analysis offers the possibility of obtaining wall sound transmission ratings in a "virtual" laboratory. That is, the transmission loss results for any construction in any laboratory could be used to predict the transmission loss for the same construction in any other laboratory, virtual or real, without the need to undertake extensive "round-robin" testing of a particular construction.

ANNs were also applied to establish the room and wall parameters that influence sound level difference between rooms at low frequencies (40 – 100 Hz) (Fora-Moncada and Gibbs, 2002). The inputs and outputs of the network were generated by a Finite Element Model (FEM) (Maluski, 1999). The accuracy of the FEM was such that the eigenfrequencies in each room were processed within an error of 10%. From this work (Fora-Moncada and Gibbs, 2002), it was concluded that, in the frequency range of 40 – 100 Hz, Radial Basis Function and General Regression Neural Network performed better than Backpropagation. Moreover, General Regression Neural Network exhibited rapid learning and prediction. The input variables that yielded the best prediction of sound level difference between rooms were: volume of the source room, volume of the receiving room, ratio of the source room length to the wavelength, ratio of the receiver room length to the wavelength, wavelength at the third octave band frequency, and edge fixing conditions of the partition. The cross-validation average prediction error was 4 dB, with all cases included, or 3 dB, if equal room configurations were excluded. Fifteen room pairs (of unequal room configurations and with the larger volumes) had correlation coefficients greater than 0.8 with the average error usually less than 3 dB, and often less than 2 dB. The remaining cases had coefficients less than 0.8. Therefore, the best results were obtained when predicting for bigger and unequal room volumes.

1.2.6 Optimising the Design of Classical Shoebox Type Concert Halls Using GAs

The theory of subjective preference allows a sound field to be evaluated in terms of the following four orthogonal acoustical parameters (Ando, 1998): the listening level (LL), T_1, the subsequent reverberation time (T_{sub}), and IACC for a particular seat in a concert hall. Several experiments have been carried out to examine the independent effects of the four orthogonal parameters on subjective preference (Ando, 1998). Linear scale values of preference were obtained by using the law of comparative judgment. The units derived from experiments with different sound sources and different subjects were almost constant, so the scale values may be added to obtain (Sato et al, 2002):

$$S \approx S_1 + S_2 + S_3 + S_4, \tag{1.1}$$

where S_i (i = 1, 2, 3, 4) are the scale values for the respective orthogonal parameters.

On the basis of this theory, it was proposed that for designing sound fields in a concert hall, the ultimate goal is to maximize the scale values of preference, and subsequently a maximum overall S (Sato et al, 2002). A genetic algorithm (GA), a branch of evolutionary algorithms, was applied to search architectural design schemes that would produce high scale values of subjective preferences. At the start of a GA search, a shoebox shape was defined as the initial scheme for the hall. Using the image method, the orthogonal parameters were then calculated for the initial shape and various shapes generated by the GA. The scale values of subjective preference were employed as fitness functions. Those hall shapes that produced higher scale values were selected as parent chromosomes, that is, binary strings. To create a new generation, the room shapes were modified and the corresponding movement of the vertices of the walls was encoded in chromosomes. After GA operations that included crossover and mutation, new offspring were created. The fitness of the offspring was then evaluated in terms of the scale values of subjective preference. This process was repeated until the end condition (2000 generations) had been satisfied.

Two models were investigated in the work (Sato et al, 2002). In the first model, the geometric proportions of the shoebox were optimised and in the second model the floor plan was optimised with the results for the first model as the starting point of the search. The optimisation for the first model produced a shoebox shape with the length/width ratio almost the same as that of the Grosser Musikvereinsaal, in Vienna, a widely acknowledged excellent concert hall. However, conflicting height/width ratios were required for the maximum S_1 and maximum S_4 due to the different reflection requirements of the ceiling and walls to achieve the optimum LL and the optimum IACC. The height/width ratio of the Grosser Musikvereinsaal is intermediate between those for the maximum S_1 and maximum S_4. The optimisation for the second model indicates that a leaf-shaped plan was optimal with regard to the sidewalls. However, (again due to the different reflection requirements), to maximise S_1 and S_4, front walls and rear walls took on opposite characteristics, one requiring concave shape and the other requiring convex shape.

Although the work concluded that the maximisation of S_1 might take priority over that of S_4, a more useful study may be the use of multi-objective optimisation evolutionary algorithms to optimise S_1 and S_4 at the same time and find a "compromised" solution, such as that achieved in the Grosser Musikvereinsaal.

1.3 OBJECTIVES OF THE THESIS

The general objective of the present research is to assess the application of ANNs and EAs to build a methodological framework for design and research associated with architectural and building acoustics. This methodological framework should be easily understood and handled, and is either usable as a black box method or open to the incorporation of new or old recipes for further sophistication, specialization or hybridisation. Furthermore, it is hoped that the ongoing research will lead to other applications of ANNs and EAs in the field of architectural and building acoustics.

The literature review in section 1.2 indicated that most of the work using ANNs has been dedicated to the study of rooms for music (Nannariello *et al.*, 2001a). The application of the ANNs to rooms for speech and building acoustics has not been fully explored although some pilot work (Nannariello *et al.*, 2001b; Coomes and Fricke, 2001; Fora-Moncada and Gibbs, 2002) has been conducted. Only one application (Sato et al, 2002) of EAs to the architectural and building acoustics was found in the literature review. The topics for the investigation in the present work were chosen on the basis of need and the availability of data. Thus it was decided to concentrate the research effort in the following specific topics: 1) predicting architectural speech intelligibility and security that involve multiple decision parameters; 2) optimising the design of flat-walled multi-layered anechoic linings that features multiple criteria decision making, multiple decision parameters and discontinuous decision spaces; 3) developing a new method for deriving the bulk acoustic properties of a rigid porous medium from a single impedance test, which needs to deal with a large quantity of measured data; and 4) predicting and optimising the airborne sound transmission of floor-ceiling constructions that involves multiple decision parameters.

1.4 LAYOUT OF THE THESIS

The preceding sections in this chapter presented the background of the study, reviewed the recent developments in the application of ANNs and EAs to architectural and building acoustics and described the objectives of the present thesis.

Chapter 2 describes the architecture and procedures of ANNs applied in the present thesis. It also introduces the statistical assessment of the performance of ANNs and the neural-computational software that is applied in the present thesis. A general discussion of the advantages and limitations of ANNs is also provided in this chapter.

Chapter 3 first introduces some basic definitions relating to optimisation to help towards the understanding of basic optimisation problems. Next, it reviews the history and current state of EAs, illustrates the general EA structure, explains how constraints can be handled

in EAs, describes an evolutionary approach to the multi-objective optimisation problems (MOPs) and introduces a program that implements general EA operators and multi-objective genetic algorithms (MOGA). The advantages and limitations of EAs are also presented in this chapter.

Chapter 4 investigates an approach that uses the artificial neural networks (ANNs) to directly represent the functional relationship of the octave band (250 Hz – 8 kHz) S/N ratios to the speech intelligibility score and to security thresholds. The objectives of the ANNs are to predict a) the speech intelligibility score (namely the percentage of words correctly identified by each individual), b) the intelligibility threshold (namely the percentage of listeners able to correctly identify at least one word), c) the cadence threshold (namely the percentage of listeners able to detect the cadence of the speech), and d) the audibility threshold (namely the percentage of listeners able to hear the presence of the speech). On the basis of the statistical analysis of the prediction results, the accuracy of the prediction using ANNs is then compared with those using conventional methods.

Chapter 5 demonstrates that a multi-objective EA can be successfully employed to solve a difficult MOP in architectural and building acoustics, i.e. the optimisation of flat-walled multi-layered anechoic linings. Two types of materials, fully-reticulated (open-cell) polyurethane foams and fibrous building insulation material, are investigated. The investigation of fibrous building insulation material is shown in the form of an application case, in which the effectiveness of EAs for solving combinatorial-type problems featuring discontinuous decision space is also illustrated.

Chapter 6 first reviews traditional methods for determining the bulk acoustical properties of rigid porous media and then proposes a new method requiring only one impedance measurement and an optimisation process of function coefficients. The results of the new method are compared with those obtained by one of the traditional methods. This chapter also, from the application point of view, compares the effectiveness, robustness and

efficiency of evolutionary algorithms (EAs) and traditional calculus-based optimisation methods.

In chapter 7, an ANN is first developed on the basis of the data from laboratory tests on floors to predict the STC of typical floor-ceiling constructions. The predictions of STC using ANNs are compared with those obtained using the multivariate regression analysis. Then an evolutionary algorithm is applied to search the multi-dimensional space created by the ANN to find a floor-ceiling construction that meets the STC requirement set out by the architect. The success of the work implies that from the application point of view, it is promising to use ANNs and EAs to form a general problem-solving framework for architectural and building acoustics problems that feature high dimensionality and non-linear relationship.

Chapter 8 concludes the thesis and points out the directions for further work.

REFERENCES FOR CHAPTER 1

- Ando Y., 1998. *Architectural acoustics – Blending sound sources, sound fields, and listeners.* AIP Press/Springer Verlag, New York, NY.
- Bethke A.D., 1981. *Genetic algorithms as function optimisers.* Thesis (PhD). University of Michigan.
- Beranek L.L., 1996. *Concert and opera halls: how they sound.* Acoustical Society of America, Woodbury, NY.
- Barron M. and Lee L-J., 1988. "Energy relation in concert auditoria I," *Journal of the Acoustical Society of America*, 84 (2), pp 618-628.
- Bradley J.S., 1994. "Comparison of concert hall measurements of spatial quality," *Journal of the Acoustical Society of America*, 96 (6), pp 3525-3535.
- Coomes J. and Fricke F.R., 2001. "The prediction of wall sound insulation using neural networks," *Journal of Building Acoustics*, 8 (2), pp 103-119.
- Choi Y.J., 2004. *Towards better predictions of concert hall acoustic quality.* Thesis (PhD). The University of Sydney, Australia.
- Davis D. and Davis C., 1991. "Audio measurements," *In:* Ballou G., editor. *Handbook for sound engineers: the new audio cyclopaedia,* 2ne ed., SAMS, Indiana, pp 1365-1412.
- Fora-Moncada A. and Gibbs M., 2002. "Prediction of sound insulation at low frequencies using artificial neural networks," *Journal of Building Acoustics*, 9 (1), pp 49-71.
- Fricke, F.R. and Haan, C.H., 1995. "Predicting the acoustics of concert halls using an artificial neural network," *Acoustics Australia*, 23 (3), pp 87-95.
- Fricke F.R. and Han Y.G., 1999. "A neural network analysis of concert hall acoustics," *Acustica*, 85 (1), pp 113-120.
- Fricke F.R., 2000a. "Visual assessments of the surface diffusion properties of concert halls," *Applied Acoustics*, 60 (2), pp 253-261.
- Fricke F.R., 2000b. "Concert hall acoustics: an alternative approach," *Journal of Building Acoustics*, 7 (4), pp 233-246.

- Gade A.C., 1991. "Prediction of room acoustical parameters," A paper presented on the *121st meeting of the acoustical society of America*, 29 April-3 May 1991, Baltimore.
- Gade A.C., 1996. "Room acoustic properties of concert halls: quantifying the influence of size, shape and absorption area," *3rd ASA/ASJ meeting*, paper 5aAA1, Honolulu, pp 1-6.
- Hodgson M., 1996. "When is diffuse-field theory applicable," *Applied Acoustics*, 49 (3), pp 197-207.
- Hodgson M., Rempel R. and Kennedy S., 1999. "Measurement and prediction of typical speech and background noise levels in university classrooms during lectures," *Journal of the Acoustical Society of America*, 105 (1), pp 226-233.
- Lynge C., 1998. *ODEON room acoustical program version 3.1 manual.* The Department of Acoustic Technology, Technical University of Denmark, Denmark.
- Maluski S. 1999. *Low frequencies sound insulation in dwellings.* Thesis (PhD). Sheffield Hallam University, UK.
- Marks R.E., 1992. "Breeding optimal strategies: optimal behaviour for oligopolists," *Journal of Evolutionary Economics*, 2, pp 17-38.
- Nannariello J, Osman M.R. and Fricke F.R., 2001a. "Recent developments in the application of neural network analysis to architectural and building acoustics," *Acoustics Australia*, 29 (3), pp 103-110.
- Nannariello J. and Fricke, F.R., 1999. "The prediction of reverberation time using neural network analysis," *Applied Acoustics*, 58 (3), pp 305-325.
- Nannariello J., Hodgson M. and Fricke F.R., 2001b. "Neural network predictions of speech levels in university classrooms," *Applied Acoustics*, 62 (7), pp 749-767.
- Nannariello J. and Fricke F.R., 2001a. "The use of neural network analysis to predict the acoustic performance of large rooms: Part I Predictions of the parameter G utilizing numerical simulations," *Applied Acoustics*, 62 (8), pp 917-950.
- Nannariello J. and Fricke F.R., 2001b. "The use of neural network analysis to predict the acoustic performance of large rooms: Part II Predictions of the acoustical attributes of concert halls utilizing measured data," *Applied Acoustics*, 62 (8), pp 951-977.

- Nannariello J. and Fricke F.R., 2001c. "A neural network analysis of the effect of geometric variables on concert hall G values," *Applied Acoustics*, 62 (12), pp 1397-1410.
- Nannariello J and Fricke F.R., 2002a. "The prediction of reverberation time using optimal neural networks," *Journal of Building Acoustics*, 9 (1), pp 5-28.
- Nannariello J. and Fricke F.R., 2002b. "A neural computation method of predicting the interaural cross-correlation coefficient. $IACC_{E3}$ for auditoria," *Applied Acoustics*, 63 (6), pp 627-641.
- Osman M.R. and Fricke F.R., 1996. "Predicting the acoustical quality of small music rooms," *Proceedings of 1996 Australian acoustical society conference*, pp 13-15.
- Sato S., Otori K., Takizawa A., Sakai H., Ando Y. and Kawamura H., 2002. "Applying genetic algorithms to the optimum design of a concert hall," *Journal of Sound and Vibration*, 258 (3), pp 517-526.
- Vorlander M., 1995. "International round robin on room acoustical computer simulation," *Proceedings of 15th international congress on acoustics*, pp 689-692.

CHAPTER 2

ARTIFICIAL NEURAL NETWORKS

2.1 INTRODUCTION

There has been an explosion of interest in artificial neural networks (ANNs) over the last two decades. They are being successfully applied across an extraordinary range of problem domains, in areas as diverse as finance, medicine, engineering, geology and physics. Indeed, almost anywhere that there are problems of prediction, classification or control, ANNs are being introduced. A review of the application of ANNs in the area of architectural and building acoustics has been provided in chapter 1 of this thesis.

ANNs grew out of research in artificial intelligence, specifically, attempts to mimic the fault-tolerance and capacity to learn of biological neural systems by modelling the low-level structure of the brain and using this capability to represent and manipulate knowledge in the form of patterns (Patterson, 1996). Based on these patterns, ANNs model input–output functional relationships and make predictions about other combinations of unseen inputs (inputs not used in the training process). This ability enables ANNs to be used to extract patterns and detect trends that are too complex to be noticed by other techniques. In particular, ANNs are non-linear models and have a direct way of acquiring information and knowledge about a given problem domain through the training phase (Nannariello and Fricke, 2001).

Many publications (e.g. Bishop, 1995; Fausett, 1994; Haykin, 1994; Ripley, 1996; Taylor, 1996; Nannariello *et al.*, 2001; Nannariello and Fricke, 2001) have discussed the history, theories and applications of the ANNs. This chapter mainly focuses on the basic theory of ANNs relating to this thesis. First, the basic feed-forward ANN architecture, with emphasis on its modus operandi, is introduced. Then issues that are related to the training of ANNs are discussed. Following this, a brief introduction to the statistical assessment of the performance of ANNs is given. This chapter also introduces the neural-

computational software that is applied in this thesis and discusses the advantages and limitations of ANNs.

2.2 FEED-FORWARD ANN ARCHITECTURE

To capture the essence of biological neural systems, an artificial neuron (or unit) is defined as follows (Haykin, 1994):

- It receives a number of inputs (either from original data, or from the output of other neurons in the network). Each input comes via a connection that has a strength (or weight); these weights correspond to synaptic efficacy in a biological neuron. Each neuron also has a single threshold (or bias) value. The weighted sum of the inputs is formed, and the threshold subtracted, to compose the activation of the neuron.
- The activation signal is passed through an activation function (also known as a transfer function) to produce the output of the neuron.

If a network is to be of any use, there must be inputs (which carry the values of variables of interest in the outside world) and outputs (which form predictions). Inputs and outputs correspond to sensory and motor nerves such as those coming from the eyes and leading to the hands. However, there can also be hidden neurons that play an internal role in the network. The input, hidden and output neurons need to be connected.

A simple network has a feed-forward structure: signals flow from inputs, forwards through any hidden units, eventually reaching the output units. Such a structure has stable behavior. However, if the network is recurrent (contains connections back from later to earlier neurons) it can be unstable, and has very complex dynamics. Recurrent networks are very interesting to researchers in neural networks, but so far it is the feed-forward structures that have proved most useful in solving real problems (Haykin, 1994). The stable feed-forward network is employed throughout this thesis.

A typical feed-forward network has neurons arranged in a distinct layered topology. The input layer is not really neural at all: these units simply serve to introduce the values of the input variables. The hidden and output layer neurons are each connected to all of the units in the preceding layer. It is possible to define networks that are partially-connected to only some units in the preceding layer; however, for most applications fully-connected networks are better.

When the network is executed (used), the input variable values are placed in the input units, and then the hidden and output layer neurons are progressively executed. Each of them calculates its activation value by taking the weighted sum of the outputs of the units in the preceding layer, and subtracting the threshold. The activation value is passed through the activation function to produce the output of the neuron. When the entire network has been executed, the outputs of the output layer act as the output of the entire network.

The above network architecture, *Multilayer Perceptrons* (MLP), is perhaps the most popular in use today, due originally to Rumelhart and McClelland (1986) and discussed at length in most neural network textbooks (e.g., Bishop, 1995). It can model functions of almost arbitrary complexity, with the number of layers, as well as the number of units in each layer, determining the complexity of the function.

Figure 2.1 below provides a simple example of an MLP feed-forward ANN. This network has m inputs, one hidden layer with n hidden neurons, two biases, *B#H* and *B#OP*, and an output neuron, *OP*. In the real-world application of ANNs, the number of input and output neurons is defined by the problem. The number of hidden units to use is far from clear. As good a starting point as any is to use one hidden layer, with the number of neurons equal to half the sum of the number of input and output units. The following paragraphs in this section explain numerically the modus operandi of this MLP feed-forward ANN.

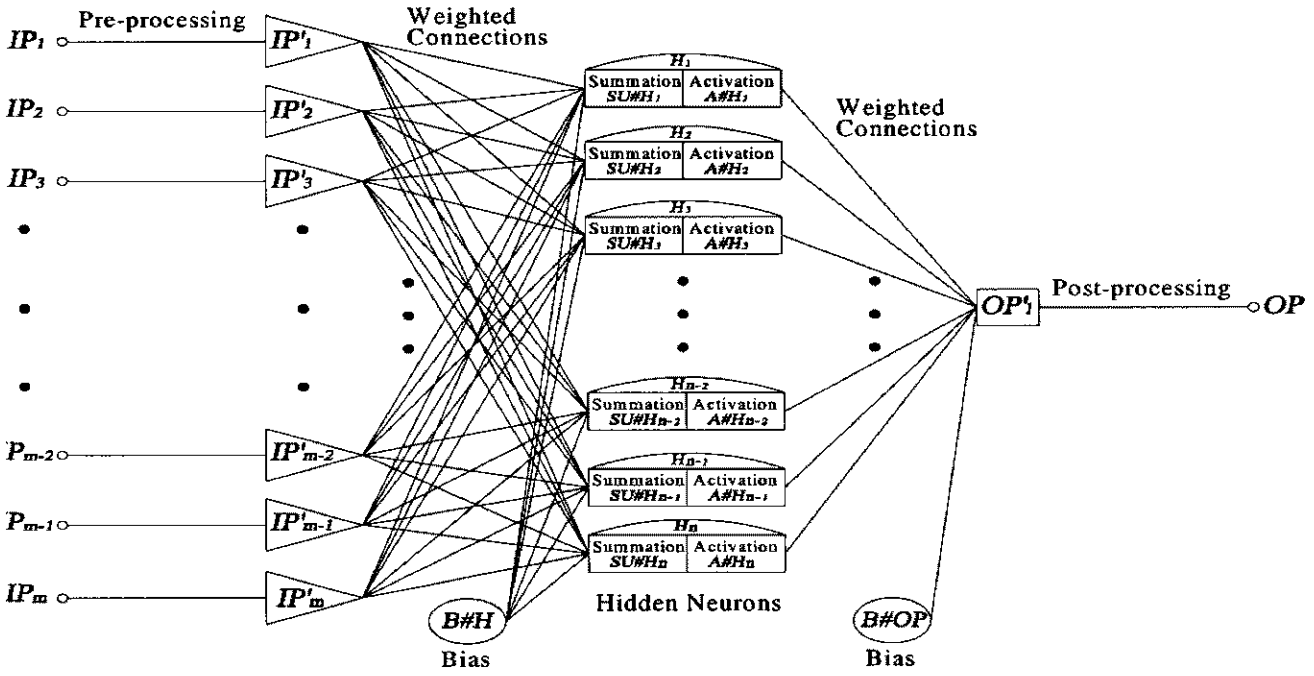

Figure 2.1 Illustration of a simple MLP feed-forward ANN model.

Pre-processing: All neural networks take numeric inputs and produce numeric outputs. The transfer function of a neuron is typically chosen so that it can accept inputs in any range, and produces an output in a strictly limited range (it has a squashing effect). Although the input can be in any range, there is a saturation effect so that the unit is only sensitive to inputs within a fairly limited range. One of the most common transfer functions is the logistic function (also sometimes referred to as the "sigmoid function"). In this case, the output is in the range (0, 1), and the input is sensitive in a range not much larger than (-1, +1). The function is also smooth and easily differentiable, facts that are critical in allowing the network training algorithms to operate. The limited numeric response range, together with the fact that information has to be in numeric form, implies that, in real applications, neural network approaches require a pre-processing stage, which may involve conversion of nominal values, scaling of numeric values, and substitution of missing values. The pre-processing also requires replication of values if predicting time series values from a data set. Throughout this thesis, only numeric input variables are dealt with.

Numeric values have to be scaled into a range that is appropriate for the network. Typically, raw variable values are scaled linearly, which involves multiplication by an input scale factor, $SC\#IP_i$ where i is the index for the first-layer units, followed by the addition of an input shift factor, $SH\#IP_i$. The pre-processing operation at each input can be expressed as:

$$IP_i' = IP_i \times SC\#IP_i + SH\#IP_i, \tag{2.1}$$

where IPi is the input and IP_i' is the pre-processed input.

Summation at hidden neurons: Each pre-processed input is multiplied by a scalar weight ($W\#H_{ij}$, where j is the index for the hidden-layer neurons) connecting the first-layer units to the hidden-layer neurons. At each neuron within the hidden layer, the weighted inputs are summed and bias value, $B\#H$, is subtracted from the summed weighted inputs. The threshold is used to adjust the 'saturation' of the hidden neuron during the training. The weighting operation that happens at each hidden neuron H_j numerically can be expressed as:

$$SU\#H_j = \sum_{i=1}^{m} (IP_i' \times W\#H_{ij}) - B\#H, \tag{2.2}$$

where SU#H_j is the resulting value after the summation at the each hidden neuron H_j.

Activation at hidden neurons: The resulting value from the summation is then passed through a non-linear activation function. In this thesis, the most popular logistic function is applied. The activation operation that occurs at each hidden neuron H_j can be numerically expressed as:

$$A\#H_j = \frac{1}{1+\exp(-SU\#H_j)}, \tag{2.3}$$

where A#H_j is the resulting value after the activation at each hidden neuron H_j.

Post synaptic potential transfer: The output value of each hidden neuron is passed through a linear post synaptic potential transfer function. In other words, the output value of each hidden neuron is multiplied by a scalar weight ($W\#OP_j$) for each connection between the hidden-layer neurons and the output neuron. Then the weighted outputs are summed and a bias value, $B\#OP$, is subtracted from the sum to produce a single output value OP'. The post synaptic potential transfer operation can be numerically expressed as:

$$OP' = \sum_{k=1}^{n} (A\#H_j \times W\#OP_j) - B\#OP. \tag{2.4}$$

Post-processing: Neural networks also require a post-processing stage. The output value of the post synaptic potential transfer needs to be post-processed to return to the original scale of the output variable. The post-processing involves descaling (subtracting the output shift factor, $SH\#OP$, followed by division by the output scale factor, $SC\#OP$). The post-processing operation can be numerically expressed as:

$$OP = \frac{OP' - SH\#OP}{SC\#OP}. \tag{2.5}$$

2.3 TRAINING OF ANNs

The training of the network is an iterative process to optimally adjust the weights (connections between neurons) of the network in order to optimally predict the sample data on which the training is performed. The best-known example of a neural network training algorithm is *Back Propagation* (Patterson, 1996; Haykin, 1994; Fausett, 1994). Modern second-order algorithms such as *Conjugate Gradient Descent* and *Levenberg-Marquardt* (Bishop, 1995) are substantially faster (that is., an order of magnitude faster) for many problems. There are also heuristic modifications of back propagation which

work well for some problem domains, such as *Quick Propagation* (Patterson, 1996) and *Delta-Bar-Delta* (Patterson, 1996).

The role of training algorithm is to set the network's weights and biases so as to minimise the prediction error made by the network. However, a problem commonly seen in neural networks is over-fitting (also called over-learning) (Reed, 1993). A network with more weights models a more complex function, and is therefore prone to over-fitting. A network with fewer weights may not be sufficiently powerful to model the underlying function. For example, a network with no hidden layers actually models a simple linear function.

The answer for selecting the right complexity of network is to check progress against an independent data set, the *verification* set. Some of the cases are reserved, and not actually used for training in the algorithm. Instead, they are used to keep an independent check on the progress of the algorithm. It is invariably the case that the initial performance of the network on training and verification sets is the same (if it is not at least approximately the same, the division of cases between the two sets is probably biased). As training progresses, the training error naturally drops, and provided training is minimising the true error represented by the root mean squared (RMS) error, the verification error drops too. However, if the verification error stops dropping, or indeed starts to rise, this indicates that the network is starting to overfit the data, and training should cease.

The problems associated with local minima, and decisions over the size of network to use, imply that using a neural network typically involves experimenting with a large number of different networks, probably training each one a number of times (to avoid being misled by local minima), and observing individual performances. The key guide to performance here is the verification error. However, following the standard scientific precept that, all else being equal, a simple model is always preferable to a complex model, then a smaller network is preferable to a larger one with a negligible improvement in verification error.

A problem with this approach of repeated experimentation is that the verification set plays a key role in selecting the model. This means that it is actually part of the training process and, therefore, its reliability as an independent guide to performance of the model is compromised. To increase confidence in the performance of the final model, it is therefore normal practice (at least where the volume of training data allows it) to reserve a third set of cases - the *test* set. The final model is tested with the test set data to ensure that the results on the verification and training set are real, and not artifacts of the training process. Of course, to fulfill this role properly the test set should be used only once - if it is in turn used to adjust and reiterate the training process, it effectively becomes verification data.

The division into multiple subsets is very unfortunate, given that the number of data is usually less than ideally desired. This problem can be avoided by resampling. Experiments can be conducted using different divisions of the available data into training, verification, and test sets. There are a number of approaches to this subset, including random (monte-carlo) resampling, cross-validation, and bootstrap (Statsoft, 1999). If design decisions, such as the best configuration of neural network to use, are made based upon a number of experiments with different subset examples, the results will be much more reliable.

To overcome over-fitting, two other strategies are 1) adding some noise to the training cases during training, which forces the neural network to model a smoothed version of the data; 2) using a *Weigened weight regularisation* technique, which explicitly penalises networks with large curvature, thus encouraging the development of a smoother model.

2.4 STATISTICAL PARAMETERS FOR ASSESSING ANNs

Throughout this thesis, ANNs are employed to solve regression type problems – a category of problems where the objective is to estimate the value of a continuous output variable from some input variables.

Statistical parameters, such as root mean square (RMS) error, correlation coefficients R^2 (the "coefficient of determination") and standard deviations ratio (SDR), can be applied to assess the prediction performance of the network.

The RMS error and R^2 provide ways to compare the performance of neural networks by way of indicating how well the predicted output matches the patterns over the entire set of facts. In a regression problem, the standard deviations of both the prediction error and original output data are important and they can be related by the SDR. The SDR in a regression problem is the ratio of the standard deviation of the prediction error to that of the original output data (an SDR of 0.1 is considered an excellent fit of the data and an SDR of 1.0 indicates that the neural network does no better than a simple average) (Statsoft, 1999). A close agreement between performance of the verification data set and that of the test data set is a strong indicator that the network has learned to generalize reliably.

2.5 NEURAL-COMPUTATIONAL SOFTWARE

Statistica Neural Networks (Statsoft, 1999) is a comprehensive neural networks analysis program which has been extensively used throughout this thesis.

Statistica Neural Networks software supports a number of practical architectures of neural networks including the MLP feedforward network used in this study. The network architectures are supported by highly optimised training algorithms including *Back-Propagation, Levenberg-Marquardt, Conjugate Gradient Descent, Quick Propagation, Delta-Bar-Delta* and many others. Furthermore, the software package provides automatic data scaling for both inputs and outputs.

2.6 ADVANTAGES AND LIMITATIONS OF ANNs

Neural networks are applicable in virtually every situation in which a relationship between the predictor variables (independents, inputs) and predicted variables

(dependents, outputs) exists, even when that relationship is very complex and not easily articulated in the usual terms of "correlations" or "differences between groups."

This sweeping success can be attributed to a few key factors (Statsoft, 1999; Nannariello *et al.*, 2001):

- Neural network analysis is a very sophisticated modelling technique capable of modelling extremely complex functions. In particular, neural networks are nonlinear. For many years linear modelling has been the commonly used technique in most modelling domains since linear models have well-known optimization strategies. Where the linear approximation was not valid (which was frequently the case) the models suffered accordingly. Neural networks also keep in check the 'curse of dimensionality' problem that frustrates attempts to model nonlinear functions with a large numbers of variables.
- Neural networks learn by example. The neural network user gathers representative data, and then invokes training algorithms to automatically learn the structure of the data. Although the user does need to have some heuristic knowledge of how to select and prepare data, how to select an appropriate neural network, and how to interpret the results, the level of user knowledge needed to successfully apply neural networks is much lower than would be the case using (for example) some more traditional nonlinear statistical methods.
- Neural networks can work with nominal data, which would be difficult to deal with by other means.
- Neural networks can directly represent the functional relationship between the input(s) and output(s).

While neural networks can be used to solve complex problems, they do suffer from a number of shortcomings (Nannariello *et al.*, 2001):

- The performance of a network can be sensitive to the quality of the input data. The input data used to train neural networks should ideally contain information that is spread evenly throughout the entire envelope of the system.
- There is no guarantee of finding an acceptable solution to a problem.

- There are limited opportunities to rationalise the solutions provided. Unlike expert systems, neural networks neither automatically explain their reasoning nor provide an audit trail account that fully explains how the system reaches its conclusion. Hence, the conclusions arrived at using neural network analysis are considered by some as "black box" solutions.
- There is limited theory to assist in the design of neural networks.

REFERENCES FOR CHAPTER 2

- Bishop C., 1995. *Neural networks for pattern recognition.* Oxford University Press, New York.
- Nannariello J., Osman M.R. and Fricke F.R., 2001. "Recent developments in the application of neural network analysis to architectural and building acoustics," *Acoustics Australia*, 29 (3), pp 103-110.
- Nannariello J. and Fricke F.R., 2001. "Introduction to neural network analysis and its application to building services engineering," *Building Services Engineering Research and Technology*, 22 (1), pp 58-68.
- Fausett L., 1994. *Fundamentals of neural networks: architectures, algorithms, and applications.* Prentice Hall, Englewood Cliffs, NJ.
- Haykin S., 1994. *Neural networks: a comprehensive foundation.* Macmillan Publishing, New York.
- Reed R., 1993. "Pruning algorithms – A survey," *IEEE transactions on neural networks*, 4 (5), pp 740-747.
- Ripley B.D., 1996. *Pattern recognition and neural networks.* Cambridge University Press, Cambridge.
- Rumelhart D.E. and McLelland J.L., 1986. *Parallel distributed processing: explorations in the microstructures of cognition.* MIT Press, Cambridge.
- StatSoft, 1999. *STATISTICA neural networks version 4.0A manual.* StatSoft Inc, Tulsa, OK.
- Taylor J.G., 1996. *Neural networks and their applications.* John Wiley and Sons, Chichester.

CHAPTER 3

OPTIMISATION AND EVOLUTIONARY ALGORITHMS

3.1 INTRODUCTION

In general, the accomplishment of any abstract task can be thought of as problem-solving, which, in turn, can be perceived as a search through a space of potential solutions. Since we are after the "best" solution, we can view this task as an optimisation process. Some problems only involve the optimisation at a single objective dimension. However, many real-world problems involve multiple measures of objectives, which need to be optimised simultaneously. Many powerful stochastic techniques for solving these large dimensional optimisation problems have arisen out of operations research, decision science, engineering, computer science and other related disciplines. The explosion in computing power continues to arouse extraordinary interest in stochastic search algorithms that require high computational speed and very large memories. Evolutionary algorithms, a generic stochastic approach, have been demonstrated to be very powerful and generally applicable for solving difficult single objective problems. Their fundamental algorithmic structures can also be applied for solving many multi-objective problems (MOPs) (Coello Coello *et al.*, 2002).

This chapter first introduces some basic definitions related to optimisation to help towards the understanding of basic optimisation problems. Next, it reviews the history and current state of the evolutionary algorithms (EAs), illustrates the general EA structure, explains how constraints can be handled in EAs, describes an evolutionary approach to the multi-objective optimisation problems (MOPs), and introduces a program that implements general EA operators and multi-objective genetic algorithms (MOGA). The advantages and limitations of EAs are also presented in this chapter.

In addition to this chapter, an instructive introductory overview of EAs can be found in Bäck *et al.* (1997a) and Fogel (1994) and more detailed discussions can be found in Bäck

et al. (1997b), Coello Coello *et al.* (2002), Fogel (1998), Fonseca and Fleming (1995) and Fonseca and Fleming (1998). These publications represent important milestones in the acceptance of EAs as practical tools for addressing complex optimisation problems and include numerous references that will assist readers just entering or not familiar with the field.

3.2 OPTIMISATION

To help in the understanding of basic optimisation problems, in this section some basic definitions related to optimisation are introduced.

3.2.1 Decision Variables

The *decision variables* are the numerical quantities for which values are to be chosen in an optimisation problem. These quantities are denoted as x_j, $j = 1, 2,\ldots,n$. The vector of n decision variables $\boldsymbol{x}$ is represented by:

$$\boldsymbol{x} = (x_1, \cdots, x_n). \tag{3.1}$$

3.2.2 Constraints

In most optimisation problems there are always restrictions imposed by the particular characteristics of the environment or resources available (e.g., physical limitations, time restrictions, etc.). These restrictions must be satisfied in order that a certain solution be considered acceptable. All these restrictions in general are called *constraints*, and they describe dependences among decision variables and constants (or parameters) involved in the problem. These constraints are expressed in the form of mathematical inequalities:

$$b_i(\boldsymbol{x}) \geq 0 \quad i = 1, \ldots, m, \tag{3.2}$$

or equalities:

$$h_i(\boldsymbol{x}) = 0 \quad i = 1, \ldots, p. \tag{3.3}$$

The number of equality constraints, p, must be less than the number of decision variables, n, because if $p \geq n$ the problem is said to be over-constrained, since there are no degrees of freedom left for optimising, in other words, there should be more unknowns than equations. The number of degrees of freedom is given by $n - p$. The constraints given by Eqs. (3.2) and (3.3) define the *parameter space* or the *feasible region X*.

3.2.3 Commensurable vs Non-commensurable

In order to ascertain how "good" a certain solution is, it is necessary to have some criteria to evaluate it. These criteria are expressed as computable functions of the decision variables that are called *objective functions*. In real world problems, some of them are in conflict with others and some have to be minimised while others are maximised. These objective functions may be *commensurable* (measured in the same units) or *non-commensurable* (measured in different units). The multiple objectives being optimised almost always conflict, placing a partial, rather than total, ordering on the search space (Bäck, 1996).

3.2.4 Attributes, Criteria, Goals and Objectives

In operations research, it is common practice to differentiate among attributes, criteria, objectives and goals. *Attributes* are often thought of as differentiating aspects, properties or characteristics of alternatives or consequences. *Criteria* generally denote evaluative measures, dimensions or scales against which alternatives may be gauged in a value or worth sense. *Objectives* are sometimes viewed in the same way, but may also denote specific desired levels of attainment or vague ideals. *Goals* usually indicate either of the latter notions.

In this thesis, the terms *objective*, *criteria* and *attribute* are used interchangeably to represent an MOP's goals or objectives (i.e., distinct mathematical functions) to be achieved. This convention is also adopted by several other researchers, for instance Horn (1997) and Fishburn (1978). The terms *objective space* or *objective function space* are also used to denote the coordinate space within which vectors resulting from evaluating an MOP are plotted.

3.2.5 Objective Functions

The *Objective functions* are designated as: $f_1(\boldsymbol{x}), f_2(\boldsymbol{x}),\ldots, f_k(\boldsymbol{x})$, where k is the number of objective functions in the MOP being solved. Therefore, the objective function forms a vector function $f(\boldsymbol{x})$ which is defined by:

$$f(\boldsymbol{x}) = (f_1(\boldsymbol{x}), f_2(\boldsymbol{x}),\ldots, f_k(\boldsymbol{x})). \tag{3.4}$$

3.2.6 Euclidean *n*-space

The set of all n-tuples of real numbers denoted by R^n is called *Euclidean n-space*. Two Euclidean spaces are considered:

1) The n-dimensional space of the decision variables in which each coordinate axis corresponds to a component of vector $\boldsymbol{x}$.
2) The k-dimensional space of the objective functions in which each coordinate axis corresponds to a component vector $f(\boldsymbol{x})$.

Every point in the first space represents a solution and gives a certain point in the second space, which determines a quality of this solution in terms of the values of the objective functions.

3.2.7 Single-objective Optimisation

The *single-objective optimisation problem* can be formally defined as follows (Bäck, 1996):

Given a function f: $X \subseteq S = R^n \rightarrow R$, $X \neq 0$, *for* $\boldsymbol{x} \in X$, *the value* $f^* \equiv f(\boldsymbol{x}^*) > -\infty$ *is called a global minimum if and only if*

$$\forall \boldsymbol{x} \in X : f(\boldsymbol{x}^*) \leq f(\boldsymbol{x}), \tag{3.5}$$

where S is the search space, $\boldsymbol{x}^*$ *is the global minimum solution* and f *is the single objective function.*

3.2.8 General MOP

A general *multi-objective optimisation problem* (also called multi-criteria optimisation, multi-performance or vector optimisation problem) can be formally defined as follows (Coello Coello *et al.*, 2002):

Find the vector $\boldsymbol{x}^* = [x_1^*, x_2^*, ..., x_n^*]$ *which satisfies the constraints, namely in the feasible region X, and optimises the vector function* $\boldsymbol{f}(\boldsymbol{x}) \in Y$ *(the objective space).*

In other words, it is aimed at determining from among the set of all numbers in the feasible region X the particular set $x_1^*, x_2^*, ..., x_n^*$ that yields the optimum values of all the objective functions.

Any point $\boldsymbol{x}$ in X defines a feasible solution. The vector function $\boldsymbol{f}(\boldsymbol{x})$ is a function which maps the set X into the objective space Y that represents all possible values of the objective functions. All the components of the vector $\boldsymbol{f}(\boldsymbol{x})$ represent the non-commensurable criteria which must be considered. The vector $\boldsymbol{x}^*$ is reserved to denote the optimal solutions.

3.2.9 Pareto Optimum

Single-objective optimisation problems may have a unique optimal solution but MOPs present a possibly uncountable set of solutions, which when evaluated, produce vectors whose components represent trade-offs in objective space. This set of non-dominated alternative solutions is known as *Pareto-optimal set* (Ben-Tal, 1980). A decision-maker (DM) then implicitly chooses an acceptable solution (or solutions) by selecting one or more of these vectors.

Pareto dominance (Fonseca and Fleming, 1998): A given vector $\boldsymbol{u} = (u_1, \cdots, u_k)$ *is said to dominate* $\boldsymbol{v} = (v_1, \cdots, v_k)$ *if and only if* $\boldsymbol{u}$ *is partially less than* $\boldsymbol{v}$ $(\boldsymbol{u}_p < \boldsymbol{v})$, *i.e.* $\forall i \in \{1, \cdots, n\} : u_i \leq v_i \wedge \exists i \in \{1, \cdots, n\} : u_i < v_i$.

Pareto optimality (Fonseca and Fleming, 1998): A solution $x_u \in X$ *is said to be Pareto-optimal if and only if there is no* $x_v \in X$ *for which* $v = f(x_v) = (v_1, \cdots, v_k)$ *dominates* $u = f(x_u) = (u_1, \cdots, u_k)$.

Pareto-optimal solutions are also called efficient, non-dominated, and non-inferior solutions. The corresponding objective vectors are simply called *non-dominated*. The set of all non-dominated vectors is known as the *non-dominated set*, or the *trade-off surface*, of the problem.

3.3 EVOLUTIONARY ALGORITHMS

Evolution provides inspiration for computing the solutions to problems that have previously appeared intractable. It is quite natural, therefore, to seek to describe evolution in terms of an algorithm that can be used to solve difficult optimisation problems. This section provides a simple introduction to the history and current state of EAs, the general EA structure, constraints handling in EAs and the EAs approach to the MOPs.

3.3.1 History and Current State

Although the origins of evolutionary algorithms can be traced back to the late 1950's [e.g., the influencing works of Bremermann (1962), Friedberg (1958), Friedberg *et al.* (1958) and Box (1957)], the field remained relatively unknown to the broader scientific community for almost three decades. This was largely due to the lack of available computer powers at that time, but also to some methodological shortcomings of those early approaches (Fogel, 1995). The fundamental work of Holland (1962), Rechenberg (1973), Schwefel (1975) and Fogel (1962) served to slowly change this picture during the 1970's and currently a remarkable and steady (still exponential) increase in the number of publications and conferences in this field can be observed in the work of Bäck *et al.* (1997a).

The majority of current implementations of evolutionary algorithms descend from three strongly related but independently developed approaches: genetic algorithms introduced

by Holland (1962), evolutionary programming introduced by Fogel (1962) and evolutionary strategies introduced by Rechenberg (1973) and Schwefel (1975). The differences between them are characterised by the typical data representation, the types of variations that imposed on solutions to create offspring, and the methods employed for selecting new parents. Over time, however, these differences have become increasingly blurred, and will likely become of historical interest only (Fogel, 1998).

3.3.2 A General Structure

EAs are stochastic search methods that mimic the metaphor of natural biological evolution on a computer. Figure 3.1 shows the structure of a simple EA (Pohlheim, 2004).

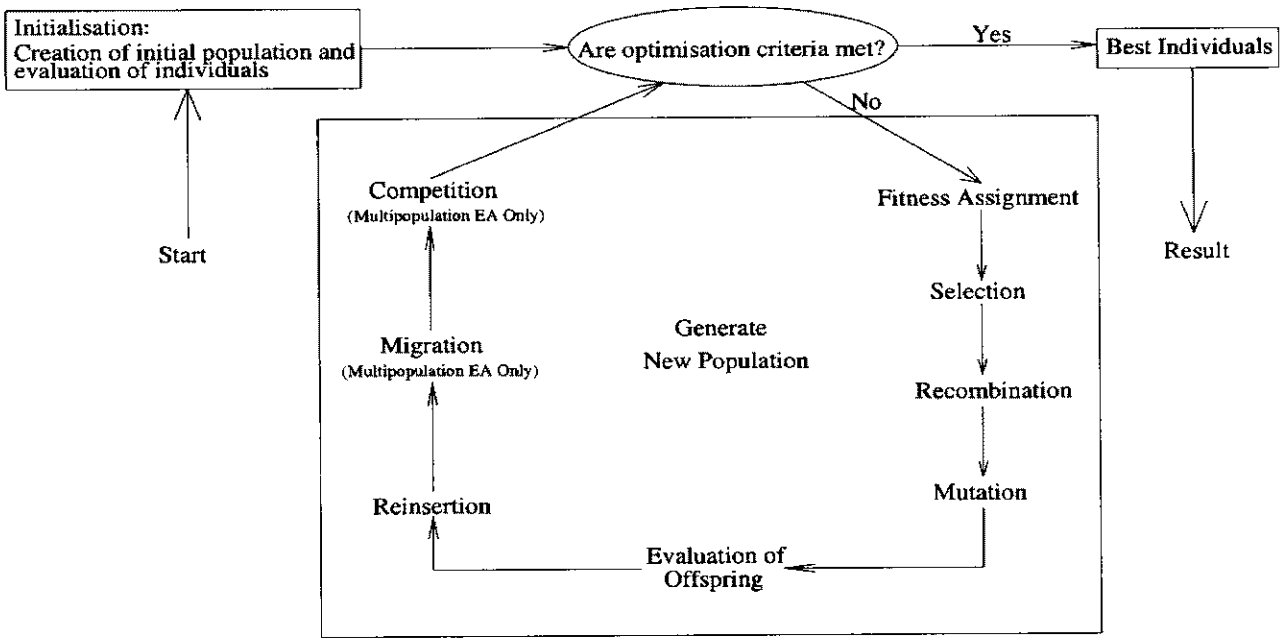

Figure 3.1 General structure of a simple EA.

The EA starts the search by randomly generating a set of a specified number of solutions, which is known as the population. Each solution within the population is known as an individual. After the size of the population is specified, individuals of the first/initial generation are randomly generated. To do this, decision variable values are generated randomly within the corresponding parameter space.

The objective function is then evaluated for these individuals. The first/initial generation (a set of potential solutions) is produced. If the optimisation criteria are not met the creation of a new generation starts. Individuals are assigned with certain fitness. Throughout this thesis, Rank-based Fitness Assignment technique (Goldberg, 1989; Fonseca and Fleming, 1993) is applied. The fitness assigned to each individual depends only on its position in the individual rank and not on the actual objective value. Rank-based Fitness Assignment overcomes the scaling problems of the proportional fitness assignment and behaves in a more robust manner than proportional fitness assignment (Bäck and Hoffmeister, 1991).

Individuals are selected according to their assigned fitness for the production of offspring (new potential solutions). Several selection methods, such as Roulette Wheel Selection (Baker, 1987), Stochastic Universal Sampling (Baker, 1987), Local Selection (Voigt *et al.*, 1991), Truncation Selection (Blickle, and Thiele, 1995) and Tournament Selection (Goldberg and Deb, 1991), have been developed.

Parents (existing potential solutions) are recombined. In other words, the information contained in the parents is combined to produce offspring. Discrete Recombination method (Mühlenbein and Schlierkamp-Voosen, 1995) can be applied to all (real-value, integer-value and binary-value) variable representations. Intermediate Recombination (Mühlenbein and Schlierkamp-Voosen, 1995), Line Recombination (Mühlenbein and Schlierkamp-Voosen, 1995) and Extended Line Recombination (Mühlenbein, 1994) methods can only be applied to real valued variables. Single (or Double or Multi-point) Point Crossover (Booker, 1987), Uniform Crossover (Syswerda, 1989), Shuffle Crossover (Caruana *et al.*, 1989) and Crossover with Reduced Surrogate (Booker, 1987) methods can only be applied to binary valued variables.

All offspring will be mutated (randomly altered) with a certain probability, which helps to keep the diversity of the population and avoid premature convergence to local optima. Mutation methods available for different variable (real valued, integer-valued and binary)

representations have been introduced by Mühlenbein and Schlierkamp-Voosen (1993) Bäck (1996) and Hansen *et al.* (1995).

The fitness of the offspring is then computed. The offspring are inserted into the population (the existing set of potential solutions) replacing their parents, producing a new generation. This cycle is performed until the optimisation criteria or the designated maximum number of generations is reached.

Such a single population EA is powerful and performs well on a wide variety of problems. However, the chance of finding a global solution may be improved or the number of the objective function evaluations may be reduced by introducing multiple subpopulations. Every subpopulation (subset of potential solutions) evolves over a few generations independently with a periodic communication phase between subpopulations. This communication can take the form of an exchange of some good individuals, which helps regenerate the converging subpopulations by injecting new generic material to replace some of the worst individuals in the subpopulation. The multi-population EA models the evolution of a species in a way more similar to nature than the single population EA (Pohlheim, 2004).

3.3.3 Constraint Handling in EAs

The simplest approach to handling constraints in EAs has been to assign infeasible individuals an arbitrarily low fitness (Goldberg, 1989). In this approach, provided feasible solutions can be easily found, any infeasible individuals are selected out and the search is not affected much.

Certain types of constraints, however, such as bounds on the decision variables and other linear constraints, can be handled by mapping the search space so as to minimise the number of infeasible solutions it contains and/or designing the mutation and recombination operators carefully in order to minimise the production of infeasible offspring from feasible parents (Michalewicz and Janikow, 1991). This and the previous approach are complementary and often used in combination with each other.

In the case where no feasible individuals are known, and cannot easily be found, the penalty imposed on infeasible individuals can be made to depend on the extent to which they violate the constraints. Such penalty values are typically added to the unconstrained performance value before fitness is computed (Goldberg, 1989). Although penalty functions do provide a way of guiding the search toward feasible solutions, when these are not known, they are very much problem-dependent. Guidelines on the use of penalty functions have been described by Richardson *et al.* (1989).

Another approach to constraint-handling has been proposed by Powell and Skolnick (1993) and consists of rescaling the original objective function to assume values less than unity in the feasible region, while assigning penalty values greater than one to infeasible individuals. Subsequent ranking of population assigns higher fitness to all feasible points than to infeasible ones.

3.3.4 Evolutionary Approach to MOPs

EAs seem particularly suitable for solving MOPs, because they deal simultaneously with a set of possible solutions (the so-called population). This enables several members of the Pareto-optimal set to be found in a single run of the algorithm, instead of a series of separate runs having to be performed as in the case of the traditional mathematical programming techniques. Additionally, EAs are less susceptible to the shape or continuity of the boundary of the design region, whereas these two issues are a real concern for mathematical programming techniques. Also, EAs are very attractive MOP solution techniques because they address both search and multi-objective decision-making (Coello Coello *et al.*, 2002).

Many EA paradigms for solving real-world MOPs have been proposed in the last two decades. Some examples of these paradigms are "Multi-Objective Genetic Algorithm (MOGA)" (Fonseca and Fleming, 1993; 1998), "Multi-Objective Messy Genetic Algorithm (MOMGA)" (Van Veldhuizen and Lamont, 2000), "Niched-Pareto Genetic Algorithm (NPGA)" (Horn and Nafpliotis, 1993), "Nondominated Sorting Genetic Algorithm (NSGA)" (Srinivas and Deb, 1994), "Pareto Archived Evolution Strategy

(PAES)" (Knowles and Cone, 2000), "Vector Evaluated Genetic Algorithm (VEGA)" (Schaffer, 1985) and "Strength Pareto Evolutionary Algorithm (SPEA)" (Zitzler and Thiele, 1999).

A detailed discussion of these paradigms can be found in Coello Coello *et al.* (2002). Among them, MOGA, NPGA and NSGA (or improved variants thereof) are some of the literature's most cited and imitated. As all these EA architectures move towards each other in terms of data structures, parameters and operators, the affirmation that one is "better" than another is probably ill-conceived (Coello Coello *et al.*, 2002).

MOGA is applied throughout this thesis as it is efficient, flexible and relatively easy to implement (see Section 3.3.4.5 for the advantages and limitations of MOGA). The following sections discuss the several important aspects of MOGA: the multi-objective decision-making based on given goals, rank-based fitness assignment, constraint satisfaction in term of objectives, MOGA as a method for progressive articulation, and advantages and limitations of MOGA.

3.3.4.1 Multi-objective decision-making based on given goals

When presented with the trade-off surface for a given function, the DM would have to decide which of all of the non-dominated points to choose as the solution to the problem. First, the regions of the Pareto set which express good compromises according to some problem-specific knowledge would be identified. Then, having a clearer picture of what is achievable, the idea of compromise would be refined until the solution was found. As a consequence, only the "interesting" regions of the Pareto set need to be well known, which is not to reduce the scope of the search, but simply to zoom in on the region of the Pareto set of interest to the DM.

Preference articulation implicitly defines a so-called utility function which discriminates between candidate solutions. Although such a utility function can be very difficult to formalize in every detail, approaches based on weighting coefficients (Hwang and Masud, 1979), priorities (Ben-Tal, 1980) and goal values (Fonseca and Fleming, 1993)

have been widely used. Goal values indicate desired levels of performance in each objective dimension. The way in which goals are interpreted may vary. In particular, they may represent minimum levels of performance to be attained, Utopian performance levels to be approximated, or ideal performance levels to be matched as closely as possible. Goals are usually easier to set than weights and priorities, because they relate more closely to the final solution of the problem.

Assuming a minimisation problem, consider two q-dimensional objective vectors, $y_a = (y_{a,1}, y_{a,2}, \cdots, y_{a,q})$ and $y_b = (y_{b,1}, y_{b,2}, \cdots, y_{b,q})$, and the goal vector $g = (g_1, g_2, \cdots, g_q)$. Assuming a convenient permutation of the objectives, also consider that

(A) y_a is such that it meets a number, $q-d$, of the specified goals, i.e., $\exists d = 1, \cdots, q-1 : \forall i \in 1, \cdots, d, \forall j \in d+1, \cdots, q, (y_{a,i} > g_i) \wedge (y_{a,j} \leq g_j)$; or

(B) y_a meets none of the goals, i.e., $\forall i = 1, \cdots, q, (y_{a,i} > g_i)$; or

(C) y_a meets all of the goals, i.e., $\forall i = 1, \cdots, q, (y_{a,j} \leq g_j)$.

In the first situation (A), y_a meets goals $d+1, \cdots, q$ and, therefore, will be preferable to y_b simply if it dominates y_b with respect to its first d components. For the case where all of the first d components of y_a are equal to those of y_b, y_a will still be preferable to y_b if it dominates y_b with respect to the remaining components of y_b, or if the remaining components of y_b do not meet all their goals. In the second situation (B), y_a satisfies none of the goals. Then y_a is preferable to y_b, if and only if it dominates y_b. Finally, in the third situation (C) y_a meets all of the goals, which means that it is a satisfactory, though not necessarily an optimal solution. In this case, y_a is preferable to y_b, if and only if it dominates y_b or y_b is not satisfactory (Fonseca and Fleming, 1993).

The use of the relation *preferable to* as just described, instead of the simpler relation *partially less than*, implies that the solution set is delimited by those non-dominated

points which tangentially achieve one or more goals. In fact, degradation in vector components which meet their goals is now acceptable provided it results in the improvement of other components which do not satisfy their goals and it does not go beyond the goal boundaries (Fonseca and Fleming, 1993).

3.3.4.2 The MOGA as a method for progressive articulation

When goals can be supplied interactively at each EA generation, the DM can reduce the size of the solution set gradually while learning about the trade-off between objectives. The variability of the goals acts as a changing environment to the EA, and does not impose any constraints on the search space.

In general, as shown in Figure 3.2 (Fonseca and Fleming, 1993), the EA (MOGA in this case) would present the DM at each generation with a set of points to be assessed. The DM makes use of the concept of Pareto optimality and of any a priori information available to express its preferences, and communicates them to the EA, which in turn replies with the next generation. At the same time, the DM learns from the data it is presented with and eventually refines its requirements until a suitable solution has been found.

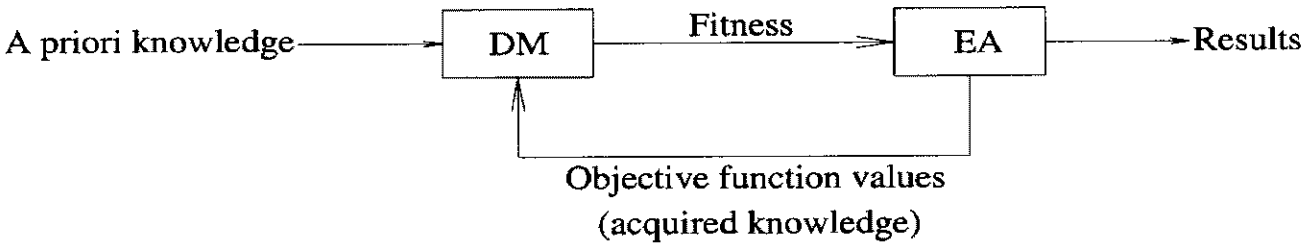

Figure 3.2 General EA optimiser with progressive articulation.

3.3.4.3 Rank-base fitness assignment for MOGA

Individuals in a population can be ranked in accordance to the preference decided using the multi-objective decision-making strategy introduced in the Section 3.3.4.1. Consider an individual x_u at generation t and let $r_u^{(t)}$ be the number of individuals in the current

population that are preferable to it. The current position of x_u in the individuals' ranks can be simply given by

$$rank(x_u, t) = r_u^{(t)}. \tag{11}$$

This ensures that all preferred individuals in the current population are assigned rank zero (Fonseca and Fleming, 1998). The ranking of a population provides sufficient relative quality information to guide evolution. Ranked based fitness assignment can be described as follows (Fonseca and Fleming, 1993):

1) Sort population according to rank;
2) Assign fitness by interpolating from the best individual to the worst according to some function, usually linear or exponential, but possibly another type;
3) Average the fitness assigned to individuals with the same rank, so that all of them are sampled at the same rate while keeping the global population fitness constant.

Fitness is understood here as the number of offspring an individual is expected to produce through selection.

3.3.4.4 Constraint satisfaction in term of objectives

Constraints can be seen as hard objectives, which must be jointly satisfied before the optimisation of the remaining, soft objectives, takes place. Satisfying a number of violated constraints can be regarded as an MOP problem of minimizing the associated functions until given goals are reached. The concept of non-inferiority is, therefore, readily applicable, and even particularly appropriate when constraints are themselves non-commensurable. When not all goals can be simultaneously met, a family of violating, non-dominated points is the closest one can get to a solution to the problem. Goal-based multi-objective optimisation extends simple constraint satisfaction in the sense that the optimisation continues even after all goals are met. In this case, solutions should both be non-dominated and meet all goals (Fonseca and Fleming, 1998).

3.3.4.5 Advantages and limitations of MOGA

The main advantage of MOGA is that it is efficient, relatively easy to implement and flexible. It potentially reduces the number of function evaluations, compared to the posteriori articulation of preferences where the DM is presented by the optimiser with a set of candidate non-dominated solutions before expressing any preferences. It also provides fewer alternative points at each iteration, which means that it is easier for the DM to discriminate between alternatives than it would be if it were presented with the whole Pareto set at once.

The main disadvantage is that it requires the DM to know beforehand the ranges of variation of each objective in order to establish coherent goals. This could be an expensive process in terms of computer processing time, if not impossible in many real-world applications (Coello Coello *et al.*, 2002). Also the use of an interactive method may require reasonable interaction times for it to become attractive. The natural solution to speed up the process is to run the EA on a parallel architecture. The most appealing of all, however, would be the use of an automated DM, such as an expert system (Fonseca and Fleming, 1993).

3.4 A PROGRAM IMPLEMENTING GENERAL EA OPERATORS AND MOGA

The above introduced general EA structure and operators (see Section 3.3.2) and MOGA (see Section 3.3.4) have been implemented as MATLAB (Mathworks, 2002) M and MEX files (Chipperfield *et al.*, 1994) and further developed and incorporated into the Genetic and Evolutionary Algorithm Toolbox for Use with Matlab (GEATbx) (Pohlheim, 2004). This toolbox offers the user several "default" EA instantiations (e.g., real-, integer-, or binary-valued genetic algorithms and evolutionary strategy) and excellent visualisation output to aid in analysis. GEATbx requires only a limited amount of user effort to implement a specific EA.

Throughout this thesis, GEATbx has been used as the tool for implementing the evolutionary approach to solve the optimisation problems investigated in chapters 5, 6 and 7 of the present thesis.

3.5 ADVANTAGES AND LIMITATIONS OF EAs

There will always remain a dichotomy between efficiency and general applicability and between reliability and effort of problem-solving, especially with optimum-seeking algorithms. Any specific knowledge about the given situation may be used to specify an adequate specific solution algorithm, the optimal situation being that one knows the solution in advance. On the other hand, there cannot exist one method that solves all problems effectively as well as efficiently.

The current literature identifies three main types of search methods: calculus-based, enumerative and random (Goldberg, 1989). Calculus-based methods have been studied extensively. These subdivide into two main classes: indirect and direct. Indirect methods seek local extrema by solving the usually nonlinear set of equations resulting from setting the gradient of the objective function equal to zero. Given a smooth, unconstrained function, finding a possible peak starts by restricting search to those points with slopes of zero in all directions. This is the multi-dimensional generalisation of the elementary calculus notion of extremal points. On the other hand, direct methods seek local optima by hopping on the function and moving in a direction related to the local gradient. This is simply the notion of hill-climbing: to find the local best and climb the function in the steepest permissible direction.

Both of these calculus-based methods have been improved, extended, hashed and rehashed and they are effective and efficient in solving the problem that features a unimodal objective space. However, there are inherent limitations in these methods. First, they are local in scope: the optima they seek are the best in a neighbourhood of the current starting point. When the objective space is multimodal, starting the search or zero-finding procedures in the neighbourhood of a lower peak will not enable the finding

of the highest peak. Furthermore, once the lower peak is reached, further improvement must be sought through random restart (or other trickery). The restarting point, however, cannot be guaranteed in the neighbourhood of the highest peak. In other words, calculus-based methods lack robustness for optimisation problems featuring multimodal objective space. Second, calculus-based methods depend upon the existence of derivatives (well-defined slope values). Even if numerical approximation of derivatives is allowed, this is a severe shortcoming. Many practical decision spaces have little respect for the notion of a derivative and the smoothness this implies. The real world of search is fraught with discontinuities and vast multimodal, noisy search spaces as depicted in a less calculus-friendly function. Therefore, it comes as no surprise that calculus-based search methods, characterised by the local scope of search and the restrictive requirements of continuity and derivative existence, are unsuitable for optimisation problems that are combinatorial (featuring discontinuous decision space) and/or multimodal.

Enumerative schemes have been considered in many shapes and sizes. The idea is fairly straightforward: within a finite search space, or a discretized infinite search space, the search algorithm starts looking at objective function values at every point in the space, one at a time. Although the simplicity of this type of algorithm is attractive, such schemes are discounted for their inefficiency. Many practical spaces are simply too large to search for one at a time and still have a chance of using the information to some practical end.

Random search algorithms have achieved increasing popularity as researchers have recognised the shortcomings of calculus-based and enumerative schemes. The EA algorithm is an example of a search procedure that uses random choice as a tool to guide a highly exploitative search. Using random choice as a tool in a directed search process seems strange at first, but nature contains many examples. Another currently popular search technique "simulated annealing", uses random processes to help guide its form of search for minimal energy states [see Laarhoven and Aarts (1987) and Booker (1987)]. The important thing to recognise is that randomised search does not necessarily imply directionless search, as shown in Section 3.3.2 of this thesis.

It is generally accepted that EAs are robust and useful search algorithms when the problem domain has multidimensional decision variables. They are applicable even in dynamic situations where the goals or constraints are moving over time or changing, either exogenously or self-induced, where parameter adjustments and fitness measurements are disturbed, and where the landscape is rough, discontinuous, multimodal, fractal or cannot otherwise be handled by traditional methods, especially those that need global prediction from local surface analysis. EAs are also particularly suitable for solving MOPs (see Section 3.3.4) and the evolutionary approach towards the MOPs has been becoming increasingly accepted in scientific, engineering and management areas since the late 1990s (Coello Coello *et al.*, 2002). Sometimes striking is the fact that even obviously wrong parameter settings do not prevent fairly good results. This can be described as robustness. Not yet well understood, but nevertheless very successful, are those EAs which self-adapt some of their internal parameters, a feature that can be described as collective learning of the environmental conditions (Schwefel, 1997).

However, if there is already a traditional method that solves a given problem, EAs should not be used because they cannot do it better or with less computational effort. EAs always present an intermediate compromise; the enthusiasm of its inventors is not yet taken into account here, nor are the insights available from the analysis of the algorithms for natural evolutionary processes which they try to mimic (Schwefel, 1997).

In the present thesis, chapter 5 demonstrates that a multi-objective EA can be successfully employed to solve a difficult MOP in architectural and building acoustics and its effectiveness for solving combinatorial-type problems featuring discontinuous decision space; and chapter 6, from an application point of view, compares the robustness, effectiveness and efficiency of EAs and traditional calculus-based optimisation methods.

REFERENCES FOR CHAPTER 3

- Bäck T. and Hoffmeister F., 1991. "Extended selection mechanisms in genetic algorithms," *Proceedings of the fourth international conference on genetic algorithms*, San Mateo, California, Morgan Kaufmann, pp 92-99.
- Bäck T., 1996. *Evolutionary algorithms in theory and practice*. Oxford University Press, New York.
- Bäck T., Hammel U. and Schwefel, H.P., 1997a. "Evolutionary computation: comments on the history and current state," *IEEE transaction on evolutionary computation*, 1 (1), pp 3-17.
- Bäck T., Fogel D.B. and Michalewicz Z., 1997b. *Handbook of evolutionary computation*. Oxford University Press, New York.
- Baker J.E., 1987. "Reducing bias and inefficiency in the selection algorithm," *Proceedings of the second international conference on genetic algorithms and their application*, Hillsdale, New Jersey, Lawrence Erlbaum Associates, pp 14-21.
- Ben-Tal A., 1980. "Characterization of Pareto and lexicographic optimal solutions." *In:* Fandel G. and Gal T., editors, *Multiple criteria decision making theory and application, vol. 177 of Lecture notes in economics and mathematical systems*, Springer-Verlag, Berlin, pp 1-11.
- Blickle T. and Thiele L., 1995. *A comparison of selection schemes used in genetic algorithms 2nd Edition. TIK report No. 11.* Computer Engineering and Communication Networks Lab (TIK), Swiss Federal Institute of Technology (ETH) Zürich, Switzerland.
- Booker L., 1987. "Improving search in genetic algorithms," *In*: Davis, L.D., editor, *Genetic algorithms and simulated annealing*, San Mateo, California, Morgan Kaufmann Publishers, pp 61-73.
- Box G.E.P., 1957. "Evolutionary operation: A method for increasing industrial productivity," *Applied Statistics*, 6 (2), pp 81-101.
- Bremermann H.J., 1962. "Optimization through evolution and recombination," *In:* Yovits *et al.*, editors, *Self-organizing systems*, Spartan, Washington DC.

- Caruana R.A., Eshelmann L.A. and Schaffer J.D., 1989. "Representation and hidden bias II: Eliminating defining length bias in genetic search via shuffle crossover," *In*: Sridharan N.S., editor, *Eleventh international joint conference on artificial intelligence*, San Mateo, California, Morgan Kaufmann Publishers, 1, pp 750-755.
- Chipperfield A., Fleming P.J., Pohlheim H. and Fonseca C.M., 1994. *Genetic algorithm toolbox for use with matlab. Technical report No. 512.* Department of Automatic Control and Systems Engineering, University of Sheffield, UK.
- Coello Coello A.C., Veldhuizen D.A.V. and Lamont G.B., 2002. *Evolutionary algorithms for solving multi-objective problems*. Kluwer Academic Publishers, New York.
- Hwang C.L. and Masud A.S.M., 1979. *Multiple objective decision making – methods and applications, vol. 164 of Lecture notes in economics and mathematical systems*, Springer-Verlag, Berlin.
- Fishburn P.C., 1978. "A survey of multiattribute/multicriterion evaluation theories," *In:* Zionts S., editor, *Multiple criteria problem solving*, Springer-Verlag, Berlin, pp 181-124.
- Fogel D.B., 1994. "An introduction to simulated evolutionary optimization," *IEEE transactions on neural networks: special issue on evolutionary computation*, 5 (1), pp 3-14.
- Fogel D.B., 1995. *Evolutionary computation: toward a new philosophy of machine intelligence*. IEEE Press, Piscataway.
- Fogel D.B., 1998. *Evolutionary computation*. IEEE Press, Piscataway.
- Fogel L.J., 1962. "Autonomous automata," *Industrial research*, 4, pp 14-19.
- Fonseca C.M. and Fleming P.J., 1993. "Genetic algorithms for multiobjective optimization: formulation, discussion and generalization," *Proceedings of the fifth international conference on genetic algorithms*, San Mateo, California, Morgan Kaufmann, pp 416-423.
- Fonseca C.M. and Fleming P.J., 1995. "An overview of evolutionary algorithms in multiobjective optimization," *Evolutionary Computation*, 3 (1), pp 1-16.
- Fonseca C.M. and Fleming P.J. (1998). "Multiobjective optimization and multiple constraint handling with evolutionary algorithms – part I: a unified formulation,"

IEEE transactions on systems, man, and cybernetics – Part A: system and humans, 28 (1), pp 26-37.

- Friedberg R.M., 1958. "A learning machine: Part I," *IBM Journal*, 2 (1), pp 2-13.
- Friedberg R.M., Dunham B. and North J.H., 1959. "A learning machine: Part II," *IBM Journal*, 3 (7), pp 282-287.
- Goldberg D.E., 1989. *Genetic algorithms in search, optimisation and machine learning*. Addison-Wesley Publishing Company, Reading, Massachusetts.
- Goldberg D.E. and Deb K., 1991. "A comparative analysis of selection schemes used in genetic algorithms," *In:* Rawlins G.J.E., editor, *Foundations of genetic algorithms*, San Mateo, California, Morgan Kaufmann Publishers, pp 69-93.
- Hansen N., Ostermeier A. and Gawelczyk A., 1995. "On the adaptation of arbitrary mutation distributions in evolution strategies: the generating set adaptation," *Proceedings of the sixth international conference on genetic algorithms*, San Francisco, California, Morgan Kaufmann Publishers, pp 57-64.
- Holland J. H. (1962). "Outline for a logical theory of adaptive systems," *Journal of the Association for Computing Machinery*, 3, pp 297-314.
- Horn J. and Nafpliotis N., 1993. *Multiobjective optimization using the niched Pareto genetic algorithm. Technical report IlliGA1 Report 93005.* University of Illinois at Urbana-Champaign, Urbana, Illinois.
- Horn J., 1997. "Multicriterion decision making," *In:* Bäck T., Fogel D.B. and Michalewicz Z., editors, *Handbook of Evolutionary Computation*, Oxford University Press, New York, 1, pp F1.9:1-F1.9:15.
- Knowles J.D. and Corne D.W., 2000. "Approximating the nondominated front using the Pareto archived evolution strategy," *Evolutionary Computation*, 8 (2), pp 149-172.
- Laarhoven P.J.M. and Aarts E.H.L., 1987. *Simulated annealing: theory and applications*. Kluwer Academic Publishers, Norwell, MA.
- Lamont G.B., 1993. *Compendium of parallel programs for the Intel iPSC computers.* Department of Electrical and Computer Engineering, Graduate School of Engineering, Air Force Institute of Technology, Wright-Patterson AFB, OH 45433.
- MathWorks Inc, 2002. *MATLAB reference guide (version 6.5 R13).* Natick, MA.

- Michalewicz Z. and Janikow C.Z., 1991. "Handling constraints in genetic algorithms," *Proceedings of the fourth international conference on genetic algorithms*, San Mateo, California, Morgan Kaufmann, pp 151-157.
- Michalewicz Z. and Fogel D.B., 2000. *How to solve it: modern heuristics*. Springer, Berlin.
- Mühlenbein H. and Schlierkamp-Voosen D., 1993. "Predictive models for the breeder genetic algorithm: I. Continuous parameter optimization," *Evolutionary Computation*, 1 (1), pp 25-49.
- Mühlenbein H., 1994. "The breeder genetic algorithm - a provable optimal search algorithm and its application," *Colloquium on applications of genetic algorithms*, IEE 94/067, London.
- Mühlenbein H. and Schlierkamp-Voosen D., 1995. "Analysis of selection, mutation and recombination in genetic algorithms," *In*: Banzhaf W. and Eeckman F.H., editors, *Evolution as a computational process Vol 899 of Lecture notes in Computer Science*, Berlin, Springer-Verlag, pp 142-168.
- Pohlheim H., 2004. *Genetic and evolutionary algorithm toolbox for use with MATLAB version 3.5*, http://www.geatbx.com/, Berlin.
- Powell D. and Skolnick M.M., 1993. "Using genetic algorithms in engineering design optimization with nonlinear constraints," *Proceedings of the fifth international conference on genetic algorithms*, San Mateo, California, Morgan Kaufmann, pp 424-431.
- Rechenberg I., 1973. *Evolutionsstrategie: optimierung technischer systeme nach prinzipien der biologischen evolution*. Frommann-Holzboog, Stuttgart.
- Richardson J.T., Palmer M.R., Liepins G. and Hilliard M., (1989). "Some guidelines for genetic algorithms with penalty functions," *Proceedings of the third international conference in genetic algorithms*, San Mateo, California, Morgan Kaufmann, pp 191-197.
- Schaffer J.D., 1984. *Multiple objective optimization with vector evaluated genetic algorithms*. Thesis (PhD). Vanderbilt University, Nashville, Tennessee.

- Schwefel H.P., 1975. *Evolutionsstrategie und numerische optimierung.* Thesis (PhD). Technische Universitat, Berlin, Germany.
- Schwefel H.P., 1981. *Numerical optimization of computer models.* Wiley & Sons, Chichester.
- Schwefel H.P., 1997. "Advantages (and disadvantages) of evolutionary computation over other approaches," *In*: Bäck T., Fogel D.B. and Michalewicz Z., editors, *Handbook of Evolutionary Computation (release 97/1)*, IOP Publishing Ltd and Oxford University Press, New York, pp A1.3:1 – A1.3:2.
- Srinivas N. and Deb K., 1994. "Multiobjective optimization using nondominated sorting in genetic algorithms," *Evolutionary Compuation*, 2 (3), pp 221-248.
- Syswerda G., 1989. "Uniform crossover in genetic algorithms," *Proceedings of the third international conference in genetic algorithms*, San Mateo, California, Morgan Kaufmann, pp 2-9.
- Van Veldhuizen D.A. and Lamont G.B., 2000. "Multiobjective optimization with messy genetic algorithms," *Proceedings of the 2000 ACM symposium on applied computing*, Villa Olmo, Como, Italy, pp 470-476.
- Voigt H.M., Born J. and Santibanez-Koref I., 1991. "Modeling and simulation of distributed evolutionary search processes for function optimization," *In*: Schwefel H.P. and Männer R., editors, *Parallel problem solving from nature - PPSN I. Vol 496 of Lecture notes in Computer Science*, Berlin, Heidelberg, New York, Springer-Verlag, pp 373-380.
- Zitzler E. and Thiele L., 1999. "Multiobjective evolutionary algorithms: a comparative case study and the strength Pareto approach," *IEEE transactions on evolutionary computation*, 3 (4), pp 257-271.

CHAPTER 4

PREDICTING ARCHITECTURAL SPEECH SECURITY USING ARTIFICIAL NEURAL NETWORKS

4.1 INTRODUCTION

Offices and meeting rooms are often intended for confidential discussions where eavesdroppers and others outside the room should not be able to hear what is being said. The acoustical privacy of such rooms can be referred to as architectural speech security. Improved speech security is achieved by constructing the boundaries of the room to have higher sound transmission loss. When speech security is of concern, it is desirable to be able to predict the degree to which the "transmitted" speech is audible or intelligible at positions outside the room.

Defining the problem of speech security in terms of the fraction of speech that can be understood makes it one of speech intelligibility. Investigations into speech privacy for open-plan office situations have used this same approach (ASTM, 2002). The distinction being made by security designers is that "privacy" is a less stringent description of sound isolation than "security". A condition where overheard speech is audible but only slightly intelligible corresponds to excellent *privacy*, but could be described as imperfect *security*. Therefore, a high degree of speech security implies not only very low speech intelligibility but in some cases minimal audibility of the transmitted speech sounds.

Speech security can be described on three different levels. The first level would be when only a very small percentage or none of the overheard words is intelligible; the second level is when no words are intelligible but when it is often still possible to recognise the cadence or rhythm of the speech; and finally, the highest level of speech security would be when all speech sounds from the adjacent space are completely inaudible (Gover and Bradley, 2004). Speech privacy and speech security have been related to Signal-to-noise (S/N) type measures, where the signal is the speech from the adjacent space. The simplest

measure is the difference of A-weighted speech and noise levels. More sophisticated measures such as the Articulation Index (AI) (ANSI, 1965) and its more recent replacement the Speech Intelligibility Index (SII) (ANSI, 1997) are known to be better related to speech intelligibility within rooms. However, Gover and Bradley (2004) have shown that SII and AI cannot be used to describe conditions for high levels of speech security which would correspond to acoustical conditions below SII=0 or AI=0, where SII or AI is not defined. The difference in A-weighted levels is not limited in this way but is much less accurately related to intelligibility scores. A more successful measure is the SII-weighted S/N ratio, which is a weighted sum of one-third-octave band S/N ratios using the same frequency weightings as the SII measure. Although the SII-weighted S/N ratio predicts the intelligibility score and threshold reasonably well, the S/N loudness ratio provides a more accurate estimate of the thresholds of cadence and audibility (Gover and Bradley, 2004).

This chapter investigates an approach that uses the artificial neural networks (ANNs) to directly represent the functional relationship of the octave band (250 Hz – 8 kHz) S/N ratios to the speech intelligibility score and to security thresholds. The objectives of the ANNs are to predict a) the speech intelligibility score (namely the percentage of words correctly identified by each individual), b) the intelligibility threshold (namely the percentage of listeners able to correctly identify at least one word), c) the cadence threshold (namely the percentage of listeners able to detect the cadence of the speech) and d) the audibility threshold (namely the percentage of listeners able to hear the presence of the speech). On the basis of the statistical analysis of the prediction results, the accuracy of the prediction using ANNs is then compared with those using conventional methods.

4.2 DATABASE FOR ANN MODELS

Two speech intelligibility and security experiments were carried out by Gover and Bradley (2004) at the Institute for Research in Construction (IRC), Canadian National Research Council (CNRC). In their work, subjects (with negligible hearing loss) rated

simulated speech security situations. The subjects sat in a sound-isolated room and heard speech sounds combined with typical ambient noises. The speech and noise sounds were spatially separated and were precisely measured at the listener's head position in an acoustically dead environment.

In the first intelligibility experiment (intelligibility scores and the intelligibility threshold), 36 subjects, who had passed a standard audiometric hearing threshold test and a short trial of an intelligibility test, each listened to 340 test sentences. The phonetically balanced and low predictability Harvard sentences (Subjective Measurements Subcommittee of the Standards Committee of IEEE Audio and Electroacoustics Group, 1969) were used with five different sentences for each physical condition. Each condition was one of 68 combinations of ambient noise, wall transmission loss characteristics and S/N ratio. The conditions were chosen so that the percentage of subjects detecting intelligibility ranged from 0 to 100%. Subjects were then divided into two groups, 19 "better" subjects and 17 "worse" subjects, in accordance with their mean intelligibility scores across all 340 sentences.

A follow-up experiment was conducted to determine not only the intelligibility score and the intelligibility threshold but the thresholds of cadence of the speech and audibility of any speech sounds. In this second experiment the 19 "better" subjects from the first experiment each listened to 160 sentences. Again there were five sentences for each condition and a range of ambient noise and wall transmission loss values. However, in the second experiment conditions had, on average, much lower S/N values so that they included situations where no speech sounds were audible to the listeners. Details of these two experiments are provided in Gover and Bradley, 2004.

The results of the 19 "better" subjects in the above two experiments constitute the database for the ANN models in the present work. The 9500 [19 x (340 + 160)] individual intelligibility score test cases were used as the database for predicting the intelligibility score. Of the 9500 cases, 7600 were used for training, 950 for verification and 950 for testing. All the sentences in the first and second experiments, viz. 500

(340+160) sentences (cases), were used as the database for predicting the intelligibility threshold. Of the 500 cases, 310 were used for training, 95 for verification and 95 for testing. For predicting the cadence threshold and the audibility threshold the 160 sentences (cases) in the second experiment were used as the database. Of the 160 cases, 128 were used for training, 16 for verification and 16 for testing.

4.3 INPUTS AND OUTPUTS OF ANN MODELS

The inputs of the ANN models for all the four prediction situations are the octave band (250 Hz – 8 kHz) S/N ratios, that is to say, the difference in the transmitted speech level and the background noise level at each octave frequency band from 250 Hz to 8 kHz. The range of the input variables for predicting the intelligibility score and the intelligibility threshold when considering both experiments is different from that for predicting the audibility and the cadence thresholds when accounting for only the second experiment. Table 4.1 provides the range of each input variable of the four ANN models. The outputs of the ANN models are the intelligibility score, the intelligibility threshold, the cadence threshold and the audibility threshold, and are within the range of 0 – 100%.

Table 4.1 Ranges of input variables

	The Range of Input Variables for Predicting the Intelligibility Scores and the Intelligibility Threshold		**The Range of Input Variables for Predicting the Cadence Threshold and the Audibility Threshold**	
Input Variables	**Minimum dB**	**Maximum dB**	**Minimum dB**	**Maximum dB**
S/N Ratio at 250 Hz	-34.8	6.2	-34.8	-8.3
S/N Ratio at 500 Hz	-30.2	13.1	-30.2	-2.3
S/N Ratio at 1 kHz	-32.7	1.3	-32.7	-15.7
S/N Ratio at 2 kHz	-28.2	7.1	-28.2	-1.8
S/N Ratio at 4 kHz	-27.4	10.0	-21.8	0.5
S/N Ratio at 8 kHz	-23.2	8.7	-16.6	-6.3

4.4 ARCHITECTURE OF ANN MODELS AND PROCEDURES OF ANN ANALYSIS

Figure 4.1 illustrates the 3-layer feed-forward ANN architecture applied in the present work. One hidden neuron layer, with 3 hidden neurons, was used. The ANN analysis was undertaken using STATISTICA Neural Networks (Statsoft, 1999). The weights, which were initialised to uniformly-distributed random values using the "uniform method", were adjusted by using "back propagation" and "conjugate gradient" algorithms to minimize the prediction error during the training. Conditions were set within the STATISTICA Neural Networks program by altering the model's parameters. "Early stopping" and "Weigend weight regularization" techniques were used to control over-fitting. Training of ANNs was stopped when the RMS error of the verification set could no longer be improved. The test set was used to independently check the performance of the network when an entire network design procedure was completed.

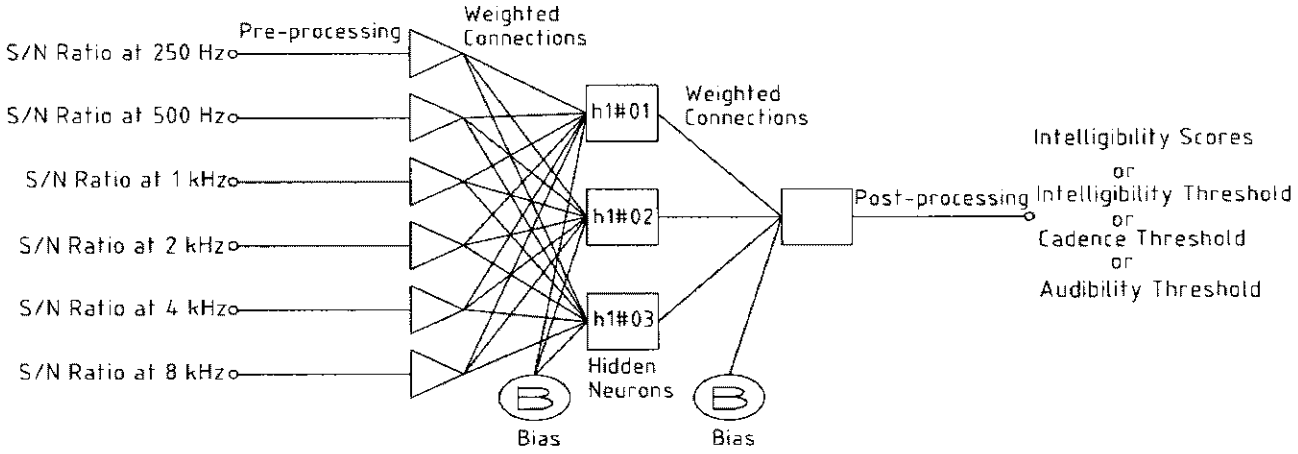

Figure 4.1 Illustration of the 3-layer feed-forward artificial neural network for predicting architectural speech intelligibility and security thresholds.

4.5 MODUS OPERANDI OF ANN MODELS

For the present work, the pre-processing of the inputs involves scaling input values to an appropriate range suitable for use in the ANN. Input values are multiplied by a scale

factor, followed by the addition of a shift factor. Table 4.2 provides the shift and scale factors to input variables of each ANN model. These factors are automatically generated by the scaling algorithm of the STATISTICA Neural Networks (Statsoft, 1999).

Table 4.2 Shift and scale factors to inputs of each ANN model

Input Variables	ANN Model for Predicting Intelligibility Scores		ANN Model for Predicting Intelligibility Threshold		ANN Model for Predicting Cadence Threshold		ANN Model for Predicting Audibility Threshold	
	Shift	Scale	Shift	Scale	Shift	Scale	Shift	Scale
S/N Ratio at 250 Hz	0.8478	0.0244	0.8561	0.0251	1.3117	0.0377	1.3117	0.0377
S/N Ratio at 500 Hz	0.6984	0.0231	0.6984	0.0231	1.0840	0.0363	1.0953	0.0362
S/N Ratio at 1 kHz	0.9629	0.0295	0.9748	0.0298	1.9676	0.0605	1.9299	0.0590
S/N Ratio at 2 kHz	0.7990	0.0284	0.7990	0.0284	1.1847	0.0421	1.0704	0.0382
S/N Ratio at 4 kHz	0.7333	0.0268	0.7333	0.0268	0.9791	0.0450	1.0969	0.0503
S/N Ratio at 8 kHz	0.7276	0.0314	0.7254	0.0316	1.6072	0.0968	1.6063	0.0966

Each pre-processed neuron is multiplied by a scalar weight connecting the first layer neurons to the hidden layer neurons. At each neuron within the hidden layer, the weighted inputs are summed and a bias value is subtracted from the summed weighted inputs. The resulting value is passed through a non-linear activation function which in this work is a sigmoidal logistic function ($1 / (1 + e^{-x})$, where x is the resulting value). Table 4.3 provides the weights and biases linked to hidden neurons of each trained ANN model.

Table 4.3 Weights and biases to hidden neurons of each ANN model

	ANN Model for Predicting Intelligibility Scores			ANN Model for Predicting Intelligibility Threshold			ANN Model for Predicting Cadence Threshold			ANN Model for Predicting Audibility Threshold		
	h1#01	h1#02	h1#03	h1#01	h1#02	h1#03	h1#01	h1#02	h1#03	h1#01	h1#02	h1#03
Bias	11.5184	3.4952	2.4780	4.7585	21.0361	23.6038	21.3096	23.4213	0.0453	1.6085	20.0568	0.8694
S/N Ratio at 250 Hz	1.1366	1.4757	0.7391	2.3090	4.7684	20.5849	20.6167	22.5940	0.9785	3.0270	4.2765	21.6642
S/N Ratio at 500 Hz	10.5723	2.7610	4.5765	2.9866	20.8594	24.8108	20.7203	21.2851	0.3082	1.9515	2.4088	21.6567
S/N Ratio at 1 kHz	20.2854	4.9302	7.2539	3.1024	22.6401	29.3399	21.8440	20.1070	0.4341	21.3097	0.1111	1.1948
S/N Ratio at 2 kHz	8.0602	1.3246	1.8921	2.1874	1.4327	21.4269	1.0129	24.0315	2.1161	4.1976	1.1180	21.7192

	ANN Model for Predicting Intelligibility Scores			ANN Model for Predicting Intelligibility Threshold			ANN Model for Predicting Cadence Threshold			ANN Model for Predicting Audibility Threshold		
	h1#01	h1#02	h1#03	h1#01	h1#02	h1#03	h1#01	h1#02	h1#03	h1#01	h1#02	h1#03
S/N Ratio at 4 kHz	2.0982	2.0439	20.0099	2.4986	0.7054	20.0970	2.5294	26.9358	2.9931	6.7447	1.3925	23.6152
S/N Ratio at 8 kHz	1.1966	21.0482	22.9519	1.5709	2.3245	20.1919	21.8705	3.6446	20.4777	23.5032	20.2028	2.2250

The output value of each hidden neuron is multiplied by the scalar weights for each connection between the hidden layer and the output neuron. The weighted outputs are summed and a bias value is subtracted from the sum to produce a single output value. Table 4.4 shows the weights and biases linked to the output neuron of each trained ANN model.

Table 4.4 Weights and biases to the output neuron of each ANN model

	ANN Model for Predicting Intelligibility Scores	ANN Model for Predicting Intelligibility Threshold	ANN Model for Predicting Cadence Threshold	ANN Model for Predicting Audibility Threshold
	Output (Intelligibility Scores)	Output (Intelligibility Threshold)	Output (Cadence Threshold)	Output (Audibility Threshold)
Bias	0.0086	-0.6521	-1.5510	-0.9244
h1#01	0.5257	2.2279	-0.0603	2.8098
h1#02	1.5923	-1.8808	-1.2885	-2.7274
h1#03	-1.1333	1.0384	-0.4996	1.1762

The output is post-processed by subtracting the shift factor, followed by division by the scale factor. In the present work, the shift factor and scale factor are 0 and 1 respectively in all the four situations as the range of outputs has already been normalised between 0 and 1 in the original database.

A more detailed numerical description of the modus operandi of an ANN can be found in Section 2.2 of the present thesis.

4.6 STATISTICAL RESULTS OF ANN ANALYSIS

Table 4.5 presents the statistical analysis results based on the ANN models specified in the above section. In Table 4.5, the numbers in parentheses are the results based on the work of Gover and Bradley (2004). In a regression problem, the standard deviations (SD) of both the prediction error and original output data are important and they can be related by the standard deviation ratio (SDR). The SDR in a regression problem is the ratio of the SD of the prediction error to that of the original output data (an SDR of 0.1 is considered an excellent fit of the data and an SDR of 1.0 is a poor fit) (Statsoft, 1999). The correlation coefficients R^2 (the "coefficient of determination") of the ANN predictions over the entire data sets for the intelligibility scores, intelligibility threshold, cadence threshold and audibility threshold were 0.773, 0.929, 0.967 and 0.942 respectively. For comparison, in the work of Gover and Bradley (2004), the SII-weighted S/N measure has an R^2 of 0.762 for predicting the intelligibility scores and an R^2 of 0.919 for predicting the intelligibility threshold and the S/N loudness ratio has an R^2 of 0.956 for predicting the cadence threshold and an R^2 of 0.899 for predicting the audibility threshold.

Table 4.5 Statistical analysis results for ANN predictions

	ANN Model for Predicting Intelligibility Scores				ANN Model for Predicting Intelligibility Threshold				ANN Model for Predicting Cadence Threshold				ANN Model for Predicting Audibility Threshold			
	Tr[a]	Ve[b]	Te[c]	En[d]	Tr[a]	Ve[b]	Te[c]	En[d]	Tr[a]	Ve[b]	Te[c]	En[d]	Tr[a]	Ve[b]	Te[c]	En[d]
RMS error	0.205	0.208	0.208	0.206	0.116	0.098	0.104	0.111	0.079	0.056	0.072	0.076	0.096	0.089	0.033	0.091
Error SD[e]	0.205	0.208	0.208	0.206	0.117	0.099	0.105	0.111	0.079	0.049	0.067	0.077	0.096	0.088	0.034	0.091
SDR.[f]	0.477	0.476	0.475	0.476	0.280	0.246	0.244	0.267	0.192	0.115	0.139	0.183	0.254	0.211	0.096	0.240
R^2	0.773	0.773	0.774	0.773 (0.762)	0.921	0.940	0.941	0.929 (0.919)	0.963	0.987	0.982	0.967 (0.956)	0.936	0.958	0.992	0.942 (0.899)

[a]Tr = training data set.
[b]Ve = verification data set.
[c]Te = test data set.
[d]En = entire data set.
[e]Error SD = standard deviation of the prediction error.
[f]SDR = standard deviation ratio.

4.7 DISCUSSIONS AND CONCLUSIONS

The present work indicates that the ANN approach provides a direct and accurate method for predicting speech intelligibility scores and security thresholds. The current method for predicting speech intelligibility and privacy first requires the development of an index and then requires the index to be related to subjective scores using a transfer function (ANSI, 1969; ANSI, 1997; Gover and Bradley, 2004). The ANN approach can avoid this two step process by using the signal-to-noise (S/N) ratio information to directly predict the subjective speech intelligibility score and security thresholds. Compared with the previous work (Gover and Bradley, 2004) that used one-third-octave band S/N ratios, the ANN approach used only the "octave band" S/N ratios and performed comparably for the predictions of the intelligibility score, the intelligibility threshold and the cadence threshold, and better for the prediction of the audibility threshold.

Specifics of the ANN models for predicting the speech security and intelligibility scores were also provided in the present work. With this information, ANN models can be embedded into standard spreadsheet applications, thus allowing predictions to be made in a transparent and direct fashion.

Similar investigations using one-third-octave band (160 Hz – 8000 Hz) S/N ratios have also been conducted in the present work. Table A.1 – Table A.5 in Appendix A show the specifics and statistical analysis results of the ANNs using one-third-octave band (160 Hz – 8000 Hz) S/N ratios as the inputs. However, the statistical results of the one-third-octave band analysis were only slightly better than those of the octave band analysis. This may be due to the information in adjacent one-third-octave bands being highly correlated and therefore not contributing any significant new information to the ANN.

The present work only takes into account the S/N ratios in predicting the architectural speech intelligibility score and security thresholds. Other factors, such as talker gender and voice characteristics, speech material, room characteristics and so on, could be

included in the ANN models to investigate the possibility of further improving the prediction accuracy.

REFERENCES FOR CHAPTER 4

- ANSI, 1969. *S3.5-1969 American national standard methods for the calculation of the articulation index.* American National Standards Institute, New York, NY.
- ANSI, 1997. *S3.5-1997 American national standard methods for calculation of the speech intelligibility index.* American National Standards Institute, New York, NY.
- ASTM, 2002. *E1130-02e1 Standard test method for objective measurement of speech privacy in open offices using articulation index.* ASTM International, West Conshohocken, PA.
- Gover B.N. and Bradley J.S., 2004. "Measures for assessing architectural speech security (privacy) of closed offices and meeting rooms," *Journal of the Acoustical Society of America*, 116, pp 3480-3490.
- StatSoft, 1999. *STATISTICA neural networks version 4.0A manual.* StatSoft Inc, Tulsa, OK.
- Subjective Measurements Subcommittee of the Standards Committee of IEEE Audio and Electroacoustics Group, 1969. "IEEE recommended practice for speech quality measurements," *IEEE transactions on audio and electroacoustics*, 17, pp 225-246.

CHAPTER 5

OPTIMISING THE DESIGN OF FLAT-WALLED MULTI-LAYERED ANECHOIC LININGS USING EVOLUTIONARY ALGORITHMS

5.1 INTRODUCTION

The concept of flat-walled multi-layered absorbent linings for anechoic rooms was proposed three decades ago. Flat-walled linings have the advantage of being less complicated and, hence, less costly to manufacture and install than the individual units such as wedges. Recently, flat-walled multi-layered absorbent linings were also applied as the anechoic termination for other types of enclosures, such as the duct-type noise measurement enclosure (Bracciali and Cascini, 2000), which required anechoic conditions for their internal surfaces.

An ideal acoustic absorbent material should have a low frontal acoustic reflection and a high internal acoustic attenuation. However, these two requirements for the same material are in conflict with each other. A method of partially overcoming this conflict is to use a multi-layered lining system (Dunn and Davern, 1986). Davern (1980) carried out work on the design of flat-walled multi-layered anechoic linings as an alternative to the more conventional wedge-type system. The approach taken was to use conventional measurements in an impedance tube. Davern's measurements indicated that a flat-walled, multi-layered, graded density lining could achieve anechoic conditions with an overall thickness slightly less than a quarter of a wavelength at the cut-off frequency, e.g. 0.727 m, at 110 Hz. However, the work (Davern, 1980) proved to be tedious and time consuming because of the numerous trial and error measurements involved.

The subsequent work undertaken by Dunn and Davern (1986) demonstrated that the overall impedance of a flat-walled multi-layered system could be calculated by the repeated application of a single layer impedance equation. They also demonstrated that the direct calculation approach could be readily programmed on a desktop computer and

good agreement between measured (impedance tube) and calculated values could be achieved.

The ability to rapidly test potential layer combinations using a computer has marked advantages over repeated impedance tube measurements. Nonetheless, a problem remained unsolved: how to efficiently optimise the design of a flat-walled multi-layered lining; more specifically, how to efficiently find a lining composite (a combination of materials) that could achieve the target cut-off frequency with a minimum overall thickness, where there exists a large pool of materials.

A cut-off frequency is the frequency above which no pressure reflections exceed 10 per cent; this corresponds to an energy absorption exceeding 99 per cent (Beranek and Sleeper, 1946). As implied by the above definition, the design of an anechoic lining can be considered as a multi-objective optimisation problem (MOP) (see chapter 3 of this thesis for more details of MOP), which is one of the major difficulties that the designers of anechoic linings face when the optimisation of a design is required.

This chapter demonstrates that a multi-objective evolutionary algorithm (EA) can be successfully employed as an optimiser to aid and speed up the design of flat-walled multi-layered anechoic linings. Two types of materials, fully-reticulated (open-cell) polyurethane foams and fibrous building insulation material, are investigated. The investigation of fibrous building insulation material is shown in the form of an application case, in which the effectiveness of EAs for solving combinatorial-type problems featuring discontinuous decision space is also illustrated.

5.2 FUNDAMENTAL EQUATIONS

The normal incidence acoustic impedance, Z_1, at the front of a layer of homogeneous material of thickness L can be calculated using the following equation (Zwicker and Kosten, 1949):

$$Z_1 = W\frac{Z_0\cosh(\gamma L)+W\sinh(\gamma L)}{Z_0\sinh(\gamma L)+W\cosh(\gamma L)}, \tag{5.1}$$

where Z_0 is the backing impedance of the layer, W is the characteristic impedance of the layer and γ is its propagation constant. Both W and γ are complex and frequency dependent. When the material has a solid backing ($Z_0 = \infty$), the single layer equation can be written as (Dunn and Davern, 1986)

$$Z_1 = W_1\coth(\gamma_1 L_1). \tag{5.2}$$

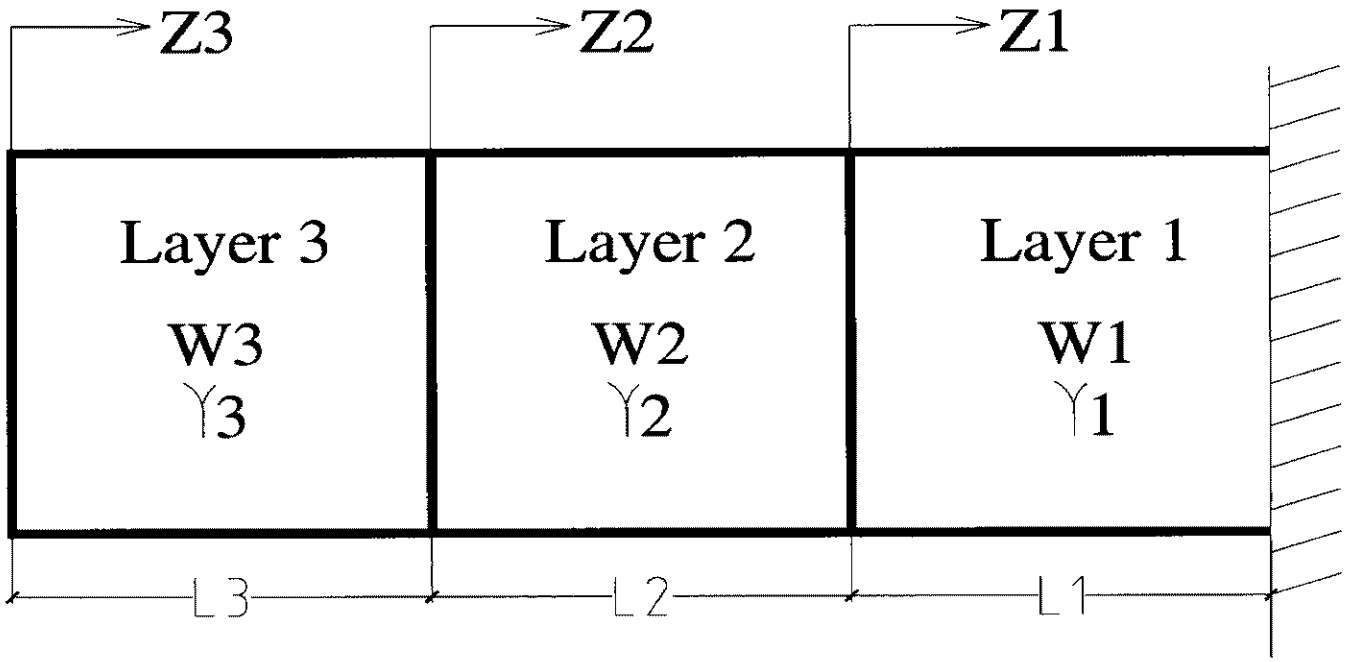

Figure 5.1 Illustration of a multi-(three-)layered system.

The impedance at the front of a composite layered material (Figure 5.1), Z_i, can be calculated by applying the single-layer equation to each material successively (Dunn and Davern, 1986), that is,

$$Z_i = W_i\frac{Z_{i-1}\cosh(\gamma_i L_i)+W_i\sinh(\gamma_i L_i)}{Z_{i-1}\sinh(\gamma_i L_i)+W_i\cosh(\gamma_i L_i)}, \tag{5.3}$$

where the subscript i refers to the i-th layer, starting from layer 1 that is closest to solid backing.

The pressure reflection factor at normal incidence, r, is the ratio of the pressure amplitude of the reflected wave to the incident wave in the reference plane for a plane wave at normal incidence and can be calculated by the following equation (ISO, 1996):

$$r = \left| \frac{Z_i / \rho c - 1}{Z_i / \rho c + 1} \right|, \tag{5.4}$$

where ρ is the air density and c is the velocity of sound in air. The relationship between r and the normal incidence sound absorption coefficient α_n (ISO, 1996) is

$$\alpha_n = 1 - r^2 . \tag{5.5}$$

Furthermore, the absolute value of the characteristic impedance W is related to r by the following equation (Dunn and Davern, 1986):

$$\left| \frac{W}{\rho c} \right| = \frac{1 + r}{1 - r} . \tag{5.6}$$

The propagation constant γ is expressed as (Dunn and Davern, 1986)

$$\gamma = \alpha + j\beta , \tag{5.7}$$

where j is $\sqrt{-1}$, α is the attenuation constant and β is the wave number that is related with the acoustic wave velocity v in the material at frequency f by the following equation (Dunn and Davern, 1986):

$$\beta = \frac{2\pi f}{v} . \tag{5.8}$$

v equals c when the acoustic wave is propagated in the air.

Hence, in the present work, the average quarter wavelength λ_a at frequency f in an N-layered lining composite can be calculated by

$$\lambda_a = \frac{1}{4}\times\frac{v_a}{f} = \frac{1}{4f}\times\frac{L_1 + L_2 + \cdots + L_N}{t_o} = \frac{1}{4f}\times\frac{\sum_{i=1}^{N} L_i}{\frac{L_1}{v_1} + \frac{L_2}{v_2} + \cdots \frac{L_N}{v_N}} = \frac{\sum_{i=1}^{N} L_i}{4f\sum_{i=1}^{N}\frac{L_i}{v_i}}, \qquad (5.9)$$

where v_a is the average sound wave velocity in the multi-layered lining composite and t_o is the overall time that it takes the sound wave to pass the multi-layered lining composite.

Equation (5.3) can also easily handle the particular case where any of the layers is a simple air space. The propagation constant γ and characteristic impedance W of an air space can be expressed as (Lee and Chen, 2001)

$$\gamma = j\beta_{air}, \qquad (5.10)$$

and

$$W = \rho c. \qquad (5.11)$$

When an air space is backed by a solid surface ($Z_0 = \infty$), the surface impedance of the air space can be expressed as (Lee and Chen, 2001)

$$Z_1 = -j\rho c\cot(\beta_{air}L). \qquad (5.12)$$

5.3 OPTIMISER

Throughout this chapter, a Genetic and Evolutionary Algorithm Toolbox for Use with Matlab (GEATbx) (Pohlheim, 2004), incorporating Multi-Objective Genetic Algorithm (MOGA) (Fonseca and Fleming, 1993; 1998), is applied as the optimiser to aid and speed

up the design of the flat-walled multi-layered anechoic linings. See chapter 3 of the present thesis for more details of EAs, MOGA and GEATbx.

5.4 APPLICATION OF FULLY-RETICULATED (OPEN-CELL) POLYURETHANE FOAMS

All materials investigated in the early work (Davern, 1980; Dunn and Davern, 1986) on flat-walled multi-layered anechoic linings were fully-reticulated (open-cell) polyurethane plastic foams. Those materials do not have small fibres and have lower susceptibility to mechanical damage than fibrous materials. Detailed research of this type of material can be found in the work of Cummings and Beadle (1993).

Dunn and Davern (1986) studied 3 foams with steady flow resistivity in the range 380 – 3200 SI rayl/m (Table 5.1) and reported the Delany and Bazley (1970) type curve-fitting equations for predicting the bulk acoustic properties, W and γ, that is,

$$W = \rho c\left[1 + 0.114(\rho f/\sigma)^{-0.369} + j\left(-0.0985(\rho f/\sigma)^{-0.758}\right)\right], \tag{5.13}$$

$$\gamma = (2\pi f/c)\left[0.168(\rho f/\sigma)^{-0.715} + j\left(1 + 0.136(\rho f/\sigma)^{-0.491}\right)\right], \tag{5.14}$$

where, f is the frequency and σ is the flow resistivity. For normalisation purposes, a value of 1.2 kg/m^3 was used for air density and 340 m/s for sound velocity. The Delany and Bazley (1970) type curve-fitting equations are discussed in more detail in chapter 6 of the present thesis.

Table 5.1 Measured values of steady flow resistivity in the work of Dunn and Davern (1986)

Foam Identity	Notional Number of Pores/Linear Inch	Flow Resistivity (SI rayl/m)
A	45	380
B	60	1340
C	80	3200

Similar curve-fitting equations for predicting the bulk acoustic properties, W and γ, of the same type of material but with a wider range of flow resistivity 60 – 6229 SI rayl/m (Table 5.2) were reported in the work of Cummings and Beadle (1993) as follows:

$$W = \rho c\left[1 + 0.0953(\rho f/\sigma)^{-0.491} + j\left(-0.0986(\rho f/\sigma)^{-0.665}\right)\right], \tag{5.15}$$

$$\gamma = (2\pi f/c)\left[0.167(\rho f/\sigma)^{-0.636} + j\left(1 + 0.174(\rho f/\sigma)^{-0.372}\right)\right]. \tag{5.16}$$

Table 5.2 Measured values of steady flow resistivity in the work of Cummings and Beadle (1993)

Notional Number of Pores/Linear Inch	Flow Resistivity (SI rayl/m)
10	60
16	79
21	176
29	287
33	356
42	671
45	816
58	1724
65	2184
72	3085
87	5745
100	6229

Equations (5.13) – (5.16) indicate that a large flow resistivity value will result in large attenuation, but at the same time, it will cause a high frontal reflection. A method of partially overcoming this conflict is to use a multi-layered lining system. By selecting a front layer material with appropriate characteristic impedance, one can obtain a low primary reflection by encouraging the incoming wave train to enter the composite layer structure. Then the inner layers of material can be selected to attenuate the wave energy within the material as much as possible without, at the same time, causing a substantial interlayer reflection (Dunn and Davern, 1986).

High correlation coefficients of the curve-fitting equations have been observed in both Dunn and Davern (1986) and Cummings and Beadle (1993). Good agreement between the measured (impedance tube) overall impedance of a flat-walled multi-layered system and calculated values using the multi-layered impedance equation and the curve-fitting equations for predicting bulk acoustic properties has also been shown in Dunn and Davern (1986). This supports the idea that the design of flat-walled multi-layered linings can be undertaken on a desktop computer.

However, it is not advisable to use the curve-fitting equations for predicting bulk acoustic properties beyond the range of the experimental data (Cummings and Beadle, 1993). The most serious consequence of extrapolation is in the case of predictions at low frequencies. See Section 6.2.2 of the present thesis for more detailed discussions. The lowest frequency at which measurements were conducted in Davern (1980), Dunn and Davern (1986) and Cummings and Beadle (1993) was 100 Hz.

5.4.1 Optimisation Procedure

This section explains the optimisation procedure for a flat-walled multi-layered anechoic lining that uses a three-layered lining system composed of fully-reticulated (open-cell) polyurethane plastic foams and targets a cut-off frequency of 100 Hz. It is considered that frequencies below 1000 Hz are the most critical in the design of anechoic linings and thus the EA search is limited to one-third-octave band frequencies between 100 and 1000 Hz.

5.4.1.1 Design criterion

Two scenarios are considered:

Scenario 1: Min $y = (r_{100}(\boldsymbol{x}), r_{125}(\boldsymbol{x}), \cdots, r_{1000}(\boldsymbol{x}), L_{overall})$

$$\text{subject to } \boldsymbol{x} = (L_1, \cdots, L_m, \delta_1, \cdots, \delta_m) \in X,$$

$$y = (y_1, \cdots, y_m) \in Y, \tag{5.17}$$

where the subscripts $(100,125,\cdots,1000)$ are the centre frequencies of a third-octave spectrum; r is the pressure reflection factor at each corresponding frequency; L and δ

are respectively the thickness and the flow resistivity of each layer; m is the number of layers; $L_{overall} = L_1 + \cdots + L_m$ is the overall thickness of the multi-layered system; $\boldsymbol{x}$ is called the decision vector; X is the parameter space; $\boldsymbol{y}$ is the objective vector; and Y is the objective space. The parameter space X may vary during the design process according to the design requirement.

The goal vector of this scenario is

$$\boldsymbol{g} = \left(g_{100}, g_{125}, \cdots, g_{1000}, g_{L_{overall}}\right), \tag{5.18}$$

where the goal values for $(r_{100}(\boldsymbol{x}), r_{125}(\boldsymbol{x}), \cdots, r_{1000}(\boldsymbol{x}))$ are $g_{100} = g_{125} = \cdots = g_{1000} = 10\%$, which are regarded as hard goals, namely, the pressure reflection over 10% at any frequency is not acceptable. The goal value for the overall thickness of the system $g_{L_{overall}}$ is soft and may vary during the design process. The three cases, Case A, Case B and Case C, presented in the Section 5.4.1.4.1 are examples of Scenario 1.

Scenario 2: Min $\boldsymbol{y} = (r_{100}(\boldsymbol{x}), r_{125}(\boldsymbol{x}), \cdots, r_{1000}(\boldsymbol{x}))$

$$\text{subject to } \boldsymbol{x} = (L_1, \cdots, L_m, \delta_1, \cdots, \delta_m) \in X \wedge \left(L_1 +, \cdots, +L_m = L_{overall\_fixed}\right),$$

$$\boldsymbol{y} = (y_1, \cdots, y_m) \in Y. \tag{5.19}$$

In this scenario the overall thickness of the system is set to a fixed value $L_{overall\_fixed}$. The goal vector of this scenario is

$$\boldsymbol{g} = \left(g_{100}, g_{125}, \cdots, g_{1000}\right), \tag{5.20}$$

where $g_{100} = g_{125} = \cdots = g_{1000} = 10\%$ and has to be reached at the end of the design. This scenario can be a situation where the overall thickness of a certain multi-layered lining system, which meets the design criterion of the anechoic lining, is known due to some

prior knowledge, and where the designer wants to know the possible compositions of the system. Case D presented in Section 5.4.1.4.2 is an example of Scenario 2.

5.4.1.2 Constraint handling

The definitions of the above two scenarios indicate that the first scenario is only constrained by the bounds on the decision variables $(L_1,\cdots,L_m,\delta_1,\cdots,\delta_m)$. However, in addition to the bounds on the decision variables, the second scenario is also constrained by a linear relationship $(L_1+,\cdots,+L_m = L_{overall\_fixed})$.

The constraint imposed by bounds on the decision variables can be simply handled by mapping the search space to minimise the number of infeasible solutions it contains, while that imposed by the linear relationship $(L_1+,\cdots,+L_m = L_{overall\_fixed})$ is handled by converting it to a penalty function and adding it to the objective function before fitness is computed, that is,

$$r = \left|\frac{Z_i/\rho c - 1}{Z_i/\rho c + 1}\right| + \kappa\left|(L_1+,\cdots,+L_m) - L_{overall\_fixed}\right|, \tag{5.21}$$

where κ is a scalar factor used to tighten or loosen the constraint. As the acceptable range of r is $0 \le r \le 10\%$, the maximum violation of the constraint $\left|(L_1+,\cdots,+L_m) - L_{overall\_fixed}\right|$ is limited to 0.01 m when the scalar factor κ is set to 1000.

Penalty functions provide a way of guiding the search toward feasible solutions but they are problem dependant. Guidelines for applying penalty functions to handle constraints and the introduction of some other constraint handling techniques can be found in chapter 3 of this thesis.

5.4.1.3 Parameter settings of GEATbx

For every operation of the EA using GEATbx, the settings for some of the relevant parameters were as follows:

- representation of variables: real value since the bulk acoustic properties of the material are calculated using Equations (5.13) – (5.16) and it is assumed that any required thickness of the material is available.
- fitness assignment: multi-objective rank-based fitness assignment (Fonseca and Fleming, 1993; 1998). See chapter 3 of this thesis for more details.
- evolutionary operator for selection: stochastic universal sampling (SUS) (Baker, 1987) which works on both real-value and integer-value data representation. Using this selection method, the individuals in the population are mapped onto contiguous segments of a line, such that each individual's segment is equal in length to its fitness. Equally spaced pointers, as many as the number of individuals to be selected, are placed along the line. This selection method has the advantage of providing zero bias and minimum spread during the selection.
- evolutionary operator for recombination: discrete recombination (Mühlenbein and Schlierkamp-Voosen, 1995) which performs an exchange of variable values between the parents. For each variable position of the offspring, the parent contributing its variable to the offspring is chosen randomly with equal probability. Discrete recombination can be applied to all (real-value, integer-value and binary-value) variable representations.
- recombination rate: 1. This means all parents have the possibility of contributing to the value of each variable of the offspring.
- evolutionary operator for mutation: real-value mutation function (Pohlheim, 2004).
- mutation rate: 1. This means that, on average, 1 variable per individual is to be mutated.
- mutation range: 0.02. This means the initial mutation step sizes will be 0.02 times the domain of each variable.
- population size: 100. This means there are 100 individuals (solutions) per population.

- generation gap: 0.9. This means 90% of the population to be reproduced every generation.
- termination method: maximum number of generations which is set 100. This means the maximum number of generations an optimisation runs is 100 and when this number is reached the optimisation terminates.

All the other internal parameters necessary for operating GEATbx were set to their default values. Details of these parameters and guidelines for setting them can be found in Pohlheim (2004). The initial population was generated randomly by the program. The computer (a desktop PC with Intel® P4 processor and 256 Mb RAM) time for each operation with the above set of parameters varied from 60 seconds to 100 seconds depending on the complexity of the search task. The non-dominated set yielded by each operation – which provided the decision maker (DM) with insight into the characteristics of the problem – was saved in a standard spreadsheet. Ten operations were conducted before any decision was made.

5.4.1.4 Searching process

The searching process for the optimum results of the two scenarios previously introduced in Section 5.4.1.1 is shown below.

5.4.1.4.1 First scenario optimisation

Three cases were involved in the first scenario optimisation. In Case A, three materials originally investigated by Davern (1980) were chosen for the construction of the multi-layered lining system; in Case B, the materials with the steady flow resistivity in the range of 380 – 3200 SI rayl/m (Dunn and Davern, 1986) were considered; and in Case C, the materials considered had a greater steady flow resistivity in the range of 60 – 6229 SI rayl/m (Cummings and Beadle, 1993).

As introduced in chapter 3 of this thesis, the searching process using MOGA is an interactive and progressive process between the DM and the algorithm. The process begins with the prior information based on the work of Davern (1980).

As previously mentioned, Davern (1980) showed that a flat-walled, multi-layered, anechoic lining, with Foam C as Layer 1 (against the solid back), foam B as Layer 2 (the mid layer) and Foam A as Layer 3 (the front layer), can achieve a cut-off frequency of 110 Hz with overall thickness of the system, 0.727 m, slightly less than a quarter of a wavelength in the air at the cut-off frequency.

Case A:

On the basis of the prior information, the decision space was set to δ_1=3200 SI rayl/m, δ_2= 1340 SI rayl/m, δ_3=380 SI rayl/m, and 0.001 m$\leq L_1, L_2, L_3 \leq$ 0.85 m. The goals were set to $g_{100} = g_{125} = \cdots = g_{1000} = 10\%$, and $g_{L_{overall}}$ =0.85 m. 0.85 m corresponds to a quarter of the wavelength in the air at the cut-off frequency of 100 Hz. The minimum thickness was set to 0.001 m to avoid the 'divided by zero' type error. All solutions, provided by the EA and meeting the anechoic lining design criterion, namely the goals set for g_{100} to g_{1000}, are shown on Figure 5.2. The minimum overall thickness of the system provided by this set of solutions was 0.802 m, which indicated that the goal set for $g_{L_{overall}}$ was slightly over-attained. Hence, the goal for $g_{L_{overall}}$ was reset to 0.8 m.

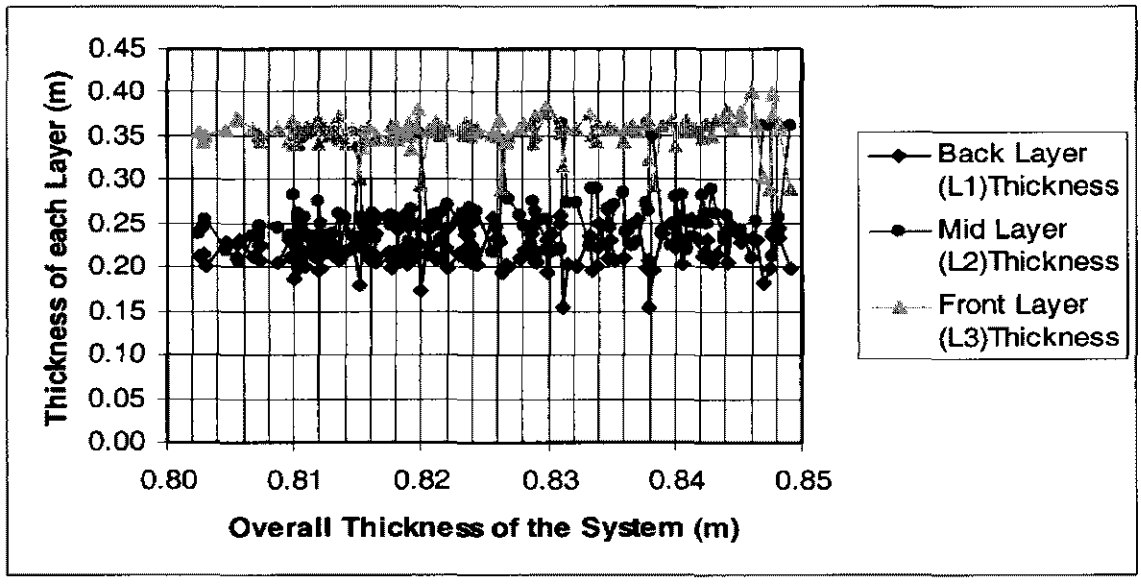

Figure 5.2 Search results of Case A. Thickness of each layer vs. overall thickness of the system.

The EA was repeated with the tightened goal for $g_{L_{overall}}$. However, no solution was found by the EA with less overall thickness. Hence it was decided that the EA had found the optimum solutions for Case A. Other preferable solutions may exist. However, they are probably more difficult to find given the encoding structure for the chromosomes and the associated genetic operators.

Case B:

It was assumed that the curve-fitting equations, Equations (5.13) and (5.14), for predicting the bulk acoustic properties of fully reticulated polyurethane plastic foams developed by Dunn and Davern (1986) could be used not only for the three materials listed in Table 5.1 but also for the same type of materials with steady flow resistivity in the range of 380 – 3200 SI rayl/m. The decision space in this case was set to 380 SI rayl/m $\leq \delta_1, \delta_2, \delta_3 \leq$ 3200 SI rayl/m and 0.001 m $\leq L_1, L_2, L_3 \leq 0.85$ m. The goals were set to $g_{100} = g_{125} = \cdots = g_{1000} = 10\%$, and $g_{L_{overall}}$ = 0.8 m. With the goal $g_{L_{overall}}$ set to 0.8 m, it was hoped that the EA could find solutions with overall thicknesses less than the minimum overall thickness, 0.802 m (found in Case A). The minimum overall thickness of the system found by EA in this case was 0.79 m. The solutions that meet the anechoic lining design criterion and have the overall thicknesses between 0.79 m and 0.802 m are shown in Figure 5.3.

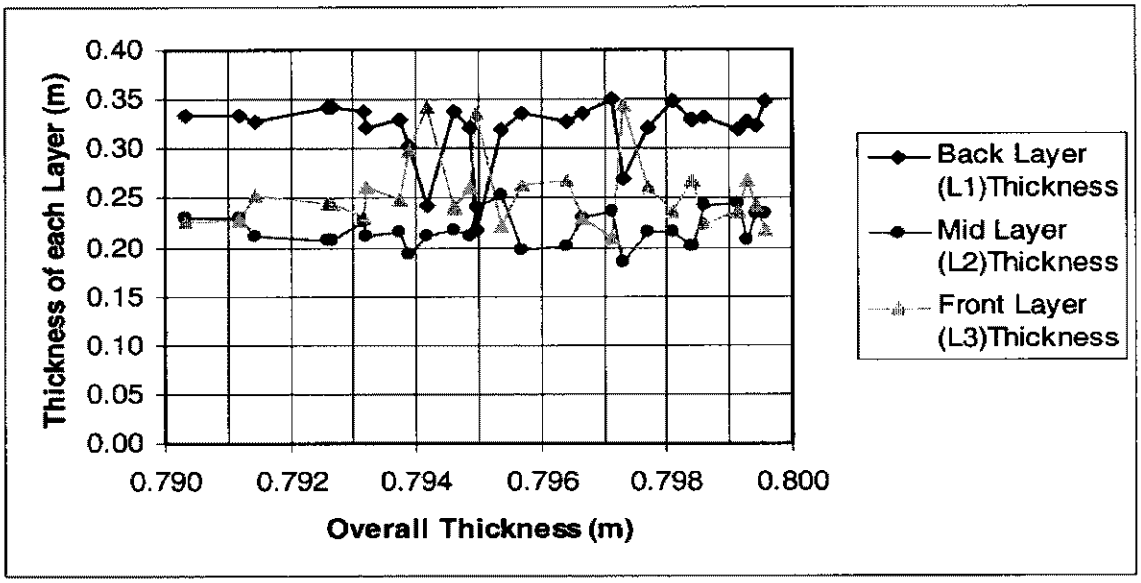

(a)

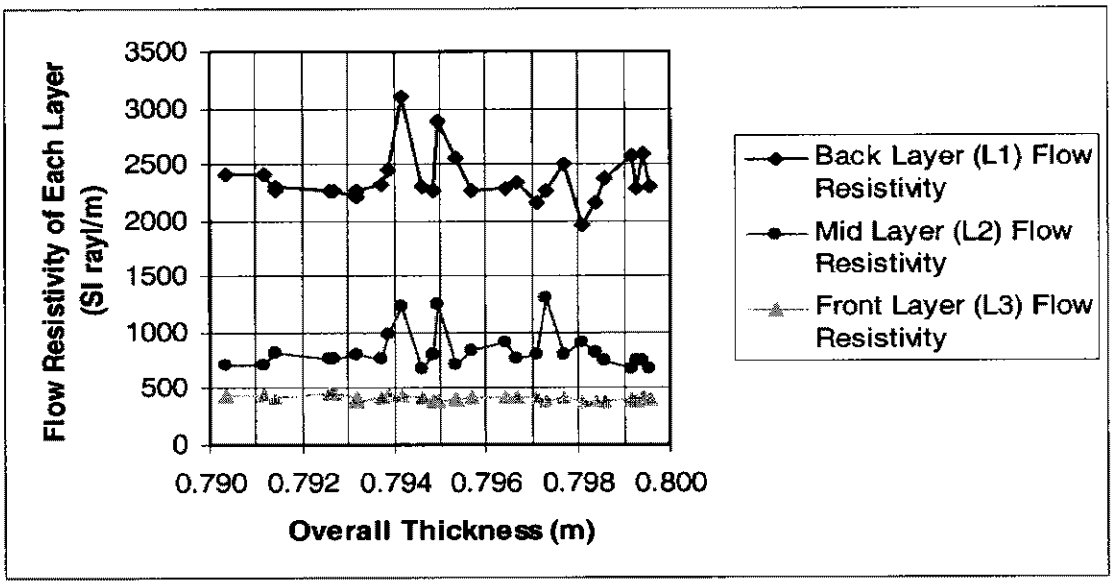

(b)

Figure 5.3 Search results of Case B. (a) Thickness of each layer vs. overall thickness of the system. (b) Steady flow resistivity of each layer vs. overall thickness of the system.

The goal for $g_{L_{overall}}$ was also set to 0.7 m, 0.75 m and 0.79 m. However, no solution was found by the EA with the overall thickness less than 0.79 m.

Case C:

Cummings and Beadle (1993) investigated the same type of fully reticulated polyurethane plastic foam materials but with a wider range of flow resistivity, 60 – 6229 SI rayl/m (Table 5.2), and developed similar curve-fitting Equations (5.15) and (5.16). In this case, in lieu of Equations (5.13) and (5.14), Equations (5.15) and (5.16) were used for predicting the bulk acoustic properties. Correspondingly the decision space in this case was set to 60 SI rayl/m $\leq \delta_1, \delta_2, \delta_3 \leq$ 6229 SI rayl/m and 0.001 m $\leq L_1, L_2, L_3 \leq$ 0.85 m. The goals were set to $g_{100} = g_{125} = \cdots = g_{1000} = 10\%$, and $g_{L_{overall}}$ = 0.8 m. It was hoped that with a greater choice of materials, solutions with less overall thickness could be found. The results produced by the first few operations of EA indicate that an overall thickness as thin as 0.61 m, slightly less than a fifth of the wave length at 100 Hz, was achievable. By further gradually tightening the goals for $g_{L_{overall}}$ from 0.68 m (a fifth of

the wave length at 100 Hz) to 0.57 m (a sixth of the wave length at 100 Hz), the minimum overall thickness found by the EA was 0.529 m. The solutions that meet the anechoic lining design criterion and have the overall thickness between 0.529 m and 0.68 m are shown in Figure 5.4. Table 5.3 presents the solution with the minimum overall thickness, 0.529 m, and Table 5.4 shows the corresponding pressure reflection factor at the frequencies from 100 to 1000 Hz.

Table 5.3 The solution with the minimum overall thickness (0.529m)

BackLayer (L1) Thickness (m)	MidLayer (L2) Thickness (m)	FrontLayer (L3) Thickness (m)	BackLayer (L1) Flow Resistivity (SI rayl/m)	MidLayer (L2) Flow Resistivity (SI rayl/m)	FrontLayer (L3) Flow Resistivity (SI rayl/m)
0.121	0.153	0.255	6188	1707	417

Table 5.4 Corresponding pressure reflection factors (%) of the solution with the minimum overall thickness (0.529m)

100 Hz	125 Hz	160 Hz	200 Hz	250 Hz	315 Hz	400 Hz	500 Hz	630 Hz	800 Hz	1000 Hz
9.941	1.409	6.318	9.876	8.533	1.677	7.410	9.026	4.501	7.181	5.155

In the above interactive and progressive optimisation process, goals were supplied interactively at each EA operation. The DM could then reduce the size of the solution set gradually while learning about the trade-off between objectives. The variability of the goals acts as a changing environment to the EA. A more general introduction of interactive and progressive articulation optimisation process and its advantages and disadvantages can be found in chapter 3 of this thesis.

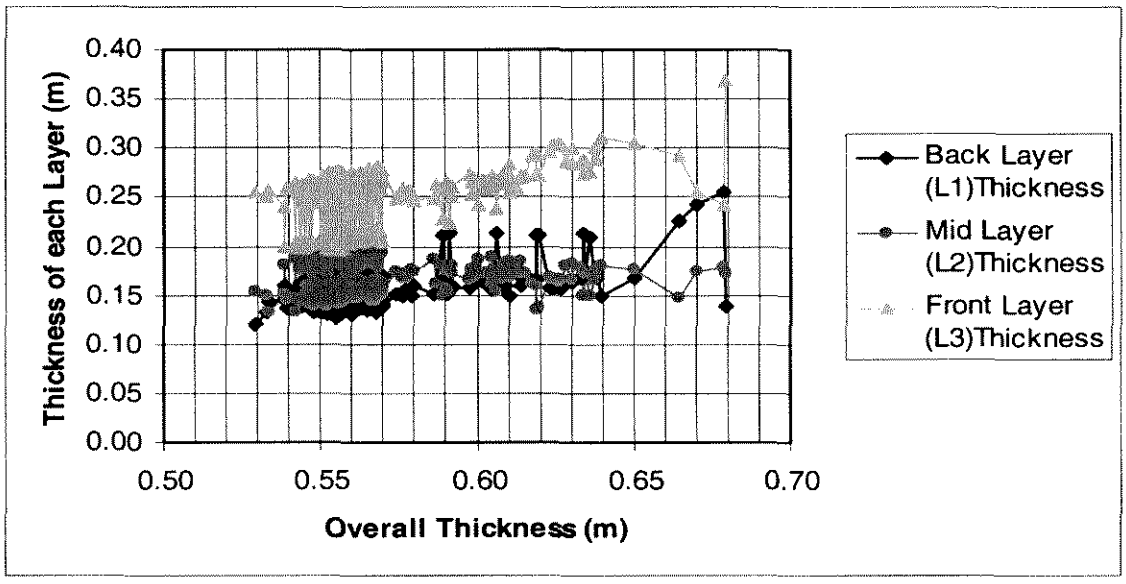

(a)

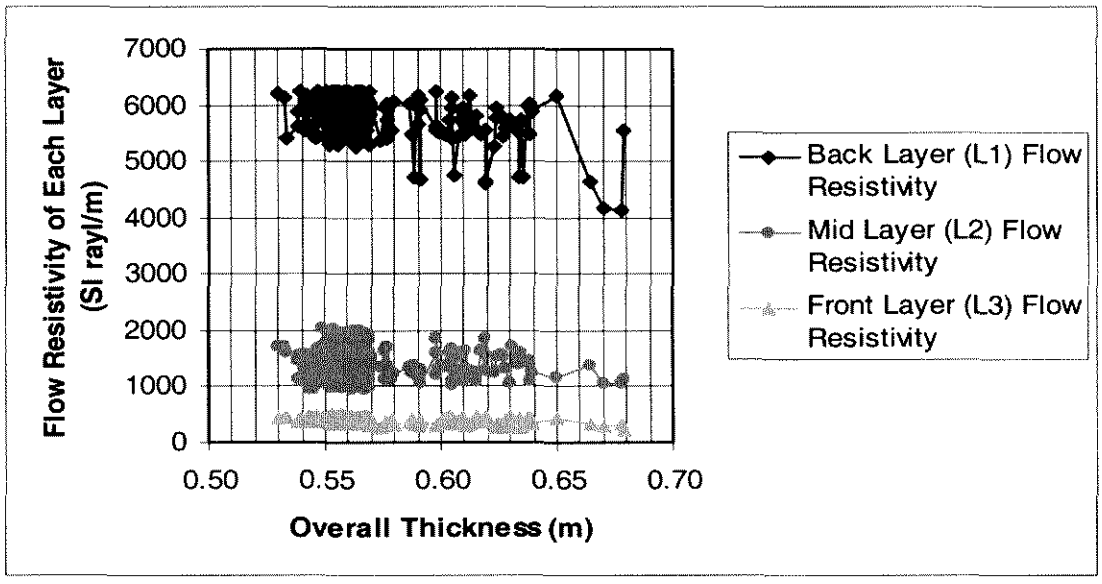

(b)

Figure 5.4 Search results of Case C. (a) Thickness of each layer vs. overall thickness of the system. (b) Steady flow resistivity of each layer vs. overall thickness of the system.

5.4.1.4.2 Second Scenario Optimisation

During the design process, the overall thickness for a certain multi-layered system, which can meet the design criterion of the anechoic lining, is sometimes known due to some prior knowledge. What is not known, and which is of interest to the designer, is the possible compositions of the system. Case D gives an example of this scenario.

Case D:

The results found in Case A in Section 5.4.1.4.1 indicate that a flat-walled, multi-layered, anechoic lining, with Foam C as Layer 1 (which is against the solid back), Foam B as Layer 2 (the mid layer) and Foam A as Layer 3 (the front layer), can achieve a cut-off frequency of 100 Hz with a minimum overall thickness of 0.802 m. The designer may want to know the required thickness for each layer if the overall thickness is 0.85 m.

Hence, the decision space in this case was set to δ_1=3200 SI rayl/m, δ_2= 1340 SI rayl/m, δ_3=380 SI rayl/m, 0.001 m$\leq L_1, L_2, L_3 \leq$ 0.85 m, and $L_1 + L_2 + L_3 = L_{overall\_fixed} = 0.85$ m. The goals were set to $g_{100} = g_{125} = \cdots = g_{1000} = 10\%$. The objective function with the penalty item can be written as

$$r = \left|\frac{Z_i/\rho c - 1}{Z_i/\rho c + 1}\right| + 1000 \times \left|(L_1 + L_2 + L_3) - 0.85\right|. \qquad (5.22)$$

This limits the possible maximum violation of the constraint to 0.01m as explained in Section 5.4.1.2. Figure 5.5 shows the search results provided by the EA. The maximum violation of the constraint of this set of results was only 0.00065m.

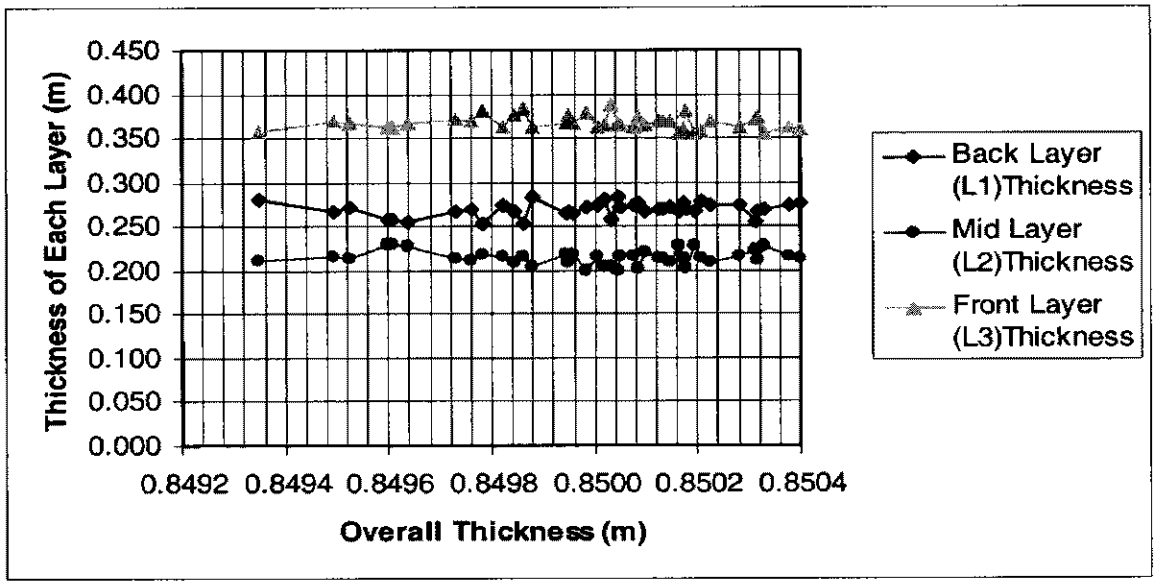

Figure 5.5 Search results of Case D. Thickness of each layer vs. overall thickness of the system.

5.4.1.5 Verification of searching results

As the bulk acoustic properties of the materials in the above searching process were calculated using curve fitting Equations (5.13) – (5.16), the materials found by the EA were ideal and might not be commercially available. Hence, the verification of searching results can only be carried out theoretically.

Davern (1972) proved that to achieve the criterion of a maximum of 10% pressure reflection (which corresponds to a normal absorption coefficient of 99% or better) for an anechoic lining, the real and imaginary parts of the specific acoustic impedance ratio should lie on, or within, the circle defined by the equation:

$$\left(\frac{R}{\rho c}-1.02\right)^2+\left(\frac{I}{\rho c}\right)^2=(0.202)^2, \tag{5.23}$$

where R and I are respectively the real part and imaginary parts of the normal incidence acoustic impedance and $\frac{R}{\rho c}$ and $\frac{I}{\rho c}$ are respectively the specific normal acoustic resistance and specific normal acoustic reactance. All results found by the EA agree with this principle. For instance, Table 5.5 shows the calculated results of Equation (5.23) for the solution with the minimum overall thickness as shown in Table 5.3.

Table 5.5 Calculated results of Equation (5.23) for the solution with the minimum overall thickness (0.529m)

Frequency	100 Hz	125 Hz	160 Hz	200 Hz	250 Hz	315 Hz	400 Hz	500 Hz	630 Hz	800 Hz	1000 Hz
Calculated Results of Equation (5.23)	0.04	0.001	0.016	0.04	0.028	0	0.023	0.032	0.007	0.018	0.011

5.4.2 A Detailed Investigation on the Application of Multi-layered Polyurethane Foams as Flat-walled Anechoic Linings

Using the same optimisation process as introduced in the above section, a detailed investigation was carried out on the application of multi-layered polyurethane foams as flat-walled anechoic linings. Curve-fitting Equations (5.15) and (5.16) developed by

Cummings and Beadle (1993) for a flow resistivity range between 60 and 6229 SI rayl/m (Table 5.2) were used to calculate the acoustic bulk properties of the material. The investigation included the following aspects: the efficacy of a single layer of material, the minimum number of layers of linings to achieve the minimum overall thickness for low (100 Hz), mid (250 Hz) and high (500 Hz) cut-off frequencies, the use of the three-layered lining composite for low to mid cut-off frequencies and the effect of air gaps. The investigation results provide the benchmark and guidelines for the design of flat-walled multi-layered anechoic linings.

5.4.2.1 Single layer

First, the performance of a single layer of material for three cut-off frequencies between 100 and 500 Hz is investigated. Figure 5.6 shows the minimum thickness of a single layer of material as a function of the cut-off frequency. Figure 5.7 shows the required flow resistivity of the single layer of material, which has the minimum overall thickness for the corresponding cut-off frequency.

Figure 5.7 indicates that with a decrease in the cut-off frequency from 500 to 100 Hz the required flow resistivity of a single layer of material is reduced from 1400 to 280 SI rayl/m and there is a near linear relationship between the cut-off frequency and required flow resistivity of the single layer of material, which can be approximately expressed as

$$\sigma = 2.82 \times f_c - 7.82 , \tag{5.24}$$

where f_c is the cut-off frequency ranging from 100 to 500 Hz. Figure 5.6 indicates that, with a decrease of the cut-off frequency from 500 to 100 Hz, the minimum thickness for a single layer of material is substantially increased, and to achieve the required cut-off frequency the minimum thickness of the single layer material needs to be equivalent to the wavelength at the corresponding cut-off frequency. Hence, it is not effective to use just a single layer of material as the flat-walled anechoic lining.

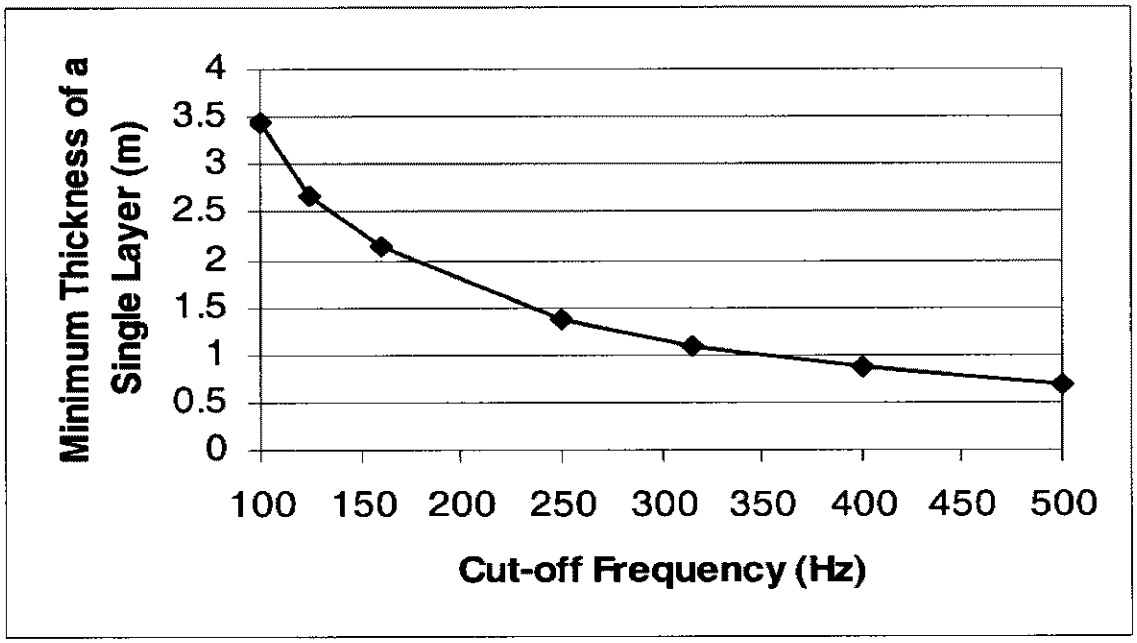

Figure 5.6 Minimum thickness of a single layer of material as a function of cut-off frequency.

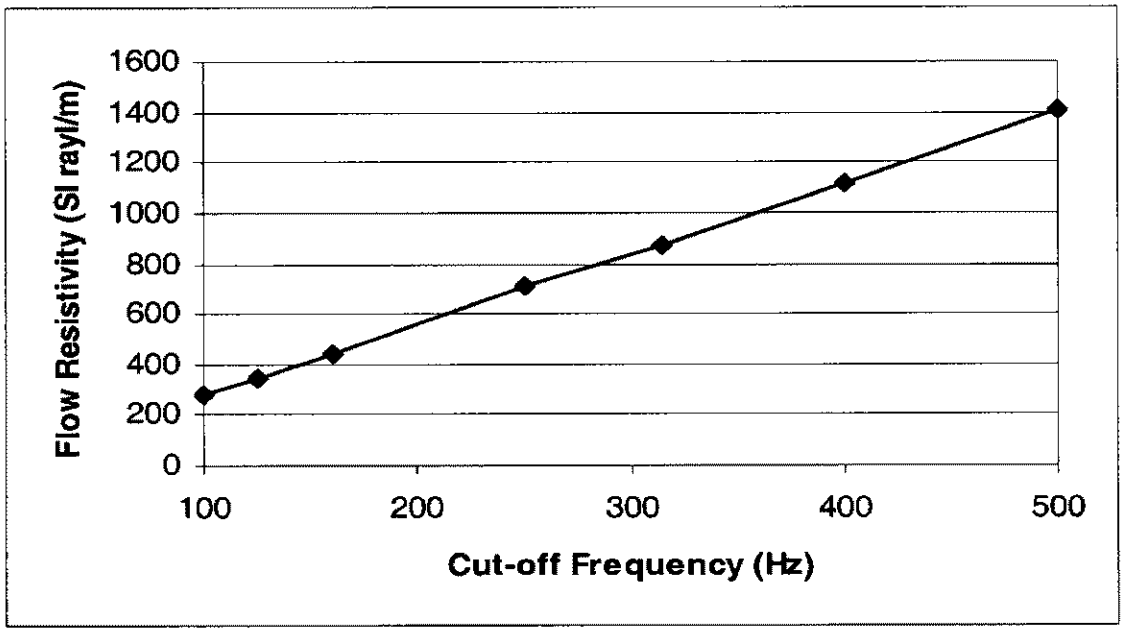

Figure 5.7 Flow resistivity of the single layer of material, which has the minimum thickness for achieving the corresponding cut-off frequency, as a function of the cut-off frequency.

5.4.2.2 Number of layers

As discussed previously, employing multi-layers of material can partially overcome the reflection versus attenuation conflict and make the use of flat-walled anechoic linings more attractive. Thus, in the design of the flat-walled multi-layered anechoic lining it is important to determine for a certain cut-off frequency the minimum number of layers of linings to achieve the minimum overall thickness.

The dependency of the minimum overall thickness on the number of layers is investigated for three cut-off frequencies, 100 Hz, 250 Hz and 500 Hz. The results of this investigation are shown in Figure 5.8.

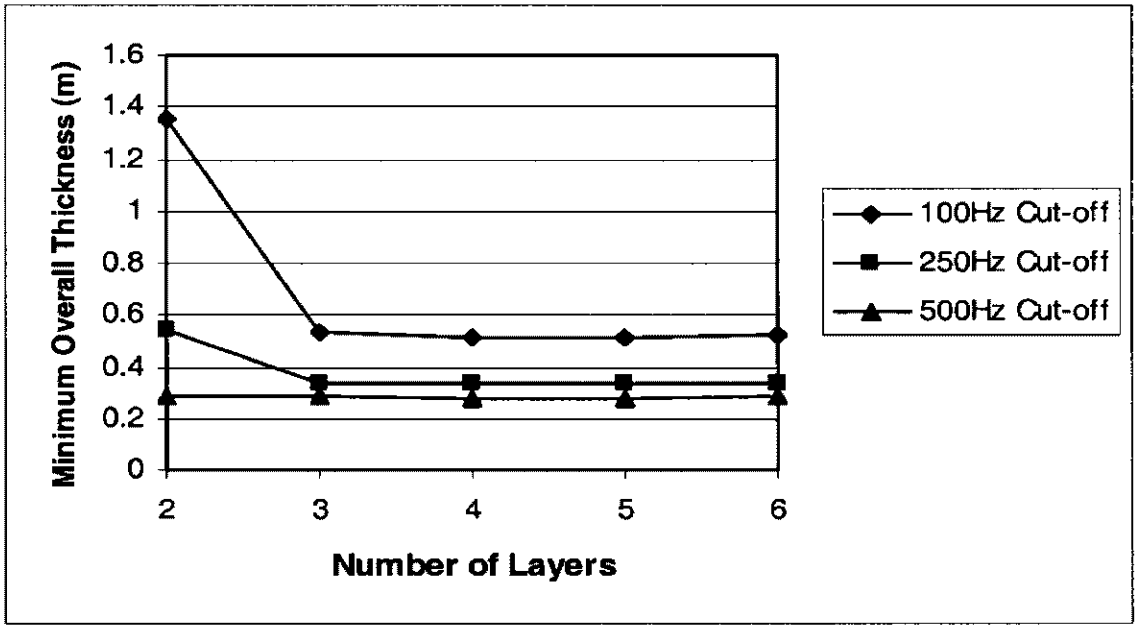

Figure 5.8 Minimum overall thickness as a function of the number of layers.

These results indicate that

a) For low (100 Hz) and mid (250 Hz) cut-off frequencies, a two-layered composite is still not sufficiently effective to overcome the reflection versus attenuation conflict. However, the minimum overall thickness can be significantly reduced by employing a three-layered composite in lieu of a two-layered one. The effect is more pronounced for the low cut-off frequency. An increase in the number of layers from three to six

can not further reduce the minimum overall thickness of the multi-layered lining composite. Therefore, for low and mid cut-off frequencies, the minimum number of layers of linings required to achieve the minimum overall thickness is three.

b) For high (500 Hz) cut-off frequency, the minimum number of layers of linings required to achieve the minimum overall thickness is two as the minimum overall thickness can not be further reduced by increasing the number of layers from two to six.

5.4.2.3 Three-layered lining composite

In most practical situations the cut-off frequency of an anechoic lining will be required to be no more than 250 Hz. Therefore, a three-layered lining composite will be of most interest. Figure 5.9 shows the minimum overall thickness of a three-layered lining composite as a function of the cut-off frequency. Figures 5.10 and 5.11 respectively show the required thickness and flow resistivity of each individual layer of the three-layered lining composite, which has the minimum overall thickness for the corresponding cut-off frequency.

Figure 5.12 shows the ratio of the minimum overall thickness of the three-layered lining composite to the average quarter wavelength in the composite as a function of the cut-off frequency. Figure 5.13 shows the ratio of the minimum overall thickness of the three-layered lining composite to the quarter wavelength in the air as a function of the cut-off frequency.

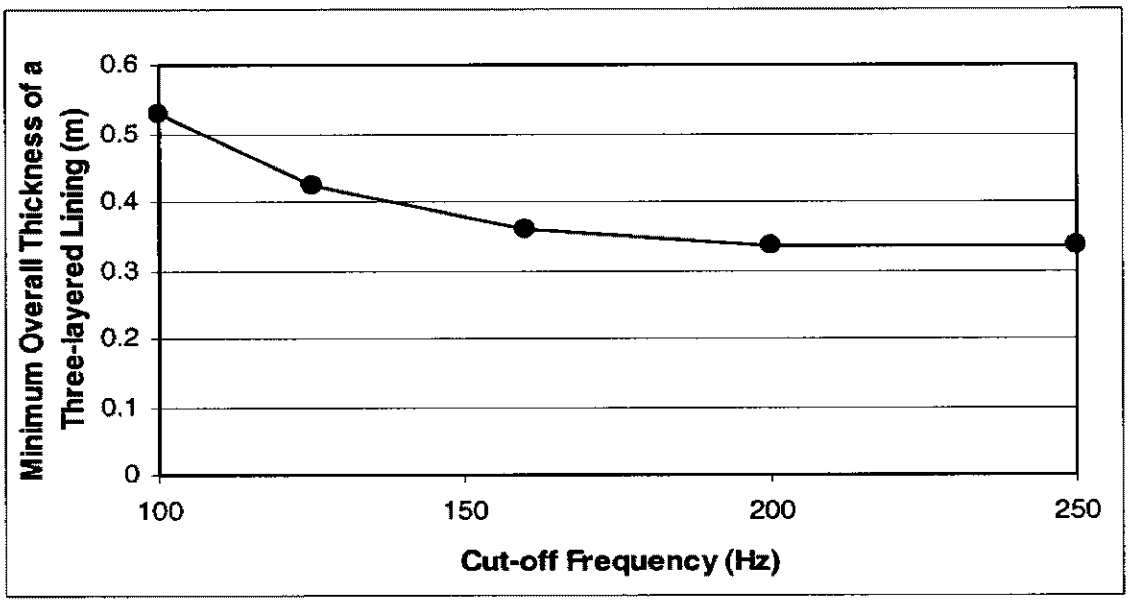

Figure 5.9 Minimum overall thickness of a three-layered lining composite as a function of the cut-off frequency.

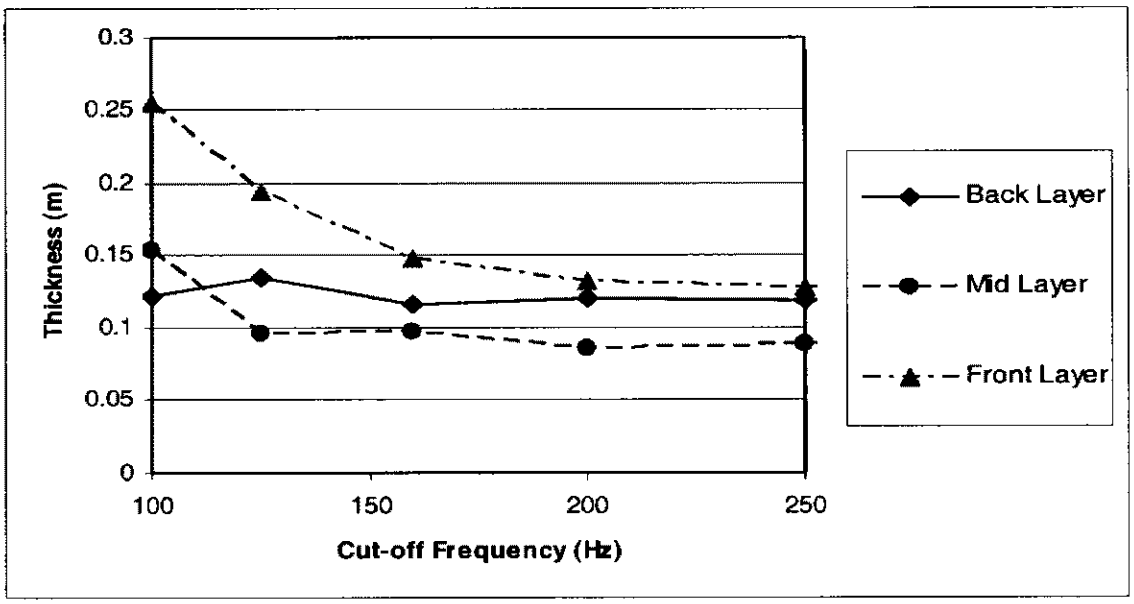

Figure 5.10 Thickness of each individual layer of the three-layered lining composite which has the minimum overall thickness for achieving the corresponding cut-off frequency, as a function of the cut-off frequency. The back layer is the layer that is closest to the solid backing; the front layer is the layer that faces the air; and the mid layer is the layer in between the back layer and the front layer.

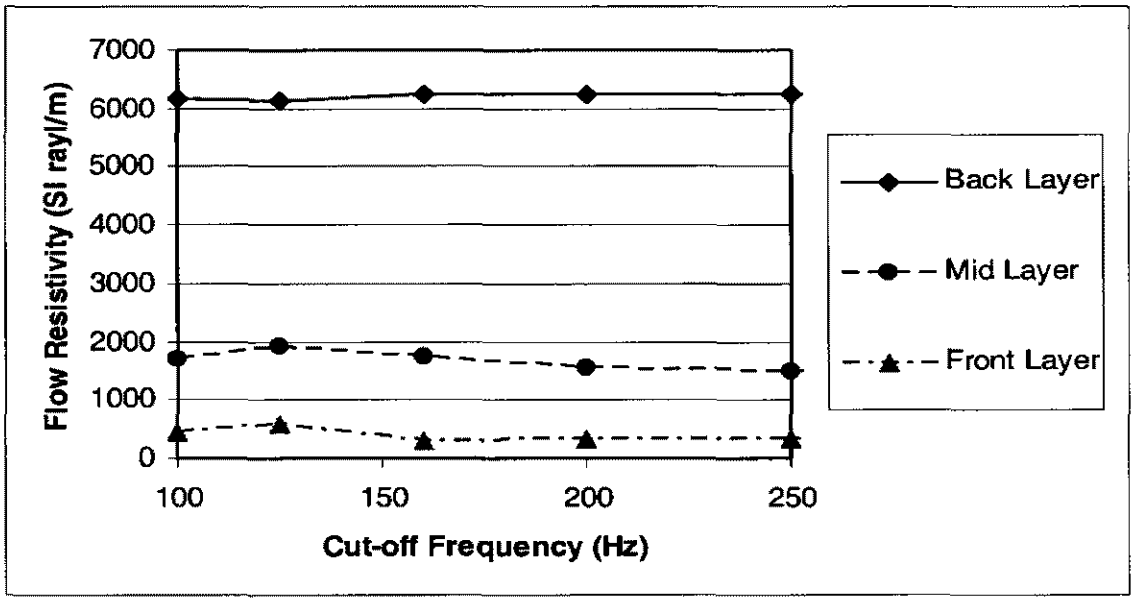

Figure 5.11 Flow resistivity of each individual layer of the three-layered lining composite, which has the minimum overall thickness for achieving the corresponding cut-off frequency, as a function of the cut-off frequency. The back layer is the layer that is closest to the solid backing; the front layer is the layer that faces the air; and the mid layer is the layer in between the back layer and the front layer.

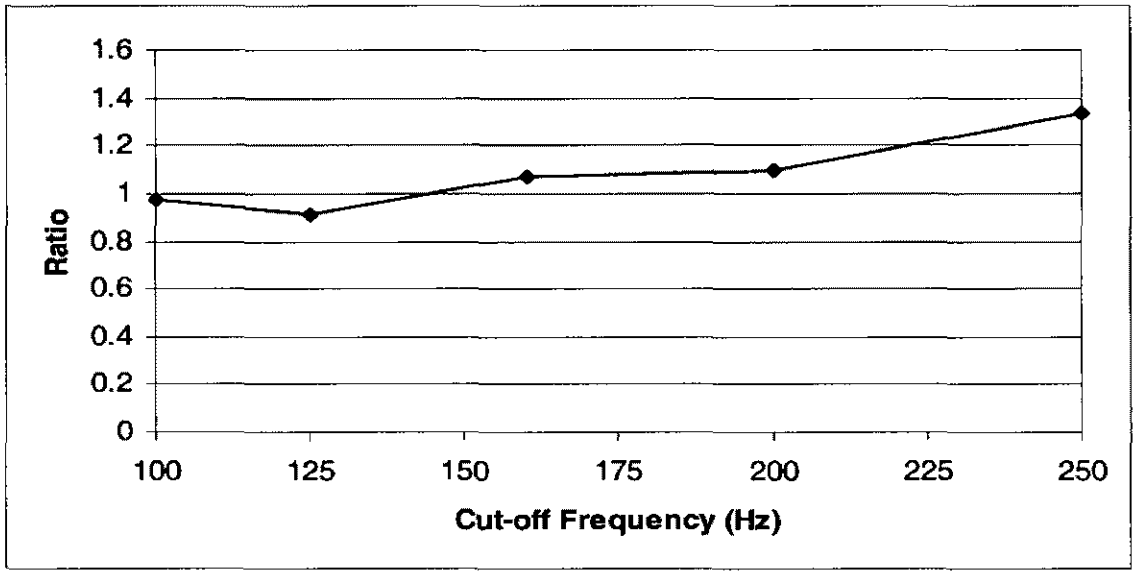

Figure 5.12 Ratio of the minimum overall thickness of the three-layered lining composite to the average quarter wavelength in the lining composite, as a function of the cut-off frequency.

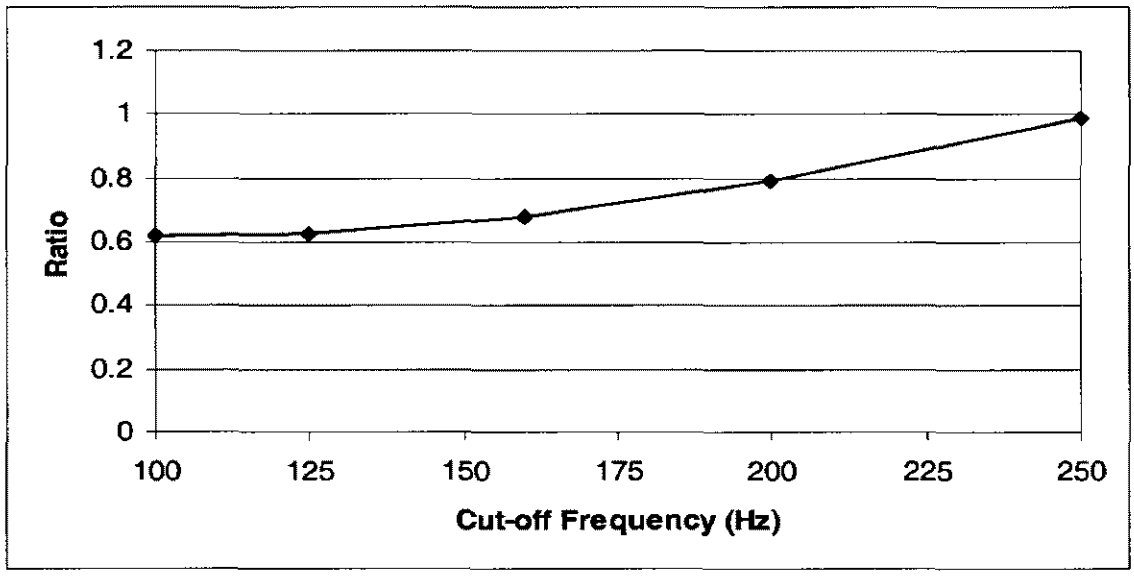

Figure 5.13 Ratio of the minimum overall thickness of the three-layered lining composite to the quarter wavelength in the air, as a function of the cut-off frequency.

From Figure 5.9 to Figure 5.13 one can observe the following:

a) The minimum overall thickness of the three-layered lining composite is close to the average quarter wavelength in the composite for cut-off frequencies between 100 and 200 Hz. It is becoming closer to the quarter wavelength in the air with the increase of cut-off frequency from 200 to 250 Hz.

b) For the three-layered lining composite the material with low flow resistivities should be placed in front of the material with high flow resistivities.

c) For the material investigated to achieve a cut-off frequency between 100 and 250 Hz, the required flow resistivity for each layer of material in the three-layered lining composite basically does not vary with the cut-off frequency. The average flow resistivity for the front layer of material is 400 SI rayl/m, which is close to the characteristic impedance of the air, and the average flow resistivities for the mid layer and back layer are 1700 and 6200 SI rayl/m respectively.

d) The required thickness of the back layer basically does not vary with the cut-off frequency and is around 0.125 m. The thicknesses of the front layer and the mid layer have to be increased to achieve the decreased cut-off frequency.

5.4.2.4 Effect of air gaps

In a practical situation, when the flat-walled multi-layered lining is not installed properly, air gaps may exist between the lining and the solid back wall and between layers of lining material. Figure 5.14 shows how the air gaps, ranging from 0 m to 0.03 m, affect the pressure reflection factors of the three-layered lining composite with the minimum overall thickness for achieving a cut-off frequency of 160 Hz. It indicates that, with the presence of air gaps, the pressure reflection factors at certain frequencies may exceed the requirement for an anechoic lining (10%) by up to 6%, although they may also be reduced at some other frequencies, especially at frequencies lower than the cut-off frequencies. A similar effect caused by air gaps on the optimum lining composites for other cut-off frequencies can be observed.

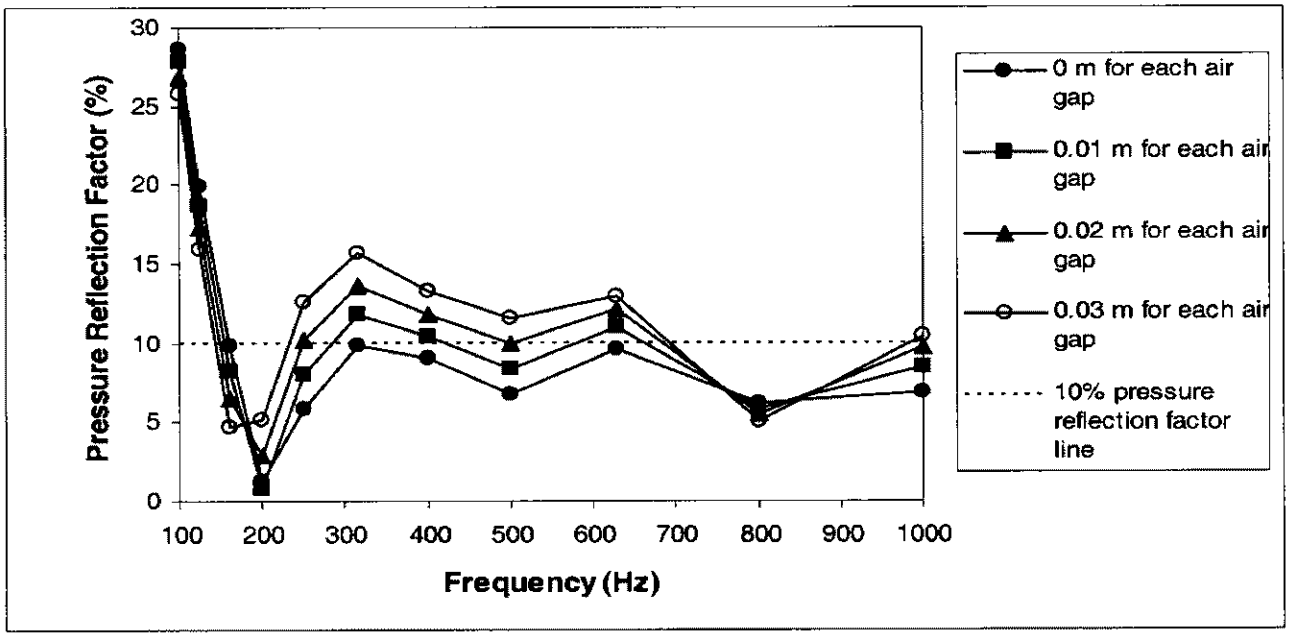

(a)

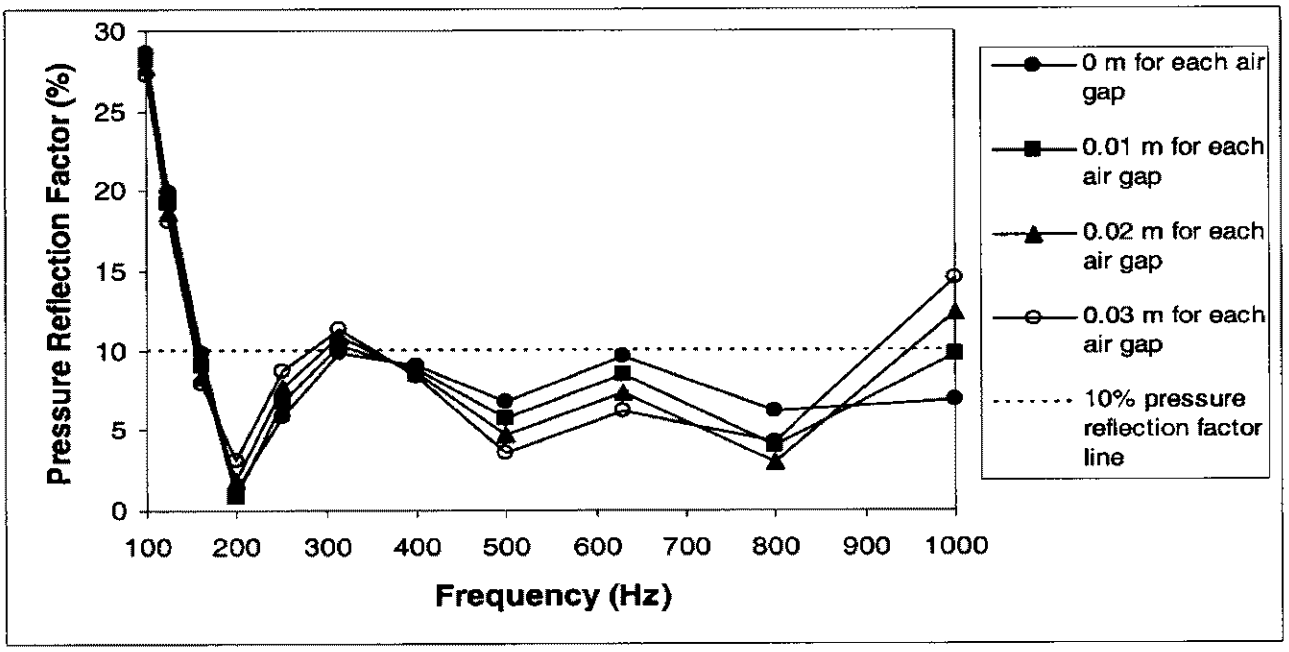
Pressure Reflection Factor (%)
30
25
20
15
10
5
0
100
200
300
400
500
600
700
800
900
1000
Frequency (Hz)
0 m for each air gap
0.01 m for each air gap
0.02 m for each air gap
0.03 m for each air gap
10% pressure reflection factor line

(b)

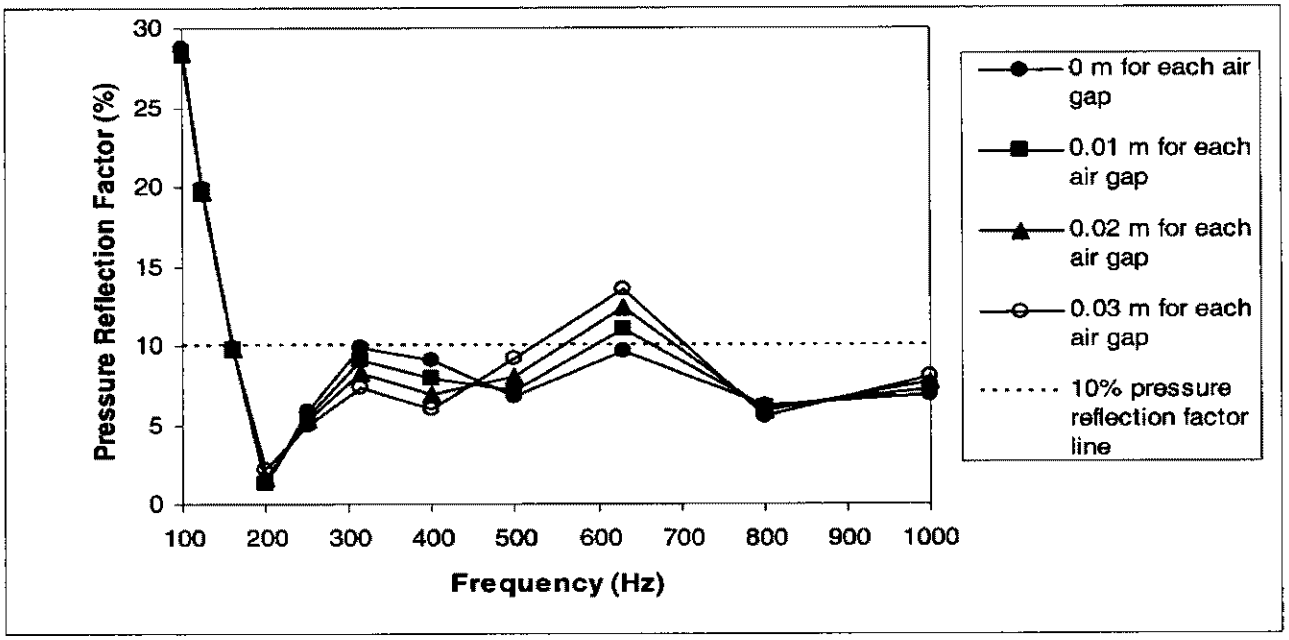
Pressure Reflection Factor (%)
30
25
20
15
10
5
0
100
200
300
400
500
600
700
800
900
1000
Frequency (Hz)
0 m for each air gap
0.01 m for each air gap
0.02 m for each air gap
0.03 m for each air gap
10% pressure reflection factor line

(c)

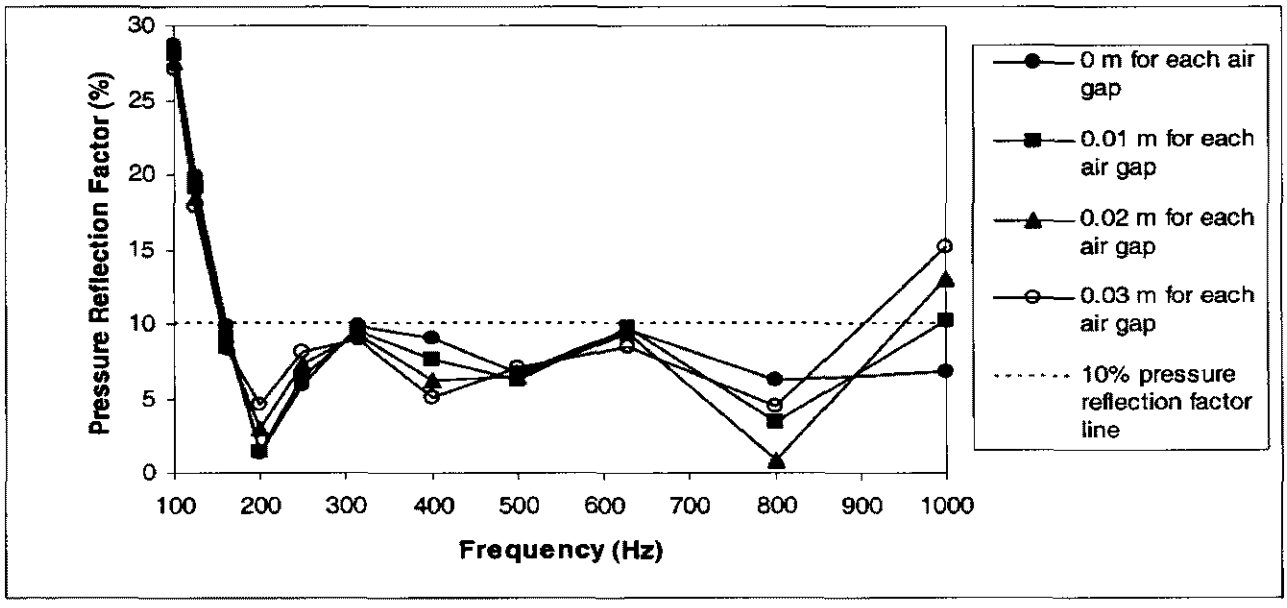

(d)

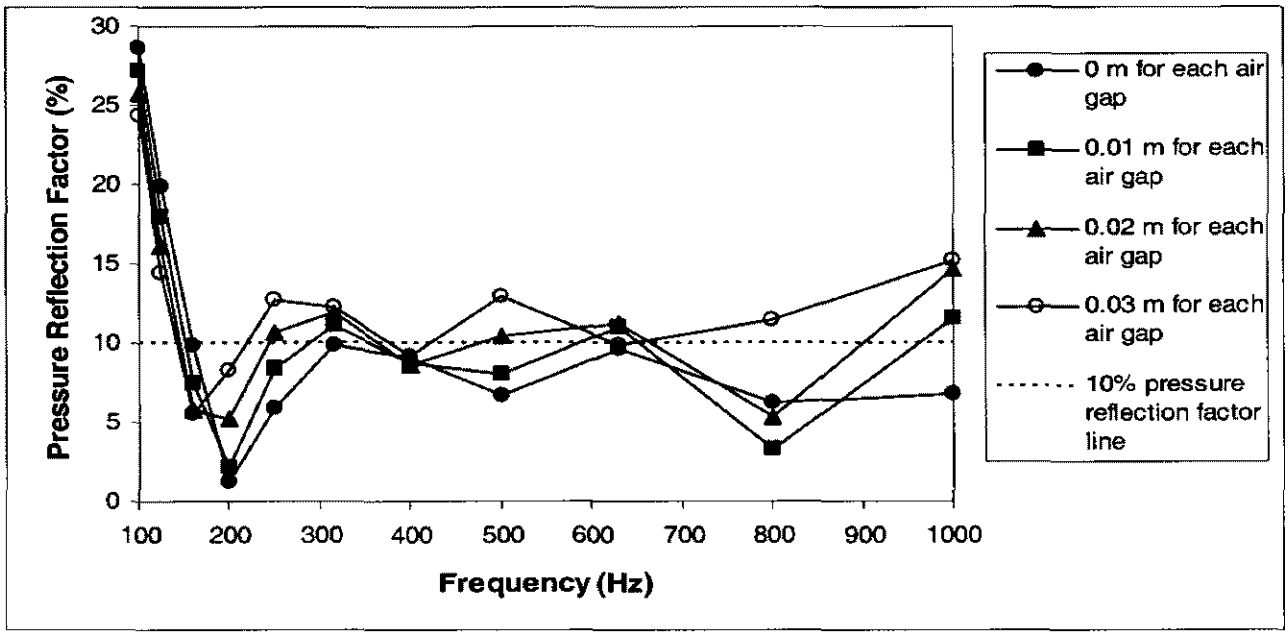

(e)

Figure 5.14 Effect of air gaps, ranging from 0 m to 0.03 m, on the pressure reflection factors of the three layered lining composite with the minimum overall thickness for achieving a cut-off frequency of 160 Hz. The back layer is the layer that is closest to the solid backing; the front layer is the layer that faces the air; and the mid layer is the layer in between the back layer and the front layer. (a) With an air gap between the solid back wall and the lining composite. (b) With an air gap between the back layer and the mid

layer of the lining composite. (c) With an air gap between the mid layer and the front layer of the lining composite. (d) With air gaps between the back layer and the mid layer and between the mid layer and the front layer of the lining composite. (e) With air gaps between the back solid wall and the back layer, between the back layer and the mid layer and between the mid layer and the front layer of the lining composite.

5.5 APPLICATION OF FIBROUS BUILDING INSULATION MATERIALS: AN APPLICATION CASE

The MARCS Auditory Laboratories at the University of Western Sydney recently decided to construct an anechoic room for its research in the area of speech communication and auditory processes. The internal size of the room is 4500 mm long, 3600 mm wide and 3500 mm high. The maximum anechoic lining thickness was limited to 300 mm due to the small size of the room, and the desired cut-off frequency was 250 Hz. As the budget for the project was limited, the conventional anechoic lining system using individual units such as wedges was not affordable. An alternative anechoic lining system, flat-walled multi-layered anechoic linings, was therefore required.

5.5.1 Fibrous Building Insulation Materials Investigated

The material investigated in the above Section 5.4 is fully-reticulated (open-cell) polyurethane foams. The detailed investigation results provide the benchmark and guidelines for the design of flat-walled multi-layered anechoic linings. However, the materials found by the EA might not be commercially available because the bulk acoustic properties of the materials in the above searching process were calculated using curve fitting Equations (5.13) – (5.16) and it was assumed that any required thickness of the material was available. The MARCS Auditory Laboratories was also reluctant to use polyurethane foams for the anechoic lining material because of the fire hazard and mechanical durability problems related to this type of material. Thus fibrous materials were required.

Hence, sixteen of the most commonly used commercial fibrous building insulation materials available in Australia were then investigated as the pool of materials for consideration. Measurements of thickness, density, and flow resistivity (ASTM, 2003) of each material were made and results of these measurements are presented in Table 5.6. The bulk acoustic properties of each material were also measured using a two-thickness method (Smith and Parrott, 1983). Generally, the cost for the glasswool type material is higher than the polyester type material.

Table 5.6 Fibrous building insulation materials investigated

Type	Material ID	Fixed Thickness (mm)	Density (kg/m3)	Flow Resistivity (Pas/m)
Low-density Glasswool	1	50	10.4	3190
Mid-density Glasswool	2	25	20.0	11180
	3	25	29.5	12378
	4	25	30.0	13915
High-density Glasswool	5	25	108.0	47637
Mid-density Polyester	6	25	33.0	6221
	7	25	40.0	7153
Low-density Polyester	8	25	10.5	1410
	9	35	7.9	453
	10	65	8.8	535
	11	75	10.8	458
	12	85	10.8	594
	13	90	11.6	659
	14	30	9.6	562
	15	40	8.2	483
	16	50	9.3	663

5.5.2 Application of GEATbx

In terms of the application of GEATbx, the main differences from that introduced in Section 5.4 are the data presentation and the corresponding evolutionary operators. In Section 5.4 the bulk acoustic properties of the material were calculated using curve fitting Equations (5.13) – (5.16) and it was assumed that any required thickness of the material was available. Hence, variables were represented as continuous real values and real valued evolutionary operators were applied accordingly. However, in the present application the sixteen materials investigated all have their own measured bulk properties and fixed thicknesses and the overall thickness of a material can only be multiples of its fixed thickness, that is, variables in the present work all have a discrete nature. In other

words, the present optimisation problem is a combinatorial-type problem. In order to apply GEATbx, the bulk properties and fixed thicknesses of the materials were organized into matrices with the index of each column of the matrix, ranging from one to sixteen, representing each material. Another variable required is the integer multiples of the fixed thickness of each material. During the EA searching process, the program would pick up the material of interest by pointing at the corresponding column of the matrix and vary the overall thickness of the material by assigning a certain integer multiple. In other words, the EA works on the integer value representation. Accordingly, the evolutionary operators (stochastic universal sampling selection (Baker, 1987), discrete recombination (Mühlenbein and Schlierkamp-Voosen, 1995), and integer mutation function (Pohlheim, 2004), which can work with integer value representation, were applied in the GEATbx.

5.5.3 Optimisation Results

In this case, a three-layered lining system was investigated because of its high efficacy compared with a two-layered lining system as indicated in Section 5.4. Taking into account the expected errors resulting from Equation (5.3) and the measurements of the materials' bulk properties, it was considered that a reflection factor of no larger than 12% was acceptable during the EA search. It was also considered that frequencies below 1000 Hz were the most critical ones in the design of anechoic linings and thus the EA search was limited to one-third-octave band frequencies between 250 and 1000 Hz. Table 5.7 shows the optimization results provided by GEATbx.

Using the sixteen materials investigated, the program found fourteen options (i.e., material combinations) that could achieve a 250 Hz cut-off frequency with an overall thickness of the lining system no larger than 300 mm. Among the fourteen options, Options 2 and 12 are the cheapest because the least amount of glasswool material was required. There were two reasons that the cost was not included as one of the optimisation goals. The first is that the primary concern of the optimisation is the physical performance of the lining system; and the second reason is to reduce the time for running the optimisation program.

The only difference between Options 2 and 12 was that Option 12 uses 40 mm more of Material 15 for Layer 3 than Option 2 does. The absorption performances of Options 2 and 12, in terms of the pressure reflection factor, were measured using an impedance tube (ISO, 1996). The measurement results, with the predicted ones, are presented in Figure 5.15. Various situations could cause the difference between the measured pressure reflection factors presented and predicted ones. Firstly, it may be due to the errors resulting from the determination of bulk acoustic properties using the two-thickness method (Smith and Parrott, 1983), which requires that two test samples have identical bulk acoustical properties and that there is no variation associated with the mounting of test samples between measurements. Although during the measurement, samples were carefully selected and the mounting of test samples was in accordance with the standard (ISO, 1996), it could not be guaranteed that there were no variations between test samples and between the mountings of test samples. In addition, because test material samples are available in only one thickness, in order to use the two-thickness method, samples had to be doubled up to achieve twice the original thickness, which introduced an unpredictable "interface impedance" effect. For this and other reasons, a detailed review of, and investigation into, different methods for determining bulk acoustic properties of rigid porous media are carried out in chapter 6 of the present thesis. Secondly, it may be due to the limitations of the experimental apparatus, for instance, the resonances of impedance tube at low frequencies. Unfortunately, all the above errors are unpredictable and unquantifiable.

Since the measured pressure reflection factors of Option 2 at frequencies of 250 Hz and 315 Hz are larger than 12, it was decided to apply Option 12 as the lining system for the anechoic room in the MARCS Auditory Laboratories.

Table 5.7 Optimization results

Option ID	Material ID of Each Layer			Multiples of the Fixed Thickness of Each Layer's Material			Overall Thickness of the Lining System (mm)	Pressure Reflection Factor (%) at Each Frequency						
	Layer 1	Layer 2	Layer 3	Layer 1	Layer 2	Layer 3		250 Hz	315 Hz	400 Hz	500 Hz	630 Hz	800 Hz	1 kHz
1	4	1	16	4	2	1	250	9.6	7.7	1.7	4.5	0.8	4.6	6.3
2	7	1	15	3	2	2	255	1.3	2.6	6.2	8.4	4.5	1.3	11.6
3	5	2	15	2	4	3	270	8.6	8.4	3.7	1.5	0.7	6.1	8.6
4	2	1	16	5	2	1	275	10.2	10.3	5.1	7.4	4.9	2.6	4.7
5	7	1	16	3	3	1	275	8.1	11.6	8.2	9.1	4.4	3.9	3.2
6	3	1	15	2	3	2	280	7.6	2.6	8.6	10.1	7.5	2.5	10.2
7	4	1	15	2	3	2	280	7.0	3.3	9.1	10.4	7.1	2.3	9.8
8	2	1	15	4	2	2	280	4.2	6.5	6.2	7.0	5.0	0.9	11.8
9	2	1	15	2	3	2	280	8.0	0.8	8.5	10.3	7.9	3.2	10.1
10	7	1	15	2	3	2	280	5.6	5.0	10.3	11.3	6.9	2.1	11.2
11	5	1	15	2	3	2	280	9.9	8.1	4.4	8.1	5.3	6.6	5.3
12	7	1	15	3	2	3	295	5.9	11.7	9.6	2.7	3.6	7.2	11.3
13	5	1	16	2	4	1	300	8.4	10.3	7.8	10.5	6.0	5.2	1.4
14	7	1	16	4	3	1	300	11.0	11.1	6.9	6.5	3.0	5.6	3.3

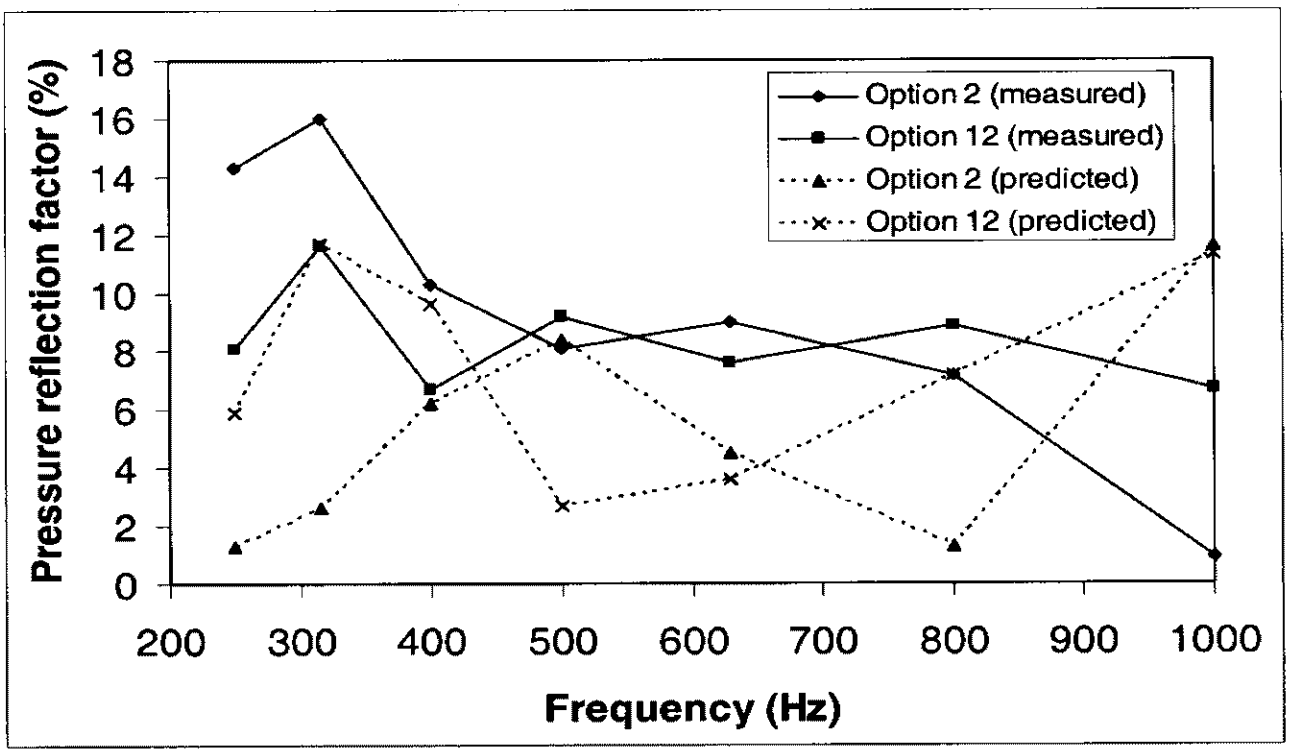

Figure 5.15 Prediction results and impedance tube measurement results of Option 2 and Option 12.

5.5.4 Installation of the Lining

Layers of insulation materials were attached to each other and to the internal surfaces of the room using spikes affixed to the internal surfaces of the room. Care was taken to

eliminate air cavities between the layers of insulation materials and between the internal surfaces of the room and the innermost layer of insulation material.

At the joints where two sheets of the same layer of material meet each other, large gaps were avoided by placing them tightly together. The joints at different layers were staggered to ensure that they did not overlap. Also, at the corners of the room, multi-layers of insulation material were staggered to ensure that their edges overlapped. Figure 5.16 provides an illustration of the arrangement of multi-layered materials. For the layer that is exposed to the air the adjoining sheets of material were loosely sewn together.

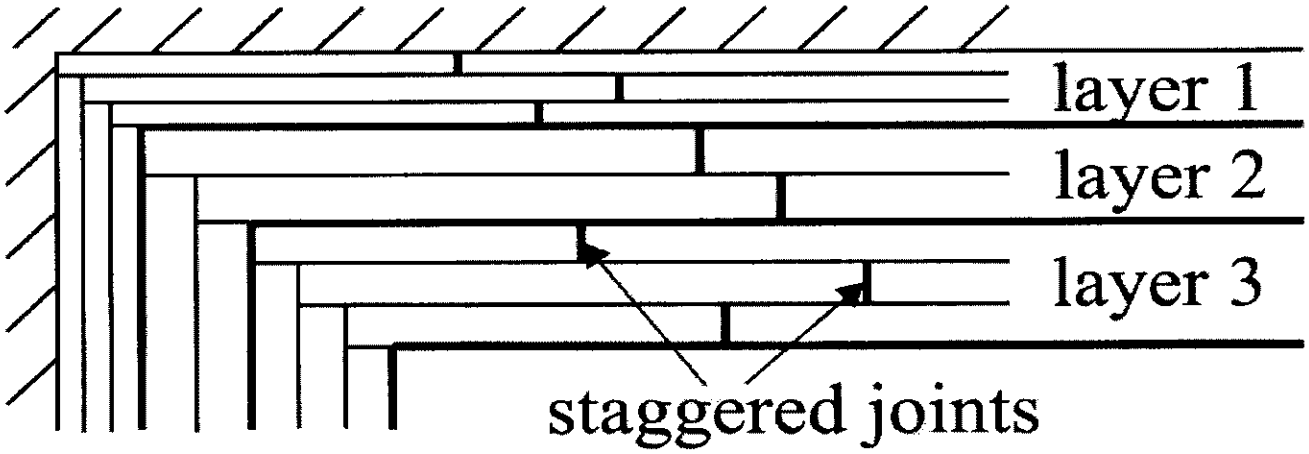

Figure 5.16 Installation of arrangements of multi-layered materials.

5.5.5 Qualification of the Completed Anechoic Room

The completed anechoic room, as shown in Figure 5.17, was qualified in accordance with the procedure set out in ISO 3745:2003 (ISO, 2003). The sound source was located so that the assumed position of its acoustic centre was at the geometric centre of the room. Five straight microphone traverses were used. Four of the five traverses were from the geometric centre of the room to the room corners (the lower southeast, lower southwest, upper northeast and upper northwest corners) and lay in an imaginary plan that passed through the geometric centre of the room. The fifth traverse was from the geometric centre of the room to the west wall, which is one of the parallel walls closest to the geometric centre of the room. One-third-octave band-filtered pink noise with the sequential midband frequencies from 250 to 10 kHz was used as the test signal. The test

signal was generated and digitally filtered (IEC, 1995) using Matlab (MathWorks, 2002). For the five traverses, the measurement of the sound pressure level was carried out starting 0.5 m from the geometric centre of the room and extending to the maximum distance that the measurement microphone could reach. The spacing between the measurement points was 0.1 m.

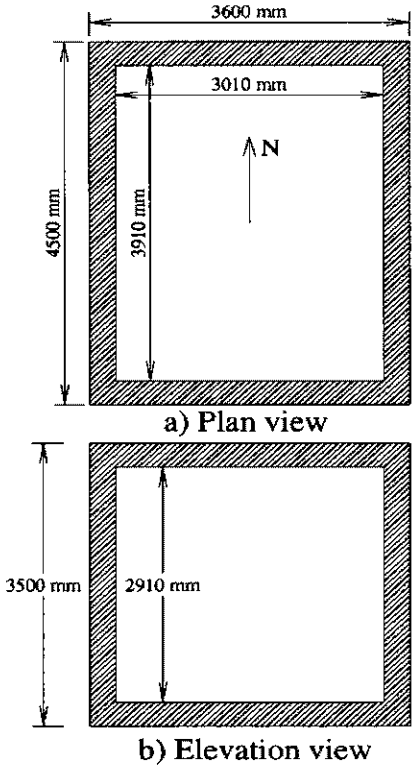

Figure 5.17 Sketch of the completed anechoic room in the MARCS Auditory Laboratories at the University of Western Sydney.

5.5.5.1 Measurement equipment

For the qualification of the room the directionality of the sound source must be uniform to within the allowable deviations as set out in ISO 3745:2003 (ISO, 2003). These limits are reproduced in Table 5.8. For the midband frequencies below 800 Hz, a Bruel & Kjaer Type 4296 OmniPower Loudspeaker, which meets the requirements of ISO 140-3 (ISO, 1995; Bruel & Kjaer, 2005), was used as the sound source (ISO, 2003). For the higher frequency bands from 800 to 10 kHz, a compression driver (TOA Electric TU-50) attached to a 1.5 m long and 6 mm inner diameter cylindrical tube was used as the sound source (ISO, 2003). The compression driver was acoustically shielded by a box wrapped

with mass-loaded vinyl material. As there was no directionality information for the custom-made high frequency sound source, its directionality was measured in accordance with the procedure set out in ISO 3745:2003 (ISO, 2003). The measurement was conducted in an anechoic room, with a 50 Hz cut-off frequency (Australian National Acoustic Laboratories, 2003), at the Australian National Acoustic Laboratories. Figure 5.18 shows the measured deviations in directionality of the custom-made high frequency sound source.

Table 5.8 Maximum allowable deviation in directionality of the sound source for an anechoic room qualification as per ISO 3745:2003 (ISO, 2003)

One-third-octave band frequency (Hz)	Allowable deviations in directionality (dB)
800 to 5000	± 2.0
6300 to 10000	± 2.5

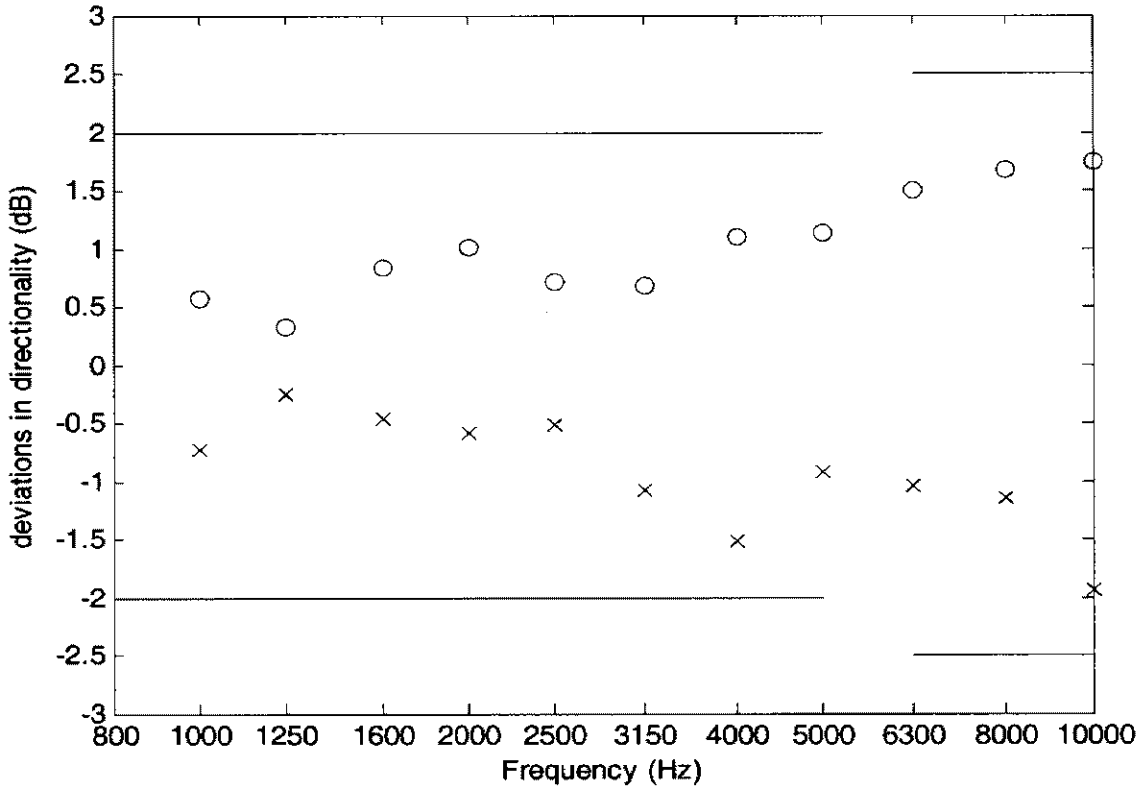

Figure 5.18 Measured deviations in directionality for the custom-made high frequency sound source.

During the measurements a reference microphone was located at an arbitrary but fixed position in the room to check the variation of the sound source output. The drift of the sound power level of the sound sources (with the associated signal generation and amplification system) in any one-third-octave band, from 250 to 630 Hz for the low frequency sound source and from 800 to 10 kHz for the high frequency sound source, was less than ± 0.2 dB at any time during the measurement.

Other equipment used in the measurement of the room was:

(1) RME Hammerfall DSP Multiface Sound Card (24 bit/96 kHz multichannel interface);
(2) RME ADI-96 Pro 24 bit/96 kHz DSP based A/D converter and conditioning amplifier;
(3) a digital SPDIF cable connecting the above sound card and A/D converter;
(4) Hafler P3000 Power Amplifier;
(5) Bruel & Kjaer Type 2804 Microphone Power Supply;
(6) Bruel & Kjaer Type 4190 Microphone with Bruel & Kjaer Type 2669 Microphone Preamplifier.

5.5.5.2 Qualification results

The maximum allowable deviation of the measured sound pressure levels from the theoretical levels, using the inverse square law as per ISO 3745:2003 {ISO, 2003), is reproduced in Table 5.9. Figure 5.19 shows the measured deviations for the traverse into the lower southeast corner of the room. Similar results can be observed for the traverses into the other corners. Figure 5.20 shows the measured deviations for the traverse into the west wall of the room.

The qualification results indicate that

(1) a minimum anechoic distance of 2.1 m is achieved for the traverses to the four corners that are on an imaginary plane passing the geometric centre of the room. This approximately corresponds to 75% of half of the diagonal distance (without taking into account the anechoic lining thickness) of the imaginary plane.

(2) a minimum anechoic distance of 1.3 m is achieved for the traverse to one of the walls closest to the geometric centre of the room. This approximately corresponds to 85% of half the distance (without taking into account the anechoic lining thickness) between the two parallel walls closest to the geometric centre of the room.

Table 5.9 Maximum allowable deviation of measured sound pressure levels from the theoretical level using the inverse square law in an anechoic room as per ISO 3745:2003 (ISO, 2003)

One-third-octave band frequency (Hz)	Allowable deviations (dB)
≤ 630	± 1.5
800 to 5000	± 1.0
≥ 6300	± 1.5

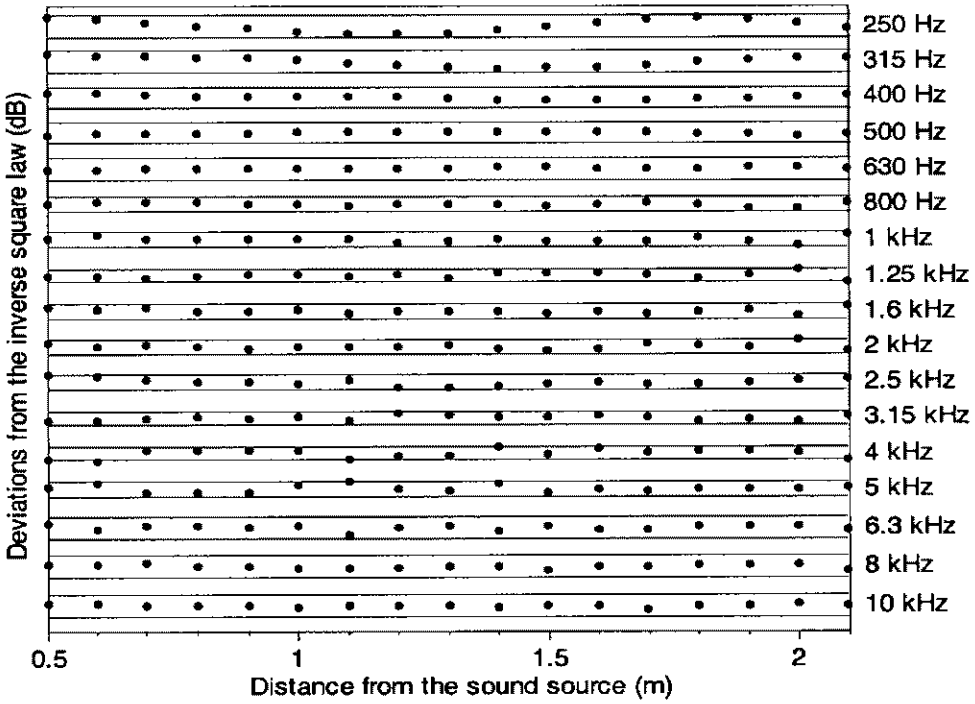

Figure 5.19 Measured deviations for the traverse into the lower southeast corner of the room. The frequency labels along the right vertical axis define the position of the 0 dB deviation for that frequency; the lines above and below the 0-dB position are the permissible variations from free-field performance in accordance with Table 5.9.

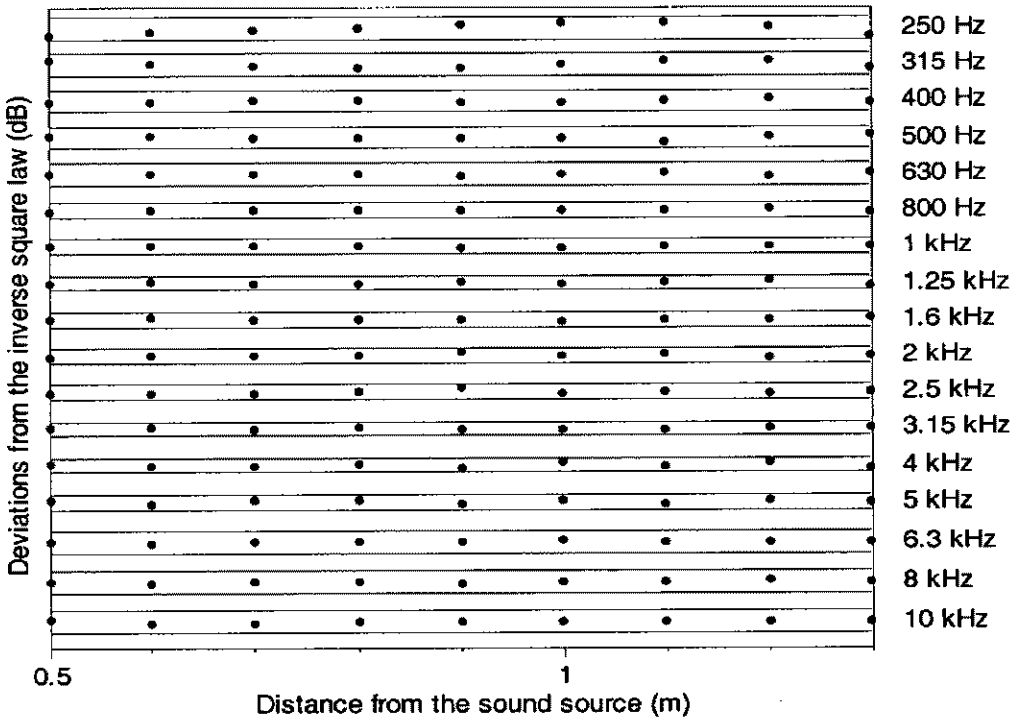

Figure 5.20 Measured deviations for the traverse into the west wall of the room. The frequency labels along the right vertical axis define the position of the 0 dB deviation for that frequency; the lines above and below the 0-dB position are the permissible variations from free-field performance in accordance with Table 5.9.

5.6 CONCLUSIONS

Simplicity of production and mounting make the flat-walled, multi-layered anechoic lining an attractive option in the design considerations of anechoic chambers. Previous investigations indicated that a flat-walled, multi-layered anechoic lining system, with an overall thickness slightly less than a quarter of a wavelength, could be used to achieve a required cut-off frequency (Davern, 1980). However, the work proved to be tedious and time consuming because of the numerous trial and error measurements involved. Good agreement between the measured (impedance tube) overall impedance of a flat-walled multi-layered system and calculated values using multi-layered impedance equation and the curve-fitting equations for predicting bulk acoustic properties has been shown in

Dunn and Davern (1986), which supports the idea that the design of flat-walled multi-layered linings can be undertaken on a desktop computer.

EAs work on populations of individuals instead of single solutions. In this way the search is performed in a parallel manner. This characteristic makes EAs very attractive for solving MOP. In this chapter, a multi-objective EA [MOGA (Fonseca and Fleming, 1993; 1998; Pohlheim, 2004)] was implemented as the optimiser to aid and speed up the design process of flat-walled multi-layered anechoic lining composite.

The general optimisation procedure was first demonstrated for a three-layered lining system composed of fully-reticulated (open-cell) polyurethane plastic foams and targeted a cut-off frequency of 100 Hz. Then, a detailed investigation was carried out on the application of multi-layered polyurethane foams as flat-walled anechoic linings. The major findings of the investigation were 1) a single layer of material was not as effective as a flat-walled multi-layered anechoic lining; 2) for low (100 Hz) and mid (250 Hz) cut-off frequencies the minimum number of layers needed to achieve the minimum overall thickness was three, and for high (500 Hz) cut-off frequency the minimum number of layers to achieve the minimum overall thickness was two; 3) for the material investigated in the present work and for cut-off frequencies between 100 and 250 Hz inclusive, using a three-layered flat-walled anechoic lining, the achievable minimum overall thickness was between a quarter wavelength in the lining composite and a quarter wavelength in the air for the corresponding cut-off frequency; 4) for a three-layered lining composite the material with low flow resistivity should be placed in front of the material with high flow resistivity. For the material investigated, to achieve a cut-off frequency between 100 and 250 Hz, the required flow resistivity for each layer of material in the three-layered lining composite basically did not vary with the cut-off frequency. The average flow resistivity for the front layer of material was 400 SI rayl/m, which is close to the characteristic impedance of the air, and the average flow resistivities for the mid and back layers were 1700 and 6200 rayl/m respectively; 5) for the three-layered lining composite, the required thickness of the back layer basically did not vary with the cut-off frequency and was around 0.125 m. The thicknesses of the front and the mid layers had to be

increased to achieve the decreased cut-off frequency; 6) to achieve the designed performance of the lining composite air gaps should be avoided. The above investigation results provide the benchmark and guidelines for the design of flat-walled multi-layered anechoic linings.

An investigation using fibrous building insulation material was also carried out in the form of an application case. The bulk acoustic properties of sixteen of the most commonly used commercial fibrous building insulation materials available in Australia were measured and, on the basis of the measurement results, a multi-objective evolutionary algorithm was used to optimise the design of a flat-walled multi-layered anechoic lining to meet the design criteria - a 250 Hz cut-off frequency with a maximum lining thickness of 300 mm. Nonetheless, because of the discrete nature of the problem, different data representation and evolutionary mutation operator to those applied in the investigation of polyurethane foams were used.

Results of the EA search indicated that for the sixteen materials investigated there were fourteen options that could achieve a cut-off frequency of 250 Hz with the overall lining thickness less than 300 mm. For all the options, the materials in the lining system exhibited a trend of a graduated increase in density and flow resistivity from the front layer (Layer 3) to the back layer (Layer 1). The options found by EA were evaluated on the basis of their costs and two options were short-listed. The acoustic performances of the short-listed options were then measured in an impedance tube. The difference between the measured and predicted performances may be due to the errors resulting from the measurement of bulk acoustical properties and the limitations of the experimental apparatus, all of which, unfortunately, are unpredictable and unquantifiable. The option that had the lower measured pressure reflection factors at low frequencies was used as the lining system for the anechoic room in the MARCS Auditory Laboratories. The lining system finally used in the anechoic room had an overall thickness of 295 mm, which is about 45 mm less than a quarter of a wavelength at the cut-off frequency of 250 Hz. The material cost of the applied lining system was about fifty Australian dollars per square metre. The completed anechoic room, where the optimised design was applied,

was qualified and the results showed that a large percentage (75% - 85%) of the distance between the sound source and the room boundaries, on the traverses made, was anechoic.

The success of this application case also shows the effectiveness of EAs for solving combinatorial-type problems featuring discontinuous decision spaces, which is difficult or even impossible, for traditional optimisation methods.

REFERENCES FOR CHAPTER 5

- ASTM, 2003. *ASTM C522-03 Standard test method for airflow resistance of acoustical materials*. American Society for Testing and Materials, Philadelphia.
- Australian National Acoustic Laboratories, 2003. *Research and development annual report 2002/2003*. Australian National Acoustic Laboratories, Sydney, pp 50-51.
- Baker J.E., 1987. "Reducing bias and inefficiency in the selection algorithm," *Proceedings of the second international conference on genetic algorithms and their application*, Hillsdale, New Jersey, Lawrence Erlbaum Associates, pp 14-21.
- Beranek L.L. and Sleeper H.P., 1946. "The design and construction of anechoic sound chambers," *Journal of the Acoustical Society of America*; 18 (1), pp 140-150.
- Bracciali A. and Cascini G., 2000. "Measurement of the lateral noise emission of an UIC 60 rail with a custom device," *Journal of Sound and Vibration*, 231, pp 653-665.
- Bruel & Kjaer, 2005. *Product data – sound sources for building acoustics: omnipower sound source – type 4269, omnisource sound source – type 4295, tapping machine – type 3207, including power amplifier – type 2716*. http:// www.bksv.com, Nœrum, Denmark.
- Cummings A. and Beadle S.P., 1993. "Acoustic properties of reticulated plastic foams," *Journal of Sound and Vibration*, 175 (1), pp 115-133.
- Davern W.A., 1972. "A design criterion for sound-absorbent lining of an anechoic chamber.," *Applied Acoustics* , 5 (1), pp 69-71.
- Davern W.A., 1980. "Flat-walled graded density anechoic lining," *Proceedings of 10th international congress on acoustics*, Sydney.
- Delany M.E. and Bazley E.N., 1970. "Acoustical properties of fibrous absorbent materials," *Applied Acoustics*, 3 (2), pp 105-116.
- Dunn I.P. and Davern W.A., 1986. "Calculation of acoustic impedance of multi-layer absorbers," *Applied Acoustics*, 19 (5), pp 321-334.
- Fonseca C.M. and Fleming P.J., 1993. "Genetic algorithms for multiobjective optimization: formulation, discussion and generalization," *Proceedings of the fifth international conference on genetic algorithms*, San Mateo, California, Morgan Kaufmann, pp 416-423.

- Fonseca C.M. and Fleming P.J., 1998. "Multiobjective optimization and multiple constraint handling with evolutionary algorithms – part I: a unified formulation," *IEEE transactions on systems, man, and cybernetics – part A: system and humans*, 28 (1), pp 26-37.
- Lee F.C. and Chen W.H., 2001. "Acoustic transmission analysis of multilayer absorbers," *Journal of Sound and Vibration*, 248 (4), pp 621-634.
- MathWorks, 2002. *MATLAB reference guide (version 6.5 R13)*. The MathWorks Inc, Natick, MA.
- Mühlenbein H. and Schlierkamp-Voosen D., 1995. "Analysis of selection, mutation and recombination in genetic algorithms," *In:* Banzhaf W. and Eeckman F.H., editors, *Evolution as a computational process vol 899 Lecture notes in Computer Science,* Berlin, Springer-Verlag, pp 142-168.
- IEC, 1995. *IEC 1260:1995 Electroacoustics: octave band and fractional-octave band filters*. International Electrotechnical Commission, Geneva, Switzerland.
- ISO, 1995. *ISO 140-3:1995(E) Acoustics – measurement of sound insulation in buildings and of building elements – part 3: laboratory measurements of airborne sound insulation of building elements*. International Organization for Standardization, Geneva, Switzerland.
- ISO, 1996. *ISO 10534-1:1996 Acoustics – determination of sound absorption coefficient and impedance in impedance tubes part 1: method using standing wave ratio*. International Organization for Standardization, Geneva.
- ISO, 2003. *ISO 3745:2003 Acoustics – determination of sound power levels of noise sources using sound pressure – precision methods for anechoic and hemi-anechoic rooms*. International Organization for Standardization, Geneva, Switzerland.
- Pohlheim H., 2004. *Genetic and evolutionary algorithm toolbox for use with MATLAB version 3.5*, http://www.geatbx.com/, Berlin.
- Smith C.D. and Parrott T.L., 1983. "Comparison of three methods for measuring acoustic properties of bulk materials," *Journal of the Acoustical Society of America*, 74, pp 1577-1582.
- Zwicker C. and Kosten C., 1949. *Sound absorbing materials*. Elsevier, Amsterdam.

CHAPTER 6

DERIVATION OF THE BULK ACOUSTIC PROPERTIES OF A RIGID POROUS MEDIUM FROM A SINGLE IMPEDANCE TEST

6.1 INTRODUCTION

Porous materials are employed as acoustic absorbents in a wide variety of applications. Examples of these are in noise control, in architectural and building acoustics[1], in the laboratory and in sound recording and reproduction. Wherever predictive design methods for sound propagation in systems involving porous media are used, the acoustic properties of these media need to be known. For many design purposes it is sufficient to regard a porous material as being rigid if it contains a gas in its pores, though in recent years much work has been focussed on the acoustics of poroelastic media, which can exhibit significant structural motion including resonant effects. Most of this work is formulated within the framework of the much earlier work by Biot (1956).

Whether structural motion in a poroelastic material is significant depends on several factors, one of the most important being the structural boundary conditions between the material and any adjacent elastic impervious solid structure. These conditions are mainly determined by whether the material and structure are bonded together. This is highlighted in the work of Bolton *et al.* (1996) for example, who examined sound transmission through a double partition with a poroelastic material filling the air-space between the panels. Here, structural motion is likely to be significant overall if the porous medium is bonded to both panels, less so if it is bonded only to one panel and even less so if it is bonded to neither panel. This is understandable, since solid contact between the poroelastic material and the impervious structure would involve relatively good structural impedance matching between the two, with consequent effective vibrational transmission. Where there is an air-space between the two, or even relatively loose

[1] For instance, as investigated in Chapter 5 of the present thesis, the application of multi-layered porous materials as anechoic linings.

contact, this is not the case and it is mainly the "air wave" that is excited in the pores of the poroelastic material, with structural motion playing a minor role.

Resonant behaviour (usually highly damped, for obvious reasons) can also be exhibited by porous media. Allard (1993) contains an example of this, and Watson and Cummings (1994) show measured data on the bulk acoustic properties of lightweight fibrous media under differing degrees of static compression. The Watson and Cummings results show very pronounced structural resonance effects and resonance frequencies increasing with the extent of compression. However, any resonant effects are usually apparent only in narrow frequency bands, and can – as a first approximation at least – be ignored in many applications.

If a porous material is taken to be effectively rigid, it behaves as an "equivalent fluid" and its acoustic characteristics are conveniently expressible in the form of two complex, frequency-dependent, "bulk" properties such as characteristic impedance and propagation constant (alternatively "propagation coefficient"), or effective density and effective sound speed[2]. Once these two complex (i.e., four real) properties are known, it is usually more or less straightforward to include the porous medium in an acoustic – or vibroacoustic – model of the system being investigated. Examples of such models are those of Astley *et al.* (1991) and Cummings *et al.* (1999), both cases involving flat plates placed near or adjacent to – but *not* bonded to – layers of an equivalent fluid porous medium. The good correspondence between predicted and measured data in their work is an indication that a porous material in loose contact with, but not bonded to, a solid structure behaves as though there is no structural contact between the two. This clearly cannot always be the case, but experience has shown that in the majority of practical cases, unless mechanical bonding between a solid structure and a porous layer is deliberately ensured, vibrational transmission between the structure and the solid frame of the porous medium is minimal and the equivalent fluid description is adequate for design purposes at least.

[2] It is immaterial how the bulk properties are expressed, provided they offer a complete description of the porous medium; and it is, of course, a simple matter to find one pair of complex parameters from the other, as is the case in the two aforementioned examples.

This chapter first reviews traditional methods for determining the bulk acoustic properties of rigid porous media and then proposes a new method requiring only a single surface impedance measurement and an optimisation process of function coefficients to derive the bulk acoustic properties. The results of the proposed new method are compared with those obtained by one of the traditional methods. This chapter also, from an application point of view, compares the effectiveness, robustness and efficiency of evolutionary algorithms (EAs) and traditional calculus-based optimisation methods.

6.2 TRADITIONAL METHODS FOR DETERMINING BULK ACOUSTIC PROPERTIES

Traditionally, two approaches for determining the bulk acoustic properties of porous acoustic materials have been used. One is to measure these properties directly by acoustic experiments and the other is to calculate them using theoretical models or empirical curve-fitting formulae.

6.2.1 Measuring Bulk Acoustic Properties

Probably the most straightforward method for measuring the bulk acoustic properties was originally developed by Scott (1946) though it has been employed later by other authors such as Delany and Bazley (1970) and Cummings and Chang (1987). This method requires a direct measurement of the attenuation and phase change of a progressive plane wave system inside the test material sample to measure the propagation constant. This can be achieved by means of a probe microphone penetrating the interior of the material and detection of the sound pressure, at fixed points in the axial direction, in the measurement tube. A surface impedance measurement, performed on the test material sample with a standing wave technique, serves to measure the characteristic impedance of the material. Scott's method, though simple in principle to implement, is beset by two disadvantages: first, an *effectively* infinite (i.e., sufficiently great) length of homogeneous material is required to ensure that an essentially progressive wave system exists in the material for an appropriate distance beyond the surface presented to the standing-wave system, and second, the probe microphone must traverse a sufficient length of the

material and detect sound pressure either at discrete points or continuously in order to define the spatial attenuation and phase changes adequately (Smith and Parrott, 1983).

The inconvenience and other disadvantages of Scott's method have motivated the development of other measurement methods that rely only on surface impedance measurements on thinner samples. Surface impedance methods, for determining the bulk acoustic properties directly from measured data at each frequency of measurement, require two separate impedance tests with differing sample geometry (to find two complex bulk properties requires knowledge of two complex surface impedances). This can be accomplished by one of two procedures: in the first of these (the "two-thickness method"), each of two test material samples of differing thicknesses is terminated by a rigid wall, and in the second (the "two-cavity method"), a single thickness of the test material is terminated by two different cavity backing depths.

The two-thickness method was first developed by Smith and Parrot (1983). The measured surface impedances are related to the characteristic impedance W and the propagation constant γ by

$$Z_{d1} = W \coth(\gamma d_1), \tag{6.1}$$

$$Z_{d2} = W \coth(\gamma d_2), \tag{6.2}$$

where Z_{d1} is the measured surface impedance corresponding to the test sample thickness d_1 and Z_{d2} is the measured surface impedance corresponding to the test sample thickness d_2. It is experimentally convenient to make $d_2 = 2\ d_1$. The solutions for W and γ then become

$$W = [Z_{d1}(2Z_{d2} - Z_{d1})]^{1/2}, \tag{6.3}$$

$$\gamma = \left(\frac{1}{2d_1}\right) \ln\left[\frac{1 + [(2Z_{d2} - Z_{d1})/Z_{d1}]^{1/2}}{1 - [(2Z_{d2} - Z_{d1})/Z_{d1}]^{1/2}}\right]. \tag{6.4}$$

The two-thickness method is efficient. However, it requires that two test samples have identical bulk acoustic properties and that there is no variation associated with the mounting of test samples between measurements. Also, in the case of materials available in only one thickness, "doubling up" the material to achieve twice the original thickness introduces an unpredictable "interface impedance" effect, which could cause experimental errors in determining the bulk acoustic properties.

Compared with the two-thickness method, the two-cavity method only requires impedance measurements of one test sample. This method appears to have been originally suggested by Zwikker and Kosten (1949) and was subsequently employed by various workers including Delany and Bazley (19). Yaniv (1973) investigated this version of the two-cavity method in some detail by applying the electrical transmission line theory to an acoustic transmission line: when the line is terminated in a high-impedance (which can be achieved by terminating the acoustic material in a rigid wall) or a low-impedance (which can be achieved by terminating the acoustic material in an air cavity with a depth equal to a quarter-wavelength, itself terminated in a rigid wall), the impedance of the line can be expressed by

$$Z_{0S} = W \coth(\gamma d), \tag{6.5}$$

$$Z_{qS} = W \tanh(\gamma d), \tag{6.6}$$

where Z_{0S} is the surface impedance to an acoustic line terminated with zero air cavity between the line and the rigid wall; Z_{qS} is the surface impedance to an acoustic line terminated with an air cavity having a depth equal to a quarter-wavelength between the line and the rigid wall; and d is the thickness of the acoustic test material. Solving Equations (6.5) and (6.6) gives

$$W = \left(Z_{0S} Z_{qS}\right)^{1/2}, \tag{6.7}$$

$$\gamma = \left(\frac{1}{2d}\right) \ln\left[\frac{1+\left(Z_{qS}/Z_{0S}\right)^{1/2}}{1-\left(Z_{qS}/Z_{0S}\right)^{1/2}}\right]. \tag{6.8}$$

Since the characteristic impedance and the propagation constant are frequency dependent, the depth of the air cavity must be changed for every frequency of interest, which results in a very tedious measurement procedure. To implement this method, a movable rigid piston has sometimes been used to terminate the sample holder of the test material. In practice, however, such a piston would often be associated with some slight air leakage around its edge, thereby introducing a measurement error which cannot be taken into account quantitatively (ISO, 1998).

To avoid changing the air cavity depth at every frequency, as is required in Yaniv's method, and therefore to improve the efficiency of the two-cavity method, Utsuno *et al.* (1989) developed a method that requires surface impedance measurements of the test material sample with two different *arbitrary* depths of air cavity between the test material sample and the rigid wall. The surface impedance of the test material sample with an arbitrary depth of air cavity between the test material sample and the rigid wall, Z_{aS}, can be calculated by (Zwicker and Kosten, 1949)

$$Z_{aS} = W\frac{Z_a\cosh(\gamma d)+W\sinh(\gamma d)}{Z_a\sinh(\gamma d)+W\cosh(\gamma d)}, \tag{6.9}$$

where Z_a is the surface impedance of an arbitrary depth of air cavity between the test material sample and the rigid wall. On the basis of the Equation (6.9), Utsuno derived the following equations for calculating the characteristic impedance and propagation constant:

$$W = \pm\left[\frac{Z_{aS1}Z_{aS2}(Z_{a1}-Z_{a2})-Z_{a1}Z_{a2}(Z_{aS1}-Z_{aS2})}{(Z_{a1}-Z_{a2})-(Z_{aS1}-Z_{aS2})}\right]^{1/2}, \tag{6.10}$$

$$\gamma = \left(\frac{1}{2d}\right)\ln\left[\frac{Z_{aS1}+W}{Z_{aS1}-W}\frac{Z_{a1}-W}{Z_{a1}+W}\right], \tag{6.11}^{3}$$

[3] Equation (6.11) in (Utsuno et al, 1989) is $\gamma = \left(\frac{1}{2jd}\right)\ln\left[\frac{Z_{aS1}+W}{Z_{aS1}-W}\frac{Z_{a1}-W}{Z_{a1}+W}\right]$, where j is $\sqrt{-1}$. This is not correct.

where the sign in Equation (6.10) is selected so as to let the real part of W be positive; Z_{aS1} and Z_{aS2} are respectively the surface impedance of the test material sample with air cavity depth a_1 and a_2 between the test material sample and the rigid wall; and Z_{a1} and Z_{a2} are respectively the surface impedance of air cavity depth a_1 and a_2 between the test material sample and the rigid wall and can be calculated by

$$Z_{a1} = -j\rho c \cot\left(\frac{2\pi f}{c} a_1\right), \tag{6.12}$$

$$Z_{a2} = -j\rho c \cot\left(\frac{2\pi f}{c} a_2\right), \tag{6.13}$$

where ρ is the air density; c is the velocity of sound in air; and f is the frequency.

To avoid the problem of the elimination of the term (Z_{aS1} - Z_{aS2}) in Equation (6.10), an appropriate set of air cavity depths needs to be selected so that the following equation is not satisfied:

$$(a_1 - a_2) = nc/2f, \tag{6.14}$$

where n = 1, 2, 3, ... This implies that, for a high-resolution broadband application, Utsuno's method requires more than one pair of cavities (and therefore more than two measurements). It should also be pointed out that the aforementioned limitation (involving the possibility of air leakage) inherent in the Yaniv's two-cavity method would also apply to that of Utsuno's improved two-cavity method if a movable piston were to be used to vary the depth of the air cavity.

The two-cavity method can become inaccurate in the case of samples having high steady flow resistivities because the spatial attenuation rate in the material tends to increase with flow resistivity (other parameters remaining the same) and sound waves travelling along the length of the test sample can therefore be highly attenuated. The surface impedance in such cases will be determined primarily by the characteristic impedance of the material,

with the presence of the backing cavity having only a minor influence. Hence the two measured surface impedances required by the two-cavity method are nearly the same and uncertainties in the derived quantities (particularly the propagation constant) will be relatively large. To measure the bulk properties of materials having high flow resistivities, Champoux and Stinson (1991) developed a method that relates the characteristic impedance and propagation constant to the surface impedance of the test material sample and a transfer function measured along its length. However, to realise this method, a specially fabricated impedance tube has to be used.

6.2.2 Calculating Bulk Acoustic Properties

In vibroacoustical design methods involving equivalent fluid porous media, there are, in general, two ways of calculating the frequency-dependent pair of complex properties. The first is from theoretical models, such as those developed by Beranek (1947), Zwikker and Kosten (1949), Lambert (1982) and Attenborough (1983), for which the various nonacoustic properties (volume porosity, tortuosity, viscous and thermal characteristic lengths, for example) need to be known; and the second is by the use of empirical curve-fitting formulae, such as those of Delany and Bazley (1970). They involve the use of eight experimentally-determined function coefficients c_1-c_8, characteristic of a particular type of material though independent of its steady flow resistivity, provided that the microstructural geometry remains substantially similar and the fluid Prandtl number and ratio of principal specific heats remain effectively constant, and a *single* dimensionless frequency parameter $\rho f/\sigma$ (where σ is the flow resistivity of the material) as shown by Equations (6.15) and (6.16) (Cummings and Beadle, 1993):

$$W = \rho c\left[1 + c_1(\rho f/\sigma)^{c_2} + j\left(c_3(\rho f/\sigma)^{c_4}\right)\right], \tag{6.15}$$

$$\gamma = (2\pi f/c)\left[c_5(\rho f/\sigma)^{c_6} + j\left(1 + c_7(\rho f/\sigma)^{c_8}\right)\right]. \tag{6.16}$$

It should be noted that the formulae in their original form (Delany and Bazley, 1970) involved a *dimensional* parameter containing the frequency and flow resistivity. Delany and Bazley's formulae have proved very successful over many years for a wide variety of porous media including fibrous materials and plastic foams and have gained fairly wide

acceptance. These empirical formulae normally yield accurate predictions of the bulk acoustic properties of effectively rigid porous media, provided they are employed within the range of frequency parameter values used in determining the eight coefficients. However, if these formulae are extrapolated to lower values of the frequency parameter, they can yield physically meaningless predictions which are useless for predictive purposes - see Mechel (1988). This problem does not occur if the formulae are extrapolated beyond the high-frequency limit of the data. One way of overcoming the low-frequency problem to some extent, by at least producing "physical" predictions as the frequency parameter tends to zero, is to employ a (usually geometrically idealized or "phenomenological") predictive model at frequencies below the range of measured data. The phenomenological model of Morse and Ingård (1968) is about the simplest, though it does not generally yield particularly accurate predictions. In the absence of any knowledge of the microstructural geometry of the material it may, however, be appropriate. Estimates of the effective compressibility and density (both assumed to be real quantities) – at acoustic frequencies – of the gas contained in the pores of the material are required in this model. Models involving a specified microstructure are preferable - see Zwikker and Kosten (1949) - and an example of these is the parallel-fibre model of Mechel (1976/1977). This can be cast in a simplified form to give predictions of bulk properties that are valid at low frequencies, and this low-frequency forecast can be applied at frequencies below the range of measured data. Usually, however, there is some degree of mismatch between the low-frequency predictions and those from the empirical curve-fitting formulae, at the chosen transition point (in the frequency parameter) between the two prediction methods. For many purposes this would be of little consequence, but where the bulk acoustic properties are to be used in predictive schemes in which it is desirable or necessary for them to vary continuously with frequency (such as dissipative silencers and other sound attenuating devices), a jump in values of the bulk parameters at a certain frequency can upset the predictive process, particularly if some kind of extrapolation procedure in the frequency domain is employed. Mechel (1976) overcame this problem by slightly adjusting the empirical coefficients in the Delany and Bazley formulae so that a smooth transition between the low-frequency approximation and the empirical predictions was achieved. Unfortunately this method somewhat

degrades the prediction accuracy of the empirical formulae, sometimes to an unacceptable extent.

Kirby and Cummings (1999) have re-examined the problem of low-frequency modelling of the bulk properties of rigid fibrous media, and have proposed an improved semi-empirical prediction method for the low-frequency region which yields physically reasonable predictions at low frequencies, whilst at the same time giving accurate prediction at higher frequencies (in agreement with the Delany and Bazley formulae) as well as continuity in bulk property values between low and higher frequencies. This model is based on a parallel-fibre geometry, which is used in conjunction with the Delany and Bazley formulae and their associated empirically-determined coefficients.

If one is to use measurements as the basis for prediction of the bulk acoustic properties of rigid porous media with geometrically similar microstructures, then the Delany and Bazley formulae are ideally suited for this purpose, and extrapolation to low frequencies can be achieved by methods such as those of Mechel (1976/1977;1976), or Kirby and Cummings (1999). Although the formulae of Delany and Bazley (1970) were originally conceived for fibrous media, they are applicable to porous media with a wide variety of microstructural geometries. Not surprisingly, differing sets of values of the eight coefficients are found for different types of material - see Cummings and Beadle (1993). For example, geometrically similar, fully reticulated, polyurethane foams have a set of values differing significantly from those for typical fibrous materials - see Delany and Bazley (1970).

6.3 DERIVING BULK ACOUSTIC PROPERTIES FROM A SINGLE IMPEDANCE TEST

The aforementioned experimental techniques in Section 6.2.1 are largely unrelated to the notion of employing curve-fitting formulae or theoretical models, such as those introduced in Section 6.2.2, to describe the bulk acoustic properties of rigid porous media. Rather they are concerned with (more or less) directly measuring the bulk

properties themselves at each measurement frequency. If, however, formulae such as those of Delany and Bazley, or a theoretical model involving experimentally-determined parameters, are to be "fitted" to a series of experimental data taken at a number of frequencies (preferably over a fairly wide frequency range), then the requirement of conducting two separate impedance measurements at each frequency is removed. Indeed, surface impedance data on one sample with a rigid backing surface will suffice very well. By this means, optimum values of the coefficients in the curve-fitting formulae, or the physical parameters in the theoretical formulae, may be found. An example of this approach is the work of Braccesi and Bracciali (1998), who employed a least squares regression method and the model of Zwikker and Kosten (1949) to fit measured acoustic pressure reflection coefficient data from a rigidly-backed sample of porous material mounted in a tube. The inferred parameters were steady flow resistivity and structure factor. This method proved successful, its main drawback being the inability of using the simple theoretical model to give very accurate predictions over a broad frequency range.

The method using curve-fitting formulae such as those of Delany and Bazley (1970) – with an appropriate mathematical form and enough empirical coefficients to allow an accurate fit to data – in an optimisation procedure to yield a best fit to experimental data taken from a *single sample* over a wide frequency range, has several advantages over the aforementioned two-measurement methods. First, any experimental errors arising from material inhomogeneity (in the case of the two-thickness method) or sample mounting (for example, edge effects of various kinds) between the two tests will be absent. Second, there will be no cumulative random errors in the results arising from the fact that two sets of experimental data are being combined. And third, conducting only one impedance test is less time-consuming than doing two tests, so more effort can be devoted to experimental accuracy within a given time.

6.3.1 Basis for Proposed New Method

If the characteristic impedance W and the propagation constant γ in Equation (6.9) are substituted with the Equations (6.15) and (6.16), Equation (6.9) is transformed to

$$Z_{aS} = \rho c\left[1 + c_1(\rho f/\sigma)^{c_2} + j\left(c_3(\rho f/\sigma)^{c_4}\right)\right]\bullet$$
$$\frac{Z_a \cosh\left((2\pi f/c)\left[c_5(\rho f/\sigma)^{c_6} + j\left(1 + c_7(\rho f/\sigma)^{c_8}\right)\right]d\right) + \rho c\left[1 + c_1(\rho f/\sigma)^{c_2} + j\left(c_3(\rho f/\sigma)^{c_4}\right)\right]\sinh(\gamma d)}{Z_a \sinh\left((2\pi f/c)\left[c_5(\rho f/\sigma)^{c_6} + j\left(1 + c_7(\rho f/\sigma)^{c_8}\right)\right]d\right) + \rho c\left[1 + c_1(\rho f/\sigma)^{c_2} + j\left(c_3(\rho f/\sigma)^{c_4}\right)\right]\cosh(\gamma d)}$$

, (6.17)

and if let $f(c_1, c_2, \ldots, c_8)$ represents the right hand side of Equation (6.17), it can be further transformed to

$$Z_{as} = f(c_1, c_2, \ldots, c_8). \tag{6.18}$$

When the depth of air cavity is zero, the characteristic impedance W and the propagation constant γ in Equation (6.5) can be substituted with the Equations (6.15) and (6.16), namely

$$Z_{0S} = \rho c\left[1 + c_1(\rho f/\sigma)^{c_2} + j\left(c_3(\rho f/\sigma)^{c_4}\right)\right]\coth\left((2\pi f/c)\left[c_5(\rho f/\sigma)^{c_6} + j\left(1 + c_7(\rho f/\sigma)^{c_8}\right)\right]d\right)$$

, (6.19)

and if let $f(c_1, c_2, \ldots, c_8)$ represents the right hand side of the equal mark in Equation (6.19), it can be further transformed to

$$Z_{0s} = f(c_1, c_2, \ldots, c_8). \tag{6.20}$$

On the basis of the formulae (6.18) and (6.20), the procedure for the new method can be described as first, to determine Z_{aS} or Z_{0S} by one surface impedance measurement of the test material sample with an arbitrary depth of air cavity or zero air cavity between the test material sample and the rigid wall and then, to conduct a function coefficients optimisation process to find a set of c_1-c_8 that minimises difference between $f(c_1, c_2, \ldots, c_8)$ and the measured surface impedance Z_{aS} or Z_{0S}.

6.3.2 An Application Example

An application example is given in this section to demonstrate the use of the proposed new method. In the present example, a piece of 30 mm thick open-cell foam, with a flow resistivity of 3900 SI rayls/m, is used as the test material sample. The bulk properties obtained using the proposed new method are compared with those obtained using Utsuno's improved two-cavity method (Utsuno *et al.*, 1989) and the surface impedance calculated using the bulk properties obtained from the proposed new method is verified with that measured.

6.3.2.1 Measurement of surface impedance

The surface impedance of the material sample with an air cavity of 90 mm between the test material sample and the rigid wall was measured for frequencies between 300 and 3800 Hz with a step of 12.5 Hz (provided by Shin H.-C. at the University of Cambridge, UK, personal communication, 3rd March, 2005) and the measurement result is shown in Tables B.1 in Appendix B. During the impedance measurement, the air density ρ = 1.213 kg/m^3 and the air velocity c = 342.19 m/s.

6.3.2.2 Function coefficients optimisation

To make the new method useful, an effective, efficient and robust optimisation technique is required. As discussed in Section 3.5 of the present thesis, there will always remain a dichotomy between efficiency and general applicability and between reliability and effort of problem-solving, especially with optimum-seeking algorithms. Any specific knowledge about the given situation may be used to specify an adequate solution algorithm. On the other hand, there cannot exist one method that solves all problems effectively as well as efficiently.

A theoretical comparison between the calculus-based optimisation techniques and EAs has been provided in Section 3.5 of the present thesis. In this chapter, both calculus-based optimisation techniques and evolutionary algorithms (EAs) are investigated for their effectiveness, robustness and efficiency in solving the function coefficients optimisation problem of the present example.

6.3.2.2.1 Objective function

Since both the measured surface impedance Z_{aSFoam} and $f(c_1, c_2, \ldots, c_8)$ are complex values, the object of the function coefficients optimisation in this example is to find a set of c_1-c_8 that will result in an overall minimum root mean square (RMS) error between Z_{aSFoam} and $f(c_1, c_2, \ldots, c_8)$. In other words, the objective function of the optimisation can be written as

$$\text{Min } y = \sqrt{\left[RMS\left(Re\left(f(c_1, c_2, \ldots, c_8) - Z_{as\,Form}\right)\right)\right]^2 + \left[RMS\left(Im\left(f(c_1, c_2, \ldots, c_8) - Z_{as\,Form}\right)\right)\right]^2},$$

$$\text{subject to } lb \le (c_1, c_2, \ldots, c_8) \le ub, \tag{6.21}$$

where *Re* and *Im* respectively represent the real part and the imaginary part of the difference between Z_{aSFoam} and $f(c_1, c_2, \ldots, c_8)$, *lb* and *ub* are respectively the lower and upper bounds of coefficients $(c_1, c_2, \ldots, c_8)$ and y is the objective value.

6.3.2.2.2 Optimisation techniques investigated

The calculus-based optimisation techniques considered in the present investigation are the Gauss-Newton method (Dennis, 1977) with line-search (Fletcher, 1987; Nocedal and Wright, 1999), the Levenberg-Marquardt method (Levenberg, 1944; Marquardt, 1963) with line-search, the BFGS Quasi-Newton method (Broyden, 1970; Fletcher, 1970; Goldfarb, 1970; Shanno, 1970) with line-search, and the Sequential Quadratic Programming (SQP) method (Biggs, 1975; Han, 1977; Powell, 1978a; Powell, 1978b) for constrained optimisation. At each search-iteration of the first three methods, two steps are involved: first determining the search direction by using the Gauss-Newton method, the Levenberg-Marquardt method or the BFGS Quasi-Newton method and then determining the search step-length using a line-search procedure. At each search-iteration of the SQP method for constrained optimisation, the constrained optimisation problem is transformed to a quadratic programming (QP) subproblem by linearising the nonlinear constraints and appending them to the objective function. Then the QP subproblem is solved using the BFGS Quasi-Newton method with line-search. Details of the above four calculus-based optimisation techniques are not included here as they have been studied, developed,

applied and documented at length - see Dennis (1977), Fletcher (1987), Gill *et al.* (1981), Powell (1983) and MathWorks (2002). In addition, these methods have been coded and implemented in the Matlab Optimisation Toolbox (MathWorks, 2002) as standard functions, the *lsqnonlin* function (based on Gauss-Newton method with line-search or Levenberg-Marquardt method with line-search), the *fminunc* function (based on BFGS Quasi-Newton method with line-search) and the *fmincon* function (based on SQP method), all of which are used in the present investigation.

Table 6.1 shows the settings of the main function parameters during each operation of the above Matlab functions (MathWorks, 2002) in the present investigation. Other function parameters that are not shown in Table 6.1 were set to their default values. More detailed information regarding these function parameters can be found in MathWorks (2002).

Table 6.1 Settings of the main function parameters for the Matlab calculus-based optimisation functions investigated in the present application example

Parameter Names	Descriptions	*lsqnonlin* Function (using Gauss-Newton method)	*Lsqnonlin* Function (using Levenberg-Marquardt method)	*Fminunc* Function	*Fmincon* Function
DiffMaxChange	Maximum change in variables for finite difference derivatives.	0.1	0.1	0.1	0.1
DiffMinChange	Minimum change in variables for finite difference derivatives.	1e-008	1e-008	1e-008	1e-008
LevenbergMarquardt	Preference for Levenberg-Marquardt over Gauss-Newton algorithm.	Off	On	Not applicable	Not applicable
LineSearchType	Line search algorithm choice.	Quadcubic	Quadcubic	Quadcubic	Not applicable
MaxFunEvals	Maximum number of function evaluations allowed.	150,000	50,000	1000	1000
MaxIter	Maximum number of iterations allowed.	20,000	10,000	400	400

Parameter Names	Descriptions	*lsqnonlin* Function (using Gauss-Newton method)	*Lsqnonlin* Function (using Levenberg-Marquardt method)	*Fminunc* Function	*Fmincon* Function
TolCon	Termination tolerance on the constraint violation.	Not applicable	Not applicable	Not applicable	1e-006
TolFun	Termination tolerance on the function value.	1e-009	1e-009	1e-006	1e-006
TolX	Termination tolerance on x.	1e-009	1e-009	1e-006	1e-006

If the optimisation converges, the operation of the function terminates automatically when any of the conditions set in parameters MaxFunEvals, MaxIter, TolFun and TolX is met. Otherwise, it will be terminated manually.

The Genetic and Evolutionary Algorithm Toolbox for Use with Matlab (GEATbx) (Pohlheim, 2004) introduced in chapter 3 of the present thesis was applied to investigate the efficiency and robustness of EAs for the present function coefficients optimisation problem. For every operation of the EA using GEATbx, the settings for the main parameters were:

- representation of variables: real value.
- fitness assignment: rank-based fitness assignment (Fonseca and Fleming, 1993; 1998). See chapter 3 of this thesis for more details.
- evolutionary operator for selection: stochastic universal sampling (SUS) (Baker, 1987) which works on both real-value and integer-value data representation. Using this selection method, the individuals in the population are mapped onto contiguous segments of a line, such that each individual's segment is equal in length to its fitness. Equally spaced pointers, as many as the number of individuals to be selected, are placed along the line. This selection method has the advantage of providing zero bias and minimum spread during the selection.
- evolutionary operator for recombination: discrete recombination (Mühlenbein and Schlierkamp-Voosen, 1995) which performs an exchange of variable values between the parents. For each variable position of the offspring, the parent contributing its variable to the offspring is chosen randomly with equal

probability. Discrete recombination can be applied to all (real-value, integer-value and binary-value) variable representations.

- recombination rate: 1. This means all parents have the possibility of contributing to the value of each variable of the offspring.
- evolutionary operator for mutation: real-value mutation function (Pohlheim, 2004).
- mutation rate: 1. This means on the average 1 variable per individual to be mutated.
- mutation range: 0.02. This means the initial mutation step sizes will be 0.02 times the domain of each variable.
- population size: 100. This means there are 100 individuals (solutions) per population.
- generation gap: 0.9. This means 90% of the population to be reproduced every generation. Since in every generation there are 100 individuals as defined by the population size, the reproduction of 90% of the population will result in $100 \times 0.9 = 90$ function evaluations for every generation after the initial population, which requires 100 function evaluations because they are new individuals.
- termination method: running mean method or maximum number of generations. Based on these two methods, the optimisation operation terminates either when, for 15 consecutive generations, the improvement of the objective value is less than 1e-6 or when the maximum number of generations is reached.

All the other internal parameters necessary for operating GEATbx were set to their default values. Details of these parameters and guidelines for setting them can be found in Pohlheim (2004).

6.3.2.3 Optimisation and statistical analysis results

Table 6.2 shows all optimisation conditions using surface impedance measurement results between 300 and 3800 Hz. Table 6.3 shows optimised coefficients c_1-c_8 of each condition in Table 6.2 and the statistical analysis results in terms of the overall RMS error between Z_{aSFoam} and the optimised $f(c_1, c_2, \ldots, c_8)$; the RMS error between the real part of Z_{aSFoam} and the real part of the optimised $f(c_1, c_2, \ldots, c_8)$; the RMS error between the

imaginary part of Z_{aSFoam} and the imaginary part of the optimised $f(c_1, c_2, \ldots, c_8)$; the correlation coefficients R^2 (the "coefficient of determination") between the real part of Z_{aSFoam} and the real part of the optimised $f(c_1, c_2, \ldots, c_8)$; and the correlation coefficients R^2 between the imaginary part of Z_{aSFoam} and the imaginary part of the optimised $f(c_1, c_2, \ldots, c_8)$.

Table 6.2 Optimisation conditions using surface impedance measurement results between 300 and 3800 Hz

Optimisation Condition ID	Optimisation Method Used	Initial Value(s) of c_1-c_8	*lb* of c_1-c_8	*ub* of c_1-c_8	Search Termination Condition
1	*lsqnonlin* Function (using Gauss-Newton method)	[0.0953, -0.491, 0.0986, -0.665, 0.167, -0.636, 0.174, -0.372] (Cummings and Beadle, 1993)	Not applicable	Not applicable	Termination tolerance on the function value, 1e-9, set in TolFun reached
2	*lsqnonlin* Function (using Gauss-Newton method)	[3, 3, 3, 3, 3, 3, 3, 3]	Not applicable	Not applicable	Not converged
3	*Lsqnonlin* Function (using Levenberg-Marquardt method)	[0.0953, -0.491, 0.0986, -0.665, 0.167, -0.636, 0.174, -0.372] (Cummings and Beadle, 1993)	Not applicable	Not applicable	Termination tolerance on the function value, 1e-9, set in TolFun reached
4	*Lsqnonlin* Function (using Levenberg-Marquardt method)	[3, 3, 3, 3, 3, 3, 3, 3]	Not applicable	Not applicable	Not converged
5	*Fminunc* Function	[0.0953, -0.491, 0.0986, -0.665, 0.167, -0.636, 0.174, -0.372] (Cummings and Beadle, 1993)	Not applicable	Not applicable	Termination tolerance on the function value, 1e-6, set in TolFun reached
6	*Fminunc* Function	[3, 3, 3, 3, 3, 3, 3, 3]	Not applicable	Not applicable	Not converged
7	*Fmincon* Function	[0.0953, -0.491, 0.0986, -0.665, 0.167, -0.636, 0.174, -0.372] (Cummings and Beadle, 1993)	[0,-1,0,-1,0,-1,0,-1]	[1,0,1,0,1,0,1,0]	Termination tolerance on the function value, 1e-6, set in TolFun reached
8	*Fmincon* Function	[3, 3, 3, 3, 3, 3, 3, 3]	[-10 -10 -10 -10 -10 -10 -10 -10]	[10 10 10 10 10 10 10 10]	Termination tolerance on the function value, 1e-6, set in TolFun reached
9	*Fmincon* Function	[0, 0, 0, 0, 0, 0, 0, 0]	[0,-1,0,-1,0,-1,0,-1]	[1,0,1,0,1,0,1,0]	Termination tolerance on the function value,

Optimisation Condition ID	Optimisation Method Used	Initial Value(s) of c_1-c_8	*lb* of c_1-c_8	*ub* of c_1-c_8	Search Termination Condition
					1e-6, set in TolFun reached
10	*Fmincon* Function	[0, 0, 0, 0, 0, 0, 0, 0]	[-10 -10 -10 -10 -10 -10 -10 -10]	[10 10 10 10 10 10 10 10]	Not converged
11	EAs	[0.0953, -0.491, 0.0986, -0.665, 0.167, -0.636, 0.174, -0.372] (Cummings and Beadle, 1993)	[0,-1,0,-1,0,-1,0,-1]	[1,0,1,0,1,0,1,0]	Terminated when for 15 consecutive generations the improvement of the objective value is less than 1e-6.
12	EAs	Randomly initialised (Pohlheim, 2004)	[0,-1,0,-1,0,-1,0,-1]	[1,0,1,0,1,0,1,0]	Terminated when for 15 consecutive generations the improvement of the objective value is less than 1e-6.
13	EAs	[3, 3, 3, 3, 3, 3, 3, 3]	[-10 -10 -10 -10 -10 -10 -10 -10]	[10 10 10 10 10 10 10 10]	Terminated when for 15 consecutive generations the improvement of the objective value is less than 1e-6.
14	EAs	The resulted last generation of optimisation condition 13	[-10 -10 -10 -10 -10 -10 -10 -10]	[10 10 10 10 10 10 10 10]	Terminated after 300 generations.
15	EAs	Randomly initialised (Pohlheim, 2004)	[-10 -10 -10 -10 -10 -10 -10 -10]	[10 10 10 10 10 10 10 10]	Terminated when maximum number of generations (4,800) reached.

Different initial values, except those of the optimisation condition 14, were used to test the sensitivity of different optimisation techniques to the starting point of the search. The initial values of c_1-c_8 for optimisation conditions 1, 3, 5, 7 and 10 are based on the work of Cummings and Beadle (1993), in which they studied twelve different open-cell foams and obtained a generic set of c_1-c_8 for open-cell foams with flow resistivities in the range of 60 – 6229 SI rayls/m. The optimisation condition 14 is a continuation of the optimisation condition 13 so its initial values (initial population) were the last generation of the optimisation condition 13. Matlab functions *lsqnonlin* and *fminunc* are for unconstrained optimisation problems and, therefore, boundary constraints cannot be assigned to them. Different boundary constraints were assigned to the Matlab function *fmincon* and EAs to test the sensitivity of each optimisation method to the range of the search.

Table 6.3 Optimisation and statistical analysis results using surface impedance measurement results between 300 and 3800 Hz

Optimisation Condition ID	Optimisation Results of c_1-c_8	Number of Function Evaluations When Optimised Results Found	Statistical Analysis Results				
			Overall RMS Error	RMS error of the Real Part	RMS Error of the Imaginary Part	R^2 of the Real Part	R^2 of the Imaginary Part
1	[0.1408 -0.2634 0.1171 -0.6208 0.1905 -0.6908 0.1612 -0.4500]	169,619	0.0558	0.0399	0.0390	0.9991	0.9991
2	Not converged						
3	[0.1258 -0.4504 0.1110 -0.6923 0.1887 -0.7057 0.1623 -0.4608]	30,815	0.0537	0.0374	0.0386	0.9992	0.9991
4	Not converged						
5	[0.1316 -0.3818 0.1080 -0.7329 0.1896 -0.7015 0.1626 -0.4527]	157	0.0531	0.0364	0.0387	0.9992	0.9991
6	Not converged						
7	[0.1317 -0.3812 0.1081 -0.7320 0.1896 -0.7016 0.1626 -0.4528]	186	0.0531	0.0364	0.0387	0.9992	0.9991
8	[0.1318 -0.3801 0.1082 -0.7311 0.1896 -0.7015 0.1626 -0.4528]	693	0.0531	0.0364	0.0387	0.9992	0.9991
9	[0.1317 -0.3808 0.1082 -0.7309 0.1896 -0.7015 0.1626 -0.4528]	612	0.0531	0.0364	0.0387	0.9992	0.9991
10	Not converged						
11	[0.1311 -0.3878 0.1073 -0.7412 0.1895 -0.7024 0.1628 -0.4519]	70,210	0.0531	0.0364	0.0387	0.9992	0.9991
12	[0.1323 -0.3733 0.1091 -0.7192 0.1896 -0.7009 0.1624 -0.4535]	177,490	0.0531	0.0364	0.0387	0.9992	0.9991
13	[0.1361 -0.3354 0.1097 -0.7129 0.1902 -0.6970 0.1623 -0.4527]	156,430	0.0533	0.0367	0.0387	0.9992	0.9991
14	[0.1329 -0.3676 0.1085 -0.7263 0.1899 -0.6986 0.1625 -0.4525]	27,010 + 156,430 = 183,440	0.0531	0.0364	0.0387	0.9992	0.9991
15	[0.1323 -0.3744 0.1085 -0.7265 0.1898 -0.6998 0.1625 -0.4536]	432,010	0.0531	0.0364	0.0387	0.9992	0.9991

For this investigation, on average it takes the computer (IBM T41 laptop with Intel Pentium M 1.6 Gb CPU and 512 Mb Ram) 0.018 seconds for one function evaluation. The optimisation condition 14 is used as a continuation of the optimisation condition 13 to check if the objective value of condition 13 can be further minimised with the increased number of generations so the sum of the number of function evaluations of condition 13 (156,430) and the number of function evaluations of 300 generations ($100 + 99 \times 90 = 27{,}010$) is regarded as the number of function evaluations required to achieve the optimised objective value in the optimisation condition 14.

It is considered that any of the optimised sets of c_1-c_8 of optimisation conditions 5, 7, 8, 9, 11, 12, 14 and 15 is the optimised solution because they all result in the same minimum objective value (i.e. the overall RMS error) and other statistical analysis results and there are no significant differences between any set of c_1-c_8 found in these conditions. Hence, any optimised set of c_1-c_8 of optimisation conditions 5, 7, 8, 9, 11, 12, 14 and 15 can be used to calculate the characteristic impedance and the propagation constant of the test material sample of the present example for the frequency range of 300 to 3800 Hz according to Equations (6.15) and (6.16). Those calculated using the optimised set of c_1-c_8 of the optimisation 7 are presented in Table B.3 and Table B.4 in Appendix B. Substituting the derived bulk acoustic properties in Table B.3 and Table B.4 into Equation (6.9), the surface impedance of the material sample with an air cavity of 95 mm between the sample and the rigid wall can be calculated and the calculated results are shown in Table B.5 in Appendix B.

As shown by the results of optimisation conditions 1 and 3, the *lsqnonlin* function based on the Gauss-Newton method with line-search or the Levenberg-Marquardt method with line-search is neither effective nor efficient for the present example. Results of the optimisation conditions 5 and 7 show that some traditional calculus-based optimisation techniques, such as the *fminunc* function (based on the BFGS Quasi-Newton method with line-search) and the *fmincon* function (based on the SQP method), can be effective and efficient optimisation methods for the present example when the starting point and/or the range of the search are properly defined. For both of these two optimisation conditions

the optimisation process was completed in only around three seconds. However, when the starting point and/or the range of the search are not properly defined either the efficiency of search is reduced as shown by the increased number function evaluations of optimisation conditions 8 and 9 or the optimisation does not converge at all as shown by optimisation conditions 2, 4, 6 and 10.

Although, as shown by the optimisation condition 11, with the same starting point of the search the EA is more efficient and effective than the *lsqnonlin* function (based on the Gauss-Newton method with line-search or the Levenberg-Marquardt method with line-search), results of the optimisation conditions 11 to 15 show that for the present example the EA is an effective method for finding the minimum solution but it is not as efficient as the *fminunc* function (based on the BFGS Quasi-Newton method with line-search) or the *fmincon* function (based on the SQP method) . This is easily understandable because, for every operation of EA, an evaluation of a large number of potential solutions is undertaken. In the present example 90 function evaluations were made for every new generation. Nonetheless, the EA is not sensitive to the starting point (which can even be randomly generated) or to the range of the search. This certainly proves the robustness of the EA.

6.3.2.4 Bulk properties and the surface impedance obtained using Utsuno's improved two-cavity method

To utilise Utsuno's improved two-cavity method (*Utsuno et al.*, 1989), an additional surface impedance of the material sample with an air cavity of 53 mm between the sample and the rigid wall was measured for frequencies between 300 and 3800 Hz with a step of 12.5 Hz (provided by Shin H.-C. at the University of Cambridge, UK, personal communication, 3rd March, 2005) and the measurement result is shown in Tables B.2 in Appendix B. On the basis of the measured surface impedances in Table B.1 and Table B.2 bulk acoustic properties between 300 and 3800 Hz (see Tables B.6 and B.7 in Appendix B) were obtained using Equations (6.10) and (6.11).

6.3.2.5 Verification and comparison

Figure 6.1 compares the measured surface impedance in Table B.1 with the calculated surface impedance in Table B.5 obtained by the proposed new method.

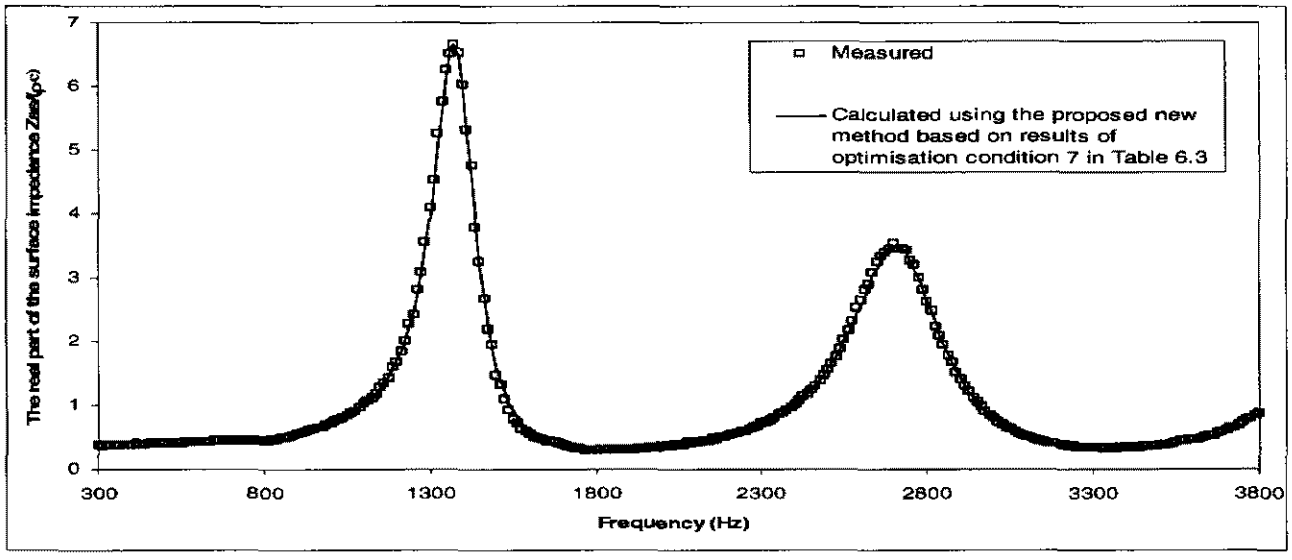

(a)

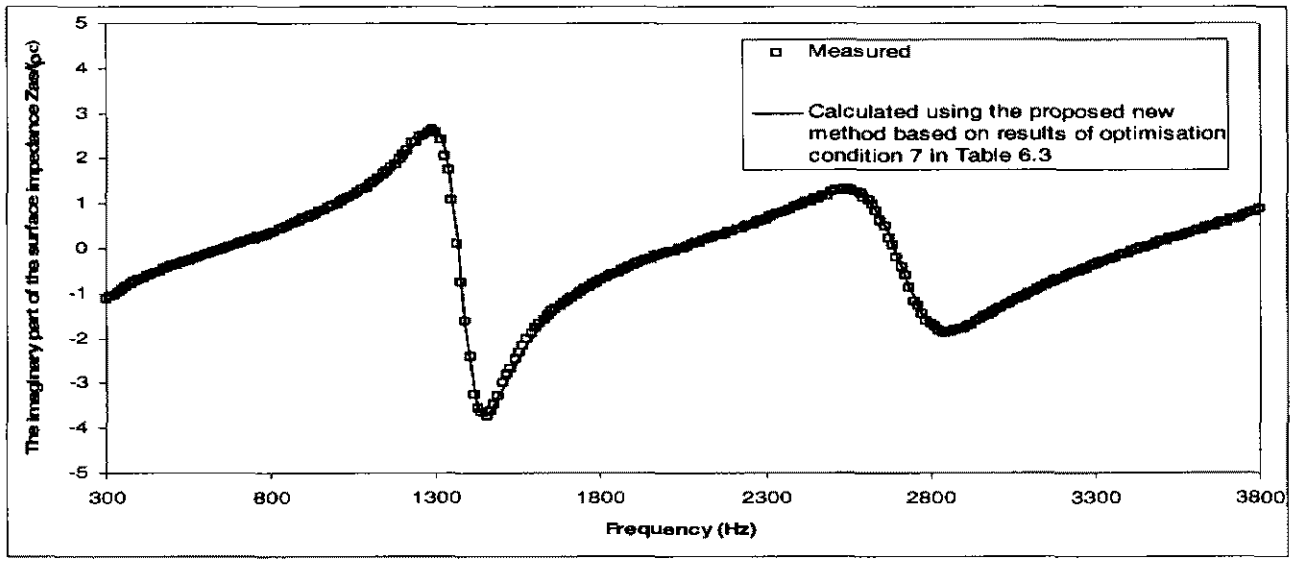

(b)

Figure 6.1 Comparison between (a) the real part and (b) the imaginary part of the measured surface impedance (normalised by the characteristic impedance of the air, ρc) in Table B.1 and those of the calculated surface impedance (normalised by the characteristic impedance of the air, ρc) in Table B.5 obtained by the proposed new method.

Figure 6.2 below compares the bulk acoustic properties, characteristic impedance and propagation constant, in Table B.3 and Table B.4 derived from the proposed new method with those in Table B.6 and Table B.7 obtained by Utsuno's improved two-cavity method.

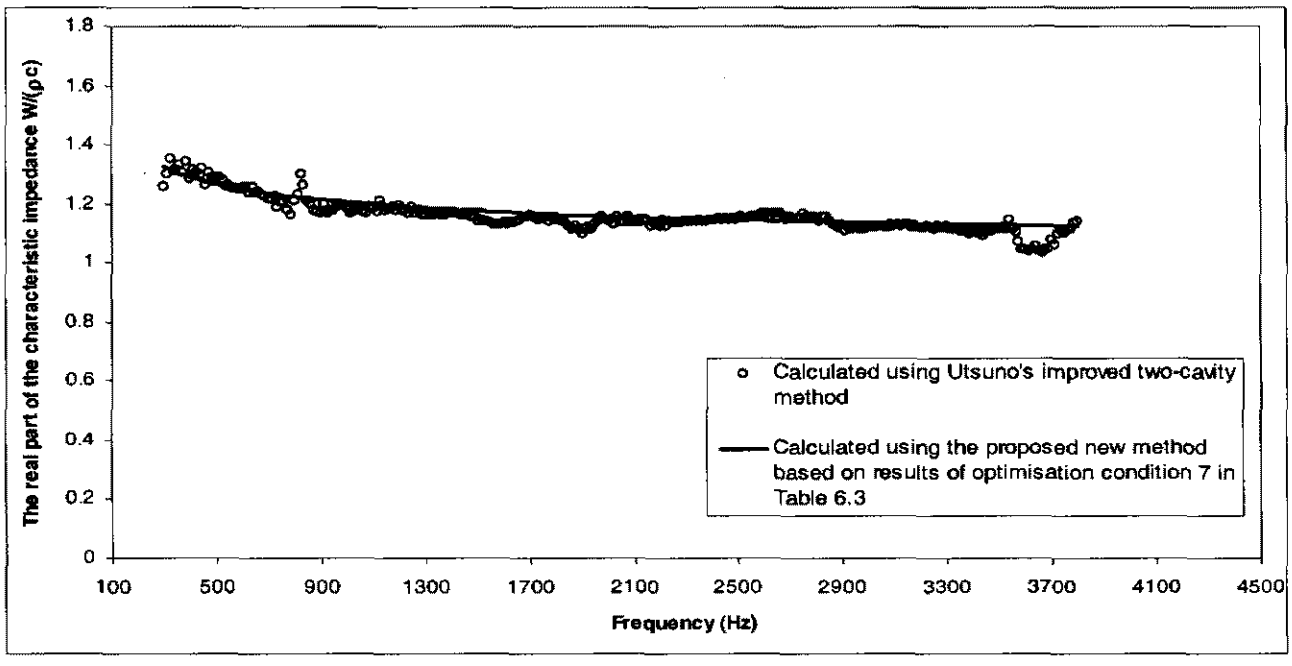

(a)

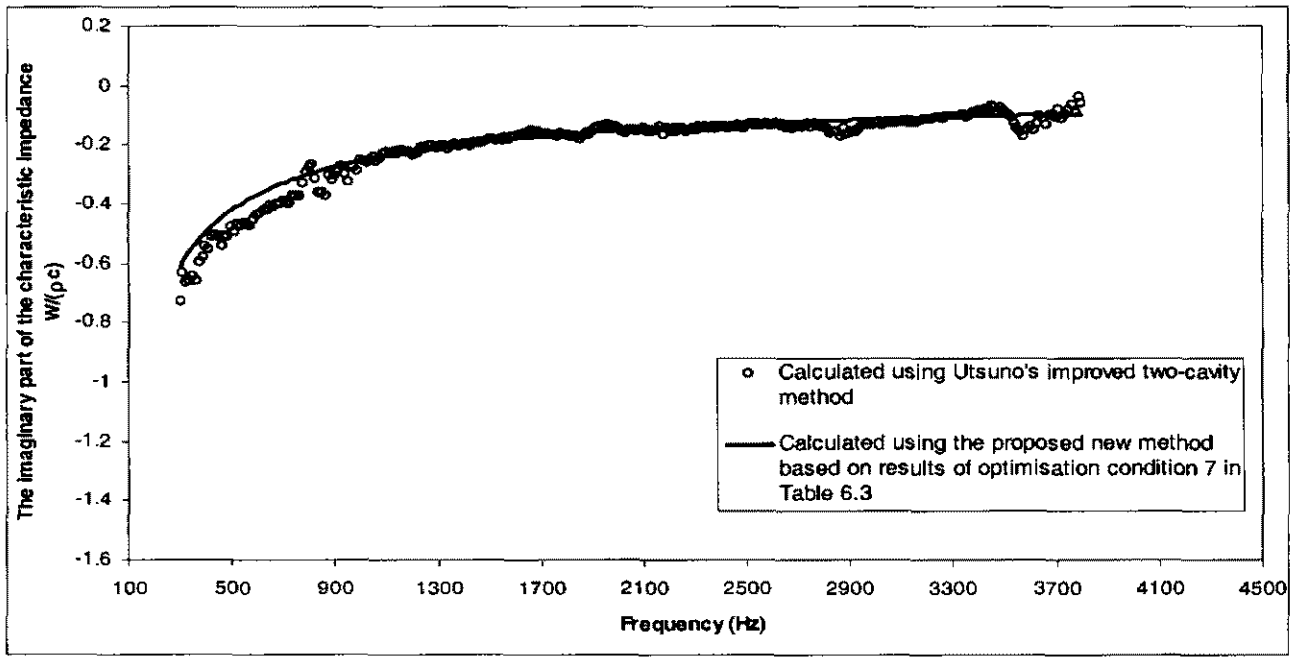

(b)

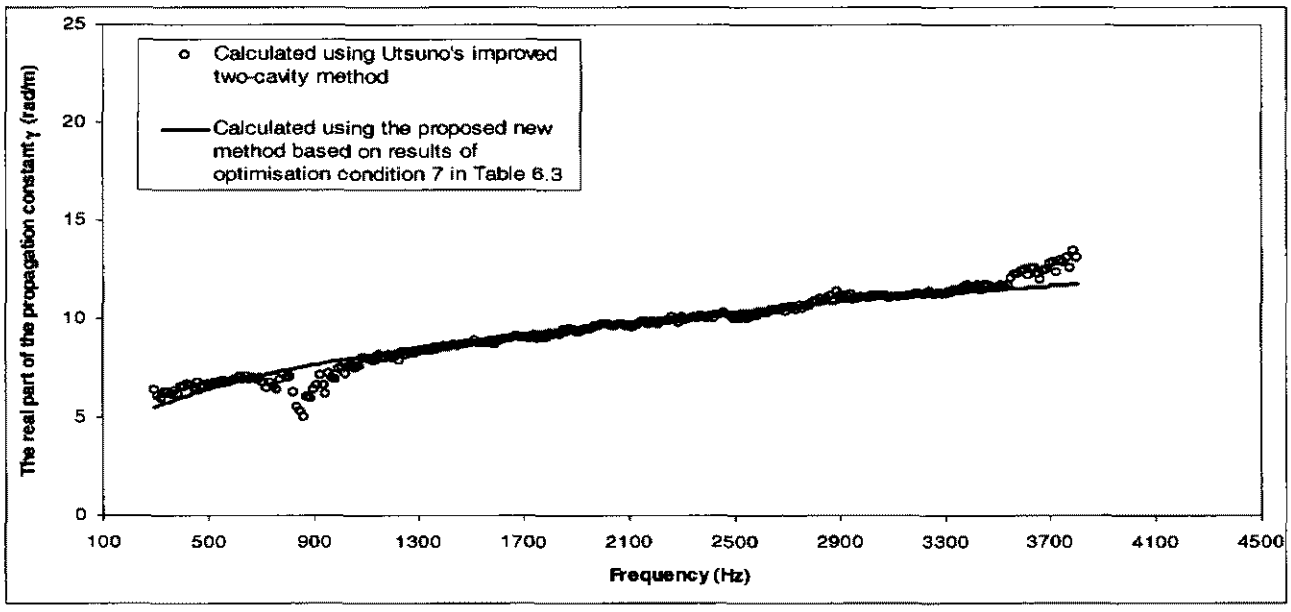

(c)

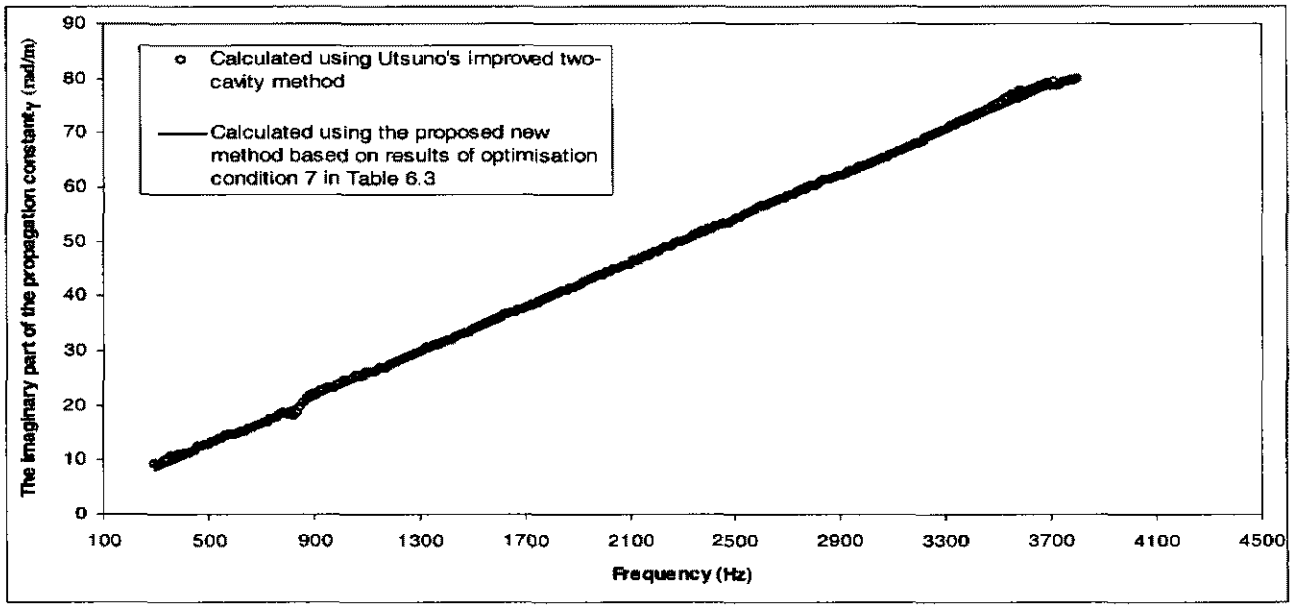

(d)

Figure 6.2 Comparison between (a) the real part and (b) the imaginary part of the characteristic impedance (normalised by the characteristic impedance of the air, ρc) between 300 and 3800 Hz derived from the proposed new method and those obtained by Utsuno's improved two-cavity method and comparison between (c) the real part and (d) the imaginary part of the propagation constant between 300 and 3800 Hz derived from the proposed new method and those obtained by Utsuno's improved two-cavity method.

An excellent fit between the surface impedance measured and that calculated using the proposed new method can be observed in Figure 6.1. Generally, the bulk properties derived from the proposed new method are also in good agreement with those obtained using Utsuno's improved two-cavity method. The discrepancies between 300 and 800 Hz in Figure 6.2 (b) and (c) are probably due to cumulative systematic and random errors in the results arising from the fact that two sets of experimental data were being combined for Utsuno's improved two-cavity method. In the "Utsuno" method, there are several possibilities for systematic errors that are rather difficult to quantify. They include (i) differing degrees of sample compression or stretching between the two experiments, caused by static friction between the tube walls and the sample, (ii) errors in a precise knowledge of the cavity depths in the two experiments, (iii) the neglect of viscothermal acoustic boundary-layer effects (Scott, 1946) in both the surface impedance measurement and the theory for processing the two sets of impedance data to find the bulk properties, (iv) possible differing structural edge-mounting effects in the sample, or small air-gaps, between the two tests. It is suspected that the discrepancies starting from about 3500 Hz in Figure 6.2 (a), (b) and (c) occur because the first half-wavelength frequency in Equation (6.14) is being approached. In the present example, since the two cavities are 90 mm and 53 mm and the air velocity is 342.19 m/s, the first half-wavelength frequency based on Equation (6.14) is 4624 Hz.

To further investigate the discrepancies at high frequencies, additional surface impedance measurement results were included to calculate the bulk acoustic properties. These are shown in Tables B.8 and B.9 in Appendix B, for the same test material sample, with both cavity depths, at high frequencies between 3812.5 and 4500 Hz with a step of 12.5 Hz (provided by Shin H.-C. at the University of Cambridge, UK, personal communication, 3rd March, 2005). In other words, to derive the bulk acoustic properties of the material, the surface impedance measurement results between 300 and 4500 Hz with an air cavity depth of 90mm were used for the proposed new method; and the surface impedance measurement results between 300 and 4500 Hz with both cavity depths were used for Utsuno's improved two-cavity method. The optimisation condition for the proposed new

method using surface impedance measurement results between 300 and 4500 Hz is shown in Table 6.4 and the optimisation results are shown in Table 6.5.

Table 6.4 Optimisation conditions using surface impedance measurement results between 300 and 4500 Hz

Optimisation Condition ID	Optimisation Method used	Initial Value(s) of c_1-c_8	*lb* of c_1-c_8	*ub* of c_1-c_8	Search Termination Condition
16	*Fmincon* Function	[0.0953, -0.491, 0.0986, -0.665, 0.167, -0.636, 0.174, -0.372] (Cummings and Beadle, 1993)	[0,-1,0,-1,0,-1,0,-1]	[1,0,1,0,1,0,1,0]	Termination tolerance on the function value, 1e-6, set in TolFun reached

Table 6.5 Optimisation and statistical analysis results using surface impedance measurement results between 300 and 4500 Hz

Optimisation Condition ID	Optimisation Results of c_1-c_8	Number of Function Evaluations When Optimised Results Found	Statistical Analysis Results				
			Overall RMS Error	RMS error of the Real Part	RMS Error of the Imaginary Part	R^2 of the Real Part	R^2 of the Imaginary Part
16	[0.1275 -0.4507 0.1007 -0.8222 0.1876 -0.7171 0.1574 -0.5061]	161	0.1052	0.0727	0.0760	0.9966	0.9962

The derived bulk acoustic properties between 300 and 4500 Hz using the results of optimisation condition 16 in Table 6.5 of the proposed new method are provided in Tables B.10 and B.11 in Appendix B. The bulk acoustic properties between 3812.5 and 4500 Hz obtained using Utsuno's improved two-cavity method are provided in Tables B.12 and B.13 in Appendix B, which is in addition to those between 300 and 3800 Hz provided in Tables B.6 and B.7. The bulk acoustic properties, in Tables B.3, B.4, B.6, B.7, B.10, B.11, B.12 and B.13, obtained by different methods are illustrated in Figure 6.3. In addition, Figure 6.3 shows the extrapolated bulk acoustic properties at high frequencies between 3812.5 and 4500 Hz (see Tables B.14 and B.15 in Appendix B) using the results of optimisation condition 7 in Table 6.3 which is based on the surface impedance measurement results between 300 and 3800 Hz.

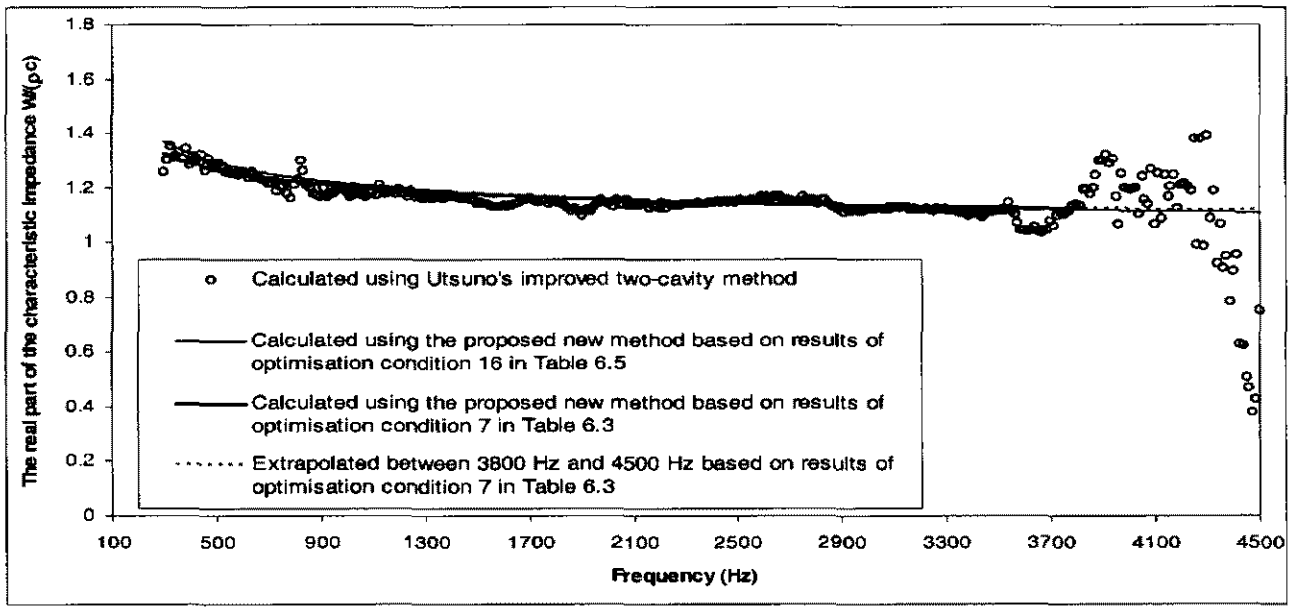
The real part of the characteristic impedance W/(ρc)
1.8
1.6
1.4
1.2
1
0.8
0.6
0.4
0.2
0
100
500
900
1300
1700
2100
2500
2900
3300
3700
4100
4500
Frequency (Hz)
Calculated using Utsuno's improved two-cavity method
Calculated using the proposed new method based on results of optimisation condition 16 in Table 6.5
Calculated using the proposed new method based on results of optimisation condition 7 in Table 6.3
Extrapolated between 3800 Hz and 4500 Hz based on results of optimisation condition 7 in Table 6.3

(a)

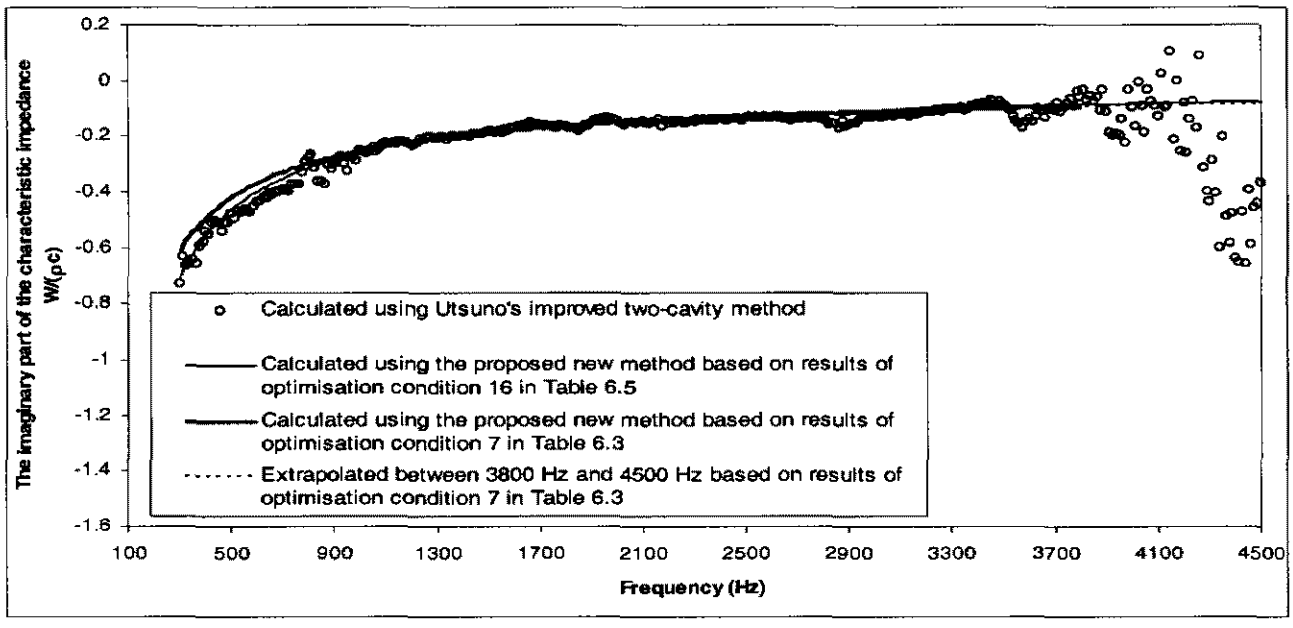
The imaginary part of the characteristic impedance W/(ρc)
0.2
0
-0.2
-0.4
-0.6
-0.8
-1
-1.2
-1.4
-1.6
100
500
900
1300
1700
2100
2500
2900
3300
3700
4100
4500
Frequency (Hz)
Calculated using Utsuno's improved two-cavity method
Calculated using the proposed new method based on results of optimisation condition 16 in Table 6.5
Calculated using the proposed new method based on results of optimisation condition 7 in Table 6.3
Extrapolated between 3800 Hz and 4500 Hz based on results of optimisation condition 7 in Table 6.3

(b)

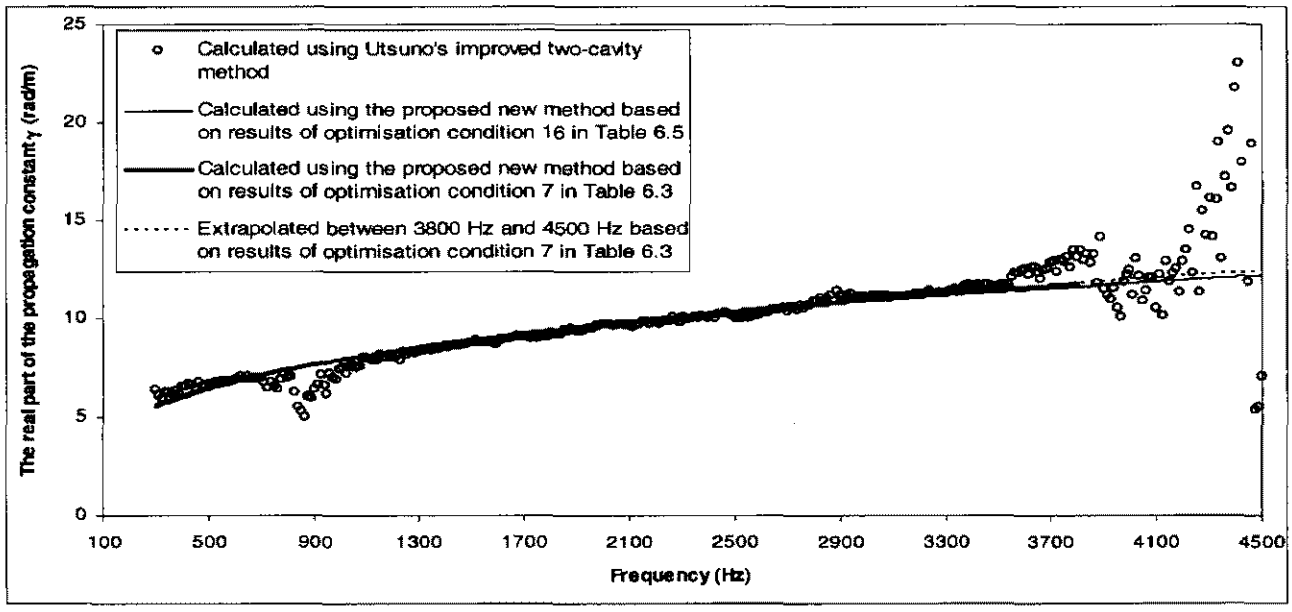

(c)

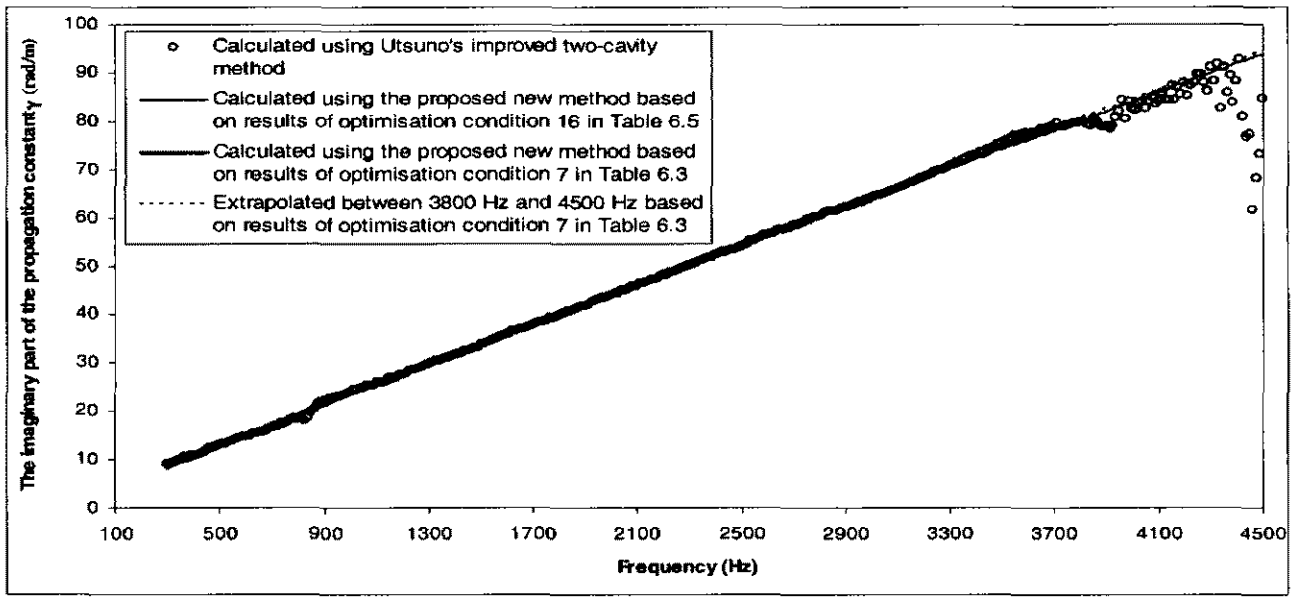

(d)

Figure 6.3 Comparison between (a) the real part and (b) the imaginary part of the characteristic impedance (normalised by the characteristic impedance of the air, ρc) between 300 and 4500 Hz obtained by the proposed new method and those obtained by Utsuno's improved two-cavity method and comparison between (c) the real part and (d) the imaginary part of the propagation constant between 300 and 4500 Hz obtained by the proposed new method and those obtained by Utsuno's improved two-cavity method.

Figure 6.3 clearly shows that Utsuno's improved two-cavity method becomes inaccurate when the half-wavelength frequency is approached. In fact it may affect a large band of frequencies - in this case about a 1000 Hz-band between 3500 and 4500 Hz. The proposed new method is certainly immune from this problem. In addition, it also shows that there is no significant problem extrapolating the Delany and Bazley (1970) type curve-fitting formulae beyond the high-frequency limit of the data.

6.4 CONCLUSIONS

This chapter proposed a new method requiring only a single surface impedance measurement and an optimisation process of the function coefficients of Delany and Bazley (1970) type curve-fitting formulae to derive the bulk acoustic properties. This method has several advantages over the traditional two-measurement methods. First, any experimental errors arising from material inhomogeneity (in the case of the two-thickness method) or sample mounting (for example, edge effects of various kinds) between the two tests will be absent. Second, there will be no cumulative random errors in the results arising from the fact that two sets of experimental data are being combined. And third, conducting only one impedance test is less time-consuming than doing two tests, so more effort can be devoted to experimental accuracy within a given time.

An application example was given to demonstrate the use of the proposed new method. The surface impedance obtained using the proposed new method was verified with that measured and an excellent fit between them was observed. The derived bulk acoustic properties using the proposed new method were compared with those obtained using Utsuno's improved two-cavity method and generally they were in agreement. The discrepancies between 300 and 800 Hz were probably due to cumulative random errors in the results arising from the fact that two sets of experimental data were being combined for Utsuno's improved two-cavity method. The discrepancies at high frequencies between 3500 and 4500 Hz occurred because the first half-wavelength frequency in Equation (6.14) was being approached. In addition, it was also shown that there was no

significant problem extrapolating the Delany and Bazley (1970) type curve-fitting formulae beyond the high-frequency limit of the data.

Using the same example, a comparison of the effectiveness, robustness and efficiency of EAs and traditional calculus-based optimisation methods was also made. Results of the different optimisation conditions showed that some traditional calculus-based optimisation techniques could be effective and efficient optimisation methods for the present example, when the starting point and/or the range of search were properly defined. The optimisation process could be completed in approximately three seconds. However, when the starting point and/or the range of search were not properly defined, either the efficiency of search was reduced or the optimisation did not converge at all. In the present example, the EA was an effective method for finding the minimum solution but it was not as efficient as some traditional calculus-based optimisation techniques with properly defined starting points and/or range of search. This was easily understandable because, for every operation of EA, an evaluation of a large number of potential solutions was undertaken. In the example 90 function evaluations were made for every new generation. Nonetheless, the EA was not sensitive to the starting point (which could even be randomly generated) or to the range of the search. This certainly proved the robustness of the EA.

In the present investigation, the flow resistivity of the test material sample is 3900 SI rayls/m. Further study is required to investigate how the proposed new method can work for materials having high steady flow resistivities.

REFERENCES FOR CHAPTER 6

- Allard J.-F., 1993. *Propagation of sound in porous media.* Elsevier Science Publishers Ltd., Barking.
- Astley R.J., Cummings A. and Sormaz N., 1991. "A finite element scheme for acoustical propagation in flexible walled ducts with bulk reacting liners, and comparison with experiment," *Journal of Sound and Vibration*, 150, pp 119-138.
- Attenborough K., 1983. "Acoustical characteristics of rigid fibrous absorbents and granular materials," *Journal of the Acoustical Society of America*, 73, pp 785-799.
- Baker J.E., 1987. "Reducing bias and inefficiency in the selection algorithm," *Proceedings of the second international conference on genetic algorithms and their application*, Hillsdale, New Jersey, Lawrence Erlbaum Associates, pp 14-21.
- Beranek L.L., 1947. "Acoustic properties of homogeneous porous medium isotropic rigid tiles and flexible blankets," *Journal of the Acoustical Society of America*, 19, pp 556-568.
- Biggs M.C., 1975. "Constrained minimization using recursive quadratic programming," *In:* Dixon L.C.W. and Szergo G.P., editors, *Towards global optimization*, North-Holland, Amsterdam, pp 341-349.
- Biot M.A., 1956. "Theory of propagation of elastic waves in a fluid-saturated porous media," *Journal of the Acoustical Society of America*, 28, pp 168-191.
- Bolton J. S., Shiau N.-M and Kang J.Y., 1996. "Sound transmission through multi-panel structures lined with elastic porous materials," *Journal of Sound and Vibration*, 191, pp 317-347.
- Braccesi C. and Bracciali A., 1998. "Least squares estimation of main properties of sound absorbing materials through acoustical measurements," *Applied Acoustics*, 54, pp 59-70.
- Broyden C.G., 1970. "The convergence of a class of double-rank minimization algorithms," *Journal of the Institute of Mathematics and Its Applications*, 6, pp 76-90.
- Champoux Y. and Stinston M.R., 1991. "Measurement of the characteristic impedance and propagation constant of materials having high flow resistivity," *Journal of the Acoustical Society of America*, 90, pp 2182-2191.

- Cummings A. and Beadle S.P., 1993. "Acoustic properties of reticulated plastic foams," *Journal of Sound and Vibration*, 175 (1), pp 115-133.
- Cummings A. and Chang I.-J., 1987. "Acoustic propagation in porous media with internal mean flow," *Journal of Sound and Vibration*, 114, pp 565-581.
- Cummings A., Rice H.J. and Wilson R., 1999. "Radiation damping in plates, induced by porous media," *Journal of Sound and Vibration*, 221, pp 143-167.
- Delany M.E. and Bazley E.N., 1970. "Acoustical properties of fibrous absorbent materials," *Applied Acoustics*, 3 (2), pp 105-116.
- Dennis J.E. Jr., 1977. "Nonlinear least-squares," *In:* Jacobs D., editor, *State of the art in numerical analysis*, Academic Press, New York, pp 269-312.
- Dunn I.P. and Davern W.A., 1986. "Calculation of acoustic impedance of multi-layer absorbers," *Applied Acoustics*, 19 (5), pp 321-334.
- Han S.P., 1977. "A globally convergent method for nonlinear programming," *Journal of Optimization Theory and Applications*, 22, p 297.
- Fletcher R., 1970. "A new approach to variable metric algorithms," *Computer Journal*, 13, pp 317-322.
- Fletcher R., 1987. *Practical methods of optimization*. John Wiley and Sons, New York.
- Fonseca C.M. and Fleming P.J., 1993. "Genetic algorithms for multiobjective optimization: formulation, discussion and generalization," *Proceedings of the fifth international conference on genetic algorithms*, San Mateo, California, Morgan Kaufmann, pp 416-423.
- Fonseca C.M. and Fleming P.J., 1998. "Multiobjective optimization and multiple constraint handling with evolutionary algorithms – part I: a unified formulation," *IEEE transactions on systems, man, and cybernetics – part A: system and humans* 28 (1), pp 26-37.
- Gill P.E., Murray W. and Wright M.H., 1981. *Practical optimization*. Academic Press, London.
- Goldfarb D., 1970. "A family of variable metric updates derived by variational means," *Mathematics of Computing*, 24, pp 23-26.

- ISO, 1998. *ISO 10534-2 Acoustics – determination of the sound absorption coefficient and impedance in impedance tubes – part 2: transfer-function method.* The International Organisation for Standardization, Geneva, Switzerland.
- Kirby R. and Cummings A., 1999. "Prediction of the bulk acoustic properties of fibrous materials at low frequencies," *Applied Acoustics*, 56, pp 101-125.
- Lambert R.F., 1982. "The acoustical structure of highly porous open-cell foams," *Journal of the Acoustical Society of America*, 72, pp 879-887.
- Lee F.C. and Chen W.H., 2001. "Acoustic transmission analysis of multilayer absorbers," *Journal of Sound and Vibration*, 248 (4), pp 621-634.
- Levenberg K., 1944. "A method for the solution of certain problems in least-squares," *Quarterly Applied Math.*, 2, pp 164-168.
- Marquardt D., 1963. "An algorithm for least-squares estimation of nonlinear parameters," *SIAM Journal Applied Math.*, 11, pp 431-441.
- MathWorks Inc, 2002. *Optimisation toolbox for use with MATLAB user's Guide (version 2.2).* Natick, MA.
- Mechel F.P., 1976/1977. "Eine Modelltheorie zum Faserabsorber. Teil I: Regulare Faseranordnung; Teil II: Absorbermodell aus Elementarzellen und numerische Ergelnisse," *Acustica*, 36, pp 53-89.
- Mechel F.P., 1976. "Ausweitung der Absorberformel von Delany and Bazley zu tiefen Frequenzen," *Acustica*, 35, pp 210-213.
- Mechel F.P., 1988. "Design charts for sound absorber layers," *Journal of the Acoustical Society of America* 83, pp 1002-1013.
- Morse P.M. and Ingard K.U., 1968. *Theoretical acoustics*. McGraw-Hill, New York.
- Mühlenbein H. and Schlierkamp-Voosen D., 1995. "Analysis of selection, mutation and recombination in genetic algorithms," *In:* Banzhaf W. and Eeckman F.H., editors, *Evolution as a computational process vol 899 Lecture notes in Computer Science*, Springer-Verlag, Berlin, pp 142-168.
- Nocedal J. and Wright S.J., 1999. *Numerical optimization.* Springer Series in Operations Research, Springer Verlag, New York.

- Pohlheim H., 2004. *Genetic and evolutionary algorithm toolbox for use with MATLAB version 3.5*, http://www.geatbx.com/, Berlin.
- Powell M.J.D., 1978a. "A fast algorithm for nonlineary constrained optimization calculations," *In:* Watson G.A., editor, *Numerical analysis vol 603 Lecture notes in Mathematics,* Springer Verlag, Berlin.
- Powell M.J.D., 1978b. "The convergence of variable metric methods for nonlinearly constrained optimization calculations," *In:* Mangasarian O.L., Meyer R.R., and Robinson S.M., editors, *Nonlinear programming 3*, Academic Press, New York.
- Powell M.J.D., 1983. "Variable metric methods for constrained optimization," *In:* Bachem A., Grotschel M. and Korte B., editors, *Mathematical programming: the state of the art*, Springer Verlag, Berlin, pp 288-311.
- Scott Y.A., 1946. "The absorption of sound in a homogeneous porous medium," *Proceedings of the physical society of London*, 58, pp 165-183.
- Shanno D.F., 1970. "Conditioning of quasi-Newton methods for function minimization," *Mathematics of Computing*, 24, pp 647-656.
- Smith C.D. and Parrott T.L., 1983. "Comparison of three methods for measuring acoustic properties of bulk materials," *Journal of the Acoustical Society of America*, 74 (5), pp 1577-1582.
- Utsuno H., Tanaka T., Fujikawa T. and Seybert A.F., 1989. "Transfer function method for measuring characteristic impedance and propagation constant of porous materials," *Journal of the Acoustical Society of America*, 86 (2), pp 637-643.
- Watson A.P. and Cummings A., 1994. *"Equivalent fluid" behaviour and further mechanical properties of the thermal insulation materials.* Brite/Aero Contract no. CT92 0032, deliverable no. 8.
- Yaniv S.L., 1973. "Impedance tube measurement of propagation constant and characteristic impedance of porous acoustical material," *Journal of the Acoustical Society of America*, 54 (5), pp 1138-1142.
- Zwicker C. and Kosten C., 1949. *Sound absorbing materials.* Elsevier, Amsterdam.

CHAPTER 7

PREDICTING AND OPTIMISING THE AIRBORNE SOUND TRANSMISSION OF FLOOR-CEILING CONSTRUCTIONS USING COMPUTATIONAL INTELLIGENCE

7.1 INTRODUCTION

The acoustic performance of various types of floor-ceiling constructions has become more and more important in the field of architectural acoustics as residential densities and occupant amenity expectations increase. Building codes and occupant satisfaction require the architects to be fully informed as to the sound insulation performance of floor-ceiling constructions. Manufacturers must have their products tested in standard test facilities to ensure compliance with building codes. However, in the product development stage, there are vast ranges of building materials and construction assemblies available for manufacturers to select. Therefore, numerical analysis, as a complement to the expensive and time consuming laboratory tests, is needed to predict the sound insulation performance of constructions that have not been measured. Once an accurate and reliable numeric model is obtained, the optimisation of the sound insulation performance of the constructions may be carried out on the basis of this model.

However, there are a large number of parameters (such as surface mass of the constructions, joint depth, joist spacing, resilient channel spacing, insulation density and insulation thickness) that may affect the sound insulation performance of floor-ceiling constructions. Furthermore, the relationship between the parameters and sound insulation performance of floor-ceiling constructions may also be non-linear. For these reasons, an accurate prediction and efficient optimisation of the sound insulation performance of the floor-ceiling constructions has been difficult.

It is an enticing challenge to a theoretician to develop a new method suitable for solving the given problem. However, from the application point of view, the time for developing

the technique has to be added to the computer time invested. In that respect, utilising a non-specialised and robust procedure, to which Computational Intelligence (CI) belongs, may be worthwhile. CI is one of the approaches to program computers in order to make them behave as if they were humans who can understand and tackle highly complex problems. The three major domains of CI are Artificial Neural Networks (ANNs), Evolutionary Algorithms (EAs), and Fuzzy Logic (FL). As discussed and demonstrated in the previous chapters, ANNs and EAs are very much capable of handling the problems that involve multi-parameters and non-linear relationship.

Coomes and Fricke (2001), using the results from acoustic laboratory tests of known wall partitions, investigated the application of ANNs for predicting the sound transmission class (STC), and transmission loss (TL) at specific frequencies, for steel and timber stud drywall constructions. The results obtained were highly encouraging with neural network designs achieving predictions for STC values within a similar range to those determined by a number of acoustic laboratories for comparable wall constructions. Fora-Moncada and Gibbs (2002) applied ANNs to establish the room and wall factors that influence sound level difference between rooms at low frequencies (40 – 100 Hz). In their work, the cross-validation average prediction error was 4 dB, with all cases included, or 3 dB, if equal room configurations were excluded. More details of the above two investigations can be found in the Literature Review, Section 1.2, of this thesis.

In this chapter, an ANN is first developed on the basis of the data from laboratory tests on floors to predict the STC of typical floor-ceiling constructions. The predictions of STC using ANNs are compared with those obtained using the multivariate regression analysis. Then an evolutionary algorithm is applied to search the multi-dimensional space created by the ANN in order to find a floor-ceiling construction that meets the STC requirement set out by the architect. The success of the work presented in this chapter implies that from the application point of view, it is promising to use ANNs and EAs to form a general problem-solving framework for architectural and building acoustics problems that feature high dimensionality and non-linear relationship.

7.2 PREDICTIONS OF STC USING ANNs

Using the laboratory measurement data, Warnock and Birta (1998) carried out a multivariate regression analysis to calculate the STC of floor-ceiling constructions. In this section, on the basis of the same set of laboratory measurement data as used in their work, an ANN approach for predicting STC of floor-ceiling constructions is first investigated and then the performance of the predictions is compared with that of multivariate regression analysis.

7.2.1 Database for the ANN Model

The Institute for Research in Construction (IRC), National Research Council Canada (CNRC), in collaboration with 18 industry and government partners, carried out a major research study over the period 1995 to 1998 to measure the acoustical and fire resistance performance of floor assemblies: Acoustical and Fire Performance of Floor Assemblies. In this IRC research project, airborne sound transmissions were measured in the floor test facility to ASTM standard E90 (ASTM, 1999b), and STC values were subsequently calculated in accordance to ASTM standard E413 (ASTM, 1999a). Most of the floors in the project incorporated wood joists or trusses. Joist type, length, spacing and depth were varied. There were only 14 steel joist systems and 4 concrete slab floors. The joist types comprised solid wood, wood trusses, I-joists, and steel joists. Three types of sound absorbing material were used: glass wool, rock wool and cellulose fibre. The measurements provide an extensive, consistent data set for analysis and testing of computer models (Warnock and Birta, 1998; Warnock, 1999; Warnock, 2000a; Warnock, 2000b).

One category of floor-ceiling constructions which contained sufficient data to allow a meaningful analysis was of solid timber joist floors with resilient channels directly attached to the joists and with sound absorbing material in the cavity. There are seventy one cases in this category and the ranges of input parameters are shown in Table 7.1. Warnock's laboratory study (Warnock, 1996) indicated that floor joist length made no significant difference to the floor sound transmission; therefore, the joint length was not

included as one of the input parameters. Of the 71 cases, 53 were used for training, 8 for verification and 10 for testing.

Table 7.1 Ranges of input and output parameters

Variable	Minimum	Maximum
Sound Transmission Class (STC)	47	70
Sound Absorbing Material Density (InsDensity), kg/m^3	10.1	58.35
Sound Absorbing Material Thickness (InsThick), mm	59	270
Joist Spacing (JstSpace), mm	305	610
Joist Depth (JstDepth), mm	184	286
Resilient Metal Channel Spacing (RCSpace), mm	200	610
Floor and Ceiling Layer Surface Density (FCMass), kg/m^2	13	127

7.2.2 ANN Model

Figure 7.1 illustrates a three-layer feed-forward ANN architecture applied in the present chapter. The floor and ceiling layer surface density in kg/m^2 was converted to its logarithmic value, which yielded a better data distribution than the non-logarithmic value. One hidden neuron layer, with 3 hidden neurons, was used.

The ANN analysis was undertaken using STATISTICA Neural Networks (Statsoft, 1999). The weights, which were initialised to uniformly-distributed random values using the "uniform method", were adjusted by using "back propagation", "conjugate gradient" and "quick propagation" algorithms to minimize the prediction error during the training. Conditions were set within the STATISTICA Neural Networks program by altering the model's parameters. "Early stopping" and "Weigend weight regularization" techniques were used to control over-fitting. Training of ANNs was stopped when the RMS error of the verification set could no longer be improved. The test set was used to independently check the performance of the network when an entire network design procedure was completed.

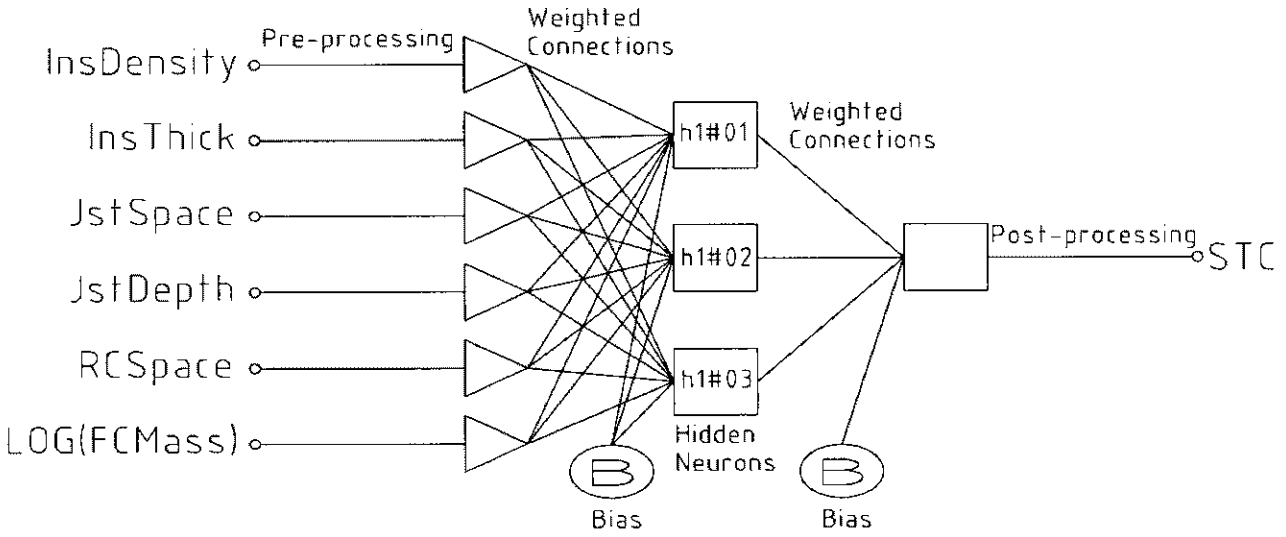

Figure 7.1 Illustration of the 3-layer feed-forward artificial neural network for predicting STC of floor-ceiling constructions (see Table 7.1 for information on the inputs and the output).

Table C.1 – Table C.4 in Appendix C provides the specifics of the neural network model. They include the shift and scale factors of inputs, weights and thresholds to each hidden neuron of the neural network, weights and thresholds to the output neuron of the neural network and shift and scale factor of the output. The same modus operandi of the ANN model as introduced in chapter 2 and chapter 4 of this thesis can be applied with these specifics.

7.2.3 Comparisons of the Predictions of ANN Analysis and Multivariate Regression Analysis

Table 7.2 presents the statistical analysis results (numbers without brackets) based on the ANN models specified in the above section. In a regression problem, the standard deviations (SD) of both the prediction error and original output data are important and can be related by the standard deviation ratio (SDR). The SDR in a regression problem is the ratio of the SD of the prediction error to that of the original output data (an SDR of

0.1 is considered an excellent fit of the data and an SDR of 1.0 is a poor fit) (Statsoft, 1999).

Table 7.2 Statistical analysis results for predictions of ANN analysis and multivariate regression analysis (in parentheses)

	Tr[a]	Ve[b]	Te[c]	En[d]
RMS error	0.758	1.090	0.880	0.821 (1.347)
Error SD[e]	0.765	1.170	0.906	0.844 (1.219)
SDR[f]	0.231	0.160	0.179	0.206 (0.297)
R^2	0.947	0.988	0.973	0.960 (0.918)

[a]Tr = training data set.
[b]Ve = verification data set.
[c]Te = test data set.
[d]En = entire data set.
[e]Error SD = standard deviation of the prediction error.
[f]SDR= standard deviation ratio.

Warnock and Birta (1998) carried out a multivariate regression analysis on the same category of data as that discussed here. The equation they derived for calculating the STC of this category of floor-ceiling constructions is as follows:

$$STC = 1.31 + 24.4 \times \log(FCMass) + 0.02 \times JstDepth + 0.01 \times JstSpace + 0.02 \times InsThick + 0.01 \times RCSpace + 0.023 \times InsDensity \quad (7.1)$$

Table 7.2 also shows the statistical analysis results (numbers in parentheses) of the calculations using Equation (7.1). Since Equation (7.1) was derived on the basis of the entire data set, only the results of the entire data set are shown. All the statistical results in Table 7.2 indicate that the ANN model provides more accurate predictions than the multivariate regression equation does. This may also imply that the relationship between the input floor parameters and the output STC is indeed non-linear.

Another advantage of ANN is its ability to work with nominal values, which is not possible when using multivariate regression analysis. This enables the ANN to directly

acquire additional information and knowledge about a given problem domain. In future work, for instance, a nominal input, "joist type" (timber or other material), could be included in the ANN model. Also, a sound absorbing material type or code containing both the information about the density and thickness of the material can be used as one of inputs of the ANN model. Architects are often more familiar with the sound absorbing material type or code than the relevant density and thickness of a certain material. The replacement of two numerical inputs (sound absorbing material density and thickness) with one nominal input (sound absorbing material type or code) would further simplify the prediction model.

7.3 OPTIMISATIONS OF STC USING EAs

Since the search for an appropriate floor-ceiling construction which would meet the design requirements of the architect involves the evaluation of different combinations of floor-ceiling construction parameters and, since the non-linear ANN model is more complex than the linear regression equation, the classic optimisation techniques are inefficient or unsatisfactory for searching for solutions provided by the ANN model. A better approach is to use EAs which have the ability and robustness to search a large non-linear multidimensional space (potential solutions), and which are capable of solving combinatorial-type problems (Goldberg, 1989).

The parametric study indicated that the most important parameter determining STC performance of floor-ceiling constructions is the mass of the floor and ceiling layers. However, other parameters also have an effect on the overall STC performance of floor-ceiling systems. Hence, there is a need to resolve – once we have an ANN model that accurately predicts the STC of a certain floor-ceiling construction – how we can optimize the STC performance of floor-ceiling constructions within the range of design parameters utilised in buildings. For instance, an architect may wish to know the construction required to achieve an STC 55 rated floor-ceiling using a relatively low depth type of solid timber joists (say 235mm deep) and the least mass possible. Consequently, the

question is posed as to which type of floor-ceiling construction can meet these requirements.

Genetic and Evolutionary Algorithm Toolbox for Use with Matlab (Pohlheim, 2004) was used to search the multidimensional space provided by the ANN model presented in Section 7.2 of this chapter and find an appropriate floor-ceiling construction which would meet the design requirements of the architect. The searching ranges of the parameters are those listed in Table 7.1. The ANN model developed was used as the objective function. Real value variable representations and multipopulation searching were used. Initial values were randomly generated by the GEATbx (Pohlheim, 2004) within the range of parameters at the start of the searching. Discrete recombination (Mühlenbein and Schlierkamp-Voosen, 1995) and real value mutation genetic operators (Pohlheim, 2004) were employed.

To achieve an STC 55 floor-ceiling construction using 235mm deep solid timber joists, the searching results indicate that

- the minimum surface weight of the floor and ceiling layers should be 20 kg/m^2;
- 235mm thick cellulose fibre sound absorbing material, with a density of 58 kg/m^3, should be applied;
- the joist spacing should be 610mm; and
- the resilient metal channel spacing should be 610mm.

This construction was not included in the original laboratory tests (Warnock and Birta, 1998; Warnock, 2000b).

Nonetheless, the original laboratory tests (Warnock and Birta, 1998; Warnock, 2000b) show that the following floor-ceiling construction can achieve an STC rating of 52:

- the floor layer is 1 layer of 15mm thick oriented strandboard with a surface weight of 8.8 kg/m2;
- the ceiling layer is 1 layer of 16mm thick gypsum board with a surface weight of 11.3 kg/m2;
- floor joists are 235mm deep solid timber joists with a spacing of 406mm;

- the sound absorbing material is 152mm thick glass fibre with a density of 11.1 kg/m3; and
- resilient metal channels are spaced 610mm apart.

The differences in construction methods between the tested laboratory floor-ceiling system and the one found by EA are the type (density) and thickness of sound absorbing material and the spacing of joists. From the laboratory tests, Warnock (1999) concluded that

- each increase in sound absorbing material thickness of about 65mm results in an increases of 1 STC point;
- for the same thickness of material, cellulose fibre gives an STC that is higher than that of glass fibre by about 1 STC point;
- an increase in joist spacing of approximately 200mm will increase the STC by 1 point.

On the basis of Warnock's conclusions, the increase of sound absorbing material thickness from 152mm to 235mm will result in an increase of 1 STC point. Furthermore, a change of sound absorbing material from glass fibre to cellulose fibre will increase STC by 1 point, and changing the spacing of joists from 406mm centres to 610mm centres will result in an increase of STC by 1 point. Hence, the overall STC performance of the floor-ceiling construction tested can be increased from 52 to 55 if its construction is changed to the searched result of EAs. In other words, the searched result of EAs is in agreement with laboratory test results and studies. However, the limitation of this verification process is that it assumes the behaviour of the floor-ceiling construction is linear.

7.4 CONCLUSIONS

The prediction of the airborne sound transmission of floor-ceiling constructions using ANNs and the optimisation of the airborne sound transmission of floor-ceiling constructions using EAs were investigated in this chapter. The results of the investigation showed that ANNs and EAs can be used together to solve architectural and building acoustics problems that feature high dimensionality and non-linear relationships. From

the application point of view, the general framework can be briefly described as first developing an ANN to numerically describe the input-output relationship of a particular acoustic problem, and then using an EA to search the multi-dimensional space created by the ANN to find a particular solution that meets the architect's requirements.

For solving the particular problem introduced in this chapter (predicting and optimising the airborne sound transmission performance of floor-ceiling constructions - airborne STC), initially an ANN model that could predict the STC of timber joist type floor-ceiling constructions was established, and then an EA was applied to search for an appropriate floor-ceiling construction capable of meeting the architect's design requirements. For the purpose of comparison with Warnock's work (Warnock and Birta, 1998; Warnock, 1999; Warnock, 2000a; Warnock, 2000b), the same type of measure of airborne sound transmission, namely STC, was used. A similar analysis to that described in this paper can be carried out using weighted sound reduction index, Rw, or sound transmission loss values at any frequency of interest.

The comparison of statistical parameters of predictions made using the ANN and calculated using multivariate regression equations indicated that the ANN model provided a more accurate prediction. This may also imply that the relationship between the input floor parameters and the output STC is non-linear. Future work may investigate the feasibility of reducing the complexity of the ANN model and providing a more user-friendly application environment by including nominal inputs, such as "joist type" or "sound absorbing material type or code", which is not achievable using multivariate regression analysis.

In the present study, due to the high cost, it is not feasible to test in a laboratory the optimised floor-ceiling construction found by the EA. Therefore, the findings from Warnock's laboratory tests (Warnock, 1999), which assumed the linear performance of floor-ceiling constructions, were applied to verify the EA result. With sufficient funding available in the future, the result found by EAs should be further verified by laboratory tests.

Another aspect of the acoustic performance of floor-ceiling constructions, namely impact transmission, could also be investigated using the same method as that introduced in this chapter. Multiple-objective EAs could also be applied to optimise STC and IIC (or other measures of sound transmission) of floor-ceiling constructions together. Optimising IIC or IIC together with STC is probably a more appropriate use of CI techniques, as the output may not be dominated by a single input parameter such as mass (which is the situation with airborne sound transmission).

REFERENCES FOR CHAPTER 7

- ASTM, 1999a. *E413-87 Classification for Rating Sound Insulation.* ASTM International, West Conshohocken, PA.
- ASTM, 1999b. *E90-99 Standard Test Method for Laboratory Measurement of Airborne Sound Transmission Loss of Building Partitions and Elements.* ASTM International, West Conshohocken, PA.
- Coomes J. and Fricke F.R., 2001. "The prediction of wall sound insulation using neural networks," *Journal of Building Acoustics*, 8 (2), pp 103-119.
- Goldberg D.E., 1989. *Genetic algorithms in search, optimization, and machine learning.* Addison-Wesley Publishing Company INC, Reading.
- Fora-Moncada A. and Gibbs B., 2002. "Prediction of sound insulation at low frequencies using artificial neural networks," *Journal of Building Acoustics*, 9 (1), pp 49-71.
- Mühlenbein H. and Schlierkamp-Voosen D., 1995. "Analysis of selection, mutation and recombination in genetic algorithms," *In:* Banzhaf W. and Eeckman F.H., editors, *Evolution as a computational process Vol 899 of Lecture notes in Computer Science,* Berlin, Springer-Verlag, pp 142-168.
- Pohlheim H., 2004. *Genetic and evolutionary algorithm toolbox for use with MATLAB version 3.5*, Available from: http://www.geatbx.com/.
- Warnock A.C.C., 1996. "Effect of joist length on sound transmission though a wood joist floor," *Proceedings of InterNoise 1996*, pp 1842-1846.
- Warnock A.C.C. and Birta J.A., 1998. *Summary report for consortium on fire resistance and sound insulation of floors: sound transmission class and impact insulation class results, internal report IRC-IR-766.* Institute for Research in Construction, National Research Council Canada.
- Warnock A.C.C., 1999. "Controlling the transmission of airborne sound through floors," *Construction technology update*, 25, pp 4.
- Warnock A.C.C., 2000a. "Airborne and impact sound insulation of joist floor systems: A collection of data," *Proceedings of InterNoise 2000*, pp 1-6.

- Warnock A.C.C., 2000b. *Detailed report for consortium on fire resistance and sound insulation of floors: sound transmission and impact insulation data in 1/3 octave bands, IRC internal report IRC-IR-811*. Institute for Research in Construction, National Research Council Canada.

CHAPTER 8

CONCLUSIONS AND FURTHER WORK

8.1 SUMMARY OF OBJECTIVES

The development of architectural and building acoustics research and design activity has long been frustrated by issues such as multiple parameters, multiple criteria, discontinuous decision spaces and a large quantity of measured data. These complex situations are not easily reconcilable and therefore remain difficult to resolve using conventional methods. Computational Intelligence (CI) is one of the approaches to programming computers that make them behave more like they were human, that is, having the ability to understand and tackle highly complex problems. Two of the major domains of CI are Artificial Neural Networks (ANNs) and Evolutionary Algorithms (EAs). The present work aimed to show the potential of these techniques when applied to some architectural research and design issues.

It is an enticing challenge to a theoretician to develop a new method suitable for solving the given problem. However, from the application point of view, the time for developing the technique has to be added to the computer time invested. In that respect, utilising a non-specialised and robust procedure, to which ANNs and EAs belong, may be worthwhile. With the inherent power of CI, it is promising to use ANNs and EAs to solve architectural and building acoustics problems that feature high dimensionality, multiple criteria, discontinuous decision spaces and a large amount of data collection.

The general objective of the present research was to assess the application of ANNs and EAs to build a methodological framework for design and research associated with architectural and building acoustics. This methodological framework should be easily understood and handled, and is either usable as a black box method or open to the incorporation of new or old recipes for further sophistication, specialization or

hybridisation. It is hoped that the ongoing research will lead to other applications of ANNs and EAs in the field of architectural and building acoustics.

The topics for the investigation in the present work were chosen on the basis of need and the data available. Thus it was decided to concentrate the research effort in the following specific topics: 1) predicting architectural speech intelligibility and security that involve multiple decision parameters; 2) optimising the design of flat-walled multi-layered anechoic linings that features multiple criteria decision making, multiple decision parameters and discontinuous decision spaces; 3) developing a new method for deriving the bulk acoustic properties of a rigid porous medium from a single impedance test, which needs to deal with a large quantity of measured data; and 4) predicting and optimising the airborne sound transmission of floor-ceiling constructions that involves multiple decision parameters.

In the present work, the application of ANNs to architectural acoustic issues has been extended to those not considered previously; and, perhaps more importantly, EA techniques have been applied to optimise acoustic designs, which has been difficult in the past.

8.2 CONCLUSIONS

The investigation in chapter 4 indicates that the ANN approach provides a direct and accurate method for predicting architectural speech intelligibility scores and security thresholds. The current method for predicting speech intelligibility and privacy first requires the development of an index and then requires the index to be related to subjective scores using a transfer function (ANSI, 1969; ANSI, 1997; Gover and Bradley, 2004). The ANN approach can avoid this two step process by using the signal-to-noise (S/N) ratio information to directly predict the subjective speech intelligibility score and security thresholds. Compared with the previous work (Gover and Bradley, 2004) that used one-third-octave band S/N ratios, the ANN approach used only "octave band" S/N ratios and performed comparably for the predictions of the intelligibility score, the

intelligibility threshold and the cadence threshold, and better for the prediction of the audibility threshold.

Specifics of the ANN models for predicting the speech security and intelligibility scores were also provided. With this information, ANN models can be embedded into standard spreadsheet applications, thus allowing predictions to be made in a transparent and direct fashion.

Similar investigations using one-third-octave band (160 Hz – 8000 Hz) S/N ratios have also been conducted in the present work. However, the statistical results of the one-third-octave band analysis were only slightly better than those of the octave band analysis. This may be due to the information in adjacent one-third-octave bands being highly correlated and therefore not contributing any significant new information to the ANN.

Chapter 5 demonstrates that a multi-objective evolutionary algorithm (EA) can be successfully employed as an optimiser to aid and speed up the design of flat-walled multi-layered anechoic linings. Two types of material, fully-reticulated (open-cell) polyurethane foams and fibrous building insulation material, were investigated. The general optimisation procedure was first demonstrated for a three-layered lining system composed of fully-reticulated (open-cell) polyurethane plastic foams and targeted a cut-off frequency of 100 Hz. Then, a detailed investigation was carried out on the application of multi-layered polyurethane foams as flat-walled anechoic linings. The major findings of the investigation were 1) a single layer of material was not as effective as a flat-walled multi-layered anechoic lining; 2) for low (100 Hz) and mid (250 Hz) cut-off frequencies the minimum number of layers needed to achieve the minimum overall thickness was three, and for high (500 Hz) cut-off frequency the minimum number of layers to achieve the minimum overall thickness was two; 3) for the material investigated in the present work and for cut-off frequencies between 100 and 250 Hz inclusive, using a three-layered flat-walled anechoic lining, the achievable minimum overall thickness was between a quarter wavelength in the lining composite and a quarter wavelength in the air for the corresponding cut-off frequency; 4) for a three-layered lining composite the material with

low flow resistivity should be placed in front of the material with high flow resistivity. For the material investigated, to achieve a cut-off frequency between 100 and 250 Hz, the required flow resistivity for each layer of material in the three-layered lining composite basically did not vary with the cut-off frequency. The average flow resistivity for the front layer of material was 400 SI rayl/m, which is close to the characteristic impedance of air, and the average flow resistivities for the mid and back layers were 1700 and 6200 SI rayl/m respectively; 5) for the three-layered lining composite, the required thickness of the back layer basically did not vary with the cut-off frequency and was around 0.125 m. The thicknesses of the front and the mid layers had to be increased to achieve the decreased cut-off frequency; 6) to achieve the designed performance of the lining composite air gaps should be avoided. The above investigation results provide the benchmark and guidelines for the design of flat-walled multi-layered anechoic linings.

An investigation using fibrous building insulation material was also carried out in the form of an application case. The bulk acoustic properties of sixteen of the most commonly used commercial fibrous building insulation materials available in Australia were measured and, on the basis of the measurement results, a multi-objective evolutionary algorithm was used to optimise the design of a flat-walled multi-layered anechoic lining to meet the design criteria - a 250 Hz cut-off frequency with a maximum lining thickness of 300 mm. Nonetheless, because of the discrete nature of the problem, different data representation and evolutionary mutation operator to those applied in the investigation of polyurethane foams were used.

Results of the EA search indicated that for the sixteen materials investigated there were fourteen options that could achieve a cut-off frequency of 250 Hz with the overall lining thickness less than 300 mm. For all the options, the materials in the lining system exhibited a trend of a graduated increase in density and flow resistivity from the front layer (Layer 3) to the back layer (Layer 1). The options found by EA were evaluated on the basis of their costs and two options were short-listed. The acoustic performances of the short-listed options were then measured in an impedance tube. The difference between the measured and predicted performances may be due to the errors resulting

from the measurement of bulk acoustical properties, the inaccuracy of the prediction equation and the limitations of the experimental apparatus, all of which, unfortunately, are unpredictable and unquantifiable. The option that had the lower measured pressure reflection factors at low frequencies was used as the lining system for the anechoic room in the MARCS Auditory Laboratories at the University of Western Sydney. The lining system finally used in the anechoic room had an overall thickness of 295 mm, which is about 45 mm less than a quarter of a wavelength at the cut-off frequency of 250 Hz. The material cost of the applied lining system was about fifty Australian dollars per square metre. The completed anechoic room, where the optimised design was applied, was qualified and the results showed that a large percentage (75% - 85%) of the distance between the sound source and the room boundaries, on the traverses made, was anechoic.

The success of this application case also shows the effectiveness of EAs for solving combinatorial-type problems featuring discontinuous decision spaces, which is difficult or even impossible, for traditional optimisation methods.

A new method of deriving the bulk acoustic properties of a rigid porous medium was proposed in chapter 6. The method required only a single surface impedance measurement and an optimisation process of the function coefficients of Delany and Bazley (1970) type curve-fitting formulae. This method has several advantages over the traditional two-measurement methods. First, any experimental errors arising from material inhomogeneity (in the case of the two-thickness method) or sample mounting (for example, edge effects of various kinds) between the two tests will be absent. Second, there will be no cumulative random errors in the results arising from the fact that two sets of experimental data are being combined. And third, conducting only one impedance test is less time-consuming than doing two tests, so more effort can be devoted to experimental accuracy within a given time.

An application example was given to demonstrate the use of the proposed new method. The surface impedance obtained using the proposed new method was verified with that measured and an excellent fit between them was observed. The derived bulk acoustic

properties using the proposed new method were compared with those obtained using Utsuno's improved two-cavity method and generally they were in agreement. The discrepancies between 300 and 800 Hz were probably due to cumulative random errors in the results arising from the fact that two sets of experimental data were being combined for Utsuno's improved two-cavity method. The discrepancies at high frequencies between 3500 and 4500 Hz occurred because the first half-wavelength frequency in Equation (6.14) was being approached. In addition, it was also shown that there was no significant problem extrapolating the Delany and Bazley (1970) type curve-fitting formulae beyond the high-frequency limit of the data.

There will always remain a dichotomy between efficiency and general applicability and between reliability and effort of problem-solving, especially with optimum-seeking algorithms. Any specific knowledge about the given situation may be used to specify an adequate solution algorithm. On the other hand, there cannot exist one method that solves all problems effectively as well as efficiently. Using the same example, also in chapter 6, a comparison of the effectiveness, robustness and efficiency of EAs and traditional calculus-based optimisation methods was made. Results of the different optimisation conditions showed that some traditional calculus-based optimisation techniques could be effective and efficient optimisation methods for the present example when the starting point and/or the range of search were properly defined. The optimisation process could be completed in approximately three seconds. However, when the starting point and/or the range of search were not properly defined, either the efficiency of search was reduced or the optimisation did not converge at all. In the present example, the EA was an effective method for finding the minimum solution but it was not as efficient as some traditional calculus-based optimisation techniques with properly defined starting points and/or range of search. This was easily understandable because, for every operation of EA, an evaluation of a large number of potential solutions was undertaken. In the example 90 function evaluations were made for every new generation. Nonetheless, the EA was not sensitive to the starting point (which could even be randomly generated) or to the range of the search. This certainly proved the robustness of the EA.

The prediction of the airborne sound transmission of floor-ceiling constructions using ANNs and the optimisation of the airborne sound transmission of floor-ceiling constructions using EAs were investigated in this chapter. The investigation results showed that ANNs and EAs can be used together to solve architectural and building acoustics problems that feature high dimensionality and non-linear relationships. From the application point of view, the general framework can be briefly described as first developing an ANN to numerically describe the input-output relationship of a particular acoustic problem, and then using an EA to search the multi-dimensional space created by the ANN to find a particular solution that meets the requirement of the architect or other designers.

For solving the particular problem introduced in chapter 7 (predicting and optimising the airborne sound transmission performance of floor-ceiling constructions), initially an ANN model that could predict the sound transmission class (STC) of timber joist type floor-ceiling constructions was established, and then an EA was applied to search for an appropriate floor-ceiling construction capable of meeting the architect's design requirements. The comparison of statistical parameters of predictions made using the ANN and calculated using multivariate regression equations indicated that the ANN model provided a more accurate prediction. This may also imply that the relationship between the input floor parameters and the output STC is non-linear.

8.3 FURTHER WORK

The investigation carried out in chapter 4 only takes into account the S/N ratios in predicting the architectural speech intelligibility score and security thresholds. Other factors, such as talker gender and voice characteristics, speech material, room characteristics and so on, could be included in the ANN models to investigate the possibility of further improving the prediction accuracy.

In chapter 5, in the design of the lining system for the anechoic room in the MARCS Auditory Laboratories at the University of Western Sydney, some difference between the

measured and predicted pressure reflection factors were observed. One of the reasons for this discrepancy may have been because of the errors resulting from the measurement of bulk acoustical properties. The method applied in chapter 5 for the determination of bulk acoustic properties was the two-thickness method (Smith and Parrott, 1983), which requires that two test samples have identical bulk acoustical properties and that there is no variation associated with the mounting of test samples between measurements. Further work should be undertaken to investigate whether the difference between the measured results and the predicted results can be reduced by applying other techniques for deriving the bulk acoustic properties, especially the proposed new method in chapter 6 of the present thesis. Further work should also investigate the lining composite for achieving different cut-off frequencies with a wider selection of materials. To improve the sound absorption performance of a single layer of material, cooperation with sound-absorbent material manufacturers could also be undertaken to develop a material that has graduated flow resistivities and densities.

The proposed new method for deriving the bulk acoustic properties of a rigid porous medium (see chapter 6) may not be effective for material having a very high flow resistivity. Further study is required to investigate how the proposed new method can be used or modified to be used for this type of material.

As an extension of the study in chapter 7, to provide a more user-friendly application environment and reduce the complexity of the ANN model, further work may investigate the feasibility of including nominal inputs, such as "joist type" or "sound absorbing material type or code" - which is not achievable using multivariate regression analysis - for predicting the acoustic performance of floor-ceiling constructions. Also, with sufficient funding available in the future, the result found by the EA in chapter 7 could be verified by laboratory tests.

Another aspect of the acoustic performance of floor-ceiling constructions, namely impact transmission, could also be investigated using the same method as that introduced in chapter 7. Multiple-objective EAs could also be applied to optimise STC and IIC (or

other measures of sound transmission) of floor-ceiling constructions together. Optimising IIC or IIC together with STC is probably a more appropriate use of CI techniques, as the output may not be dominated by a single input parameter such as mass (which is the situation with airborne sound transmission).

Finally, the work presented in this thesis is sufficiently encouraging for the CI techniques to be applied to other areas of acoustic research and design.

REFERENCES FOR CHAPTER 8

- ANSI, 1969. *S3.5-1969 American national standard methods for the calculation of the articulation index.* American National Standards Institute, New York, NY.
- ANSI, 1997. *S3.5-1997 American national standard methods for calculation of the speech intelligibility index.* American National Standards Institute, New York, NY.
- Delany M.E. and Bazley E.N., 1970. "Acoustical properties of fibrous absorbent materials," *Applied Acoustics*, 3 (2), pp 105-116.
- Gover B.N. and Bradley J.S., 2004. "Measures for assessing architectural speech security (privacy) of closed offices and meeting rooms," *Journal of the Acoustical Society of America*, 116, pp 3480-3490.
- Smith C.D. and Parrott T.L., 1983. "Comparison of three methods for measuring acoustic properties of bulk materials," *Journal of the Acoustical Society of America*, 74 (5), pp 1577-1582.
- Utsuno H., Tanaka T., Fujikawa T. and Seybert A.F., 1989. "Transfer function method for measuring characteristic impedance and propagation constant of porous materials," *Journal of the Acoustical Society of America*, 86 (2), pp 637-643.

APPENDIX A

DETAILS AND STATISTICAL ANALYSIS RESULTS OF ARTIFICIAL NEURAL NETWORKS FOR PREDICTING ARCHITECTURAL SPEECH INTELLIGIBILITY AND SECURITY USING ONE-THIRD-OCTAVE BANDS SIGNAL-TO-NOISE RATIOS

Table A.1 Ranges of input variables of each ANN model using one-third-octave band signal-to-noise (S/N) ratios

	The Range of Input Variables for Predicting the Intelligibility Scores and the Intelligibility Threshold		The Range of Input Variables for Predicting the Cadence Threshold and the Audibility Threshold	
Input Variables	**Minimum dB**	**Maximum dB**	**Minimum dB**	**Maximum dB**
S/N Ratio at 160 Hz	-32.3	26.9	-23.7	9.9
S/N Ratio at 2000 Hz	-38.4	12.4	-38.4	-8.3
S/N Ratio at 250 Hz	-31.3	8.4	-31.3	-2.9
S/N Ratio at 315 Hz	-30.3	11.3	-30.3	0.0
S/N Ratio at 400 Hz	-29.4	13.7	-29.4	-1.9
S/N Ratio at 500 Hz	-30.9	15.0	-30.9	-2.1
S/N Ratio at 630 Hz	-32.6	10.7	-32.6	-1.5
S/N Ratio at 800 Hz	-33.4	2.7	-33.4	-13.1
S/N Ratio at 1 kHz	-32.7	2.8	-32.6	-15.5
S/N Ratio at 1.25 kHz	-32.6	-0.4	-31.9	-11.6
S/N Ratio at 1.6 kHz	-29.8	2.8	-29.8	-6.8
S/N Ratio at 2 kHz	-29.1	10.7	-28.6	-2.5
S/N Ratio at 2.5 kHz	-26.4	15.5	-25.7	2.1
S/N Ratio at 3.15 kHz	-27.6	12.3	-22.5	3.2
S/N Ratio at 4 kHz	-28.5	8.7	-22.2	-5.0
S/N Ratio at 6.3 kHz	-28.3	13.4	-20.2	-2.4
S/N Ratio at 8 kHz	-26.4	10.7	-18.5	-6.2

Table A.2 Shift and scale factors to inputs of each ANN model using one-third-octave band S/N ratios

Input variables	ANN Model for Predicting Intelligibility Scores		ANN Model for Predicting Intelligibility Threshold		ANN Model for Predicting Cadence Threshold		ANN Model for Predicting Audibility Threshold	
	Shift	Scale	Shift	Scale	Shift	Scale	Shift	Scale
S/N Ratio at 160 Hz	0.5453	0.0169	0.5249	0.0176	0.7050	0.0298	0.7480	0.0316
S/N Ratio at 2000 Hz	0.7556	0.0197	0.7684	0.0200	1.2742	0.0332	1.2740	0.0332
S/N Ratio at 250 Hz	0.7882	0.0252	0.7882	0.0252	1.1042	0.0363	1.1008	0.0351
S/N Ratio at 315 Hz	0.7292	0.0240	0.7292	0.0240	0.9992	0.0329	0.9992	0.0329
S/N Ratio at 400 Hz	0.6827	0.0232	0.6827	0.0232	1.0673	0.0363	1.0673	0.0363
S/N Ratio at 500 Hz	0.6728	0.0218	0.6728	0.0218	1.0718	0.0347	1.0718	0.0347
S/N Ratio at 630 Hz	0.7522	0.0231	0.7514	0.0232	1.0485	0.0322	1.0485	0.0322
S/N Ratio at 800 Hz	0.9263	0.0277	0.9410	0.0282	1.6450	0.0493	1.9085	0.0572
S/N Ratio at 1 kHz	0.9206	0.0281	0.9206	0.0281	1.9117	0.0586	1.9117	0.0586
S/N Ratio at 1.25 kHz	1.0139	0.0311	1.0139	0.0311	1.5746	0.0496	1.5713	0.0493
S/N Ratio at 1.6 kHz	0.9134	0.0307	0.9134	0.0307	1.2935	0.0435	1.2935	0.0435
S/N Ratio at 2 kHz	0.7320	0.0252	0.7320	0.0252	1.0973	0.0383	1.0973	0.0383
S/N Ratio at 2.5 kHz	0.6291	0.0239	0.6291	0.0239	0.9231	0.0359	0.9231	0.0359
S/N Ratio at 3.15 kHz	0.6919	0.0251	0.6919	0.0251	0.8773	0.0389	0.8773	0.0389
S/N Ratio at 4 kHz	0.7669	0.0269	0.7669	0.0269	1.2888	0.0579	1.3157	0.0591
S/N Ratio at 6.3 kHz	0.6791	0.0240	0.7492	0.0265	1.1377	0.0563	1.1377	0.0563
S/N Ratio at 8 kHz	0.7110	0.0269	0.7272	0.0276	1.5096	0.0818	1.5067	0.0816

Table A.3 Weights and biases to hidden neurons of each ANN model using one-third-octave band S/N ratios

	ANN Model for Predicting Intelligibility Scores			ANN Model for Predicting Intelligibility Threshold			ANN Model for Predicting Cadence Threshold			ANN Model for Predicting Audibility Threshold		
	h1#01	h1#02	h1#03	h1#01	h1#02	h1#03	h1#01	h1#02	h1#03	h1#01	h1#02	h1#03
Bias	0.6618	0.4631	7.4964	0.2604	-6.5581	0.0867	-0.1935	0.9061	-4.5788	4.4580	4.7960	2.6819
S/N Ratio at 160 Hz	0.2606	0.5531	-0.3364	0.8530	-0.0748	0.4031	-0.1198	0.6566	-0.2423	0.7386	2.8072	-1.7904
S/N Ratio at 2000 Hz	1.4678	0.4204	2.1696	1.7110	-3.5840	1.4639	2.9919	-0.3742	-3.4275	2.1972	1.3530	-1.9391
S/N Ratio at 250 Hz	-0.4848	0.1587	0.5699	0.6067	-1.0307	0.1605	-0.7898	0.4211	-0.9066	-0.7292	3.0498	-1.1777
S/N Ratio at 315 Hz	0.5726	0.2285	-1.0849	-0.0928	1.3142	0.8726	-2.8153	1.7774	2.1189	-1.5362	-4.5817	2.5482
S/N Ratio at 400 Hz	1.0424	0.6222	2.7649	0.6673	-2.0549	0.8079	-0.1227	-1.1665	-1.6673	1.6314	2.6688	0.4239
S/N Ratio at 500 Hz	1.7237	1.0584	4.7406	0.3650	-2.4946	0.0997	-1.6354	1.3643	1.7324	2.1388	2.5486	0.2391
S/N Ratio at 630 Hz	1.5073	1.1896	0.1833	0.8859	-0.5600	1.4410	2.5015	-3.0224	-4.4803	3.4614	2.1725	-0.3058
S/N Ratio at 800 Hz	1.0491	1.1118	-0.0876	2.7213	-2.4410	1.4857	-0.8064	1.5273	2.6156	0.0654	-3.3510	2.7679
S/N Ratio at 1 kHz	1.7880	0.6415	-0.4047	2.8141	-0.2973	0.2086	0.3829	0.0739	-0.2391	1.1607	2.4622	0.2054
S/N Ratio at 1.25 kHz	0.1493	1.1194	1.8849	0.8934	-1.5928	1.2533	-1.4178	1.5116	1.5926	-0.9453	-6.2791	2.6413
S/N Ratio at 1.6 kHz	3.3092	0.4267	0.7130	3.1996	-0.9247	0.8371	-1.8957	1.3775	4.1318	-0.3930	-1.7700	1.1078
S/N Ratio at 2 kHz	-0.5991	-0.0081	1.2408	0.7498	-0.2927	0.6531	3.9324	-2.1612	-4.0013	2.0707	3.6251	-3.8452
S/N Ratio at 2.5 kHz	-0.2268	0.2568	1.6002	-0.8551	-3.3902	0.3577	2.7284	-2.3846	-4.0365	3.3577	5.2778	-4.0614

	ANN Model for Predicting Intelligibility Scores			ANN Model for Predicting Intelligibility Threshold			ANN Model for Predicting Cadence Threshold			ANN Model for Predicting Audibility Threshold		
	h1#01	**h1#02**	**h1#03**	**h1#01**	**h1#02**	**h1#03**	**h1#01**	**h1#02**	**h1#03**	**h1#01**	**h1#02**	**h1#03**
S/N Ratio at 3.15 kHz	-0.5094	0.2727	0.1641	-1.5645	0.2797	1.4628	4.5197	-4.6323	-6.4257	5.1764	9.9580	-3.8420
S/N Ratio at 4 kHz	0.7472	-0.2862	1.3078	0.4513	0.4841	0.4002	1.6065	0.0376	-0.5232	0.8778	2.8643	-1.3171
S/N Ratio at 6.3 kHz	-0.8792	0.3984	3.5406	-1.5997	-2.7692	0.3561	2.8427	-0.8502	-1.9022	1.2908	4.3759	-0.7148
S/N Ratio at 8 kHz	-1.0926	0.0844	0.8817	-1.1649	-1.2248	0.2551	-1.3890	-0.2391	0.1133	0.0549	-0.8226	-0.1886

Table A.4 Weights and biases to the output neuron of each ANN model using one-third-octave band S/N ratios

	ANN Model for Predicting Intelligibility Scores	ANN Model for Predicting Intelligibility Threshold	ANN Model for Predicting Cadence Threshold	ANN Model for Predicting Audibility Threshold
	Output (Intelligibility Scores)	Output (Intelligibility Threshold)	Output (Cadence Threshold)	Output (Audibility Threshold)
Bias	0.4058	-0.4518	-1.6303	-0.0066
h1#01	-1.5015	-1.3673	-0.6447	-0.1512
h1#02	1.9459	-1.2363	0.0736	1.1394
h1#03	0.9548	1.9226	-1.2202	1.1378

Table A.5 Statistic results for ANN predictions using one-third-octave band S/N ratios

	ANN Model for Predicting Intelligibility Scores				ANN Model for Predicting Intelligibility Threshold				ANN Model for Predicting Cadence Threshold				ANN Model for Predicting Audibility Threshold			
	Tr[a]	Ve[b]	Te[c]	En[d]	Tr[a]	Ve[b]	Te[c]	En[d]	Tr[a]	Ve[b]	Te[c]	En[d]	Tr[a]	Ve[b]	Te[c]	En[d]
RMS error	0.203	0.195	0.200	0.202	0.100	0.099	0.118	0.102	0.077	0.042	0.049	0.072	0.067	0.089	0.101	0.069
Error SD[e]	0.203	0.195	0.200	0.202	0.100	0.098	0.119	0.102	0.077	0.042	0.050	0.072	0.069	0.016	0.095	0.069
SDR.[f]	0.471	0.452	0.468	0.469	0.242	0.235	0.277	0.245	0.185	0.107	0.122	0.172	0.182	0.049	0.229	0.182
R^2	0.778	0.795	0.781	0.780	0.942	0.945	0.924	0.940	0.966	0.989	0.987	0.971	0.967	0.998	0.955	0.967

[a]Tr = training data set.
[b]Ve = verification data set.
[c]Te = test data set.
[d]En = entire data set.
[e]Error SD = standard deviation of the prediction error.
[f]SDR = standard deviation ratio.

APPENDIX B

SURFACE IMPEDANCES AND BULK ACOUSTICAL PROPERTIES OF THE TEST MATERIAL SAMPLE (A PIECE OF 30 MM THICK CELLULAR FOAM) USED IN CHAPTER 6

Table B.1 Measured surface impedance (normalised by the characteristic impedance of the air, ρc), between 300 and 3800 Hz, of the material sample with an air cavity of 90 mm between the test material sample and the rigid wall

Frequency (Hz)	Real Part	Imaginary Part	Frequency (Hz)	Real Part	Imaginary Part
300	0.3652	-1.1391	700	0.4365	0.0818
312.5	0.3608	-1.0741	712.5	0.4373	0.1089
325	0.3676	-1.0219	725	0.4389	0.1424
337.5	0.3709	-0.9604	737.5	0.4395	0.1684
350	0.3739	-0.9076	750	0.4409	0.2017
362.5	0.3798	-0.8502	762.5	0.4462	0.2357
375	0.3705	-0.8028	775	0.4439	0.2621
387.5	0.3779	-0.7443	787.5	0.4403	0.2911
400	0.3737	-0.7067	800	0.4373	0.3368
412.5	0.3852	-0.6672	812.5	0.4435	0.3762
425	0.3818	-0.6234	825	0.4571	0.4220
437.5	0.3781	-0.5818	837.5	0.4625	0.4523
450	0.3849	-0.5396	850	0.4703	0.4953
462.5	0.3923	-0.5031	862.5	0.4854	0.5460
475	0.3890	-0.4636	875	0.4984	0.5787
487.5	0.3916	-0.4293	887.5	0.5208	0.6244
500	0.3910	-0.3919	900	0.5456	0.6588
512.5	0.3965	-0.3581	912.5	0.5570	0.6973
525	0.3980	-0.3273	925	0.5884	0.7240
537.5	0.3985	-0.2966	937.5	0.6006	0.7737
550	0.4034	-0.2632	950	0.6128	0.8225
562.5	0.4087	-0.2355	962.5	0.6429	0.8529
575	0.4129	-0.2026	975	0.6534	0.9009
587.5	0.4115	-0.1748	987.5	0.6795	0.9451
600	0.4144	-0.1457	1000	0.7016	0.9864
612.5	0.4165	-0.1164	1012.5	0.7498	1.0416
625	0.4201	-0.0886	1025	0.7587	1.0957
637.5	0.4246	-0.0570	1037.5	0.7977	1.1377
650	0.4271	-0.0296	1050	0.8290	1.1861
662.5	0.4298	-0.0013	1062.5	0.8797	1.2648
675	0.4315	0.0248	1075	0.9001	1.3038
687.5	0.4350	0.0549	1087.5	0.9460	1.3403

Frequency (Hz)	Real Part	Imaginary Part	Frequency (Hz)	Real Part	Imaginary Part
1100	1.0206	1.4346	1687.5	0.3908	-1.2265
1112.5	1.0520	1.4811	1700	0.3764	-1.1701
1125	1.0922	1.5627	1712.5	0.3499	-1.1010
1137.5	1.1579	1.6322	1725	0.3358	-1.0344
1150	1.2733	1.6964	1737.5	0.3140	-0.9729
1162.5	1.3252	1.7880	1750	0.3092	-0.9205
1175	1.4075	1.8656	1762.5	0.2991	-0.8668
1187.5	1.5710	1.9682	1775	0.3003	-0.8019
1200	1.6548	2.0715	1787.5	0.2950	-0.7619
1212.5	1.8274	2.1695	1800	0.2966	-0.7081
1225	1.9905	2.3385	1812.5	0.2900	-0.6649
1237.5	2.2562	2.3428	1825	0.2907	-0.6199
1250	2.4013	2.4790	1837.5	0.2851	-0.5724
1262.5	2.7981	2.5076	1850	0.2824	-0.5338
1275	3.0740	2.5677	1862.5	0.2851	-0.4882
1287.5	3.5502	2.6366	1875	0.2992	-0.4460
1300	4.0878	2.5685	1887.5	0.2915	-0.4135
1312.5	4.5291	2.4103	1900	0.2907	-0.3723
1325	5.2627	2.0442	1912.5	0.3002	-0.3361
1337.5	5.7482	1.7375	1925	0.3071	-0.2988
1350	6.2547	1.0640	1937.5	0.3116	-0.2638
1362.5	6.5046	0.0857	1950	0.3203	-0.2287
1375	6.6546	-0.7516	1962.5	0.3260	-0.1943
1387.5	6.5182	-1.6125	1975	0.3400	-0.1659
1400	6.0225	-2.4000	1987.5	0.3416	-0.1336
1412.5	5.3219	-3.2559	2000	0.3476	-0.1035
1425	4.7540	-3.5681	2012.5	0.3592	-0.0718
1437.5	3.7879	-3.6606	2025	0.3598	-0.0539
1450	3.2448	-3.7435	2037.5	0.3732	-0.0041
1462.5	2.6629	-3.6382	2050	0.3726	0.0145
1475	2.1870	-3.4725	2062.5	0.3825	0.0447
1487.5	1.9256	-3.2882	2075	0.4053	0.0886
1500	1.4495	-2.9764	2087.5	0.4024	0.1132
1512.5	1.3127	-2.8011	2100	0.4064	0.1364
1525	1.0890	-2.6768	2112.5	0.4243	0.1769
1537.5	0.9082	-2.4558	2125	0.4336	0.2003
1550	0.7747	-2.3044	2137.5	0.4457	0.2307
1562.5	0.7105	-2.1540	2150	0.4705	0.2685
1575	0.6333	-2.0213	2162.5	0.4655	0.2892
1587.5	0.5733	-1.8802	2175	0.4963	0.3117
1600	0.5341	-1.7759	2187.5	0.4999	0.3510
1612.5	0.5047	-1.6660	2200	0.5195	0.3750
1625	0.4834	-1.5709	2212.5	0.5330	0.4290
1637.5	0.4649	-1.4832	2225	0.5602	0.4361
1650	0.4408	-1.4087	2237.5	0.5778	0.4911
1662.5	0.4426	-1.3436	2250	0.5883	0.5154
1675	0.4172	-1.2932	2262.5	0.6298	0.5322

Frequency (Hz)	Real Part	Imaginary Part	Frequency (Hz)	Real Part	Imaginary Part
2275	0.6506	0.5840	2862.5	1.7717	-1.8616
2287.5	0.6634	0.6229	2875	1.6545	-1.8403
2300	0.7075	0.6423	2887.5	1.5009	-1.7865
2312.5	0.7187	0.6919	2900	1.3908	-1.7856
2325	0.7575	0.7168	2912.5	1.2808	-1.7256
2337.5	0.7869	0.7580	2925	1.1966	-1.6930
2350	0.8426	0.8008	2937.5	1.1007	-1.6289
2362.5	0.8646	0.8368	2950	1.0442	-1.5898
2375	0.9204	0.8640	2962.5	0.9674	-1.5323
2387.5	0.9492	0.9129	2975	0.8851	-1.4898
2400	1.0059	0.9565	2987.5	0.8339	-1.4313
2412.5	1.0591	0.9808	3000	0.7887	-1.3810
2425	1.1254	1.0264	3012.5	0.7362	-1.3297
2437.5	1.1714	1.0446	3025	0.6891	-1.2905
2450	1.2354	1.0913	3037.5	0.6537	-1.2434
2462.5	1.2950	1.1056	3050	0.6280	-1.1844
2475	1.3725	1.1547	3062.5	0.5895	-1.1372
2487.5	1.4537	1.1657	3075	0.5495	-1.0954
2500	1.5312	1.2360	3087.5	0.5271	-1.0624
2512.5	1.6472	1.2791	3100	0.5003	-1.0103
2525	1.7505	1.2843	3112.5	0.4767	-0.9690
2537.5	1.8754	1.2968	3125	0.4575	-0.9145
2550	2.0178	1.3132	3137.5	0.4315	-0.8806
2562.5	2.1580	1.2924	3150	0.4141	-0.8298
2575	2.3085	1.2564	3162.5	0.3982	-0.7809
2587.5	2.5147	1.2054	3175	0.3933	-0.7436
2600	2.6476	1.1132	3187.5	0.3849	-0.6944
2612.5	2.8049	1.0682	3200	0.3724	-0.6599
2625	2.8923	0.9624	3212.5	0.3647	-0.6249
2637.5	3.0823	0.8090	3225	0.3601	-0.5883
2650	3.2344	0.6144	3237.5	0.3559	-0.5426
2662.5	3.3215	0.4798	3250	0.3409	-0.5090
2675	3.3900	0.2253	3262.5	0.3356	-0.4802
2687.5	3.4421	0.0695	3275	0.3374	-0.4434
2700	3.5357	-0.2007	3287.5	0.3289	-0.4064
2712.5	3.4538	-0.4260	3300	0.3281	-0.3755
2725	3.4443	-0.6191	3312.5	0.3258	-0.3390
2737.5	3.4182	-0.8800	3325	0.3219	-0.3013
2750	3.2570	-1.1787	3337.5	0.3294	-0.2736
2762.5	3.1914	-1.2711	3350	0.3162	-0.2356
2775	2.9898	-1.4634	3362.5	0.3201	-0.2016
2787.5	2.8008	-1.6140	3375	0.3304	-0.1636
2800	2.6239	-1.6650	3387.5	0.3331	-0.1304
2812.5	2.4617	-1.7376	3400	0.3349	-0.1068
2825	2.2327	-1.8273	3412.5	0.3348	-0.0715
2837.5	2.0807	-1.8873	3425	0.3426	-0.0432
2850	1.9255	-1.8648	3437.5	0.3366	-0.0081

Frequency (Hz)	Real Part	Imaginary Part	Frequency (Hz)	Real Part	Imaginary Part
3450	0.3536	0.0150	3637.5	0.5054	0.4456
3462.5	0.3549	0.0435	3650	0.5143	0.4763
3475	0.3555	0.0739	3662.5	0.5273	0.5008
3487.5	0.3634	0.1085	3675	0.5555	0.5362
3500	0.3691	0.1384	3687.5	0.5777	0.5674
3512.5	0.3771	0.1660	3700	0.6116	0.5758
3525	0.3819	0.1985	3712.5	0.6396	0.6331
3537.5	0.3979	0.2208	3725	0.6527	0.6417
3550	0.4135	0.2537	3737.5	0.6952	0.6702
3562.5	0.4269	0.2761	3750	0.7268	0.7240
3575	0.4343	0.3000	3762.5	0.7585	0.7601
3587.5	0.4486	0.3373	3775	0.7890	0.7921
3600	0.4582	0.3529	3787.5	0.8256	0.8365
3612.5	0.4643	0.3812	3800	0.8775	0.8806
3625	0.4872	0.4050			

Table B.2 Measured surface impedance (normalised by the characteristic impedance of the air, ρc), between 300 and 3800 Hz, of the material sample with an air cavity of 53 mm between the test material sample and the rigid wall

Frequency (Hz)	Real Part	Imaginary Part	Frequency (Hz)	Real Part	Imaginary Part
300	0.3523	-1.7412	825	0.3618	-0.1885
312.5	0.3738	-1.6860	837.5	0.3523	-0.1723
325	0.3631	-1.6442	850	0.3443	-0.1375
337.5	0.3606	-1.5528	862.5	0.3479	-0.1052
350	0.3633	-1.4933	875	0.3537	-0.0717
362.5	0.3544	-1.4298	887.5	0.3629	-0.0452
375	0.3609	-1.3680	900	0.3751	-0.0212
387.5	0.3650	-1.3119	912.5	0.3840	0.0010
400	0.3689	-1.2493	925	0.3938	0.0199
412.5	0.3765	-1.2148	937.5	0.3976	0.0398
425	0.3808	-1.1615	950	0.4005	0.0583
437.5	0.3706	-1.1131	962.5	0.4130	0.0860
450	0.3706	-1.0764	975	0.4154	0.1066
462.5	0.3586	-1.0145	987.5	0.4238	0.1236
475	0.3625	-0.9878	1000	0.4218	0.1489
487.5	0.3585	-0.9463	1012.5	0.4341	0.1700
500	0.3641	-0.9061	1025	0.4344	0.1899
512.5	0.3607	-0.8723	1037.5	0.4452	0.2104
525	0.3656	-0.8354	1050	0.4488	0.2292
537.5	0.3579	-0.7987	1062.5	0.4606	0.2539
550	0.3627	-0.7649	1075	0.4595	0.2642
562.5	0.3618	-0.7351	1087.5	0.4714	0.2896
575	0.3593	-0.7043	1100	0.4815	0.3230
587.5	0.3610	-0.6753	1112.5	0.4815	0.3260
600	0.3648	-0.6489	1125	0.4936	0.3683
612.5	0.3658	-0.6234	1137.5	0.4992	0.3804
625	0.3658	-0.5900	1150	0.5083	0.3981
637.5	0.3679	-0.5678	1162.5	0.5124	0.4200
650	0.3692	-0.5371	1175	0.5255	0.4390
662.5	0.3667	-0.5143	1187.5	0.5360	0.4603
675	0.3665	-0.4888	1200	0.5539	0.4853
687.5	0.3646	-0.4632	1212.5	0.5591	0.5024
700	0.3637	-0.4371	1225	0.5586	0.5358
712.5	0.3606	-0.4170	1237.5	0.5702	0.5522
725	0.3569	-0.3937	1250	0.5860	0.5862
737.5	0.3542	-0.3624	1262.5	0.5865	0.6030
750	0.3539	-0.3421	1275	0.6051	0.6302
762.5	0.3531	-0.3159	1287.5	0.6163	0.6424
775	0.3529	-0.2855	1300	0.6300	0.6697
787.5	0.3499	-0.2585	1312.5	0.6478	0.6959
800	0.3509	-0.2339	1325	0.6601	0.7236
812.5	0.3547	-0.2062	1337.5	0.6836	0.7372

Frequency (Hz)	Real Part	Imaginary Part	Frequency (Hz)	Real Part	Imaginary Part
1350	0.6906	0.7768	1937.5	4.5012	-0.4594
1362.5	0.7092	0.8006	1950	4.4896	-0.7344
1375	0.7209	0.8163	1962.5	4.4706	-1.0131
1387.5	0.7480	0.8571	1975	4.4299	-1.2834
1400	0.7685	0.8762	1987.5	4.1918	-1.5510
1412.5	0.7888	0.9121	2000	3.9985	-1.7835
1425	0.8079	0.9224	2012.5	3.8228	-2.0940
1437.5	0.8310	0.9607	2025	3.6367	-2.2472
1450	0.8446	0.9943	2037.5	3.4398	-2.3724
1462.5	0.8765	1.0211	2050	3.1360	-2.4370
1475	0.9016	1.0594	2062.5	2.9318	-2.4849
1487.5	0.9126	1.0753	2075	2.7654	-2.5968
1500	0.9552	1.1184	2087.5	2.4243	-2.5842
1512.5	0.9945	1.1437	2100	2.3354	-2.5795
1525	1.0191	1.1695	2112.5	2.0190	-2.5949
1537.5	1.0635	1.2209	2125	1.8831	-2.5553
1550	1.1055	1.2443	2137.5	1.7889	-2.4758
1562.5	1.1246	1.2818	2150	1.6282	-2.4199
1575	1.1723	1.3108	2162.5	1.4587	-2.2776
1587.5	1.2203	1.3772	2175	1.3323	-2.3732
1600	1.2897	1.4104	2187.5	1.2607	-2.1982
1612.5	1.3285	1.4346	2200	1.1092	-2.1561
1625	1.4173	1.4884	2212.5	1.1340	-2.1365
1637.5	1.4533	1.5167	2225	0.9502	-2.0201
1650	1.5354	1.5641	2237.5	0.9658	-1.9757
1662.5	1.5944	1.5996	2250	0.8819	-1.8908
1675	1.7088	1.6454	2262.5	0.8209	-1.8548
1687.5	1.7839	1.6873	2275	0.7584	-1.7825
1700	1.8890	1.7306	2287.5	0.7249	-1.7287
1712.5	1.9951	1.7450	2300	0.6921	-1.6708
1725	2.1026	1.7844	2312.5	0.6619	-1.6075
1737.5	2.2302	1.7877	2325	0.6136	-1.5689
1750	2.3571	1.8272	2337.5	0.6021	-1.5107
1762.5	2.5461	1.8299	2350	0.5645	-1.4619
1775	2.6569	1.8126	2362.5	0.5390	-1.4092
1787.5	2.8338	1.8117	2375	0.5054	-1.3587
1800	3.0076	1.7167	2387.5	0.5065	-1.3288
1812.5	3.2441	1.6719	2400	0.4686	-1.2794
1825	3.3739	1.5764	2412.5	0.4596	-1.2353
1837.5	3.6118	1.4852	2425	0.4278	-1.1971
1850	3.7758	1.2743	2437.5	0.4279	-1.1445
1862.5	3.9257	1.1473	2450	0.4262	-1.1214
1875	4.1020	0.8972	2462.5	0.4110	-1.0660
1887.5	4.2945	0.7104	2475	0.3990	-1.0491
1900	4.3821	0.4725	2487.5	0.3691	-1.0053
1912.5	4.4764	0.1881	2500	0.3645	-0.9747
1925	4.5384	-0.1261	2512.5	0.3614	-0.9358

Frequency (Hz)	Real Part	Imaginary Part	Frequency (Hz)	Real Part	Imaginary Part
2525	0.3443	-0.9070	3112.5	0.4210	0.2701
2537.5	0.3414	-0.8527	3125	0.4264	0.2942
2550	0.3334	-0.8391	3137.5	0.4409	0.3158
2562.5	0.3273	-0.8006	3150	0.4493	0.3436
2575	0.3273	-0.7601	3162.5	0.4579	0.3631
2587.5	0.3170	-0.7395	3175	0.4701	0.3906
2600	0.3169	-0.7083	3187.5	0.4803	0.4121
2612.5	0.3242	-0.6790	3200	0.4933	0.4335
2625	0.3095	-0.6476	3212.5	0.5078	0.4574
2637.5	0.3179	-0.6217	3225	0.5206	0.4874
2650	0.3023	-0.5980	3237.5	0.5343	0.5082
2662.5	0.3057	-0.5735	3250	0.5460	0.5314
2675	0.2914	-0.5339	3262.5	0.5648	0.5618
2687.5	0.2988	-0.5162	3275	0.5773	0.5829
2700	0.2943	-0.4777	3287.5	0.5929	0.6100
2712.5	0.2925	-0.4569	3300	0.6170	0.6406
2725	0.2957	-0.4268	3312.5	0.6330	0.6552
2737.5	0.2954	-0.4021	3325	0.6528	0.6919
2750	0.2964	-0.3832	3337.5	0.6752	0.7111
2762.5	0.2970	-0.3570	3350	0.7079	0.7332
2775	0.3011	-0.3300	3362.5	0.7236	0.7578
2787.5	0.2962	-0.3052	3375	0.7410	0.7829
2800	0.3005	-0.2836	3387.5	0.7728	0.8100
2812.5	0.2987	-0.2596	3400	0.7864	0.8372
2825	0.3006	-0.2401	3412.5	0.8276	0.8643
2837.5	0.3016	-0.2144	3425	0.8541	0.8943
2850	0.3024	-0.1909	3437.5	0.8740	0.9197
2862.5	0.3000	-0.1740	3450	0.9074	0.9559
2875	0.3052	-0.1423	3462.5	0.9475	0.9831
2887.5	0.3124	-0.1267	3475	1.0145	1.0058
2900	0.3163	-0.1028	3487.5	1.0592	1.0526
2912.5	0.3149	-0.0812	3500	1.1278	1.0680
2925	0.3234	-0.0612	3512.5	1.1985	1.0708
2937.5	0.3297	-0.0342	3525	1.2725	1.0802
2950	0.3311	-0.0112	3537.5	1.4238	1.0924
2962.5	0.3363	0.0080	3550	1.4664	0.9970
2975	0.3429	0.0322	3562.5	1.5022	0.9535
2987.5	0.3468	0.0489	3575	1.5115	0.8761
3000	0.3548	0.0739	3587.5	1.4981	0.8742
3012.5	0.3565	0.0949	3600	1.5020	0.8894
3025	0.3688	0.1121	3612.5	1.5593	0.8943
3037.5	0.3741	0.1344	3625	1.5858	0.9046
3050	0.3823	0.1593	3637.5	1.6661	0.9665
3062.5	0.3859	0.1790	3650	1.7153	0.9417
3075	0.3935	0.1988	3662.5	1.7803	0.8948
3087.5	0.4006	0.2239	3675	1.8526	0.9304
3100	0.4089	0.2454	3687.5	1.9083	0.9112

Frequency (Hz)	Real Part	Imaginary Part	Frequency (Hz)	Real Part	Imaginary Part
3700	1.9951	0.8656	3762.5	2.4357	0.7278
3712.5	2.0913	0.8555	3775	2.5262	0.6258
3725	2.1901	0.8298	3787.5	2.5883	0.6624
3737.5	2.2531	0.7888	3800	2.7100	0.5162
3750	2.3598	0.7455			

Table B.3 Derived characteristic impedance (normalised by the characteristic impedance of the air, ρc), between 300 and 3800 Hz, using the optimised set of c_1-c_8 of the optimisation condition 7 in Table 6.3 and Equation (6.15)

Frequency (Hz)	Real Part	Imaginary Part	Frequency (Hz)	Real Part	Imaginary Part
300	0.3369	-1.1699	825	0.4979	0.4337
312.5	0.3366	-1.1009	837.5	0.5081	0.4665
325	0.3366	-1.0360	850	0.5188	0.4999
337.5	0.3368	-0.9748	862.5	0.5301	0.5340
350	0.3372	-0.9169	875	0.5422	0.5687
362.5	0.3379	-0.8620	887.5	0.5550	0.6041
375	0.3387	-0.8097	900	0.5686	0.6403
387.5	0.3397	-0.7599	912.5	0.5831	0.6775
400	0.3409	-0.7121	925	0.5986	0.7156
412.5	0.3423	-0.6663	937.5	0.6152	0.7547
425	0.3438	-0.6222	950	0.6330	0.7951
437.5	0.3455	-0.5798	962.5	0.6521	0.8366
450	0.3474	-0.5387	975	0.6727	0.8796
462.5	0.3494	-0.4990	987.5	0.6948	0.9240
475	0.3516	-0.4604	1000	0.7188	0.9700
487.5	0.3540	-0.4230	1012.5	0.7447	1.0178
500	0.3565	-0.3864	1025	0.7729	1.0675
512.5	0.3592	-0.3508	1037.5	0.8036	1.1193
525	0.3620	-0.3160	1050	0.8372	1.1733
537.5	0.3650	-0.2819	1062.5	0.8739	1.2297
550	0.3682	-0.2484	1075	0.9144	1.2887
562.5	0.3715	-0.2155	1087.5	0.9590	1.3506
575	0.3750	-0.1831	1100	1.0084	1.4155
587.5	0.3787	-0.1512	1112.5	1.0634	1.4837
600	0.3826	-0.1197	1125	1.1248	1.5555
612.5	0.3867	-0.0885	1137.5	1.1936	1.6309
625	0.3910	-0.0577	1150	1.2712	1.7103
637.5	0.3955	-0.0270	1162.5	1.3591	1.7938
650	0.4002	0.0034	1175	1.4592	1.8813
662.5	0.4052	0.0337	1187.5	1.5738	1.9728
675	0.4104	0.0639	1200	1.7056	2.0679
687.5	0.4159	0.0940	1212.5	1.8583	2.1657
700	0.4216	0.1241	1225	2.0360	2.2648
712.5	0.4276	0.1542	1237.5	2.2439	2.3626
725	0.4339	0.1844	1250	2.4883	2.4552
737.5	0.4406	0.2147	1262.5	2.7764	2.5359
750	0.4475	0.2451	1275	3.1161	2.5947
762.5	0.4549	0.2758	1287.5	3.5153	2.6162
775	0.4626	0.3067	1300	3.9794	2.5777
787.5	0.4707	0.3379	1312.5	4.5074	2.4472
800	0.4793	0.3694	1325	5.0844	2.1840
812.5	0.4884	0.4013	1337.5	5.6715	1.7432

Frequency (Hz)	Real Part	Imaginary Part	Frequency (Hz)	Real Part	Imaginary Part
1350	6.1967	1.0921	1937.5	0.3212	-0.2599
1362.5	6.5585	0.2369	1950	0.3261	-0.2248
1375	6.6544	-0.7517	1962.5	0.3314	-0.1903
1387.5	6.4324	-1.7421	1975	0.3372	-0.1564
1400	5.9270	-2.5914	1987.5	0.3435	-0.1229
1412.5	5.2432	-3.2069	2000	0.3502	-0.0897
1425	4.5018	-3.5720	2012.5	0.3573	-0.0570
1437.5	3.7943	-3.7252	2025	0.3649	-0.0245
1450	3.1695	-3.7259	2037.5	0.3729	0.0077
1462.5	2.6425	-3.6291	2050	0.3814	0.0397
1475	2.2095	-3.4770	2062.5	0.3905	0.0715
1487.5	1.8582	-3.2977	2075	0.4000	0.1031
1500	1.5748	-3.1091	2087.5	0.4102	0.1347
1512.5	1.3461	-2.9214	2100	0.4208	0.1663
1525	1.1611	-2.7405	2112.5	0.4321	0.1978
1537.5	1.0109	-2.5693	2125	0.4440	0.2293
1550	0.8882	-2.4089	2137.5	0.4566	0.2609
1562.5	0.7876	-2.2594	2150	0.4700	0.2925
1575	0.7045	-2.1206	2162.5	0.4840	0.3243
1587.5	0.6357	-1.9918	2175	0.4989	0.3563
1600	0.5783	-1.8722	2187.5	0.5147	0.3884
1612.5	0.5304	-1.7610	2200	0.5314	0.4207
1625	0.4902	-1.6575	2212.5	0.5491	0.4532
1637.5	0.4564	-1.5609	2225	0.5678	0.4861
1650	0.4279	-1.4706	2237.5	0.5878	0.5192
1662.5	0.4039	-1.3859	2250	0.6090	0.5526
1675	0.3837	-1.3064	2262.5	0.6315	0.5863
1687.5	0.3666	-1.2315	2275	0.6555	0.6204
1700	0.3523	-1.1607	2287.5	0.6811	0.6549
1712.5	0.3403	-1.0938	2300	0.7084	0.6897
1725	0.3303	-1.0303	2312.5	0.7377	0.7248
1737.5	0.3221	-0.9699	2325	0.7689	0.7603
1750	0.3154	-0.9123	2337.5	0.8024	0.7961
1762.5	0.3101	-0.8573	2350	0.8384	0.8322
1775	0.3059	-0.8046	2362.5	0.8770	0.8686
1787.5	0.3028	-0.7540	2375	0.9186	0.9051
1800	0.3007	-0.7054	2387.5	0.9633	0.9417
1812.5	0.2994	-0.6586	2400	1.0116	0.9782
1825	0.2989	-0.6134	2412.5	1.0636	1.0145
1837.5	0.2991	-0.5697	2425	1.1199	1.0504
1850	0.3000	-0.5273	2437.5	1.1808	1.0855
1862.5	0.3015	-0.4862	2450	1.2468	1.1196
1875	0.3035	-0.4462	2462.5	1.3182	1.1523
1887.5	0.3061	-0.4072	2475	1.3955	1.1829
1900	0.3091	-0.3692	2487.5	1.4794	1.2109
1912.5	0.3127	-0.3320	2500	1.5701	1.2355
1925	0.3167	-0.2956	2512.5	1.6683	1.2556

Frequency (Hz)	Real Part	Imaginary Part	Frequency (Hz)	Real Part	Imaginary Part
2525	1.7743	1.2700	3112.5	0.4742	-0.9387
2537.5	1.8885	1.2774	3125	0.4548	-0.8960
2550	2.0109	1.2760	3137.5	0.4372	-0.8544
2562.5	2.1414	1.2639	3150	0.4213	-0.8136
2575	2.2797	1.2388	3162.5	0.4069	-0.7738
2587.5	2.4247	1.1983	3175	0.3939	-0.7349
2600	2.5748	1.1396	3187.5	0.3822	-0.6968
2612.5	2.7278	1.0602	3200	0.3718	-0.6595
2625	2.8802	0.9574	3212.5	0.3624	-0.6229
2637.5	3.0278	0.8295	3225	0.3541	-0.5870
2650	3.1653	0.6751	3237.5	0.3468	-0.5518
2662.5	3.2867	0.4947	3250	0.3403	-0.5171
2675	3.3856	0.2902	3262.5	0.3347	-0.4830
2687.5	3.4558	0.0655	3275	0.3298	-0.4495
2700	3.4920	-0.1734	3287.5	0.3258	-0.4164
2712.5	3.4907	-0.4189	3300	0.3224	-0.3837
2725	3.4509	-0.6626	3312.5	0.3197	-0.3515
2737.5	3.3739	-0.8958	3325	0.3177	-0.3195
2750	3.2635	-1.1108	3337.5	0.3163	-0.2880
2762.5	3.1255	-1.3016	3350	0.3155	-0.2567
2775	2.9668	-1.4642	3362.5	0.3154	-0.2256
2787.5	2.7943	-1.5970	3375	0.3158	-0.1948
2800	2.6149	-1.7000	3387.5	0.3167	-0.1641
2812.5	2.4342	-1.7750	3400	0.3183	-0.1336
2825	2.2570	-1.8246	3412.5	0.3204	-0.1032
2837.5	2.0865	-1.8522	3425	0.3231	-0.0728
2850	1.9252	-1.8609	3437.5	0.3264	-0.0426
2862.5	1.7745	-1.8542	3450	0.3302	-0.0123
2875	1.6349	-1.8351	3462.5	0.3347	0.0180
2887.5	1.5066	-1.8061	3475	0.3397	0.0483
2900	1.3894	-1.7695	3487.5	0.3454	0.0787
2912.5	1.2827	-1.7272	3500	0.3518	0.1093
2925	1.1860	-1.6808	3512.5	0.3588	0.1400
2937.5	1.0983	-1.6315	3525	0.3666	0.1708
2950	1.0191	-1.5804	3537.5	0.3750	0.2019
2962.5	0.9474	-1.5281	3550	0.3843	0.2332
2975	0.8828	-1.4754	3562.5	0.3944	0.2647
2987.5	0.8243	-1.4227	3575	0.4054	0.2966
3000	0.7716	-1.3702	3587.5	0.4174	0.3288
3012.5	0.7239	-1.3184	3600	0.4303	0.3613
3025	0.6808	-1.2674	3612.5	0.4443	0.3943
3037.5	0.6418	-1.2172	3625	0.4595	0.4276
3050	0.6065	-1.1681	3637.5	0.4760	0.4614
3062.5	0.5746	-1.1201	3650	0.4938	0.4956
3075	0.5457	-1.0731	3662.5	0.5130	0.5303
3087.5	0.5195	-1.0272	3675	0.5339	0.5655
3100	0.4957	-0.9824	3687.5	0.5565	0.6012

Frequency (Hz)	Real Part	Imaginary Part	Frequency (Hz)	Real Part	Imaginary Part
3700	0.5810	0.6374	3762.5	0.7388	0.8250
3712.5	0.6076	0.6741	3775	0.7791	0.8634
3725	0.6364	0.7112	3787.5	0.8230	0.9019
3737.5	0.6677	0.7488	3800	0.8709	0.9403
3750	0.7018	0.7867			

Table B.4 Derived propagation constant, between 300 and 3800 Hz, using the optimised set of c_1-c_8 of the optimisation condition 7 in Table 6.3 and Equation (6.16)

Frequency (Hz)	Real Part	Imaginary Part	Frequency (Hz)	Real Part	Imaginary Part
300	5.5124	8.1517	825	7.4548	19.7654
312.5	5.5799	8.4413	837.5	7.4883	20.0334
325	5.6456	8.7298	850	7.5215	20.3012
337.5	5.7095	9.0173	862.5	7.5543	20.5688
350	5.7718	9.3039	875	7.5868	20.8360
362.5	5.8326	9.5896	887.5	7.6190	21.1031
375	5.8919	9.8744	900	7.6509	21.3699
387.5	5.9498	10.1584	912.5	7.6824	21.6365
400	6.0065	10.4416	925	7.7137	21.9029
412.5	6.0619	10.7241	937.5	7.7446	22.1690
425	6.1161	11.0059	950	7.7753	22.4349
437.5	6.1693	11.2869	962.5	7.8057	22.7006
450	6.2213	11.5674	975	7.8358	22.9662
462.5	6.2724	11.8472	987.5	7.8656	23.2315
475	6.3225	12.1264	1000	7.8952	23.4966
487.5	6.3717	12.4050	1012.5	7.9245	23.7615
500	6.4200	12.6831	1025	7.9536	24.0262
512.5	6.4675	12.9606	1037.5	7.9824	24.2907
525	6.5142	13.2376	1050	8.0110	24.5551
537.5	6.5601	13.5141	1062.5	8.0394	24.8192
550	6.6052	13.7901	1075	8.0675	25.0832
562.5	6.6497	14.0657	1087.5	8.0953	25.3470
575	6.6934	14.3408	1100	8.1230	25.6106
587.5	6.7365	14.6155	1112.5	8.1504	25.8741
600	6.7790	14.8897	1125	8.1777	26.1374
612.5	6.8208	15.1635	1137.5	8.2047	26.4005
625	6.8621	15.4370	1150	8.2315	26.6634
637.5	6.9027	15.7100	1162.5	8.2581	26.9262
650	6.9429	15.9827	1175	8.2845	27.1889
662.5	6.9824	16.2550	1187.5	8.3107	27.4514
675	7.0215	16.5269	1200	8.3367	27.7137
687.5	7.0600	16.7985	1212.5	8.3625	27.9759
700	7.0981	17.0697	1225	8.3881	28.2379
712.5	7.1357	17.3407	1237.5	8.4136	28.4998
725	7.1728	17.6113	1250	8.4388	28.7616
737.5	7.2095	17.8816	1262.5	8.4639	29.0232
750	7.2457	18.1515	1275	8.4889	29.2846
762.5	7.2816	18.4212	1287.5	8.5136	29.5459
775	7.3170	18.6906	1300	8.5382	29.8071
787.5	7.3520	18.9597	1312.5	8.5626	30.0682
800	7.3866	19.2286	1325	8.5869	30.3291
812.5	7.4209	19.4971	1337.5	8.6109	30.5899

Frequency (Hz)	Real Part	Imaginary Part	Frequency (Hz)	Real Part	Imaginary Part
1350	8.6349	30.8506	1937.5	9.6178	42.9820
1362.5	8.6587	31.1111	1950	9.6363	43.2380
1375	8.6823	31.3715	1962.5	9.6547	43.4939
1387.5	8.7058	31.6318	1975	9.6730	43.7497
1400	8.7291	31.8920	1987.5	9.6912	44.0055
1412.5	8.7523	32.1520	2000	9.7094	44.2612
1425	8.7753	32.4119	2012.5	9.7275	44.5168
1437.5	8.7982	32.6717	2025	9.7455	44.7724
1450	8.8210	32.9314	2037.5	9.7634	45.0279
1462.5	8.8436	33.1910	2050	9.7812	45.2833
1475	8.8661	33.4505	2062.5	9.7990	45.5386
1487.5	8.8884	33.7098	2075	9.8166	45.7939
1500	8.9107	33.9691	2087.5	9.8342	46.0491
1512.5	8.9328	34.2282	2100	9.8518	46.3043
1525	8.9547	34.4872	2112.5	9.8692	46.5594
1537.5	8.9766	34.7462	2125	9.8866	46.8144
1550	8.9983	35.0050	2137.5	9.9040	47.0693
1562.5	9.0199	35.2637	2150	9.9212	47.3242
1575	9.0413	35.5223	2162.5	9.9384	47.5790
1587.5	9.0627	35.7808	2175	9.9555	47.8338
1600	9.0839	36.0392	2187.5	9.9725	48.0884
1612.5	9.1051	36.2975	2200	9.9895	48.3431
1625	9.1261	36.5557	2212.5	10.0064	48.5976
1637.5	9.1470	36.8138	2225	10.0232	48.8521
1650	9.1677	37.0719	2237.5	10.0400	49.1066
1662.5	9.1884	37.3298	2250	10.0567	49.3609
1675	9.2090	37.5876	2262.5	10.0734	49.6153
1687.5	9.2294	37.8453	2275	10.0899	49.8695
1700	9.2498	38.1030	2287.5	10.1064	50.1237
1712.5	9.2700	38.3605	2300	10.1229	50.3779
1725	9.2901	38.6180	2312.5	10.1393	50.6319
1737.5	9.3102	38.8754	2325	10.1556	50.8860
1750	9.3301	39.1327	2337.5	10.1719	51.1399
1762.5	9.3500	39.3899	2350	10.1881	51.3938
1775	9.3697	39.6470	2362.5	10.2042	51.6477
1787.5	9.3893	39.9040	2375	10.2203	51.9015
1800	9.4089	40.1610	2387.5	10.2363	52.1552
1812.5	9.4283	40.4178	2400	10.2523	52.4089
1825	9.4477	40.6746	2412.5	10.2682	52.6625
1837.5	9.4670	40.9313	2425	10.2840	52.9161
1850	9.4861	41.1879	2437.5	10.2998	53.1696
1862.5	9.5052	41.4444	2450	10.3155	53.4231
1875	9.5242	41.7009	2462.5	10.3312	53.6765
1887.5	9.5431	41.9573	2475	10.3468	53.9298
1900	9.5619	42.2136	2487.5	10.3624	54.1832
1912.5	9.5806	42.4698	2500	10.3779	54.4364
1925	9.5993	42.7259	2512.5	10.3934	54.6896

Frequency (Hz)	Real Part	Imaginary Part	Frequency (Hz)	Real Part	Imaginary Part
2525	10.4088	54.9428	3112.5	11.0792	66.7887
2537.5	10.4241	55.1959	3125	11.0925	67.0398
2550	10.4394	55.4489	3137.5	11.1057	67.2908
2562.5	10.4547	55.7019	3150	11.1189	67.5418
2575	10.4699	55.9549	3162.5	11.1320	67.7927
2587.5	10.4850	56.2078	3175	11.1451	68.0436
2600	10.5001	56.4606	3187.5	11.1582	68.2945
2612.5	10.5151	56.7134	3200	11.1712	68.5453
2625	10.5301	56.9662	3212.5	11.1842	68.7961
2637.5	10.5450	57.2189	3225	11.1972	69.0468
2650	10.5599	57.4715	3237.5	11.2101	69.2975
2662.5	10.5748	57.7241	3250	11.2230	69.5482
2675	10.5896	57.9767	3262.5	11.2359	69.7989
2687.5	10.6043	58.2292	3275	11.2487	70.0495
2700	10.6190	58.4817	3287.5	11.2615	70.3000
2712.5	10.6336	58.7341	3300	11.2743	70.5506
2725	10.6482	58.9865	3312.5	11.2870	70.8011
2737.5	10.6628	59.2388	3325	11.2997	71.0516
2750	10.6773	59.4911	3337.5	11.3124	71.3020
2762.5	10.6918	59.7433	3350	11.3250	71.5524
2775	10.7062	59.9955	3362.5	11.3376	71.8028
2787.5	10.7205	60.2476	3375	11.3501	72.0531
2800	10.7349	60.4997	3387.5	11.3627	72.3034
2812.5	10.7491	60.7518	3400	11.3752	72.5537
2825	10.7634	61.0038	3412.5	11.3876	72.8039
2837.5	10.7776	61.2558	3425	11.4001	73.0541
2850	10.7917	61.5077	3437.5	11.4125	73.3043
2862.5	10.8058	61.7596	3450	11.4248	73.5544
2875	10.8199	62.0115	3462.5	11.4372	73.8045
2887.5	10.8339	62.2633	3475	11.4495	74.0546
2900	10.8479	62.5150	3487.5	11.4618	74.3046
2912.5	10.8618	62.7667	3500	11.4740	74.5546
2925	10.8757	63.0184	3512.5	11.4862	74.8046
2937.5	10.8895	63.2701	3525	11.4984	75.0545
2950	10.9033	63.5216	3537.5	11.5105	75.3045
2962.5	10.9171	63.7732	3550	11.5227	75.5543
2975	10.9308	64.0247	3562.5	11.5348	75.8042
2987.5	10.9445	64.2762	3575	11.5468	76.0540
3000	10.9582	64.5276	3587.5	11.5588	76.3038
3012.5	10.9718	64.7790	3600	11.5709	76.5536
3025	10.9853	65.0304	3612.5	11.5828	76.8033
3037.5	10.9989	65.2817	3625	11.5948	77.0530
3050	11.0123	65.5330	3637.5	11.6067	77.3026
3062.5	11.0258	65.7842	3650	11.6186	77.5523
3075	11.0392	66.0354	3662.5	11.6304	77.8019
3087.5	11.0526	66.2865	3675	11.6423	78.0515
3100	11.0659	66.5377	3687.5	11.6541	78.3010

Frequency (Hz)	Real Part	Imaginary Part	Frequency (Hz)	Real Part	Imaginary Part
3700	11.6658	78.5505	3762.5	11.7243	79.7977
3712.5	11.6776	78.8000	3775	11.7359	80.0470
3725	11.6893	79.0495	3787.5	11.7475	80.2963
3737.5	11.7010	79.2989	3800	11.7590	80.5456
3750	11.7127	79.5483			

Table B.5 Calculated surface impedance (normalised by the characteristic impedance of the air, ρc), between 300 and 3800 Hz, using the derived bulk acoustic properties in Tables B.3 and B.4 and Equation (6.9)

Frequency (Hz)	Real Part	Imaginary Part	Frequency (Hz)	Real Part	Imaginary Part
300	0.3369	-1.1699	825	0.4979	0.4337
312.5	0.3366	-1.1009	837.5	0.5081	0.4665
325	0.3366	-1.0360	850	0.5188	0.4999
337.5	0.3368	-0.9748	862.5	0.5301	0.5340
350	0.3372	-0.9169	875	0.5422	0.5687
362.5	0.3379	-0.8620	887.5	0.5550	0.6041
375	0.3387	-0.8097	900	0.5686	0.6403
387.5	0.3397	-0.7599	912.5	0.5831	0.6775
400	0.3409	-0.7121	925	0.5986	0.7156
412.5	0.3423	-0.6663	937.5	0.6152	0.7547
425	0.3438	-0.6222	950	0.6330	0.7951
437.5	0.3455	-0.5798	962.5	0.6521	0.8366
450	0.3474	-0.5387	975	0.6727	0.8796
462.5	0.3494	-0.4990	987.5	0.6948	0.9240
475	0.3516	-0.4604	1000	0.7188	0.9700
487.5	0.3540	-0.4230	1012.5	0.7447	1.0178
500	0.3565	-0.3864	1025	0.7729	1.0675
512.5	0.3592	-0.3508	1037.5	0.8036	1.1193
525	0.3620	-0.3160	1050	0.8372	1.1733
537.5	0.3650	-0.2819	1062.5	0.8739	1.2297
550	0.3682	-0.2484	1075	0.9144	1.2887
562.5	0.3715	-0.2155	1087.5	0.9590	1.3506
575	0.3750	-0.1831	1100	1.0084	1.4155
587.5	0.3787	-0.1512	1112.5	1.0634	1.4837
600	0.3826	-0.1197	1125	1.1248	1.5555
612.5	0.3867	-0.0885	1137.5	1.1936	1.6309
625	0.3910	-0.0577	1150	1.2712	1.7103
637.5	0.3955	-0.0270	1162.5	1.3591	1.7938
650	0.4002	0.0034	1175	1.4592	1.8813
662.5	0.4052	0.0337	1187.5	1.5738	1.9728
675	0.4104	0.0639	1200	1.7056	2.0679
687.5	0.4159	0.0940	1212.5	1.8583	2.1657
700	0.4216	0.1241	1225	2.0360	2.2648
712.5	0.4276	0.1542	1237.5	2.2439	2.3626
725	0.4339	0.1844	1250	2.4883	2.4552
737.5	0.4406	0.2147	1262.5	2.7764	2.5359
750	0.4475	0.2451	1275	3.1161	2.5947
762.5	0.4549	0.2758	1287.5	3.5153	2.6162
775	0.4626	0.3067	1300	3.9794	2.5777
787.5	0.4707	0.3379	1312.5	4.5074	2.4472
800	0.4793	0.3694	1325	5.0844	2.1840
812.5	0.4884	0.4013	1337.5	5.6715	1.7432

Frequency (Hz)	Real Part	Imaginary Part	Frequency (Hz)	Real Part	Imaginary Part
1350	6.1967	1.0921	1937.5	0.3212	-0.2599
1362.5	6.5585	0.2369	1950	0.3261	-0.2248
1375	6.6544	-0.7517	1962.5	0.3314	-0.1903
1387.5	6.4324	-1.7421	1975	0.3372	-0.1564
1400	5.9270	-2.5914	1987.5	0.3435	-0.1229
1412.5	5.2432	-3.2069	2000	0.3502	-0.0897
1425	4.5018	-3.5720	2012.5	0.3573	-0.0570
1437.5	3.7943	-3.7252	2025	0.3649	-0.0245
1450	3.1695	-3.7259	2037.5	0.3729	0.0077
1462.5	2.6425	-3.6291	2050	0.3814	0.0397
1475	2.2095	-3.4770	2062.5	0.3905	0.0715
1487.5	1.8582	-3.2977	2075	0.4000	0.1031
1500	1.5748	-3.1091	2087.5	0.4102	0.1347
1512.5	1.3461	-2.9214	2100	0.4208	0.1663
1525	1.1611	-2.7405	2112.5	0.4321	0.1978
1537.5	1.0109	-2.5693	2125	0.4440	0.2293
1550	0.8882	-2.4089	2137.5	0.4566	0.2609
1562.5	0.7876	-2.2594	2150	0.4700	0.2925
1575	0.7045	-2.1206	2162.5	0.4840	0.3243
1587.5	0.6357	-1.9918	2175	0.4989	0.3563
1600	0.5783	-1.8722	2187.5	0.5147	0.3884
1612.5	0.5304	-1.7610	2200	0.5314	0.4207
1625	0.4902	-1.6575	2212.5	0.5491	0.4532
1637.5	0.4564	-1.5609	2225	0.5678	0.4861
1650	0.4279	-1.4706	2237.5	0.5878	0.5192
1662.5	0.4039	-1.3859	2250	0.6090	0.5526
1675	0.3837	-1.3064	2262.5	0.6315	0.5863
1687.5	0.3666	-1.2315	2275	0.6555	0.6204
1700	0.3523	-1.1607	2287.5	0.6811	0.6549
1712.5	0.3403	-1.0938	2300	0.7084	0.6897
1725	0.3303	-1.0303	2312.5	0.7377	0.7248
1737.5	0.3221	-0.9699	2325	0.7689	0.7603
1750	0.3154	-0.9123	2337.5	0.8024	0.7961
1762.5	0.3101	-0.8573	2350	0.8384	0.8322
1775	0.3059	-0.8046	2362.5	0.8770	0.8686
1787.5	0.3028	-0.7540	2375	0.9186	0.9051
1800	0.3007	-0.7054	2387.5	0.9633	0.9417
1812.5	0.2994	-0.6586	2400	1.0116	0.9782
1825	0.2989	-0.6134	2412.5	1.0636	1.0145
1837.5	0.2991	-0.5697	2425	1.1199	1.0504
1850	0.3000	-0.5273	2437.5	1.1808	1.0855
1862.5	0.3015	-0.4862	2450	1.2468	1.1196
1875	0.3035	-0.4462	2462.5	1.3182	1.1523
1887.5	0.3061	-0.4072	2475	1.3955	1.1829
1900	0.3091	-0.3692	2487.5	1.4794	1.2109
1912.5	0.3127	-0.3320	2500	1.5701	1.2355
1925	0.3167	-0.2956	2512.5	1.6683	1.2556

Frequency (Hz)	Real Part	Imaginary Part	Frequency (Hz)	Real Part	Imaginary Part
2525	1.7743	1.2700	3112.5	0.4742	-0.9387
2537.5	1.8885	1.2774	3125	0.4548	-0.8960
2550	2.0109	1.2760	3137.5	0.4372	-0.8544
2562.5	2.1414	1.2639	3150	0.4213	-0.8136
2575	2.2797	1.2388	3162.5	0.4069	-0.7738
2587.5	2.4247	1.1983	3175	0.3939	-0.7349
2600	2.5748	1.1396	3187.5	0.3822	-0.6968
2612.5	2.7278	1.0602	3200	0.3718	-0.6595
2625	2.8802	0.9574	3212.5	0.3624	-0.6229
2637.5	3.0278	0.8295	3225	0.3541	-0.5870
2650	3.1653	0.6751	3237.5	0.3468	-0.5518
2662.5	3.2867	0.4947	3250	0.3403	-0.5171
2675	3.3856	0.2902	3262.5	0.3347	-0.4830
2687.5	3.4558	0.0655	3275	0.3298	-0.4495
2700	3.4920	-0.1734	3287.5	0.3258	-0.4164
2712.5	3.4907	-0.4189	3300	0.3224	-0.3837
2725	3.4509	-0.6626	3312.5	0.3197	-0.3515
2737.5	3.3739	-0.8958	3325	0.3177	-0.3195
2750	3.2635	-1.1108	3337.5	0.3163	-0.2880
2762.5	3.1255	-1.3016	3350	0.3155	-0.2567
2775	2.9668	-1.4642	3362.5	0.3154	-0.2256
2787.5	2.7943	-1.5970	3375	0.3158	-0.1948
2800	2.6149	-1.7000	3387.5	0.3167	-0.1641
2812.5	2.4342	-1.7750	3400	0.3183	-0.1336
2825	2.2570	-1.8246	3412.5	0.3204	-0.1032
2837.5	2.0865	-1.8522	3425	0.3231	-0.0728
2850	1.9252	-1.8609	3437.5	0.3264	-0.0426
2862.5	1.7745	-1.8542	3450	0.3302	-0.0123
2875	1.6349	-1.8351	3462.5	0.3347	0.0180
2887.5	1.5066	-1.8061	3475	0.3397	0.0483
2900	1.3894	-1.7695	3487.5	0.3454	0.0787
2912.5	1.2827	-1.7272	3500	0.3518	0.1093
2925	1.1860	-1.6808	3512.5	0.3588	0.1400
2937.5	1.0983	-1.6315	3525	0.3666	0.1708
2950	1.0191	-1.5804	3537.5	0.3750	0.2019
2962.5	0.9474	-1.5281	3550	0.3843	0.2332
2975	0.8828	-1.4754	3562.5	0.3944	0.2647
2987.5	0.8243	-1.4227	3575	0.4054	0.2966
3000	0.7716	-1.3702	3587.5	0.4174	0.3288
3012.5	0.7239	-1.3184	3600	0.4303	0.3613
3025	0.6808	-1.2674	3612.5	0.4443	0.3943
3037.5	0.6418	-1.2172	3625	0.4595	0.4276
3050	0.6065	-1.1681	3637.5	0.4760	0.4614
3062.5	0.5746	-1.1201	3650	0.4938	0.4956
3075	0.5457	-1.0731	3662.5	0.5130	0.5303
3087.5	0.5195	-1.0272	3675	0.5339	0.5655
3100	0.4957	-0.9824	3687.5	0.5565	0.6012

Frequency (Hz)	Real Part	Imaginary Part	Frequency (Hz)	Real Part	Imaginary Part
3700	0.5810	0.6374	3762.5	0.7388	0.8250
3712.5	0.6076	0.6741	3775	0.7791	0.8634
3725	0.6364	0.7112	3787.5	0.8230	0.9019
3737.5	0.6677	0.7488	3800	0.8709	0.9403
3750	0.7018	0.7867			

Table B.6 Calculated characteristic impedance (normalised by the characteristic impedance of the air, ρc), between 300 and 3800 Hz, using Utsuno's improved two-cavity method

Frequency (Hz)	Real Part	Imaginary Part	Frequency (Hz)	Real Part	Imaginary Part
300	1.2586	-0.7291	825	1.2970	-0.3134
312.5	1.3000	-0.6313	837.5	1.2642	-0.3639
325	1.3512	-0.6665	850	1.2071	-0.3622
337.5	1.3108	-0.6592	862.5	1.2001	-0.3743
350	1.3165	-0.6443	875	1.1744	-0.3070
362.5	1.3312	-0.6606	887.5	1.1736	-0.3186
375	1.3034	-0.5943	900	1.1683	-0.3018
387.5	1.3433	-0.5822	912.5	1.1974	-0.2914
400	1.2857	-0.5443	925	1.1659	-0.2745
412.5	1.3164	-0.5539	937.5	1.1757	-0.3000
425	1.3046	-0.5112	950	1.1745	-0.3231
437.5	1.2936	-0.5051	962.5	1.1877	-0.2704
450	1.3227	-0.5124	975	1.1969	-0.2772
462.5	1.2642	-0.5419	987.5	1.1902	-0.2880
475	1.3038	-0.5117	1000	1.1810	-0.2495
487.5	1.2875	-0.5138	1012.5	1.1638	-0.2571
500	1.2890	-0.4803	1025	1.1735	-0.2602
512.5	1.2904	-0.4936	1037.5	1.1788	-0.2501
525	1.2782	-0.4704	1050	1.1760	-0.2423
537.5	1.2570	-0.4744	1062.5	1.1702	-0.2548
550	1.2605	-0.4626	1075	1.1663	-0.2481
562.5	1.2501	-0.4687	1087.5	1.1887	-0.2293
575	1.2517	-0.4740	1100	1.1844	-0.2273
587.5	1.2454	-0.4513	1112.5	1.1705	-0.2321
600	1.2510	-0.4392	1125	1.2090	-0.2252
612.5	1.2564	-0.4318	1137.5	1.1952	-0.2281
625	1.2341	-0.4221	1150	1.1789	-0.2178
637.5	1.2545	-0.4231	1162.5	1.1849	-0.2211
650	1.2380	-0.4072	1175	1.1898	-0.2261
662.5	1.2396	-0.4114	1187.5	1.1744	-0.2227
675	1.2295	-0.4011	1200	1.1906	-0.2339
687.5	1.2269	-0.4024	1212.5	1.1774	-0.2284
700	1.2141	-0.3909	1225	1.1770	-0.2233
712.5	1.2147	-0.3924	1237.5	1.1684	-0.2093
725	1.2229	-0.3981	1250	1.1886	-0.2151
737.5	1.1867	-0.3732	1262.5	1.1665	-0.2010
750	1.2060	-0.3732	1275	1.1766	-0.2039
762.5	1.2037	-0.3743	1287.5	1.1620	-0.2105
775	1.1763	-0.3286	1300	1.1596	-0.2076
787.5	1.1601	-0.2960	1312.5	1.1660	-0.2061
800	1.2115	-0.2790	1325	1.1585	-0.2033
812.5	1.2284	-0.2647	1337.5	1.1618	-0.2127

Frequency (Hz)	Real Part	Imaginary Part	Frequency (Hz)	Real Part	Imaginary Part
1350	1.1652	-0.2022	1937.5	1.1154	-0.1388
1362.5	1.1621	-0.1991	1950	1.1292	-0.1344
1375	1.1588	-0.2014	1962.5	1.1399	-0.1320
1387.5	1.1700	-0.2009	1975	1.1562	-0.1460
1400	1.1682	-0.2007	1987.5	1.1424	-0.1414
1412.5	1.1655	-0.2004	2000	1.1394	-0.1432
1425	1.1643	-0.2041	2012.5	1.1462	-0.1574
1437.5	1.1601	-0.1949	2025	1.1315	-0.1607
1450	1.1609	-0.1929	2037.5	1.1553	-0.1504
1462.5	1.1588	-0.1940	2050	1.1329	-0.1491
1475	1.1575	-0.1905	2062.5	1.1350	-0.1483
1487.5	1.1543	-0.1863	2075	1.1583	-0.1557
1500	1.1417	-0.1835	2087.5	1.1363	-0.1506
1512.5	1.1464	-0.1825	2100	1.1367	-0.1460
1525	1.1408	-0.1875	2112.5	1.1377	-0.1543
1537.5	1.1373	-0.1831	2125	1.1347	-0.1540
1550	1.1326	-0.1872	2137.5	1.1375	-0.1483
1562.5	1.1295	-0.1788	2150	1.1438	-0.1529
1575	1.1275	-0.1799	2162.5	1.1236	-0.1417
1587.5	1.1284	-0.1715	2175	1.1335	-0.1654
1600	1.1323	-0.1729	2187.5	1.1292	-0.1460
1612.5	1.1276	-0.1684	2200	1.1238	-0.1557
1625	1.1359	-0.1652	2212.5	1.1450	-0.1428
1637.5	1.1321	-0.1593	2225	1.1241	-0.1575
1650	1.1374	-0.1585	2237.5	1.1414	-0.1447
1662.5	1.1431	-0.1514	2250	1.1319	-0.1428
1675	1.1553	-0.1578	2262.5	1.1332	-0.1558
1687.5	1.1539	-0.1579	2275	1.1367	-0.1502
1700	1.1608	-0.1586	2287.5	1.1373	-0.1439
1712.5	1.1551	-0.1641	2300	1.1376	-0.1508
1725	1.1525	-0.1612	2312.5	1.1381	-0.1404
1737.5	1.1465	-0.1686	2325	1.1379	-0.1476
1750	1.1496	-0.1648	2337.5	1.1402	-0.1418
1762.5	1.1534	-0.1700	2350	1.1453	-0.1460
1775	1.1409	-0.1599	2362.5	1.1419	-0.1415
1787.5	1.1477	-0.1638	2375	1.1415	-0.1470
1800	1.1426	-0.1651	2387.5	1.1467	-0.1394
1812.5	1.1475	-0.1708	2400	1.1468	-0.1419
1825	1.1385	-0.1697	2412.5	1.1464	-0.1420
1837.5	1.1337	-0.1694	2425	1.1487	-0.1449
1850	1.1237	-0.1844	2437.5	1.1439	-0.1407
1862.5	1.1130	-0.1694	2450	1.1510	-0.1378
1875	1.1252	-0.1606	2462.5	1.1436	-0.1371
1887.5	1.1155	-0.1680	2475	1.1509	-0.1372
1900	1.0993	-0.1533	2487.5	1.1448	-0.1430
1912.5	1.1106	-0.1467	2500	1.1493	-0.1350
1925	1.1188	-0.1410	2512.5	1.1536	-0.1310

Frequency (Hz)	Real Part	Imaginary Part	Frequency (Hz)	Real Part	Imaginary Part
2525	1.1526	-0.1359	3112.5	1.1300	-0.1265
2537.5	1.1489	-0.1305	3125	1.1248	-0.1201
2550	1.1576	-0.1333	3137.5	1.1284	-0.1288
2562.5	1.1562	-0.1333	3150	1.1267	-0.1247
2575	1.1553	-0.1306	3162.5	1.1192	-0.1228
2587.5	1.1642	-0.1360	3175	1.1250	-0.1180
2600	1.1630	-0.1370	3187.5	1.1184	-0.1134
2612.5	1.1662	-0.1281	3200	1.1187	-0.1155
2625	1.1555	-0.1334	3212.5	1.1206	-0.1152
2637.5	1.1653	-0.1300	3225	1.1244	-0.1108
2650	1.1662	-0.1397	3237.5	1.1173	-0.1071
2662.5	1.1650	-0.1357	3250	1.1152	-0.1102
2675	1.1548	-0.1427	3262.5	1.1221	-0.1109
2687.5	1.1580	-0.1385	3275	1.1188	-0.1048
2700	1.1558	-0.1326	3287.5	1.1164	-0.1050
2712.5	1.1522	-0.1420	3300	1.1215	-0.1050
2725	1.1482	-0.1328	3312.5	1.1133	-0.1041
2737.5	1.1528	-0.1295	3325	1.1140	-0.1015
2750	1.1665	-0.1416	3337.5	1.1155	-0.0976
2762.5	1.1537	-0.1301	3350	1.1089	-0.1090
2775	1.1581	-0.1326	3362.5	1.1053	-0.1021
2787.5	1.1550	-0.1397	3375	1.1001	-0.0904
2800	1.1494	-0.1424	3387.5	1.0996	-0.0899
2812.5	1.1421	-0.1428	3400	1.1018	-0.0848
2825	1.1542	-0.1608	3412.5	1.0999	-0.0889
2837.5	1.1567	-0.1539	3425	1.1024	-0.0821
2850	1.1414	-0.1562	3437.5	1.0932	-0.0830
2862.5	1.1308	-0.1706	3450	1.1044	-0.0710
2875	1.1265	-0.1443	3462.5	1.1054	-0.0737
2887.5	1.1191	-0.1678	3475	1.1085	-0.0858
2900	1.1305	-0.1597	3487.5	1.1124	-0.0783
2912.5	1.1079	-0.1558	3500	1.1145	-0.0869
2925	1.1179	-0.1532	3512.5	1.1161	-0.0967
2937.5	1.1155	-0.1463	3525	1.1154	-0.1070
2950	1.1191	-0.1279	3537.5	1.1463	-0.1287
2962.5	1.1134	-0.1305	3550	1.1148	-0.1461
2975	1.1205	-0.1366	3562.5	1.1039	-0.1546
2987.5	1.1117	-0.1328	3575	1.0731	-0.1726
3000	1.1198	-0.1270	3587.5	1.0424	-0.1517
3012.5	1.1159	-0.1233	3600	1.0418	-0.1410
3025	1.1207	-0.1346	3612.5	1.0406	-0.1481
3037.5	1.1231	-0.1300	3625	1.0417	-0.1281
3050	1.1242	-0.1218	3637.5	1.0543	-0.1046
3062.5	1.1203	-0.1213	3650	1.0397	-0.1138
3075	1.1195	-0.1272	3662.5	1.0329	-0.1332
3087.5	1.1295	-0.1246	3675	1.0461	-0.1033
3100	1.1255	-0.1240	3687.5	1.0413	-0.0958

Frequency (Hz)	Real Part	Imaginary Part	Frequency (Hz)	Real Part	Imaginary Part
3700	1.0751	-0.1057	3762.5	1.1132	-0.0664
3712.5	1.0619	-0.0823	3775	1.1108	-0.0917
3725	1.0946	-0.1152	3787.5	1.1332	-0.0380
3737.5	1.1079	-0.0966	3800	1.1420	-0.0580
3750	1.1014	-0.0835			

Table B.7 Calculated propagation constant, between 300 and 3800 Hz, using Utsuno's improved two-cavity method

Frequency (Hz)	Real Part	Imaginary Part	Frequency (Hz)	Real Part	Imaginary Part
300	6.4106	9.2567	850	5.3060	19.7686
312.5	6.0923	9.1017	862.5	5.0293	20.4311
325	5.9405	9.4121	875	6.0507	21.1853
337.5	6.2204	9.8219	887.5	5.9518	21.6843
350	6.2495	10.0133	900	6.4284	22.1115
362.5	6.1978	10.5073	912.5	6.5949	21.9052
375	6.2901	10.4544	925	7.1691	22.6204
387.5	6.2104	10.8133	937.5	6.6376	22.7563
400	6.5378	10.9141	950	6.1644	22.9977
412.5	6.5567	11.0576	962.5	7.2228	23.1137
425	6.6739	11.1829	975	6.9806	23.1784
437.5	6.6138	11.4933	987.5	6.8998	23.5011
450	6.5063	11.7292	1000	7.4148	23.8688
462.5	6.7284	12.5250	1012.5	7.4784	24.5633
475	6.5309	12.3835	1025	7.2358	24.5379
487.5	6.5638	12.7267	1037.5	7.5515	24.6893
500	6.6826	12.8457	1050	7.6642	24.8947
512.5	6.5973	13.1509	1062.5	7.4955	25.4426
525	6.7991	13.3204	1075	7.5516	25.3980
537.5	6.7553	13.7166	1087.5	7.9929	25.2945
550	6.8459	13.9236	1100	7.9825	25.9646
562.5	6.8582	14.2130	1112.5	7.9067	25.9868
575	6.7366	14.5088	1125	7.8940	25.9272
587.5	6.8551	14.6112	1137.5	7.8907	26.2160
600	6.9146	14.6982	1150	8.1926	26.7286
612.5	6.8951	14.8039	1162.5	8.0127	26.7873
625	7.0442	15.2271	1175	8.0281	26.8955
637.5	6.9090	15.2571	1187.5	8.1388	27.4765
650	7.0840	15.5874	1200	8.0349	27.4889
662.5	6.9330	15.7616	1212.5	8.1077	27.8567
675	7.0009	15.9943	1225	7.8786	28.1935
687.5	6.8885	16.2697	1237.5	8.2797	28.5154
700	6.9568	16.5645	1250	8.1439	28.5416
712.5	6.7904	16.6834	1262.5	8.2951	29.0381
725	6.5061	16.8515	1275	8.3307	29.1718
737.5	6.7606	17.4588	1287.5	8.2604	29.4879
750	6.5485	17.4296	1300	8.2933	29.8329
762.5	6.4122	17.7750	1312.5	8.3945	29.9924
775	6.9179	18.2381	1325	8.3710	30.4105
787.5	7.1772	18.5753	1337.5	8.4375	30.4417
800	6.9765	18.2260	1350	8.3906	30.7366
812.5	7.0461	18.3647	1362.5	8.5045	31.0255
825	6.2864	17.9760	1375	8.4868	31.0938
837.5	5.5153	18.5481	1387.5	8.5136	31.3675

Frequency (Hz)	Real Part	Imaginary Part	Frequency (Hz)	Real Part	Imaginary Part
1400	8.6227	31.5321	1987.5	9.6404	43.7062
1412.5	8.5347	31.9113	2000	9.6865	43.9248
1425	8.6277	31.9019	2012.5	9.7000	44.2958
1437.5	8.7059	32.3689	2025	9.6714	44.2347
1450	8.6024	32.5240	2037.5	9.6251	44.7775
1462.5	8.6836	32.8181	2050	9.6604	44.8171
1475	8.6586	33.1445	2062.5	9.7051	45.0278
1487.5	8.7209	33.1382	2075	9.7229	45.5106
1500	8.7149	33.8299	2087.5	9.6587	45.7749
1512.5	8.8927	33.9871	2100	9.6069	45.7037
1525	8.7744	34.1346	2112.5	9.5818	46.3640
1537.5	8.7333	34.6430	2125	9.6085	46.4418
1550	8.7616	34.8691	2137.5	9.7111	46.5820
1562.5	8.7250	35.0156	2150	9.8309	47.0398
1575	8.7800	35.2541	2162.5	9.8290	47.2340
1587.5	8.6771	35.6785	2175	9.7027	47.3432
1600	8.8061	35.9571	2187.5	9.8315	47.6913
1612.5	8.8679	36.0932	2200	9.7699	48.0044
1625	8.9580	36.5105	2212.5	9.6864	48.1104
1637.5	8.9738	36.5919	2225	9.8546	48.5533
1650	8.9909	36.8847	2237.5	9.8520	48.7515
1662.5	9.0738	36.9996	2250	9.8241	48.9819
1675	9.1092	37.3041	2262.5	10.0371	49.1468
1687.5	9.0352	37.4907	2275	9.8971	49.6276
1700	9.0406	37.7399	2287.5	9.8014	49.7944
1712.5	9.0565	37.9808	2300	10.0873	50.0132
1725	8.9995	38.2464	2312.5	9.9286	50.2899
1737.5	9.0194	38.4887	2325	9.9606	50.4918
1750	8.9695	38.7242	2337.5	10.0306	50.7367
1762.5	9.0106	39.1005	2350	10.0840	51.1777
1775	9.0441	39.2891	2362.5	10.0136	51.3526
1787.5	9.0415	39.5228	2375	10.1157	51.6904
1800	9.2330	39.8131	2387.5	10.0700	51.7591
1812.5	9.2049	40.1647	2400	9.9888	52.1725
1825	9.2969	40.2796	2412.5	10.1419	52.3615
1837.5	9.2143	40.6107	2425	10.0267	52.7190
1850	9.4192	40.7940	2437.5	10.2195	52.8815
1862.5	9.3451	40.9755	2450	10.2199	53.0194
1875	9.5013	41.4190	2462.5	10.3253	53.2999
1887.5	9.3877	41.5362	2475	10.2134	53.4460
1900	9.3054	41.6891	2487.5	10.1736	53.7476
1912.5	9.3704	42.0316	2500	9.9954	53.9738
1925	9.3974	42.3856	2512.5	10.0091	54.3605
1937.5	9.4713	42.6518	2525	9.9963	54.5447
1950	9.4978	42.9703	2537.5	10.0748	55.0226
1962.5	9.4591	43.2546	2550	10.0190	55.1789
1975	9.5979	43.4929	2562.5	10.0829	55.5097

Frequency (Hz)	Real Part	Imaginary Part	Frequency (Hz)	Real Part	Imaginary Part
2575	10.1942	55.8806	3162.5	11.1413	67.5146
2587.5	10.1597	56.2269	3175	11.1499	67.8152
2600	10.3181	56.4515	3187.5	11.2318	68.0829
2612.5	10.3303	56.6765	3200	11.2482	68.3221
2625	10.3270	56.7674	3212.5	11.2802	68.5909
2637.5	10.4543	57.1500	3225	11.2458	68.9209
2650	10.4055	57.4346	3237.5	11.3674	69.2136
2662.5	10.4585	57.5259	3250	11.2622	69.4755
2675	10.4601	57.9205	3262.5	11.2208	69.7912
2687.5	10.5504	57.9599	3275	11.3088	69.9796
2700	10.3908	58.4398	3287.5	11.2473	70.3232
2712.5	10.6178	58.5527	3300	11.2834	70.6664
2725	10.5698	58.7569	3312.5	11.3878	70.8632
2737.5	10.4747	59.0765	3325	11.2890	71.3136
2750	10.6497	59.5506	3337.5	11.4733	71.4498
2762.5	10.5462	59.4804	3350	11.4195	71.9431
2775	10.6774	59.9149	3362.5	11.4541	72.1761
2787.5	10.6862	60.1958	3375	11.6173	72.4731
2800	10.8812	60.3062	3387.5	11.6845	72.8475
2812.5	10.8640	60.4536	3400	11.6039	72.9034
2825	11.0540	60.9590	3412.5	11.6273	73.3816
2837.5	10.8819	61.2542	3425	11.6901	73.5890
2850	11.0054	61.3197	3437.5	11.4989	73.9157
2862.5	11.1445	61.3807	3450	11.7068	74.0274
2875	10.8924	61.6308	3462.5	11.6549	74.3027
2887.5	11.3746	61.8395	3475	11.6170	74.7399
2900	11.1702	62.2017	3487.5	11.5754	75.1264
2912.5	11.1814	62.1834	3500	11.6095	75.4835
2925	11.2042	62.4766	3512.5	11.7002	75.7721
2937.5	11.2140	62.8343	3525	11.6322	76.1605
2950	10.9585	62.9804	3537.5	11.6932	76.4803
2962.5	11.0667	63.1629	3550	12.0837	76.9073
2975	11.0717	63.6143	3562.5	12.2595	77.0001
2987.5	11.1279	63.6531	3575	12.3119	77.1949
3000	11.1055	64.0084	3587.5	12.4534	77.6577
3012.5	11.0188	64.1940	3600	12.5058	77.4295
3025	11.2064	64.4659	3612.5	12.1936	77.6036
3037.5	11.1544	64.6987	3625	12.5581	77.6958
3050	11.1880	64.9963	3637.5	12.5676	78.0223
3062.5	11.1416	65.1787	3650	12.2946	78.3670
3075	11.1526	65.4361	3662.5	12.0014	78.5539
3087.5	11.0429	65.7160	3675	12.3999	78.7716
3100	11.0916	65.9792	3687.5	12.4991	79.0855
3112.5	11.1216	66.3286	3700	12.7983	78.5582
3125	11.0946	66.5994	3712.5	12.8515	79.5093
3137.5	11.1371	66.9116	3725	12.3501	78.6442
3150	11.0949	67.2875	3737.5	12.9251	78.7568

Frequency (Hz)	Real Part	Imaginary Part	Frequency (Hz)	Real Part	Imaginary Part
3750	12.8554	79.4498	3787.5	13.4538	79.6002
3762.5	13.0946	79.4839	3800	13.0777	79.8720
3775	12.5626	79.6288			

Table B.8 Measured surface impedance (normalised by the characteristic impedance of the air, ρc), between 3812.5 and 4500 Hz, of the material sample with an air cavity of 90 mm between the test material sample and the rigid wall

Frequency (Hz)	Real Part	Imaginary Part	Frequency (Hz)	Real Part	Imaginary Part
3812.5	0.9081	0.9122	4162.5	2.5788	-0.9655
3825	0.9741	0.9554	4175	2.6487	-1.2812
3837.5	1.0051	0.9818	4187.5	2.2178	-1.2074
3850	1.1170	1.0418	4200	2.1123	-1.3211
3862.5	1.1493	1.0569	4212.5	2.0211	-1.2312
3875	1.2109	1.1427	4225	1.8740	-1.1721
3887.5	1.3249	1.1569	4237.5	1.8807	-1.4093
3900	1.4256	1.2801	4250	1.5822	-1.1977
3912.5	1.5820	1.2216	4262.5	1.7363	-1.3775
3925	1.6836	1.2200	4275	1.4906	-1.3565
3937.5	2.0128	1.1961	4287.5	1.2674	-1.1132
3950	1.9432	1.1242	4300	1.1606	-1.2813
3962.5	2.0167	1.1790	4312.5	1.2117	-1.1739
3975	2.1572	0.9460	4325	0.9969	-1.1181
3987.5	2.4229	1.2373	4337.5	1.0213	-1.0420
4000	2.3394	1.0260	4350	0.9558	-1.1062
4012.5	2.4944	0.9331	4362.5	0.9321	-0.9997
4025	2.6594	1.0182	4375	0.8047	-0.9899
4037.5	2.5075	0.7322	4387.5	0.8564	-0.9262
4050	3.0493	0.4916	4400	0.7535	-0.9604
4062.5	3.0548	0.7903	4412.5	0.7270	-0.9098
4075	2.9343	0.2691	4425	0.7245	-0.7835
4087.5	3.2998	0.0495	4437.5	0.6452	-0.8005
4100	2.8998	0.1687	4450	0.7479	-0.7167
4112.5	3.4687	-0.5264	4462.5	0.6599	-0.6911
4125	3.2033	-0.1413	4475	0.7358	-0.6738
4137.5	2.9645	-0.6478	4487.5	0.7097	-0.8816
4150	3.2344	-1.0657	4500	0.4128	-1.1411

Table B.9 Measured surface impedance (normalised by the characteristic impedance of the air, ρc), between 3812.5 and 4500 Hz, of the material sample with an air cavity of 53 mm between the test material sample and the rigid wall

Frequency (Hz)	Real Part	Imaginary Part	Frequency (Hz)	Real Part	Imaginary Part
3812.5	2.7170	0.4943	4162.5	1.4546	-1.4638
3825	2.9129	0.3591	4175	1.3621	-1.3732
3837.5	2.9183	0.3441	4187.5	1.1883	-1.4255
3850	2.9683	0.0096	4200	1.1734	-1.2659
3862.5	2.9731	0.0428	4212.5	1.2317	-1.3431
3875	3.2715	-0.1224	4225	1.1736	-1.1609
3887.5	3.1392	-0.1033	4237.5	1.0831	-1.2540
3900	3.4319	-0.5139	4250	1.1293	-1.0655
3912.5	3.3212	-0.7407	4262.5	0.9377	-1.0944
3925	3.2047	-0.8925	4275	1.0662	-1.2278
3937.5	2.8989	-1.2300	4287.5	0.8568	-1.1123
3950	2.6864	-1.2051	4300	0.8903	-1.1207
3962.5	2.4769	-1.2820	4312.5	0.8437	-1.0682
3975	2.6165	-1.1955	4325	0.7669	-0.9851
3987.5	2.4840	-1.3115	4337.5	0.8098	-1.0768
4000	2.4630	-1.2019	4350	0.6935	-0.9401
4012.5	2.4142	-1.4016	4362.5	0.7223	-0.9819
4025	2.3380	-1.2604	4375	0.6607	-0.9385
4037.5	2.1175	-1.2385	4387.5	0.6669	-0.9385
4050	2.1361	-1.6572	4400	0.6428	-0.9278
4062.5	2.1461	-1.4972	4412.5	0.6463	-0.8602
4075	1.8703	-1.3896	4425	0.5991	-0.8243
4087.5	1.9547	-1.5687	4437.5	0.6010	-0.8260
4100	1.8023	-1.4760	4450	0.5972	-0.8183
4112.5	1.6836	-1.5110	4462.5	0.6616	-0.7830
4125	1.7041	-1.5856	4475	0.6656	-0.8995
4137.5	1.6680	-1.4376	4487.5	0.5234	-1.0352
4150	1.4378	-1.4137	4500	0.2772	-1.0438

Table B.10 Derived characteristic impedance (normalised by the characteristic impedance of the air, ρc), between 300 and 4500 Hz, using the optimised set of c_1-c_8 of the optimisation condition 16 in Table 6.5 and Equation (6.15)

Frequency (Hz)	Real Part	Imaginary Part	Frequency (Hz)	Real Part	Imaginary Part
300	1.3704	-0.7045	825	1.2348	-0.3067
312.5	1.3636	-0.6813	837.5	1.2332	-0.3029
325	1.3573	-0.6597	850	1.2316	-0.2992
337.5	1.3512	-0.6395	862.5	1.2301	-0.2957
350	1.3455	-0.6207	875	1.2286	-0.2922
362.5	1.3401	-0.6030	887.5	1.2272	-0.2888
375	1.3349	-0.5864	900	1.2257	-0.2855
387.5	1.3300	-0.5708	912.5	1.2243	-0.2823
400	1.3253	-0.5561	925	1.2230	-0.2791
412.5	1.3209	-0.5422	937.5	1.2216	-0.2761
425	1.3166	-0.5291	950	1.2203	-0.2731
437.5	1.3125	-0.5166	962.5	1.2190	-0.2702
450	1.3085	-0.5048	975	1.2177	-0.2673
462.5	1.3047	-0.4936	987.5	1.2165	-0.2645
475	1.3011	-0.4829	1000	1.2153	-0.2618
487.5	1.2976	-0.4727	1012.5	1.2141	-0.2592
500	1.2942	-0.4629	1025	1.2129	-0.2566
512.5	1.2910	-0.4536	1037.5	1.2117	-0.2540
525	1.2878	-0.4447	1050	1.2106	-0.2515
537.5	1.2848	-0.4362	1062.5	1.2095	-0.2491
550	1.2818	-0.4280	1075	1.2084	-0.2467
562.5	1.2790	-0.4202	1087.5	1.2073	-0.2444
575	1.2762	-0.4127	1100	1.2062	-0.2421
587.5	1.2736	-0.4054	1112.5	1.2052	-0.2398
600	1.2710	-0.3985	1125	1.2041	-0.2377
612.5	1.2685	-0.3918	1137.5	1.2031	-0.2355
625	1.2661	-0.3853	1150	1.2021	-0.2334
637.5	1.2637	-0.3791	1162.5	1.2011	-0.2313
650	1.2614	-0.3731	1175	1.2002	-0.2293
662.5	1.2592	-0.3673	1187.5	1.1992	-0.2273
675	1.2570	-0.3617	1200	1.1983	-0.2254
687.5	1.2549	-0.3563	1212.5	1.1974	-0.2235
700	1.2528	-0.3510	1225	1.1965	-0.2216
712.5	1.2508	-0.3460	1237.5	1.1956	-0.2197
725	1.2488	-0.3411	1250	1.1947	-0.2179
737.5	1.2469	-0.3363	1262.5	1.1938	-0.2162
750	1.2451	-0.3317	1275	1.1929	-0.2144
762.5	1.2433	-0.3272	1287.5	1.1921	-0.2127
775	1.2415	-0.3229	1300	1.1913	-0.2110
787.5	1.2397	-0.3186	1312.5	1.1904	-0.2094
800	1.2380	-0.3145	1325	1.1896	-0.2077
812.5	1.2364	-0.3106	1337.5	1.1888	-0.2061

Frequency (Hz)	Real Part	Imaginary Part	Frequency (Hz)	Real Part	Imaginary Part
1350	1.1880	-0.2046	1937.5	1.1598	-0.1520
1362.5	1.1873	-0.2030	1950	1.1593	-0.1512
1375	1.1865	-0.2015	1962.5	1.1589	-0.1504
1387.5	1.1857	-0.2000	1975	1.1584	-0.1496
1400	1.1850	-0.1985	1987.5	1.1580	-0.1488
1412.5	1.1842	-0.1971	2000	1.1575	-0.1481
1425	1.1835	-0.1957	2012.5	1.1571	-0.1473
1437.5	1.1828	-0.1943	2025	1.1566	-0.1466
1450	1.1821	-0.1929	2037.5	1.1562	-0.1458
1462.5	1.1814	-0.1915	2050	1.1558	-0.1451
1475	1.1807	-0.1902	2062.5	1.1553	-0.1444
1487.5	1.1800	-0.1889	2075	1.1549	-0.1437
1500	1.1793	-0.1876	2087.5	1.1545	-0.1430
1512.5	1.1786	-0.1863	2100	1.1541	-0.1423
1525	1.1780	-0.1851	2112.5	1.1537	-0.1416
1537.5	1.1773	-0.1838	2125	1.1533	-0.1409
1550	1.1767	-0.1826	2137.5	1.1529	-0.1402
1562.5	1.1760	-0.1814	2150	1.1525	-0.1395
1575	1.1754	-0.1802	2162.5	1.1521	-0.1389
1587.5	1.1748	-0.1790	2175	1.1517	-0.1382
1600	1.1742	-0.1779	2187.5	1.1513	-0.1376
1612.5	1.1736	-0.1768	2200	1.1509	-0.1369
1625	1.1730	-0.1756	2212.5	1.1505	-0.1363
1637.5	1.1724	-0.1745	2225	1.1501	-0.1357
1650	1.1718	-0.1735	2237.5	1.1497	-0.1350
1662.5	1.1712	-0.1724	2250	1.1494	-0.1344
1675	1.1706	-0.1713	2262.5	1.1490	-0.1338
1687.5	1.1700	-0.1703	2275	1.1486	-0.1332
1700	1.1695	-0.1692	2287.5	1.1483	-0.1326
1712.5	1.1689	-0.1682	2300	1.1479	-0.1320
1725	1.1684	-0.1672	2312.5	1.1475	-0.1314
1737.5	1.1678	-0.1662	2325	1.1472	-0.1308
1750	1.1673	-0.1653	2337.5	1.1468	-0.1303
1762.5	1.1667	-0.1643	2350	1.1465	-0.1297
1775	1.1662	-0.1633	2362.5	1.1461	-0.1291
1787.5	1.1657	-0.1624	2375	1.1458	-0.1286
1800	1.1652	-0.1615	2387.5	1.1454	-0.1280
1812.5	1.1647	-0.1606	2400	1.1451	-0.1275
1825	1.1641	-0.1597	2412.5	1.1447	-0.1269
1837.5	1.1636	-0.1588	2425	1.1444	-0.1264
1850	1.1631	-0.1579	2437.5	1.1441	-0.1258
1862.5	1.1626	-0.1570	2450	1.1437	-0.1253
1875	1.1622	-0.1561	2462.5	1.1434	-0.1248
1887.5	1.1617	-0.1553	2475	1.1431	-0.1243
1900	1.1612	-0.1545	2487.5	1.1428	-0.1238
1912.5	1.1607	-0.1536	2500	1.1424	-0.1233
1925	1.1602	-0.1528	2512.5	1.1421	-0.1228

Frequency (Hz)	Real Part	Imaginary Part	Frequency (Hz)	Real Part	Imaginary Part
2525	1.1418	-0.1223	3112.5	1.1290	-0.1029
2537.5	1.1415	-0.1218	3125	1.1288	-0.1026
2550	1.1412	-0.1213	3137.5	1.1286	-0.1023
2562.5	1.1409	-0.1208	3150	1.1283	-0.1019
2575	1.1406	-0.1203	3162.5	1.1281	-0.1016
2587.5	1.1402	-0.1198	3175	1.1279	-0.1013
2600	1.1399	-0.1193	3187.5	1.1277	-0.1009
2612.5	1.1396	-0.1189	3200	1.1274	-0.1006
2625	1.1393	-0.1184	3212.5	1.1272	-0.1003
2637.5	1.1390	-0.1179	3225	1.1270	-0.1000
2650	1.1387	-0.1175	3237.5	1.1268	-0.0997
2662.5	1.1385	-0.1170	3250	1.1266	-0.0993
2675	1.1382	-0.1166	3262.5	1.1263	-0.0990
2687.5	1.1379	-0.1161	3275	1.1261	-0.0987
2700	1.1376	-0.1157	3287.5	1.1259	-0.0984
2712.5	1.1373	-0.1153	3300	1.1257	-0.0981
2725	1.1370	-0.1148	3312.5	1.1255	-0.0978
2737.5	1.1367	-0.1144	3325	1.1253	-0.0975
2750	1.1364	-0.1140	3337.5	1.1250	-0.0972
2762.5	1.1362	-0.1135	3350	1.1248	-0.0969
2775	1.1359	-0.1131	3362.5	1.1246	-0.0966
2787.5	1.1356	-0.1127	3375	1.1244	-0.0963
2800	1.1353	-0.1123	3387.5	1.1242	-0.0960
2812.5	1.1351	-0.1119	3400	1.1240	-0.0957
2825	1.1348	-0.1115	3412.5	1.1238	-0.0954
2837.5	1.1345	-0.1111	3425	1.1236	-0.0951
2850	1.1343	-0.1107	3437.5	1.1234	-0.0949
2862.5	1.1340	-0.1103	3450	1.1232	-0.0946
2875	1.1337	-0.1099	3462.5	1.1230	-0.0943
2887.5	1.1335	-0.1095	3475	1.1228	-0.0940
2900	1.1332	-0.1091	3487.5	1.1226	-0.0937
2912.5	1.1330	-0.1087	3500	1.1224	-0.0935
2925	1.1327	-0.1083	3512.5	1.1222	-0.0932
2937.5	1.1325	-0.1080	3525	1.1220	-0.0929
2950	1.1322	-0.1076	3537.5	1.1218	-0.0927
2962.5	1.1319	-0.1072	3550	1.1216	-0.0924
2975	1.1317	-0.1068	3562.5	1.1214	-0.0921
2987.5	1.1314	-0.1065	3575	1.1212	-0.0919
3000	1.1312	-0.1061	3587.5	1.1210	-0.0916
3012.5	1.1310	-0.1057	3600	1.1209	-0.0913
3025	1.1307	-0.1054	3612.5	1.1207	-0.0911
3037.5	1.1305	-0.1050	3625	1.1205	-0.0908
3050	1.1302	-0.1047	3637.5	1.1203	-0.0906
3062.5	1.1300	-0.1043	3650	1.1201	-0.0903
3075	1.1298	-0.1040	3662.5	1.1199	-0.0900
3087.5	1.1295	-0.1036	3675	1.1197	-0.0898
3100	1.1293	-0.1033	3687.5	1.1196	-0.0895

Frequency (Hz)	Real Part	Imaginary Part	Frequency (Hz)	Real Part	Imaginary Part
3700	1.1194	-0.0893	4112.5	1.1138	-0.0819
3712.5	1.1192	-0.0890	4125	1.1137	-0.0817
3725	1.1190	-0.0888	4137.5	1.1135	-0.0815
3737.5	1.1188	-0.0886	4150	1.1134	-0.0813
3750	1.1186	-0.0883	4162.5	1.1132	-0.0811
3762.5	1.1185	-0.0881	4175	1.1130	-0.0809
3775	1.1183	-0.0878	4187.5	1.1129	-0.0807
3787.5	1.1181	-0.0876	4200	1.1127	-0.0805
3800	1.1179	-0.0874	4212.5	1.1126	-0.0803
3812.5	1.1178	-0.0871	4225	1.1124	-0.0801
3825	1.1176	-0.0869	4237.5	1.1123	-0.0799
3837.5	1.1174	-0.0867	4250	1.1121	-0.0797
3850	1.1173	-0.0864	4262.5	1.1120	-0.0795
3862.5	1.1171	-0.0862	4275	1.1118	-0.0793
3875	1.1169	-0.0860	4287.5	1.1117	-0.0791
3887.5	1.1167	-0.0857	4300	1.1116	-0.0789
3900	1.1166	-0.0855	4312.5	1.1114	-0.0787
3912.5	1.1164	-0.0853	4325	1.1113	-0.0785
3925	1.1162	-0.0851	4337.5	1.1111	-0.0784
3937.5	1.1161	-0.0848	4350	1.1110	-0.0782
3950	1.1159	-0.0846	4362.5	1.1108	-0.0780
3962.5	1.1157	-0.0844	4375	1.1107	-0.0778
3975	1.1156	-0.0842	4387.5	1.1105	-0.0776
3987.5	1.1154	-0.0840	4400	1.1104	-0.0774
4000	1.1152	-0.0837	4412.5	1.1103	-0.0773
4012.5	1.1151	-0.0835	4425	1.1101	-0.0771
4025	1.1149	-0.0833	4437.5	1.1100	-0.0769
4037.5	1.1148	-0.0831	4450	1.1098	-0.0767
4050	1.1146	-0.0829	4462.5	1.1097	-0.0765
4062.5	1.1144	-0.0827	4475	1.1096	-0.0764
4075	1.1143	-0.0825	4487.5	1.1094	-0.0762
4087.5	1.1141	-0.0823	4500	1.1093	-0.0760
4100	1.1140	-0.0821			

Table B.11 Derived propagation constant, between 300 and 4500 Hz, using the optimised set of c_1-c_8 of the optimisation condition 16 in Table 6.5 and Equation (6.16)

Frequency (Hz)	Real Part	Imaginary Part	Frequency (Hz)	Real Part	Imaginary Part
300	5.6580	8.4092	825	7.5326	19.9502
312.5	5.7237	8.6982	837.5	7.5647	20.2159
325	5.7875	8.9860	850	7.5965	20.4814
337.5	5.8497	9.2727	862.5	7.6280	20.7466
350	5.9102	9.5584	875	7.6591	21.0115
362.5	5.9691	9.8431	887.5	7.6899	21.2762
375	6.0266	10.1268	900	7.7204	21.5407
387.5	6.0828	10.4097	912.5	7.7505	21.8049
400	6.1377	10.6917	925	7.7804	22.0689
412.5	6.1914	10.9729	937.5	7.8100	22.3326
425	6.2439	11.2533	950	7.8394	22.5961
437.5	6.2953	11.5330	962.5	7.8684	22.8594
450	6.3456	11.8119	975	7.8972	23.1225
462.5	6.3950	12.0902	987.5	7.9257	23.3854
475	6.4435	12.3678	1000	7.9539	23.6481
487.5	6.4910	12.6448	1012.5	7.9819	23.9105
500	6.5376	12.9212	1025	8.0097	24.1728
512.5	6.5835	13.1971	1037.5	8.0372	24.4348
525	6.6285	13.4723	1050	8.0645	24.6967
537.5	6.6728	13.7471	1062.5	8.0915	24.9584
550	6.7163	14.0213	1075	8.1183	25.2199
562.5	6.7591	14.2950	1087.5	8.1449	25.4812
575	6.8013	14.5682	1100	8.1713	25.7423
587.5	6.8428	14.8410	1112.5	8.1975	26.0033
600	6.8837	15.1133	1125	8.2234	26.2641
612.5	6.9240	15.3851	1137.5	8.2492	26.5247
625	6.9636	15.6565	1150	8.2747	26.7851
637.5	7.0028	15.9276	1162.5	8.3001	27.0454
650	7.0413	16.1982	1175	8.3252	27.3055
662.5	7.0794	16.4684	1187.5	8.3502	27.5655
675	7.1169	16.7382	1200	8.3750	27.8253
687.5	7.1540	17.0077	1212.5	8.3995	28.0849
700	7.1905	17.2768	1225	8.4240	28.3444
712.5	7.2266	17.5456	1237.5	8.4482	28.6038
725	7.2623	17.8140	1250	8.4722	28.8630
737.5	7.2975	18.0821	1262.5	8.4961	29.1220
750	7.3322	18.3499	1275	8.5198	29.3809
762.5	7.3666	18.6174	1287.5	8.5434	29.6397
775	7.4006	18.8845	1300	8.5668	29.8983
787.5	7.4342	19.1514	1312.5	8.5900	30.1568
800	7.4673	19.4179	1325	8.6131	30.4151
812.5	7.5002	19.6842	1337.5	8.6360	30.6734

Frequency (Hz)	Real Part	Imaginary Part	Frequency (Hz)	Real Part	Imaginary Part
1350	8.6587	30.9314	1937.5	9.5905	42.9398
1362.5	8.6813	31.1894	1950	9.6080	43.1931
1375	8.7038	31.4472	1962.5	9.6254	43.4464
1387.5	8.7261	31.7049	1975	9.6427	43.6996
1400	8.7483	31.9625	1987.5	9.6599	43.9527
1412.5	8.7703	32.2200	2000	9.6771	44.2058
1425	8.7922	32.4773	2012.5	9.6941	44.4588
1437.5	8.8139	32.7345	2025	9.7111	44.7117
1450	8.8355	32.9916	2037.5	9.7281	44.9646
1462.5	8.8570	33.2486	2050	9.7449	45.2173
1475	8.8784	33.5054	2062.5	9.7617	45.4700
1487.5	8.8996	33.7622	2075	9.7784	45.7227
1500	8.9207	34.0188	2087.5	9.7950	45.9752
1512.5	8.9417	34.2753	2100	9.8116	46.2278
1525	8.9625	34.5318	2112.5	9.8280	46.4802
1537.5	8.9832	34.7881	2125	9.8445	46.7326
1550	9.0038	35.0443	2137.5	9.8608	46.9849
1562.5	9.0243	35.3004	2150	9.8771	47.2371
1575	9.0447	35.5564	2162.5	9.8933	47.4893
1587.5	9.0649	35.8123	2175	9.9094	47.7414
1600	9.0851	36.0680	2187.5	9.9255	47.9934
1612.5	9.1051	36.3237	2200	9.9415	48.2454
1625	9.1250	36.5793	2212.5	9.9575	48.4974
1637.5	9.1448	36.8348	2225	9.9734	48.7492
1650	9.1645	37.0902	2237.5	9.9892	49.0010
1662.5	9.1841	37.3455	2250	10.0049	49.2528
1675	9.2036	37.6007	2262.5	10.0206	49.5044
1687.5	9.2229	37.8558	2275	10.0363	49.7561
1700	9.2422	38.1108	2287.5	10.0518	50.0076
1712.5	9.2614	38.3658	2300	10.0673	50.2591
1725	9.2805	38.6206	2312.5	10.0828	50.5106
1737.5	9.2994	38.8753	2325	10.0982	50.7620
1750	9.3183	39.1300	2337.5	10.1135	51.0133
1762.5	9.3371	39.3846	2350	10.1288	51.2646
1775	9.3558	39.6390	2362.5	10.1440	51.5158
1787.5	9.3744	39.8934	2375	10.1591	51.7669
1800	9.3929	40.1477	2387.5	10.1742	52.0180
1812.5	9.4113	40.4020	2400	10.1893	52.2691
1825	9.4296	40.6561	2412.5	10.2043	52.5201
1837.5	9.4478	40.9102	2425	10.2192	52.7710
1850	9.4660	41.1641	2437.5	10.2341	53.0219
1862.5	9.4840	41.4180	2450	10.2489	53.2727
1875	9.5020	41.6719	2462.5	10.2637	53.5235
1887.5	9.5199	41.9256	2475	10.2784	53.7743
1900	9.5377	42.1793	2487.5	10.2930	54.0249
1912.5	9.5554	42.4328	2500	10.3076	54.2756
1925	9.5730	42.6863	2512.5	10.3222	54.5261

Frequency (Hz)	Real Part	Imaginary Part	Frequency (Hz)	Real Part	Imaginary Part
2525	10.3367	54.7767	3112.5	10.9669	66.4999
2537.5	10.3511	55.0271	3125	10.9793	66.7484
2550	10.3655	55.2775	3137.5	10.9917	66.9968
2562.5	10.3799	55.5279	3150	11.0041	67.2452
2575	10.3942	55.7782	3162.5	11.0164	67.4935
2587.5	10.4084	56.0285	3175	11.0287	67.7418
2600	10.4226	56.2787	3187.5	11.0410	67.9901
2612.5	10.4368	56.5289	3200	11.0532	68.2383
2625	10.4509	56.7790	3212.5	11.0654	68.4865
2637.5	10.4650	57.0291	3225	11.0776	68.7347
2650	10.4790	57.2792	3237.5	11.0897	68.9828
2662.5	10.4929	57.5291	3250	11.1018	69.2309
2675	10.5068	57.7791	3262.5	11.1139	69.4790
2687.5	10.5207	58.0290	3275	11.1259	69.7270
2700	10.5345	58.2788	3287.5	11.1379	69.9750
2712.5	10.5483	58.5286	3300	11.1499	70.2229
2725	10.5620	58.7784	3312.5	11.1618	70.4709
2737.5	10.5757	59.0281	3325	11.1737	70.7188
2750	10.5894	59.2778	3337.5	11.1856	70.9666
2762.5	10.6029	59.5274	3350	11.1974	71.2144
2775	10.6165	59.7770	3362.5	11.2092	71.4622
2787.5	10.6300	60.0265	3375	11.2210	71.7100
2800	10.6435	60.2760	3387.5	11.2327	71.9577
2812.5	10.6569	60.5254	3400	11.2444	72.2054
2825	10.6703	60.7748	3412.5	11.2561	72.4531
2837.5	10.6836	61.0242	3425	11.2678	72.7007
2850	10.6969	61.2735	3437.5	11.2794	72.9483
2862.5	10.7101	61.5228	3450	11.2910	73.1959
2875	10.7234	61.7720	3462.5	11.3025	73.4434
2887.5	10.7365	62.0212	3475	11.3141	73.6909
2900	10.7497	62.2704	3487.5	11.3256	73.9384
2912.5	10.7627	62.5195	3500	11.3370	74.1858
2925	10.7758	62.7686	3512.5	11.3485	74.4332
2937.5	10.7888	63.0176	3525	11.3599	74.6806
2950	10.8018	63.2666	3537.5	11.3713	74.9279
2962.5	10.8147	63.5155	3550	11.3826	75.1753
2975	10.8276	63.7645	3562.5	11.3939	75.4226
2987.5	10.8404	64.0133	3575	11.4052	75.6698
3000	10.8532	64.2622	3587.5	11.4165	75.9170
3012.5	10.8660	64.5109	3600	11.4277	76.1642
3025	10.8788	64.7597	3612.5	11.4389	76.4114
3037.5	10.8915	65.0084	3625	11.4501	76.6585
3050	10.9041	65.2571	3637.5	11.4613	76.9056
3062.5	10.9167	65.5057	3650	11.4724	77.1527
3075	10.9293	65.7543	3662.5	11.4835	77.3998
3087.5	10.9419	66.0029	3675	11.4946	77.6468
3100	10.9544	66.2514	3687.5	11.5056	77.8938

Frequency (Hz)	Real Part	Imaginary Part	Frequency (Hz)	Real Part	Imaginary Part
3700	11.5167	78.1408	4112.5	11.8662	86.2754
3712.5	11.5276	78.3877	4125	11.8764	86.5215
3725	11.5386	78.6346	4137.5	11.8866	86.7676
3737.5	11.5496	78.8815	4150	11.8967	87.0136
3750	11.5605	79.1283	4162.5	11.9069	87.2596
3762.5	11.5714	79.3752	4175	11.9170	87.5056
3775	11.5822	79.6220	4187.5	11.9271	87.7515
3787.5	11.5931	79.8687	4200	11.9371	87.9974
3800	11.6039	80.1155	4212.5	11.9472	88.2433
3812.5	11.6147	80.3622	4225	11.9572	88.4892
3825	11.6254	80.6089	4237.5	11.9672	88.7351
3837.5	11.6362	80.8555	4250	11.9771	88.9809
3850	11.6469	81.1022	4262.5	11.9871	89.2267
3862.5	11.6575	81.3488	4275	11.9970	89.4725
3875	11.6682	81.5953	4287.5	12.0069	89.7183
3887.5	11.6788	81.8419	4300	12.0168	89.9640
3900	11.6895	82.0884	4312.5	12.0267	90.2098
3912.5	11.7000	82.3349	4325	12.0366	90.4555
3925	11.7106	82.5814	4337.5	12.0464	90.7011
3937.5	11.7211	82.8278	4350	12.0562	90.9468
3950	11.7317	83.0743	4362.5	12.0660	91.1924
3962.5	11.7422	83.3207	4375	12.0758	91.4380
3975	11.7526	83.5670	4387.5	12.0855	91.6836
3987.5	11.7631	83.8134	4400	12.0953	91.9292
4000	11.7735	84.0597	4412.5	12.1050	92.1747
4012.5	11.7839	84.3060	4425	12.1147	92.4202
4025	11.7943	84.5523	4437.5	12.1243	92.6657
4037.5	11.8046	84.7985	4450	12.1340	92.9112
4050	11.8149	85.0447	4462.5	12.1436	93.1567
4062.5	11.8252	85.2909	4475	12.1532	93.4021
4075	11.8355	85.5371	4487.5	12.1628	93.6475
4087.5	11.8458	85.7832	4500	12.1724	93.8929
4100	11.8560	86.0293			

Table B.12 Calculated characteristic impedance (normalised by the characteristic impedance of the air, ρc), between 3812.5 and 4500 Hz, using Utsuno's improved two-cavity method

Frequency (Hz)	Real Part	Imaginary Part	Frequency (Hz)	Real Part	Imaginary Part
3812.5	1.1359	-0.0324	4162.5	1.2060	-0.2146
3825	1.1949	-0.0692	4175	1.2480	-0.0019
3837.5	1.1940	-0.0527	4187.5	1.1231	-0.2564
3850	1.1786	-0.0760	4200	1.2093	-0.0826
3862.5	1.1966	-0.0577	4212.5	1.2141	-0.2643
3875	1.2463	-0.1077	4225	1.2051	-0.1380
3887.5	1.2984	-0.0318	4237.5	1.1865	-0.0787
3900	1.2983	-0.1134	4250	1.3779	-0.1710
3912.5	1.3199	-0.1876	4262.5	0.9912	0.0868
3925	1.2904	-0.1956	4275	1.3813	-0.3156
3937.5	1.3059	-0.1935	4287.5	0.9839	-0.3991
3950	1.1688	-0.2001	4300	1.3919	-0.4351
3962.5	1.0673	-0.1379	4312.5	1.0886	-0.2868
3975	1.2488	-0.2255	4325	1.1879	-0.4055
3987.5	1.1959	-0.0321	4337.5	0.9211	-0.6022
4000	1.1928	-0.0966	4350	1.0646	-0.2041
4012.5	1.1908	-0.1642	4362.5	0.9047	-0.4892
4025	1.1977	-0.0064	4375	0.9483	-0.5844
4037.5	1.1024	-0.0906	4387.5	0.7815	-0.4789
4050	1.2426	-0.1893	4400	0.8939	-0.6373
4062.5	1.1553	-0.0315	4412.5	0.9558	-0.6532
4075	1.1387	-0.0767	4425	0.6310	-0.4766
4087.5	1.2655	-0.0894	4437.5	0.6244	-0.6610
4100	1.0643	-0.1295	4450	0.5080	-0.3953
4112.5	1.2496	0.0268	4462.5	0.4673	-0.5932
4125	1.0886	-0.0958	4475	0.3760	-0.4587
4137.5	1.2486	-0.0932	4487.5	0.4244	-0.4412
4150	1.1681	0.1050	4500	0.7498	-0.3668

Table B.13 Calculated propagation constant, between 3812.5 and 4500 Hz, using Utsuno's improved two-cavity method

Frequency (Hz)	Real Part	Imaginary Part	Frequency (Hz)	Real Part	Imaginary Part
3812.5	13.4657	80.0473	4162.5	12.2751	84.2838
3825	12.9576	79.2600	4175	12.5358	86.9368
3837.5	13.2083	79.1591	4187.5	11.3301	85.6128
3850	12.7657	80.4595	4200	12.8323	87.9787
3862.5	13.2321	79.8588	4212.5	13.4459	85.1980
3875	11.7914	78.9935	4225	14.4702	87.4461
3887.5	14.0867	78.8082	4237.5	12.2881	87.8179
3900	11.5073	79.0847	4250	16.6769	89.6110
3912.5	11.2117	78.5855	4262.5	11.3035	89.7399
3925	10.9884	79.1795	4275	15.4759	87.8172
3937.5	11.5290	80.8844	4287.5	14.1933	86.1443
3950	10.5437	82.0235	4300	16.1143	91.0397
3962.5	10.0812	84.3337	4312.5	14.0828	88.2821
3975	11.8508	80.5340	4325	16.0389	91.6443
3987.5	12.2113	83.9334	4337.5	18.9689	82.7042
4000	12.4134	82.5633	4350	12.9888	91.0509
4012.5	11.1565	82.1763	4362.5	17.1958	85.8777
4025	13.0137	83.6557	4375	19.5518	89.2804
4037.5	12.1669	83.9952	4387.5	16.6083	83.8161
4050	10.8542	82.6074	4400	21.7501	88.2278
4062.5	11.4124	83.9379	4412.5	23.0492	92.5063
4075	12.0923	84.8399	4425	17.9605	80.7287
4087.5	12.0293	83.5935	4437.5	30.6129	76.8219
4100	10.5404	84.2023	4450	11.8569	77.4318
4112.5	12.1992	85.8761	4462.5	18.9298	61.7000
4125	10.1684	84.4064	4475	5.3399	68.1090
4137.5	12.8804	84.3632	4487.5	5.5472	73.2198
4150	11.8360	87.3907	4500	7.0812	84.6678

Table B.14 Extrapolated characteristic impedance (normalised by the characteristic impedance of the air, ρc), between 3812.5 and 4500 Hz, using the optimised set of c_1-c_8 of the optimisation condition 7 in Table 6.3 and Equation (6.15)

Frequency (Hz)	Real Part	Imaginary Part	Frequency (Hz)	Real Part	Imaginary Part
3812.5	1.1231	-0.0950	4162.5	1.1191	-0.0891
3825	1.1230	-0.0948	4175	1.1190	-0.0889
3837.5	1.1228	-0.0946	4187.5	1.1188	-0.0887
3850	1.1227	-0.0943	4200	1.1187	-0.0885
3862.5	1.1225	-0.0941	4212.5	1.1186	-0.0883
3875	1.1224	-0.0939	4225	1.1184	-0.0881
3887.5	1.1222	-0.0937	4237.5	1.1183	-0.0879
3900	1.1221	-0.0935	4250	1.1182	-0.0878
3912.5	1.1219	-0.0932	4262.5	1.1180	-0.0876
3925	1.1218	-0.0930	4275	1.1179	-0.0874
3937.5	1.1216	-0.0928	4287.5	1.1178	-0.0872
3950	1.1215	-0.0926	4300	1.1176	-0.0870
3962.5	1.1213	-0.0924	4312.5	1.1175	-0.0868
3975	1.1212	-0.0922	4325	1.1174	-0.0866
3987.5	1.1211	-0.0920	4337.5	1.1172	-0.0865
4000	1.1209	-0.0917	4350	1.1171	-0.0863
4012.5	1.1208	-0.0915	4362.5	1.1170	-0.0861
4025	1.1206	-0.0913	4375	1.1169	-0.0859
4037.5	1.1205	-0.0911	4387.5	1.1167	-0.0857
4050	1.1203	-0.0909	4400	1.1166	-0.0856
4062.5	1.1202	-0.0907	4412.5	1.1165	-0.0854
4075	1.1201	-0.0905	4425	1.1163	-0.0852
4087.5	1.1199	-0.0903	4437.5	1.1162	-0.0850
4100	1.1198	-0.0901	4450	1.1161	-0.0849
4112.5	1.1196	-0.0899	4462.5	1.1160	-0.0847
4125	1.1195	-0.0897	4475	1.1159	-0.0845
4137.5	1.1194	-0.0895	4487.5	1.1157	-0.0843
4150	1.1192	-0.0893	4500	1.1156	-0.0842

Table B.15 Extrapolated propagation constant, between 3812.5 and 4500 Hz, using the optimised set of c_1-c_8 of the optimisation condition 7 in Table 6.3 and Equation (6.16)

Frequency (Hz)	Real Part	Imaginary Part	Frequency (Hz)	Real Part	Imaginary Part
3812.5	11.7706	80.7949	4162.5	12.0831	87.7631
3825	11.7821	81.0441	4175	12.0940	88.0116
3837.5	11.7936	81.2933	4187.5	12.1048	88.2601
3850	11.8050	81.5425	4200	12.1155	88.5086
3862.5	11.8164	81.7916	4212.5	12.1263	88.7570
3875	11.8278	82.0407	4225	12.1370	89.0054
3887.5	11.8392	82.2898	4237.5	12.1477	89.2537
3900	11.8505	82.5389	4250	12.1584	89.5021
3912.5	11.8619	82.7879	4262.5	12.1690	89.7504
3925	11.8732	83.0369	4275	12.1797	89.9987
3937.5	11.8844	83.2859	4287.5	12.1903	90.2470
3950	11.8957	83.5349	4300	12.2009	90.4952
3962.5	11.9069	83.7838	4312.5	12.2115	90.7435
3975	11.9181	84.0327	4325	12.2220	90.9917
3987.5	11.9293	84.2816	4337.5	12.2325	91.2399
4000	11.9404	84.5304	4350	12.2431	91.4880
4012.5	11.9515	84.7793	4362.5	12.2535	91.7361
4025	11.9626	85.0281	4375	12.2640	91.9843
4037.5	11.9737	85.2768	4387.5	12.2745	92.2324
4050	11.9848	85.5256	4400	12.2849	92.4804
4062.5	11.9958	85.7743	4412.5	12.2953	92.7285
4075	12.0068	86.0230	4425	12.3057	92.9765
4087.5	12.0178	86.2717	4437.5	12.3160	93.2245
4100	12.0287	86.5203	4450	12.3264	93.4725
4112.5	12.0397	86.7689	4462.5	12.3367	93.7204
4125	12.0506	87.0175	4475	12.3470	93.9683
4137.5	12.0614	87.2661	4487.5	12.3573	94.2162
4150	12.0723	87.5146	4500	12.3675	94.4641

APPENDIX C

SPECIFICS OF THE ARTIFICIAL NEURAL NETWORK FOR PREDICTING SOUND TRANSMISSION CLASS OF FLOOR-CEILING CONSTRUCTIONS

Table C.1 Shift and scale factors of inputs

	Shift	Scale
InsDensity	-0.2093	0.02072
InsThick	-0.2796	0.004739
JstSpace	-1	0.003279
JstDepth	-1.803922	0.009804
RCSpace	-1	0.003279
LOG(FCMass)	-1.46187	1.232935

Table C.2 Weights and thresholds to each hidden neuron of the neural network

	h1#01	h1#02	h1#03
Threshold	0.386025	-0.1329	-2.0437
InsDensity'	-1.23369	-1.12211	-0.4246
InsThick'	0.997581	0.281194	-1.17909
JstSpace'	-1.12721	-0.1058	0.597408
JstDepth'	-1.48347	-0.5016	0.849528
RCSpace'	0.029992	0.50511	0.135541
LOG(FCMass)'	1.210527	-1.03458	-4.05432

Table C.3 Weights and thresholds to the output neuron of the neural network

	STC'
Threshold	-1.73649
h1#01	-1.92222
h1#02	1.795027
h1#03	-2.43284

Table C.4 Shift and scale factors of the output

	Shift	Scale
STC	-2.4	0.05

PUBLICATIONS BY THE AUTHOR

- Xu J. and Fricke F.R., 2003. "The prediction of airborne and impact sound transmission through floor-ceiling constructions using neural network analysis," *Proceedings of the 10th international congress on sound and vibration*, Stockholm, Sweden, pp 4543-4540.

- Xu J., Nannariello J. and Fricke F.R., 2003. "The use of evolutionary algorithms to optimize the performance of thin membrane absorbers," *Proceedings of the 32nd international congress and exposition on noise control engineering*, Jeju, Korea, pp 537-544.

- Xu J., Nannariello J. and Fricke F.R., 2004. "Predicting and optimising the airborne sound transmission of floor-ceiling constructions using computational intelligence," *Applied Acoustics*, 65 (7), pp 693-704.

- Xu J., Nannariello J. and Fricke F.R., 2004. "Optimising flat-walled multi-layered anechoic linings using evolutionary algorithms," *Applied Acoustics*, 65 (11), pp 1009-1026.

- Xu J., Bradley J. and Gover B.N., 2005. "A neural network approach for predicting architectural speech security," *Journal of the Acoustical Society of America*, 117 (4), pp 1709-1712.

- Xu J., Buchholz J. and Fricke F.R, 2005. "Flat-walled multi-layered anechoic linings: Optimization and application," *Journal of the Acoustical Society of America*, 118 (5), pp 3104-3109.

- Xu J., Buchholz J. and Fricke F.R., 2005. "Applying multi-layered polyurethane foams for flat-walled anechoic linings," *Applied Acoustics*, 67(5), pp 476-485.

- Xu J., Buchholz J. and Fricke F.R., 2005. "Multi-layered polyurethane foams for flat-walled anechoic linings," *Proceedings of the first international symposium on advanced technology of vibration and sound*, Hiroshima, Japan, pp 273-276.

- Xu J., Nannariello J. and Fricke F.R., 2005. "Application of computational intelligence techniques to architectural and building Acoustics," *In*: Kalogirou S., editor, *Artificial intelligence in energy and renewable energy systems*, to be published by Nova Publishers Inc, US.

- Xu J., Cummings A. and Shin H-C, 2006. "Derivation of the bulk acoustic properties of a rigid porous medium from a single impedance test," *Journal of Sound and Vibration* (in preparation)

Available online at www.sciencedirect.com
SCIENCE DIRECT®
Applied Acoustics 65 (2004) 693–704
applied acoustics
www.elsevier.com/locate/apacoust

Predicting and optimising the airborne sound transmission of floor–ceiling constructions using computational intelligence

Jingfeng Xu [a,*], Joseph Nannariello [a,b], Fergus R. Fricke [a]

[a] *School of Architecture, Design Science and Planning, University of Sydney, Sydney, NSW 2006, Australia*
[b] *Renzo Tonin and Associates Pty Ltd, P.O. Box 877, Strawberry Hills, Sydney, NSW 2012, Australia*

Received 1 September 2003; received in revised form 21 November 2003; accepted 5 December 2003

Abstract

Computational intelligence (CI) techniques offer powerful alternatives for investigating acoustical issues and providing acoustical solutions to problems. This paper presents information on two CI techniques by applying them to the sound transmission performance prediction and design of floor–ceiling constructions.

First a simple neural network (NN) model for predicting the airborne sound transmission of typical floor–ceiling constructions is presented and explained in detail. This model is accessible to researchers with knowledge of neural network analysis (NNA) for further sophistication, specialisation or hybridisation. The model may also be used by architects and others with no knowledge of NNA and no access to any specialised neural network software. Evolutionary algorithms (EAs) were then applied to search the multidimensional space created by the neural network model in order to optimise the airborne sound transmission of floor–ceiling constructions within the range of design parameters utilised in buildings.

Keywords: Sound transmission; Computational intelligence; Neural network analysis; Evolutionary algorithms

* Corresponding author. Fax: +61-2-9351-3031.
E-mail address: jixu4247@mail.usyd.edu.au (J. Xu).

0003-682X/$ - see front matter © 2003 Elsevier Ltd. All rights reserved.
doi:10.1016/j.apacoust.2003.12.004

1. Introduction

There are at least two factors that make architectural and building acoustics design and research difficult: (1) the multiple parameters and multiple criteria aspects involved; (2) the large quantity of data measured under non-standard conditions, which blurs the inherent acoustic phenomena. These complex situations are not easily recognizable and therefore remain difficult to resolve using conventional methods [1]. On the other hand computational intelligence (CI) is one of the approaches to program computers in order to make them behave as if they were humans who can understand and tackle highly complex problems. The three major domains of CI are neural networks (NNs), evolutionary algorithms (EAs), and fuzzy logic (FL).

In connectionist models of computation, such as neural network analysis, attempts are made to simulate the powerful cognitive and sensory functions of the human brain and to use this capability to represent and manipulate knowledge in the form of patterns. Based on these patterns, neural networks model input–output functional relationships and can make predictions about other combinations of unseen inputs (inputs not used in the training process). EAs are defined as search procedures based on the mechanics of natural selection and can be perceived as a generalisation of genetic algorithms. Classical genetic algorithms operate on fixed length binary strings, which need not be the case for evolutionary algorithms [2]. With the ability of searching a large population (potential solutions), the EA can overcome the problem of local fitness optima to obtain the optima that are almost always close to global [3].

It is an enticing challenge to a theoretician to develop a new method suitable for solving the problem at hand. However, from the application point of view, the time for developing the technique has to be added to the computer time invested. In that respect, utilising a non-specialised and robust procedure, to which NNA and EAs belong, may be worthwhile. With the inherent power of CI, it is promising to use NNA and EAs to solve architectural and building acoustics problems that feature high dimensionality and multiple criteria.

Multivariate regression analysis [4] has been used to model the airborne sound transmission performance, sound transmission class (STC), of floor–ceiling constructions using the existing measurement data. However, it does not appear that NNA has been used previously to model STC of floor–ceiling constructions although it is not the first time NNA has been used on predicting sound transmission performance of walls [5,6]. The NN model is accessible to researchers with knowledge of NNA for further sophistication, specialisation or hybridisation. The NN model can also be used by architects and others who have no knowledge of NNA and do not have access to the specialised NN software but can use any standard spreadsheet application. The current work also investigates, for the first time, the application of EAs to search the large non-linear multidimensional space (potential solutions) provided by the NN model in order to optimise the STC of floor–ceiling constructions within the range of design parameters utilised in buildings.

2. Prediction of STC using NNA

2.1. Data set

The Institute for Research in Construction (IRC), National Research Council Canada (CNRC), in collaboration with 18 industry and government partners carried out a major research study from 1995 to 1998 to measure the acoustical and fire resistance performance of floor assemblies [4,7]. In this IRC research project, airborne and impact transmission were measured for about 190 specimens, to ASTM standards, in the floor test facility but with a frequency range extended down to 50 Hz. Most of the 190 floors in the project incorporated timber joists or trusses. Joist type, length, spacing and depth were varied. There were only 14 steel joist systems and four concrete slab floors. The joist types comprised solid timber, timber trusses, I-joists, and steel joists. Three types of sound absorbing material were used: glass, rock and cellulose fibre. The measurements provide an extensive and consistent data set appropriate for analysis and testing of computer models [4,7,8].

One category of floor–ceiling constructions which contained sufficient data to allow a meaningful analysis was of solid timber joist floors with resilient channels directly attached to the joists and with sound absorbing material in the cavity. There are 71 cases in this category and the ranges of parameters are shown in Table 1.

2.2. Neural network architecture

As mentioned previously NNA can be thought of as a method of learning from precedents. The number of input and output parameters and the number of cases influence the architecture of the network. The structure of the hidden layer/s essentially defines the topology of a basic feed-forward network [9]. The network consists of an input layer of neurons (one neuron to each input), a layer or layers of hidden neurons and an output layer of one neuron for each output. A neuron, also called processing unit, is the basic unit of a NN and performs summation and activation functions to determine the output of that neuron. The number of hidden neurons in the hidden layer is approximately the average of the inputs and outputs although it does depend on the number of training cases as well. Too few hidden layer neurons can result in large training and verification and testing errors. Too

Table 1
Ranges of parameters

Variable	Minimum	Maximum
Sound transmission class (STC)	47	70
Sound absorbing material density (InsDensity), kg/m^3	10.1	58.35
Sound absorbing material thickness (InsThick), mm	59	270
Joist spacing (JstSpace), mm	305	610
Joist depth (JstDepth), mm	184	286
Resilient metal channel spacing (RCSpace), mm	200	610
Floor and ceiling layer surface density (FCMass), mm	13	127

many hidden layer neurons can result in over training (a lack of generalisation) and lead to large test errors [10].

Starting from an initially randomised weighted network system, input data are propagated through the network to provide an estimate of the output value. The error between the actual output and the predicted value is used to adjust the network weightings (on the connections between neurons) to minimize the error in the predicted outputs. In this iterative procedure, the new weights are accepted if the resulting error is smaller than that recorded using the previous set of weights [10].

2.3. NN model

There are many alternative forms of NN systems and there are many ways NNA may be applied to a given problem. The suitability of an appropriate paradigm and strategy for application is very much dependent on the type of problem to be solved [11]. Fig. 1 illustrated the basic multi-layer feed-forward NN employed by authors in the present work. The floor and ceiling layer surface density in kg/m^2 is converted to its logarithmic value, which yields a better data distribution than the non-logarithmic value.

The basic modus operandi of the NN model is as follows:

(1) The input data are first pre-processed, depending on the type of problems, which may include replication of time-shifted values for time series problems, conversion of nominal values, scaling of numeric values, missing value substitution and the normalisation of cases. For the current problem, only the scaling and shifting processes are involved to convert input values to the same order of magnitude that is suitable for use in the NN. After scaling and shifting, the minimum value of a certain input is converted to zero and the maximum value of the same input is converted to one. For instance, the minimum value and the maximum value of InsDensity (sound absorbing material density) are 10.1 and 58.35 kg/m^3, respectively, and solving Eqs. (1) and (2) found that the corresponding scale and shift factors are 0.02072 and

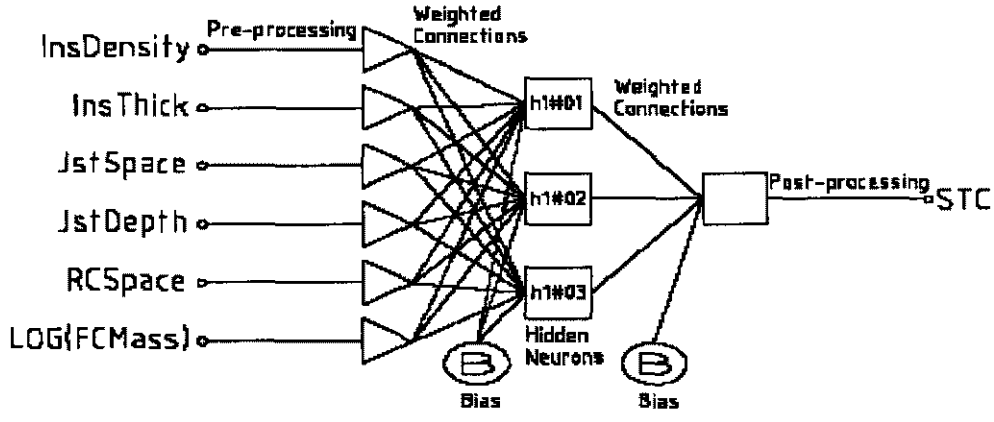

Fig. 1. Illustration of a basic multi-layer feed-forward neural network.

−0.2093 for the input InsDensity. Table 2 shows the scale and shift factors for the inputs of the network. Furthermore, the pre-processed input InsDensity' can be expressed as shown in Eq. (3). All other pre-processed inputs can be expressed in the same way:

$$10.1 \times \text{Scale} + \text{Shift} = 0, \tag{1}$$

$$58.35 \times \text{Scale} + \text{Shift} = 1, \tag{2}$$

$$\text{InsDensity'} = \text{InsDensity} \times 0.02072 - 0.2093. \tag{3}$$

(2) Each pre-processed input unit is multiplied by a scalar weight connecting the first layer neurons to the hidden layer neurons. At each neuron within the hidden layer, the weighted inputs are summed and bias value (threshold) is subtracted from the summed weighted inputs. The threshold is used to adjust the 'fullness' of the hidden neuron during the training. The resulting value is passed through a non-linear activation function, in this case, sigmoidal logistic function, $1/(1+e^{-x})$. Table 3 shows the weights and thresholds linked to each hidden neuron of the best NN attained by training.

The numeric operations at hidden neuron 1, h1#01, can be expressed as:

$$\begin{aligned} \text{h1\#01} = 1/(1+\exp(-((&0.5816121 \times \text{InsDensity'} - 0.4974 \times \text{InsThick'} \\ &+ 0.3348666 \times \text{JstSpace'} - 0.756 \times \text{JstDepth'} - 0.5216 \\ &\times \text{RCSpace'} - 0.68 \times \text{Log(FCMass)}) - (+0.05078)))). \end{aligned} \tag{4}$$

The numeric operations at the other two hidden neurons can be expressed in the same way.

Table 2
Shift and scale factors of inputs

	Shift	Scale
InsDensity	−0.2093	0.02072
InsThick	−0.2796	0.004739
JstSpace	−1	0.003279
JstDepth	−1.803922	0.009804
RCSpace	−1.990196	0.004902
log(FCMass)	−1.249962	1.12681

Table 3
Weights and thresholds to each hidden neuron of the best neural network attained

	h1#01	h1#02	h1#03
Threshold	0.05078	2.467049	0.2841709
InsDensity'	0.5816121	0.3737668	0.794076
InsThick'	−0.4974	0.3751391	0.8492002
JstSpace'	0.3348666	0.4216603	−0.4004
JstDepth'	−0.756	−0.1088	−0.824262
RCSpace'	−0.5216	0.02952	0.1421855
log(FCMass)'	−0.68	2.168416	0.4592341

(3) The output value of each hidden neuron is multiplied by the scalar weights for each connection between the hidden layer and the output neuron. The weighted outputs are summed and a bias (threshold) value is subtracted from the sum to produce a single output value (STC' which is equal to STC after post-processing). Table 4 shows the weights and threshold to the output neuron of the best NN attained during the training.

The output STC' is:

$$\mathrm{STC}' = -0.9772 \times \mathrm{h1\#01} + 2.205224 \times \mathrm{h1\#02} - 0.05104 \times \mathrm{h1\#03} - (-0.1129). \quad (5)$$

(4) The single output STC' is post-processed by subtracting the shift factor, followed by division by the scale factor. Table 5 shows the scale and shift factors for the outputs of the network.

Hence, the final output of the NN STC is:

$$\mathrm{STC} = (\mathrm{STC}' - (-2.4))/0.05. \quad (6)$$

Nannariello and Fricke [12] present a complete example of how to embed a NN model into a standard spreadsheet. A similar procedure can be applied to include the NN model into a computing program written by any standard programming languages, for instance, Matlab.

2.4. Training the NN and results

During the process of searching for the best network, the data set presented in Table 1 was divided into three sub-data sets:

- The training data set (53 cases) was used for training the network (that is the process of adjusting the weights of the network). The order in which the training cases were presented to the network was randomly altered within each epoch. The weights, which were initialised to uniformly distributed random values using the "uniform method" [13], were adjusted by using "back propagation" [14] training algorithm to minimize the prediction error over the training cases.

Table 4
Weights and thresholds to the output neuron of the best neural network attained

	STC'
Threshold	−0.1129
h1#01	−0.9772
h1#02	2.205224
h1#03	−0.05104

Table 5
Shift and scale factor of the output

	Shift	Scale
STC	−2.4	0.05

- The verification data set (8 cases) was used for periodically evaluating the predictions of the network during training, but was not used to compute adjustments to weights. Training was stopped once deterioration in the verification error was observed.
- The test data set (10 cases) was used for independently checking the performance of the network and testing the stability of the network when an entire network design procedure was completed. As the test data set has not been used in the training process at all – not even for verification of results – it presents the best measure of the NN model's ability to make accurate predictions.

Table 6 presents a statistical analysis based on the best NN model which has the lowest 'test' RMS error, the lowest 'test' standard deviation ratio and a close agreement between the verification data set and the test data set. This is a strong indicator that the network has learned to generalize reliably [13].

2.5. Comparison between NNA and multivariate regression analysis

A conventional multivariate regression analysis was carried out using the cases in the training data set and verification data set. The corresponding RMS error of the 'test' data set is 0.77. For the same set of test cases, predictions by the NN model results in an RMS error of 0.59, i.e., the NN model is more accurate than the multivariate regression equation.

Another advantage of NNA is its ability to work with nominal values, which is not possible when using multivariate regression analysis. This enables the NN to directly acquire additional information and knowledge about a given problem domain. In future work, for instance, a nominal input, "joist type" (timber or other materials), could be included into the NN model. Also, a sound absorbing material type or code which contains both the information about the density and thickness of the material can be used as one of inputs of the NN model. Often architects are more familiar with the sound absorbing material type or code than the relevant density and thickness of a certain material. The replacement of two numerical inputs, sound absorbing material density and thickness, with one nominal input, sound absorbing material type or code, would further simplify the prediction model.

As the non-linear NN model is more complex than the linear regression equation, the classic optimisation techniques are inefficient or unsatisfactory for searching for potential solutions provided by the NN model to an appropriate floor–ceiling construction. A better approach is to use EAs which have the ability to search a large non-linear multidimensional space (potential solutions).

Table 6
Statistical data of the best neural network established

	RMS error	Correlation coefficient	Standard deviation ratio
Verification (8 cases)	0.81	0.98	0.21
Test (10 cases)	0.59	0.99	0.17

3. Optimisation of STC using EAs

The parametric study indicated that the most important parameter that determines STC performance of floor–ceiling constructions is the mass of the floor and ceiling layers. However, other parameters also have an effect on the overall STC performance of floor–ceiling systems. Consequently there is a need to resolve – once we have a NN model that accurately predicts the STC of a certain floor–ceiling construction – how we can optimize the STC performance of floor–ceiling constructions within the range of design parameters utilised in buildings. For instance, an architect may wish to know the construction to achieve an STC 55 rated floor–ceiling that uses a relatively low depth type of solid timber joists, say 235 mm deep, and the least mass possible. Consequently the question is posed as to which type of floor–ceiling construction can meet these requirements? EA is a powerful tool which in this case can be utilised to search the non-linear multi-dimensional space (potential solutions) provided by the best NN model and find an appropriate floor–ceiling construction that meets the design requirement of the architect.

3.1. Introductions of EAs

Although the term EA (or evolutionary computation in some literature) was invented as recently as 1991, the field has a history that spans four decades. Three broadly similar avenues of investigation in simulated evolution have survived as main disciplines within the field: genetic algorithms mainly developed in the USA by Holland [15], evolutionary strategies, developed in Germany by Rechenberg [16] and Schwefel [17] and evolutionary programming [18]. The differences between them are characterised by the typical data representation, the types of variations that imposed on solutions to create offspring, and the methods employed for selecting new parents. Over time, however, these differences have become increasingly blurred, and will likely become of historical interest only [19]. An instructive introductory overview of EAs can be found in [19–22]. These publications represent important milestones in the acceptance of EAs as practical tools for addressing complex problems in engineering and include numerous references that will assist readers just entering or not familiar with the field.

In general, any abstract task to be accomplished can be thought of as solving a problem, which, in turn, can be perceived as a search through a space of potential solutions. Since we are after "the best" solution, we can view this task as an optimisation process. The classic techniques of gradient descent, deterministic hill climbing, and purely random search (with no heredity) have been generally unsatisfactory when applied to non-linear optimisation problems, especially with stochastic, temporal, or chaotic components. But these are the problems that nature has seemingly solved so very well. It is quite natural therefore to seek to describe evolution in terms of an algorithm that can be used to solve difficult optimisation problems. Evolution provides inspiration for computing the solutions to problems that have previously appeared intractable [23].

EAs are stochastic search methods that mimic the metaphor of natural biological evolution on a computer. They operate on a population of potential solutions applying the principle of survival of the fittest to produce better and better approximations to a solution. At each generation, a new set of approximations is created by the process of selecting individuals according to their level of fitness in the problem domain and breeding them together using operators borrowed from natural genetics, such as selection, recombination, mutation, migration, locality and neighbourhood. This process leads to the evolution of populations of individuals that are better suited to their environment than the individuals that they were created from, just as in natural adaptation. EAs work on populations of individuals instead of single solutions. In this way, the search is performed in a parallel manner [24].

Fig. 2 shows the structure of a simple EA. At the beginning of the computation a number of individuals (potential solutions) are randomly initialised. The objective function is then evaluated for these individuals. The first/initial generation (a set of potential solutions) is produced. If the optimisation criteria are not met the creation of a new generation starts. Individuals are selected according to their fitness (closeness to the optimisation criteria) for the production of offspring (new potential solutions). Parents (existing potential solutions) are recombined. In other words, the information contained in the parents is combined to produce offspring. All offspring will be mutated (randomly altered) with a certain probability. The fitness of the offspring is then computed. The offspring are inserted into the population (the existing set of potential solutions) replacing the parents, producing a new generation. This cycle is performed until the optimisation criteria are reached. Such a single population EA is powerful and performs well on a wide variety of problems. However, better results can be obtained by introducing multiple subpopulations. Every subpopulation (subset of potential solutions) evolves over a few generations isolated like the single population EA before one or more individuals are exchanged between the subpopulation. The multipopulation EA models the evolution of a species in a way more similar to nature than the single population EA [24].

EAs differ substantially from more traditional search and optimisation methods [24]. The most significant differences are:

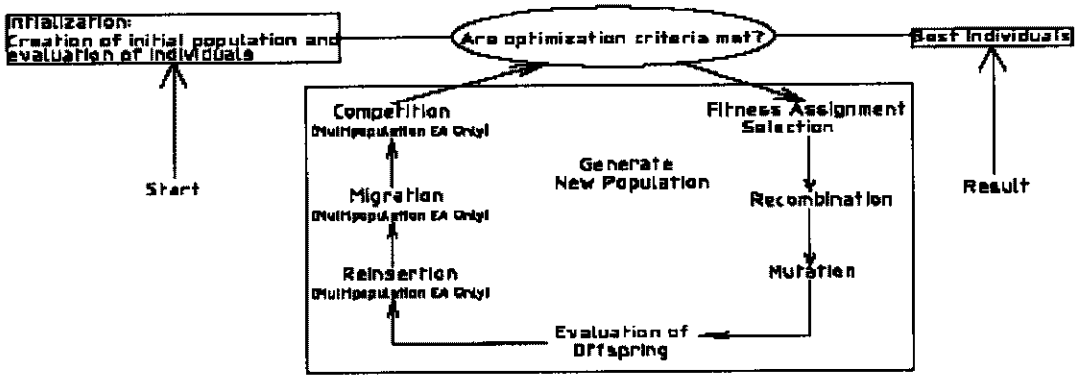

Fig. 2. Structure of a simple evolutionary algorithm.

- EAs search a population of points in parallel, not just a single point.
- EAs do not require derivative information or other auxiliary knowledge. Only the objective function and corresponding fitness levels influence the directions of search.
- EAs use probabilistic transition rules, not deterministic ones.
- EAs are generally more straightforward to apply, because no restrictions for the definition of the objective function exist.
- EAs can provide a number of potential solutions to a given problem. The final choice is left to the user. Thus in case where the particular problem does not have one individual solution, for example a family of pareto optimal solutions, as in the case of multi-objective optimisation and scheduling problems, then the EA is potentially useful for identifying these alternative solutions simultaneously.

3.2. Searching the space

Genetic and Evolutionary Algorithm Toolbox for Use with Matlab (GEATbx version 3.3) [24] was used to search the multidimensional space provided by the best NN model presented in Section 2.3 of this paper and find an appropriate floor–ceiling construction which would meet the design requirements of the architect. The searching range of the parameters is listed in Table 1. The best NN established was used as the objective function. Real value variable representations and multipopulation searching were used. Initial values were randomly generated by the GEATbx [24] within the range of parameters at the start of the searching. Discrete recombination and real value mutation genetic operators were employed. Discrete recombination is a recombination method that performs an exchange of variable values between the parents and for each variable position of the offspring the parent who contributes its variable to the offspring is chosen randomly with equal probability.

To achieve an STC 55 floor–ceiling construction using 235 mm deep solid timber joists, the searching results indicate that

- The minimum surface weight of the floor and ceiling layers should be 20 kg/m^2.
- The 235 mm thick cellulose fibre sound absorbing material, with a density of 58 kg/m^3, should be applied.
- The joist spacing should be 610 mm.
- The resilient metal channel spacing should be 610 mm.

This construction was not included in the original laboratory tests [4,7].

However, the original laboratory tests [4,7] show that the following floor–ceiling construction can achieve STC 52:

- The floor layer is 1 layer of 15 mm thick oriented strandboard with a surface weight of 8.8 kg/m^2.
- The ceiling layer is 1 layer of 16 mm thick gypsum board with a surface weight of 11.3 kg/m^2.
- Floor joists are 235 mm deep solid timber joists with a spacing of 406 mm.
- The sound absorbing material is 152 mm thick glass fibre with a density of 11.1 kg/m^3.
- The resilient metal channel is spaced 610 mm apart.

The differences in construction methods between the laboratory floor–ceiling system and the EAs searching are the type (density) and thickness of sound absorbing material and the spacing of joists. From the laboratory tests, Warnock [25] concluded that

- Each increase in sound absorbing material thickness of about 65 mm results in an increases of 1 STC point.
- For the same thickness of material, cellulose fibre gives an STC that is higher than that of glass fibre by about 1 STC point.
- An increase in joist spacing of approximately 200 mm will increase the STC by 1 point.

On the basis of Warnock's conclusions, the increase of sound absorbing material thickness from 152 to 270 mm will result in an increase of 1 STC point. Furthermore a change of sound absorbing material from glass fibre to cellulose fibre will increase STC by 1 point and changing the spacing of joists from 406 mm centres to 610 mm centres will result in an increase of STC by 1 point. Hence, the overall STC performance of the floor–ceiling construction tested can be increased from 52 to 55 if its construction is changed to the searched result of EAs. In other words, the searched result of EAs is in agreement with laboratory test results and studies.

4. Conclusions and future work

This current work indicates that the inherent power of CI makes the use of NNA and EAs to solve architectural and building acoustics problems, which are characterised by high dimensionality, multiple criteria and large quantity of measured data, a very attractive alternative to conventional approaches.

The current work also demonstrates one simple example of the use of CI: predicting and optimising the airborne sound transmission performance of floor–ceiling constructions (airborne sound transmission class (STC)). Initially a NN model which can predict the STC of timber joist type floor–ceiling constructions was established and then EAs were applied to search for an appropriate floor–ceiling construction which would meet the design requirements. For the purpose of comparison with Warnock's work [4,7,8,25], in this work the same type of measure of airborne sound transmission, namely STC, is used. A similar analysis to that described in this paper can be carried out using Rw or sound transmission loss values at any frequency of interest. Future work needs to include the other aspect of the acoustic performance of floor–ceiling constructions, namely impact transmission. Multiple-objective EAs could also be applied to optimise STC and IIC (or other measures of sound transmission) of floor–ceiling constructions at the same time. This problem is probably a more appropriate use of CI techniques as the output (IIC) may not be dominated by a single input parameter such as mass, which is the situation with airborne sound transmission.

Acknowledgements

Authors are grateful to Dr. Warnock for providing the laboratory test data, without which the present work could not have been undertaken. The current

research was conducted under an Australian Postgraduate Award and a School of Architecture, Design Science and Planning Supplementary Scholarship.

References

[1] Nannariello J, Osman MR, Fricke FR. Recent developments in the application of neural network analysis to architectural and building acoustics. Acoust Aust 2001;29(3):103–10.
[2] Michalewicz Z. Genetic algorithms + data structures = evolution programs. 3rd ed. Berlin/Heidelberg: Springer; 1996.
[3] Bethke AD. Genetic algorithms as function optimisers. Doctoral dissertation, University of Michigan. Dissertation Abstracts International 1981:41(9).
[4] Warnock ACC, Birta JA. Summary Report for Consortium on Fire Resistance and Sound Insulation of Floors: Sound Transmission Class and Impact Insulation Class Results. Internal Report IRC-IR-766, Institute for Research in Construction, National Research Council Canada, 1998.
[5] Coomes J, Fricke FR. The prediction of wall sound insulation using neural networks. J Build Acoust 2001;8(2):103–19.
[6] Moncada AF, Gibbs B. Prediction of sound insulation at low frequencies using artificial neural networks. J Build Acoust 2002;9(1):49–71.
[7] Warnock ACC. Detailed Report for Consortium on Fire Resistance and Sound Insulation of Floors: Sound Transmission and Impact Insulation Data in 1/3 Octave Bands, IRC Internal Report IRC-IR-811, Institute for Research in Construction, National Research Council Canada; 2000.
[8] Warnock ACC. Airborne and impact sound insulation of joist floor systems:a collection of data. InterNoise 2000;1–6.
[9] Nelson MN, Illingworth WT. A practical guide to neural nets. New York: Addison-Wesley; 1991.
[10] Nannariello J, Fricke FR. Introduction to neural network analysis and its application to building services engineering. Build Serv Eng Res Technol 2001;22(1):58–68.
[11] Browne A. Neural network analysis, architectures and applications. Bristol and Philadelphia: Institute of Physics; 1999.
[12] Nannariello J, Fricke FR. A neural-computation method of predicting the early interaural cross-correlation coefficient ($IACC_{E3}$) for auditoria. Appl Acoust 2002;63(6):627–41.
[13] StatSoft. Statistica neural networks manual, version 4.0A manual. Tulsa OK: StatSoft Inc; 1999.
[14] Haykin S. Neural networks: a comprehensive foundation. Upper Saddle River, NJ: Prentice-Hall; 1999.
[15] Holland JH. Adaptation in natural and artificial systems. Ann Arbor: The University of Michigan Press; 1975.
[16] Rechenberg I. Evolutions strategie – Optimierung technischer systeme nach prinzipien der biologischen evolution, Stuttgart, Frommann – Holzboog; 1973.
[17] Schwefel HP. Numerical optimization of computer models. Chichester: Wiley; 1981.
[18] Fogel LJ, Owens AJ, Walsh MJ. Artificial intelligence through simulated evolution. New York: Wiley; 1966.
[19] Fogel DB. Evolutionary computation. Piscataway: IEEE Press; 1998.
[20] Fogel DB. An introduction to simulated evolutionary optimization. IEEE Trans Neural Networks 1994;5(1):3–14 [special issue on Evolutionary Computation].
[21] Back T, Hammel U, Schwefel HP. Evolutionary computation: comments on the history and current state. IEEE Trans Evolution Comput 1997;1(1):3–17.
[22] Back T, Fogel DB, Michalewicz Z. Handbook of evolutionary computation. New York: Oxford University Press; 1997.
[23] Quagliarella D, Periaux J, Poloni C, Winter G. Genetic algorithm and evolutionary strategies in engineering and computer science. Chichester: Wiley; 1998.
[24] Pohlheim H. Genetic and evolutionary algorithm toolbox for use with Matlab version 3.3: Evolutionary Algorithms, Berlin; 2002.
[25] Warnock ACC. Controlling the transmission of airborne sound through floors. Construct Technol Update 1999;25:4.

Available online at www.sciencedirect.com
SCIENCE DIRECT®
Applied Acoustics 65 (2004) 1009–1026
applied acoustics
www.elsevier.com/locate/apacoust

Optimising flat-walled multi-layered anechoic linings using evolutionary algorithms

Jingfeng Xu [a,*], Joseph Nannariello [a,b], Fergus R. Fricke [a]

[a] School of Architecture, Design Science and Planning, University of Sydney, NSW 2006, Australia
[b] Renzo Tonin & Associates Pty Ltd, P.O. Box 877, Strawberry Hills, NSW 2012, Australia

Received 17 March 2004; received in revised form 18 May 2004; accepted 18 June 2004
Available online 5 August 2004

Abstract

Previous investigations indicated that a flat-walled, multi-layered anechoic lining system, with an overall thickness slightly less than a quarter of a wavelength, could be used to achieve a required cut-off frequency. However, the work proved to be tedious and time consuming because of the numerous trial-and-error measurements involved. On the other hand, the successful application of a method of calculating the overall acoustic impedance of multi-layered absorbing systems has indicated that the design of multi-layered absorbing systems can be carried out on a desktop computer. In the present work, a MATLAB genetic and evolutionary algorithm toolbox is implemented as the optimiser to aid and speed up the design process. The optimisation results indicate that a three-layered lining system can achieve results comparable with quality wedge-type anechoic linings with overall thickness slightly less than a sixth of a wavelength at the 100 Hz cut-off frequency.

Keywords: Anechoic lining; Multi-objective optimisation problem; Evolutionary algorithms

* Corresponding author. Fax: +61 2 9351 3031.
E-mail address: jixu4247@mail.usyd.edu.au (J. Xu).

0003-682X/$ - see front matter © 2004 Elsevier Ltd. All rights reserved.
doi:10.1016/j.apacoust.2004.06.003

1. Introduction

Flat-walled "anechoic" linings have advantages in being less complicated and, hence, less costly to install than the individual units, such as wedges, pyramids and blocks. Davern [1] carried out work on the design of flat-walled multi-layered anechoic linings as an alternative to the more conventional wedge-type system. The approach used was to design a flat-walled lining system by using conventional measurements in an impedance tube. Davern's measurements indicated that a flat-walled, multi-layered, graded density lining could achieve an overall thickness slightly less than a quarter of a wavelength at the cut-off frequency, e.g., 0.727 m, at 110 Hz. For comparison, quality wedge-type anechoic linings can achieve cut-off frequencies within thicknesses of a fifth of the wavelength [2] (Cut-off frequency is the frequency above which no pressure reflections exceed 10%; this corresponds to an energy absorption exceeding 99% [3].) However, the work [1] proved to be tedious and time consuming because of the numerous trial-and-error measurements involved.

The subsequent work undertaken by Dunn and Davern [4] demonstrated that the overall impedance of a flat-walled multi-layered system could be calculated by the repeated application of a single layer impedance equation. They also demonstrated that the direct calculation approach could be readily programmed on a desktop computer and good agreement between measured (impedance tube) and calculated values could be achieved.

The ability to rapidly test potential layer combinations using a computer has marked advantages over repeated impedance tube measurements. There is now a need to resolve how to optimise flat-walled multi-layered anechoic lining systems to achieve an acoustic performance that is comparable to wedge-type anechoic linings and lead to a more efficient design procedure. In the present work, evolutionary algorithms (EAs) are introduced and applied as the optimiser to aid and speed up the design process.

2. Impedance of a single homogeneous layer and multiple layers

2.1. Impedance of a single homogeneous layer

The normal incidence acoustic impedance, Z_1, at the front of a layer of homogeneous material of thickness L can be calculated using the following equation [5]

$$Z_1 = W\frac{Z_0\cosh(\gamma L) + W\sinh(\gamma L)}{Z_0\sinh(\gamma L) + W\cosh(\gamma L)}, \tag{1}$$

where Z_0 is the backing impedance of the layer, W is the characteristic impedance of the layer and γ is its propagation constant. Both W and γ are complex and frequency dependent. When the material is backed by solid backing ($Z_0 = \infty$), the single layer equation can be written as

$$Z_1 = W\coth(\gamma L). \tag{2}$$

2.2. Impedance of multiple layers

The impedance at the front of a composite layered material (Fig. 1), Z_i, can be calculated by applying the single-layer equation to each material successively [4], i.e.,

$$Z_i = W_i \frac{Z_{i-1}\cosh(\gamma_i L_i) + W_i \sinh(\gamma_i L_i)}{Z_{i-1}\sinh(\gamma_i L_i) + W_i \cosh(\gamma_i L_i)}, \tag{3}$$

where the subscript i refers to the ith layer, starting from the layer closest to solid backing.

3. Pressure reflection factor

The pressure reflection factor at normal incidence, r, is defined as the ratio of the pressure amplitude of the reflected wave to the incident wave in the reference plane for a plane wave at normal incidence [6] and can be calculated by the following equation:

$$r = \left|\frac{Z_i/\rho c - 1}{Z_i/\rho c + 1}\right|. \tag{4}$$

The relationship between the normal incidence sound absorption coefficient α_n and r is

$$\alpha_n = 1 - r^2. \tag{5}$$

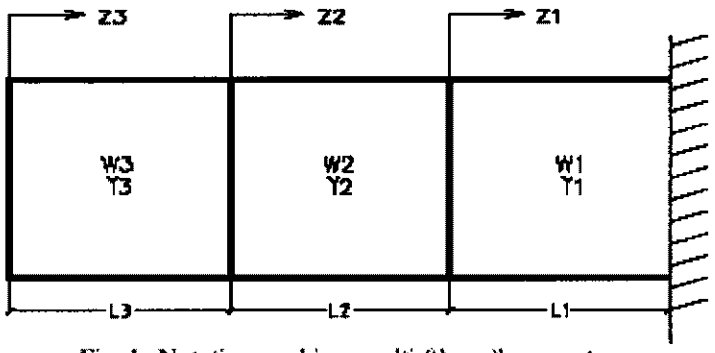

Fig. 1. Notation used in a multi-(three-)layer system.

4. Materials investigated

All materials investigated in the work [2,4] were fully reticulated polyurethane plastic foams which do not have small fibres and have lower susceptibility to mechanical damage. A detailed research of this type of material can be found in [7].

Dunn and Davern [4] studied three foams with steady flow resistivity in the range 380–3200 SI rayl/m (Table 1) and reported the curve-fitting equations for predicting the bulk acoustic properties, W and γ, i.e.,

$$W = \rho c\left[1 + 0.114(\rho f/\sigma)^{-0.369} + \mathrm{j}\left(-0.0985(\rho f/\sigma)^{-0.758}\right)\right], \tag{6}$$

$$\gamma = (2\pi f/c)\left[0.168(\rho f/\sigma)^{-0.715} + \mathrm{j}\left(1 + 0.136(\rho f/\sigma)^{-0.491}\right)\right], \tag{7}$$

where ρ is the air density, c is the velocity of sound in air, f is the frequency and σ is the flow resistivity. For normalisation purposes, a value of 1.2 kg/m^3 is used for air density and 340 m/s for sound velocity.

Similar curve-fitting equations for predicting the bulk acoustic properties, W and γ, of the same type of material but with a wider range of flow resistivity 60–6229 SI rayl/m (Table 2) were reported in [7] as follows:

$$W = \rho c\left[1 + 0.0953(\rho f/\sigma)^{-0.491} + \mathrm{j}\left(0.0986(\rho f/\sigma)^{-0.665}\right)\right], \tag{8}$$

$$\gamma = (2\pi f/c)\left[0.167(\rho f/\sigma)^{-0.636} + \mathrm{j}\left(1 + 0.174(\rho f/\sigma)^{-0.372}\right)\right]. \tag{9}$$

High correlation coefficients of the curve-fitting equations have been observed in both [4] and [7]. Good agreement between the measured (impedance tube) overall impedance of a flat-walled multi-layered system and calculated values using multi-layered impedance equation and the curve-fitting equations for predicting bulk acoustic properties has also been shown in [4]. This supports the confidence that the design can indeed be conducted on a desktop computer.

However, it is not advisable to use the curve-fitting equations for predicting bulk acoustic properties beyond the range of the experimental data [4,7,8]. The most serious consequence of extrapolation is in the case of predications at low frequencies. The lowest frequency measurements were conducted in [1,4,7] was 100 Hz.

In the present work, the fully reticulated polyurethane plastic foams are also investigated as materials for anechoic linings.

Table 1
Measured values of steady flow resistivity in [4]

Foam Identity	Notional number of pores/linear inch	Flow resistivity (SI rayl/m)
A	45	380
B	60	1340
C	80	3200

Table 2
Measured values of steady flow resistivity in [7]

Notional number of pores/linear inch	Flow resistivity (SI rayl/m)
10	60
16	79
21	176
29	287
33	356
42	671
45	816
58	1724
65	2184
72	3085
87	5745
100	6229

5. Multi-objective optimisation problems (MOP)

Most practical problems require the simultaneous optimisation of multiple, often competing, objectives (or criteria). In applications of optimisation techniques, the solution to such problems is usually computed by combining the objectives into a single-objective optimisation problem according to some utility function which expresses the relative importance of the objectives. In many cases, however, the utility function is not well known prior to the optimisation process, and therefore, the whole problem should then be treated as a multi-objective optimisation problem with non-commensurable objectives. In this way, a number of solutions can be found which provide the decision maker (DM) with insight into the characteristics of the problem before a final solution is chosen.

A general MOP can be described as a vector function, f, that maps a group of m parameters (decision variables) to a group of n objectives. Formally:

$$\begin{aligned} \min \quad & y = f(x) = (f_1(x), \ldots, f_n(x)) \\ \text{s.t.} \quad & x = (x_1, \ldots, x_m) \in X, \\ & y = (y_1, \ldots, y_n) \in Y, \end{aligned} \tag{10}$$

where x is called the decision vector, X is the parameter space, y is the objective vector, and Y is the objective space [9].

The MOP usually has no unique, perfect solutions, but a set of non-dominated, alternative solutions, known as the Pareto-optimal set [10]. Still assuming a minimisation problem, dominance is defined as follows.

Pareto dominance: A given vector $u = (u_1, \ldots, u_n)$ is said to dominate $v = (v_1, \ldots, v_n)$ if and only if u is partially less than v ($u_p \prec v$), i.e., $\forall i \in \{1, \ldots, n\}: u_i \leqslant v_i \wedge \exists i \in \{1, \ldots, n\}: u_i < v_i$.

Pareto optimality: A solution $x_u \in X$ is said to be Pareto-optimal if and only if there is no $x_v \in X$ for which $v = f(x_v) = (v_1, \ldots, v_n)$ dominates $u = f(x_u) = (u_1, \ldots, u_n)$.

Pareto-optimal solutions are also called efficient, non-dominated, and non-inferior solutions. The corresponding objective vectors are simply called non-dominated. The set of all non-dominated vectors is known as the non-dominated set, or the trade-off surface, of the problem.

6. Multi-objective decision making based on given goals

When presented with the trade-off surface for a given function, the DM has to decide which of the non-dominated points will solve the problem at hand. First, the regions of the Pareto set which express good compromises according to some problem-specific knowledge needs to be identified. Then, having a clearer picture of what is achievable, the idea of compromise would be refined until the solution is found. As a consequence, only the "interesting" regions of the Pareto set need to be well known. Reducing the size of the solution set calls for higher level decision making to be incorporated in the selection algorithm. The idea is not to reduce the scope of the search, but simply to zoom in on the region of the Pareto set of interest to the DM by providing external information to the selection algorithm.

Such information can be provided in the form of goals to be attained. Goal values indicate desired levels of performance in each objective dimension. In fact, degradation in vector components which meet their goals is also acceptable provided it results in the improvement of other components that do not satisfy their goals and it does not go beyond the goal's boundaries. This makes it possible to prefer one individual to another even though they are both non-dominated. A detailed discussion of multi-objective decision making based on given goals can be found in [11,12].

7. Evolutionary approaches to MOP

Generating the non-dominated set can be computationally expensive and is often infeasible, because the complexity of the underlying application prevents exact methods from being applicable. EAs are an alternative. They usually do not guarantee to identify optimal tradeoffs but try to find a good approximation for a given problem, i.e., a set of solutions whose objective vectors are not too far away from the optimal objective vectors [13].

EAs are stochastic search methods that mimic the metaphor of natural biological evolution on a computer. They operate on a population of potential solutions applying the principle of survival of the fittest to produce better and better approximations to a solution. At each generation, a new set of approximations is created by the process of selecting individuals according to their level of fitness in the problem domain and breeding them together using operators borrowed from natural genetics, such as selection, recombination, and mutation. This process leads to the evolution of populations of individuals that are better suited to their environment than the individuals that they were created from, just as in natural adaptation.

EAs work on populations of potential individuals. In this way, the search is performed in a parallel manner. This characteristic makes EAs very attractive for solving MOP. A good introductory survey of EAs can be found in [14].

There are six basic steps in an EA search: initialisation, fitness assignment, selection, recombination, mutation and reinsertion.

7.1. Initialisation

The EA starts the search by randomly generating a set of a specified number of solutions, which is known as the population. Each solution within the population is known as an individual. After the size of the population is specified, individuals of the first/initial generation are randomly generated. To do this, decision variable values are generated randomly within the corresponding parameter space.

7.2. Rank-based fitness assignment for EAs

Individuals in a population can be ranked in accordance with the preference decided using the strategy introduced in Section 6. Consider an individual x_m at generation t and let $r_m^{(t)}$ be the number of individuals in the current population that are preferable to it. The current position of x_m in the individuals' rank can be simply given by

$$\text{rank}(x_m, t) = r_m^{(t)}. \tag{11}$$

This ensures that all preferred individuals in the current population are assigned rank zero [12]. The ranking of a population provides sufficient relative quality information to guide evolution.

Fitness is understood here as the number of offspring an individual is expected to produce through selection. Ranked based fitness assignment can be described as follows [11,12]:

1) Sort population according to rank.
2) Assign fitness by interpolating from the best individual to the worst according to some function, usually linear or exponential, but possibly of other type.
3) Average the fitness assigned to individuals with the same rank, so that all of them are sampled at the same rate while keeping the global population fitness constant.

7.3. Selection

Individuals with high fitness in a population are selected as parents and take part in recombination operations by suitably combining to produce offspring. In the present work, the stochastic universal sampling (SUS) [15] selection method is employed. The individuals are mapped to contiguous segment of a line, such that each individual's segment is equal in length to its fitness. Equally spaced pointers are placed along the line, as many as there are individuals to be selected. The SUS

selection method has the advantage of providing zero bias and minimum spread during the selection [15].

7.4. Recombination

Once the parents of the next generation have been selected from the old generation, they are recombined. In other words, the information contained in the parents is combined to produce offspring. The discrete recombination method [16] is applied in the present work. The method performs an exchange of variable values between the parents. For each variable position of the offspring, the parent which contributes its variable to the offspring is chosen randomly with equal probability.

7.5. Mutation

After the recombination individuals are mutated (randomly altered), which helps to keep the diversity of the population and to avoid premature convergence to local optima. In the present work, the real value mutation approach is adopted. Mutation of real value means that randomly created values are added to the variables with a low probability [16].

7.6. Reinsertion

Once the offspring have been produced by selection, recombination and mutation of individuals from the old population, the fitness of the offspring is determined. Only fitter offspring are then reinserted into the population and replace the existing individuals with lower fitness.

Four steps, namely selection, recombination, mutation and reinsertion are part of an iterative process which comes to an end when a satisfactory set of solutions is found or a given number of generations is reached.

8. Implementation

The above multi-objective evolutionary approach has been implemented as MATLAB [17] M and MEX files [18] and further developed and incorporated into the Genetic and Evolutionary Algorithm Toolbox for use with Matlab (GEATbx) [19]. In the work presented here, GEATbx has been used as the tool for implementing the evolutionary approach to aid the design of flat-walled multi-layered anechoic lining.

8.1. Design criterion

As the valid lowest frequency for Eqs. (6)–(9) is 100 Hz, it is decided that the design criterion of the present work is to optimise the flat-walled multi-layered anechoic lining to a cut-off frequency of 100 Hz. To simplify the problem, the highest frequency is capped at 1000 Hz.

In the present work, two scenarios are considered:

Scenario 1:

$$\begin{aligned} \text{Min} \quad & y = (r_{100}(x), r_{125}(x), \ldots, r_{1000}(x), L_{\text{overall}}) \\ \text{s.t.} \quad & x = (L_1, \ldots, L_m, \delta_1, \ldots, \delta_m) \in X, \\ & y = (y_1, \ldots, y_m) \in Y, \end{aligned} \tag{12}$$

where the subscripts (100, 125, ..., 1000) are the centre frequencies of a third octave spectrum, r is the pressure reflection factor at each corresponding frequency, L and δ are respectively the thickness and the flow resistivity of each layer, m is the number of layers and $L_{\text{overall}} = L_1 + \cdots + L_m$ is the overall thickness of the multi-layered system. The parameter space X may vary during the design process according to the design requirement.

The goal vector of this scenario is

$$g = (g_{100}, g_{125}, \ldots, g_{1000}, g_{L_{\text{overall}}}), \tag{13}$$

where the goal values for $(r_{100}(x), r_{125}(x), \ldots, r_{1000}(x))$ are $g_{100} = g_{125} = \cdots = g_{1000} = 10\%$, which are regarded as hard goals, namely, the pressure reflection over 10% at any frequency is not acceptable. The goal value for the overall thickness of the system $g_{L_{\text{overall}}}$ is soft and may vary during the design process. The three cases, Case A, Case B and Case C, presented in Section 8.4.1 are examples of Scenario 1.

Scenario 2:

$$\begin{aligned} \text{Min} \quad & y = (r_{100}(x), r_{125}(x), \ldots, r_{1000}(x)) \\ \text{s.t.} \quad & x = (L_1, \ldots, L_m, \delta_1, \ldots, \delta_m) \in X \wedge (L_1 + \cdots + L_m = L_{\text{overall\_fixed}}), \\ & y = (y_1, \ldots, y_m) \in Y. \end{aligned} \tag{14}$$

In this scenario, the overall thickness of the system is set to a fixed value $L_{\text{overall\_fixed}}$. The goal vector of this scenario is

$$g = (g_{100}, g_{125}, \ldots, g_{1000}), \tag{15}$$

where $g_{100} = g_{125} = \cdots = g_{1000} = 10\%$ and have to be reached at the end of the design. This scenario can be the case that the overall thickness of a certain multi-layered system, which meets the design criterion of the anechoic lining, is known due to some prior knowledge and the designer wants to know the possible compositions of the system. Case D presented in Section 8.4.2 is an example of Scenario 2.

8.2. Constraint handling

The definitions of the above two scenarios indicate that the first scenario is only constrained by the bounds on the decision variables $(L_1, \ldots, L_m, \delta_1, \ldots, \delta_m)$. However, in addition to the bounds on the decision variables, the second scenario is also constrained by a linear relationship $(L_1 + \cdots + L_m = L_{\text{overall\_fixed}})$.

The constraint imposed by bounds on the decision variables can be simply handled by mapping the search space to minimise the number of infeasible solutions

it contains. While the constraint imposed by the linear relationship ($L_1 + \cdots + L_m = L_{\text{overall\_fixed}}$) is handled by converting it to a penalty function and adding it to the objective function before fitness is computed, i.e.,

$$r = \left|\frac{Z_i/\rho c - 1}{Z_i/\rho c + 1}\right| + \lambda|(L_1 + \cdots + L_m) - L_{\text{overall\_fixed}}|, \tag{16}$$

where λ is a scalar factor used to tighten or loosen the constraint. As the acceptable range of r is $0 \leqslant r \leqslant 10$, the maximum violation of the constraint $|(L_1 + \cdots + L_m) - L_{\text{overall\_fixed}}|$ is limited to 0.01 m when the scalar factor λ is set to 1000.

Penalty functions provide a way of guiding the search toward feasible solutions but they are problem dependant. Guidelines for applying penalty functions to handle constraints can be found in [20] and the introduction of some other constraint handling techniques can be found in [12].

8.3. Parameters of EAs

In the present work, for every operation of the EA using GEATbx, the setting for some of the relevant parameters is:

- Maximum number of Generations: 100.
- Population size: 100.
- Generation Gap: 0.9 (which means 90% of the population to be reproduced every generation).
- Recombination rate: 1 (which means all parents have the possibility of contributing to the value of each variable of the offspring).
- Mutation rate: 1 (which means on the average 1 variable per individual to be mutated).
- Mutation range: 0.02 (which means the initial mutation step sizes will be 0.02 times the domain of each variable).

All the other parameters necessary for operating GEATbx are set to their default values. Details of these parameters and guidelines for setting these parameters can be found in [19]. The initial population are generated randomly by the program. In the present work, the computer (a desktop PC with Intel® P4 processor and 256 Mb RAM) time for each operation with above set of parameters varies from 60 to 100 s depending on the complexity of the search task. The non-dominated set yielded by each operation – which provides the DM with insight into the characteristics of the problem – is saved in a standard spreadsheet. In the work presented here, ten operations were conducted before any decision was made.

8.4. Evolutionary optimisation process and results

In the present work, the evolutionary optimisation of two scenarios previously introduced in Section 8.1 is considered.

8.4.1. First scenario optimisation

Three cases were involved in the first scenario optimisation. In Case A, three materials originally investigated by Davern [1] were chosen for the construction of the multi-layered lining system; in Case B, the materials with the steady flow resistivity in the range of 380–3200 SI rayl/m were chosen; and in Case C, the materials chosen had a greater steady flow resistivity in the range of 60–6229 SI rayl/m.

The evolutionary optimisation process is an interactive process between the DM and the evolutionary algorithm (EA). The process begins with the prior information based on Davern's work [1].

As previously mentioned, Davern's work [1] indicates that a flat-walled, multi-layered, anechoic lining, with Foam C as Layer 1 (against the solid back), foam B as Layer 2 (the mid layer) and Foam A as Layer 3 (the front layer), can achieve a cut-off frequency of 110 Hz with overall thickness of the system, 0.727 m, slightly less than a quarter of a wavelength at the cut-off frequency.

Case A. On the basis of the prior information, the decision space was set to $\delta_1 = 3200$ SI rayl/m, $\delta_2 = 1340$ SI rayl/m, $\delta_3 = 380$ SI rayl/m, and $0.001\ \text{m} \leqslant L_1, L_2, L_3 \leqslant 0.85$ m. The goals were set to $g_{100} = g_{125} = \cdots = g_{1000} = 10\%$, and $g_{L_{overall}} = 0.85$ m. 0.85 m corresponds to a quater of the wavelength at the cut-off frequency 100 Hz. The minimum thickness was set to 0.001 m to avoid the 'divided by zero' type error. All solutions, provided by the EA and meeting the anechoic lining design criterion, namely the goals set for g_{100} to g_{1000}, are shown in Fig. 2. The minimum overall thickness of the system provided by this set of solutions was 0.802 m, which indicated that the goal set for $g_{L_{overall}}$ was slightly over attained. Hence, the goal for $g_{L_{overall}}$ was reset to 0.8 m.

The EA was repeated with the tightened goal for $g_{L_{overall}}$. However, no solution was found by the EA with less overall thickness. Hence it was decided that the EA had found the optimum solutions for Case A. Other preferable solutions may exist

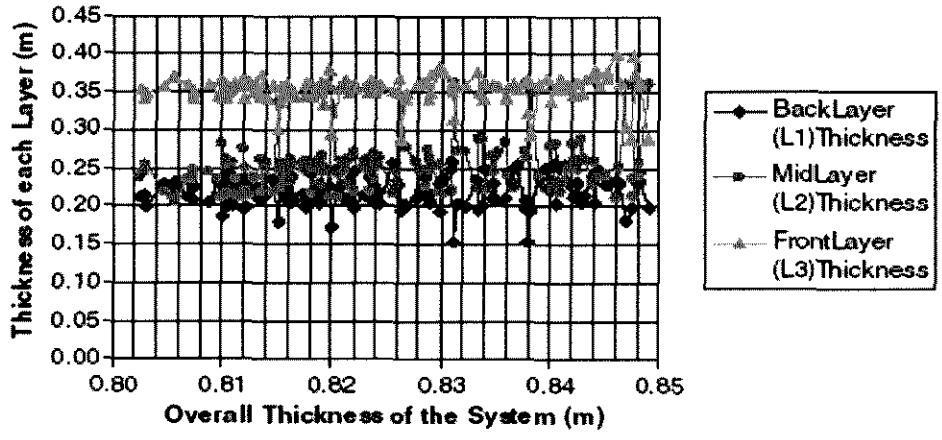

Fig. 2. Search results of Case A. Thickness of each layer vs. overall thickness of the system.

however they are most likely to be more difficult to be found given the encoding structure for the chromosomes and the associated genetic operators.

Case B. It was assumed that the curve-fitting equations, Eqs. (6) and (7), for predicting the bulk acoustic properties of fully reticulated polyurethane plastic foams developed by Dunn and Davern [4] could be used not only for the three materials listed in Table 1 but also for the same type of materials with steady flow resistivity in the range 380–3200 SI rayl/m. The decision space in this case was set to 380 SI rayl/m $\leqslant \delta_1, \delta_2, \delta_3 \leqslant$ 3200 SI rayl/m and 0.001 m $\leqslant L_1, L_2, L_3 \leqslant$ 0.85 m. The goals were set to $g_{100} = g_{125} = \cdots = g_{1000} = 10\%$, and $g_{L_{overall}} = 0.8$ m. With the goal $g_{L_{overall}}$ set to 0.8 m, it was hoped that the EA could find solutions with overall thicknesses less than the minimum overall thickness, 0.802 m, found in Case A. The minimum overall thickness of the system found by EA in this case was 0.79 m. The solutions that meet the anechoic lining design criterion and have the overall thicknesses between 0.79 and 0.802 m are shown in Fig. 3.

The goal for $g_{L_{overall}}$ was also set to 0.7, 0.75 and 0.79 m. However, no solution was found by the EA with the overall thickness less than 0.79 m.

Case C. Cummings and Beadle [7] investigated the same type of fully reticulated polyurethane plastic foam materials but with a wider range of flow resistivity, 60–6229 SI rayl/m (Table 2), and developed similar curve-fitting Eqs. (8) and (9). In this case, in lieu of Eqs. (6) and (7), Eqs. (8) and (9) were used for predicting the bulk acoustic properties. Correspondingly the decision space in this case was set to 60 SI rayl/m $\leqslant \delta_1, \delta_2, \delta_3 \leqslant$ 6229 SI rayl/m and 0.001 m $\leqslant L_1, L_2, L_3 \leqslant$ 0.85 m. The goals were set to $g_{100} = g_{125} = \cdots = g_{1000} = 10\%$, and $g_{L_{overall}} = 0.8$ m. It was hoped that with a greater choice of materials, solutions with less overall thickness could be found. The results produced by the first few operations of EA indicate that an overall thickness as thin as 0.61 m, slightly less than a fifth of the wave length at 100 Hz, was achievable. By further gradually tightening the goals for $g_{L_{overall}}$ from 0.68 m (a fifth of the wave length at 100 Hz) to 0.57 m (a sixth of the wave length at 100 Hz) the minimum overall thickness found by the EA was 0.529 m. The solutions that meet the anechoic lining design criterion and have the overall thickness between 0.529 m and 0.68 m are shown in Fig. 4.

The above interactive optimisation process has the advantage of reducing computational effort by concentrating optimisation effort on the region from which satisfying solutions are likely to emerge, while simultaneously providing the DM with trade-off information [21]. A more general introduction of interactive multi-objective evolutionary optimisation process can be found in [11].

A similar process was applied to search a two-layer system. However, no results were found with the overall thickness less than 1 m when using the materials with the steady flow resistivity in the range 60–6229 SI rayl/m.

8.4.2. Second scenario optimisation

During the design process, the overall thickness for a certain multi-layered system, which can meet the design criterion of the anechoic lining, is sometimes

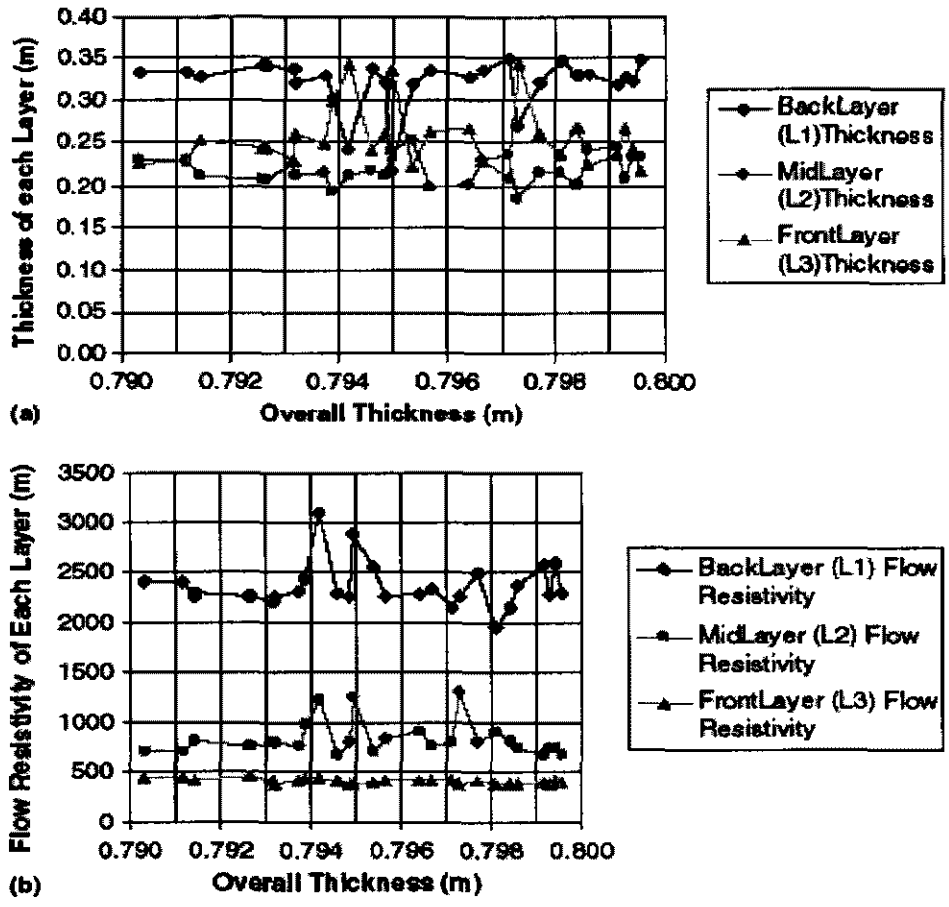

Fig. 3. Search results of Case B. (a) Thickness of each layer vs. overall thickness of the system. (b) Steady flow resistivity of each layer vs. overall thickness of the system.

known due to some prior knowledge. What is not known and of interest to the designer is the possible compositions of the system. Case D gives an example of this scenario.

Case D. The results found in Case A in Section 8.4.1 indicate that a flat-walled, multi-layered, anechoic lining, with Foam C as Layer 1 (which is against the solid back), Foam B as Layer 2 (the mid layer) and Foam A as Layer 3 (the front layer), can achieve a cut-off frequency of 100 Hz with a minimum overall thickness of 0.802 m. The designer may want to know the required thickness for each layer if the overall thickness is 0.85 m.

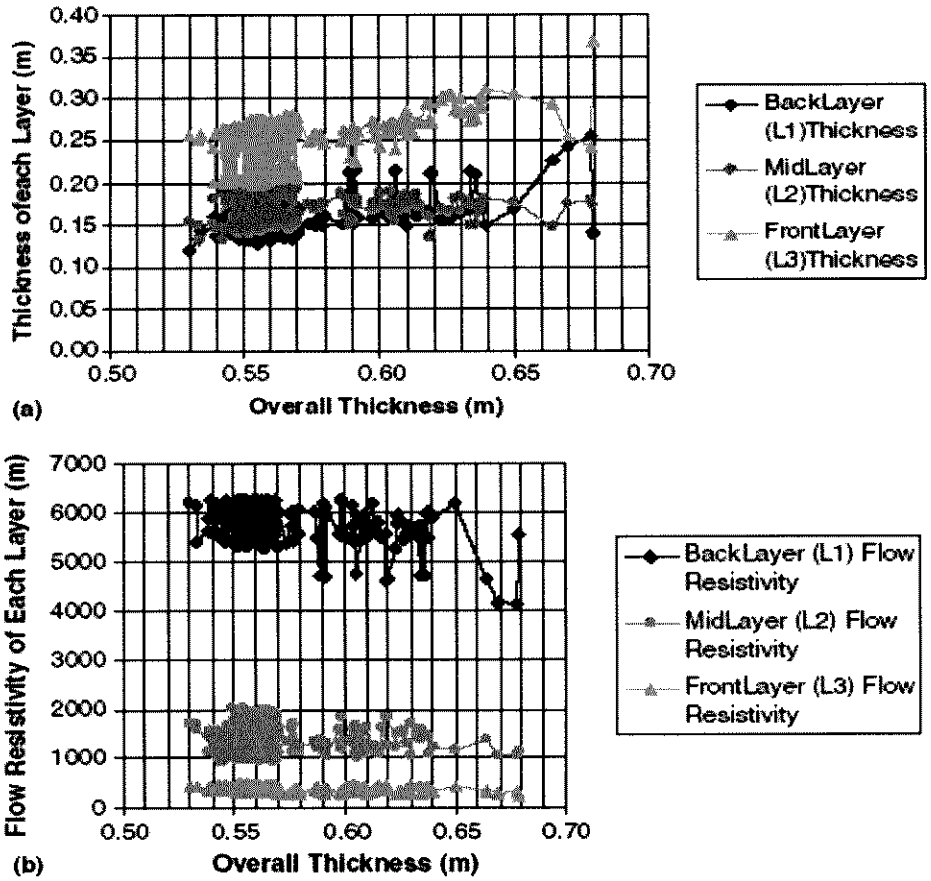

Fig. 4. Search results of Case C. (a) Thickness of each layer vs. overall thickness of the system. (b) Steady flow resistivity of each layer vs. overall thickness of the system.

Hence, the decision space in this case was set to $\delta_1 = 3200$ SI rayl/m, $\delta_2 = 1340$ SI rayl/m, $\delta_3 = 380$ SI rayl/m, 0.001 m $\leqslant L_1, L_2, L_3 \leqslant 0.85$ m, and $L_1 + L_2 + L_3 = L_{\text{overall\_fixed}} = 0.85$ m. The goals were set to $g_{100} = g_{125} = \cdots = g_{1000} = 10\%$. The objective function with the penalty item can be written as

$$r = \left|\frac{Z_t/\rho c - 1}{Z_t/\rho c + 1}\right| + 1000 \times |(L_1 + L_2 + L_3) - 0.85|. \tag{17}$$

This limits the possible maximum violation of the constraint to 0.01 m as explained in Section 8.2. Fig. 5 shows the search results provided by the EA. The maximum violation of the constraint of this set of results was only 0.00065 m.

8.5. Discussion of results

The optimisation results indicate that a flat-walled three-layered anechoic lining system can achieve results comparable with quality wedge-type anechoic linings with overall thickness slightly less than a sixth of a wavelength at a cut-off frequency of 100 Hz. Table 3 presents the solution with the minimum overall thickness, 0.529 m, and Table 4 shows the corresponding pressure reflection factor at the frequencies from 100 to 1000 Hz. However, a similar two-layered system (made of the fully reticulated polyurethane plastic foams with the steady flow resistivity in the range 60–6229 SI rayl/m) cannot achieve an overall thickness less than 1 m.

Davern [22] proved that to achieve the criterion of a maximum of 10% pressure reflection (which corresponds to a normal absorption coefficient of 99% or better) for an anechoic lining, the real and imaginary parts of the specific acoustic impedance ratio should lie on, or within, the circle defined by the equation

$$\left(\frac{R}{\rho c} - 1.02\right)^2 + \left(\frac{X}{\rho c}\right)^2 = (0.202)^2, \tag{18}$$

where R and X are, respectively, the real part and imaginary parts of the normal incidence acoustic impedance and $R/\rho c$ and $X/\rho c$ are, respectively, the specific normal

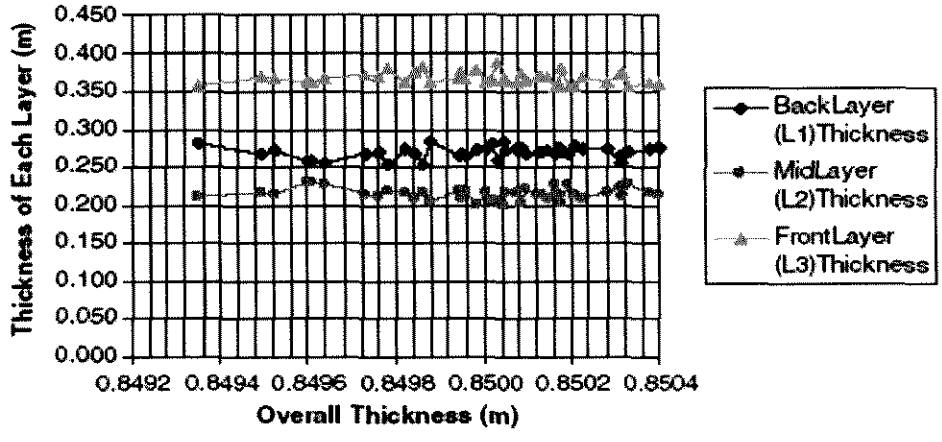

Fig. 5. Search results of Case D.

Table 3
The solution with the minimum overall thickness (0.529m)

BackLayer (L1) Thickness (m)	MidLayer (L2) Thickness (m)	FrontLayer (L3) Thickness (m)	BackLayer (L1) Flow Resistivity (SI rayl/m)	MidLayer (L2) Flow Resistivity (SI rayl/m)	FrontLayer (L3) Flow Resistivity (SI rayl/m)
0.121	0.153	0.255	6188	1707	417

Table 4
Corresponding pressure reflection factors (%) of the solution with the minimum overall thickness (0.529m)

100 Hz	125 Hz	160 Hz	200 Hz	250 Hz	315 Hz	400 Hz	500 Hz	630 Hz	800 Hz	1000 Hz
9.941	1.409	6.318	9.876	8.533	1.677	7.410	9.026	4.501	7.181	5.155

Table 5
Calculated results of Eq. (18) for the solution with the minimum overall thickness (0.529m)

100 Hz	125 Hz	160 Hz	200 Hz	250 Hz	315 Hz	400 Hz	500 Hz	630 Hz	800 Hz	1000 Hz
0.04	0.001	0.016	0.04	0.028	0	0.023	0.032	0.007	0.018	0.011

acoustic resistance and specific normal acoustic reactance. All results found by the EA agree with this principle. For instance, Table 5 shows the calculated results of Eq. (18) for the solution with the minimum overall thickness as shown in Table 3.

The search results provided by EA as shown in Figs. 3(b) and 4(b) also indicate that a flat-walled multi-layered system should be designed in a fashion that the material with lower flow resistivity should always be arranged in front of the material with higher flow resistivity.

9. Conclusions and future work

Simplicity of production and mounting make the flat-walled, multi-layered anechoic lining an attractive option in the design considerations of anechoic chamber. Previous investigations indicated that a flat-walled, multi-layered anechoic lining system, with an overall thickness slightly less than a quarter of a wavelength, could be used to achieve a required cut-off frequency [1]. However, the work proved to be tedious and time consuming because of the numerous trial-and-error measurements involved. Good agreement between the measured (impedance tube) overall impedance of a flat-walled multi-layered system and calculated values using multi-layered impedance equation and the curve-fitting equations for predicting bulk acoustic properties has been shown in [4], which provides the confidence to conduct the design on a desktop computer.

EAs work on populations of individuals instead of single solutions. In this way the search is performed in a parallel manner. This characteristic makes EAs very attractive for solving MOP. In the present work, an EA is implemented as the optimiser to aid and speed up the design process. The optimisation results indicate that a three-layered lining system can achieve results comparable with quality wedge-type anechoic linings with overall thickness slightly less than a sixth of a wavelength at the 100 Hz cut-off frequency.

Similar work could be carried out for other types of materials or combinations of different types of materials, provided that the models for predicting bulk acoustic properties are available for these materials. The models for predicting bulk acoustic properties are not limited to the regression curve fitting equations. Other models, for

instance, a neural network (NN) model for predicting bulk acoustic properties [23], could also be utilized. An example of combining NN model with EAs can be found in [24].

The model applied in the present work for predicting bulk acoustic properties takes into account only the flow resistivity of the material. Future work needs to investigate the more elaborate models which make use of a combination of material parameters, such as flow resistivity, density, porosity and tortuosity.

Acknowledgements

Authors here are grateful to Dr. John Davy at Commonwealth Scientific and Industrial Research Organisation (CSIRO), Australia for providing the original laboratory measurement results in Davern and Dunn's work [1] and [4] and the valuable comments on the present work. Special thanks also go to Professor Alan Cummings for providing the original laboratory measurement results in the work [7] and the valuable comments. Also thanks to Dr. Hartmut Pohlheim for the valuable technical advice in applying the GEATbx [19]. The current research was conducted under an Australian Postgraduate Award and a School of Architecture, Design Science and Planning Supplementary Scholarship.

References

[1] Davern WA. Flat-walled graded density anechoic lining. In: Proceedings of 10th international congress on acoustics. Sydney; 1980.
[2] Davern WA, Hutchinson J. Polyurethane ether foam wedge for anechoic chamber. Appl Acoust 1971;4(4):287–302.
[3] Beranek LL, Sleeper HP. The design and construction of anechoic sound chambers. J Acoust Soc Am 1946;18(1):140–150.
[4] Dunn IP, Davern WA. Calculation of acoustic impedance of multi-layer absorbers. Appl Acoust 1986;19(5):321–334.
[5] Zwicker C, Kosten C. Sound absorbing materials. Amsterdam: Elsevier; 1949.
[6] International Organization for Standardization. ISO 10534-1:1996 Acoustics – Determination of sound absorption coefficient and impedance in impedance tubes Part 1: Method using standing wave ratio; 1996.
[7] Cummings A, Beadle SP. Acoustic properties of reticulated plastic foams. J Sound Vib 1993;175(1):115–133.
[8] Delany ME, Bazley EN. Acoustical properties of fibrous absorbent materials. Appl Acoust 1970;3(2):105–116.
[9] Fonseca CM, Fleming PJ. An overview of evolutionary algorithms in multiobjective optimization. Evolut Comput 1995;3(1):1–16.
[10] Ben-Tal A. Characterization of Pareto and lexicographic optimal solutions. In: Fandel G, Gal T, editors. Multiple criteria decision making theory and application, vol. 177 of lecture notes in economics and mathematical systems. Berlin: Springer-Verlag; 1980.
[11] Fonseca CM, Fleming PJ. Genetic algorithms for multiobjective optimization: formulation, discussion and generalization. In: Proceedings of the fifth international conference in genetic algorithms. San Mateo, CA: Morgan Kaufmann; 1993.
[12] Fonseca CM, Fleming PJ. Multiobjective optimization and multiple constraint handling with evolutionary algorithms – part I: a unified formulation. IEEE Trans Syst Man Cybernet Part A 1998;28(1):26–37.

[13] Zitzler E, Thiele L, Laumanns M, Fonseca CM, Fonseca VG. Performance Assessment of Multiobjective Optimizers: An Analysis and Review. IEEE Trans Evolut Comput 2003;7(2):117–132.
[14] Fogel DB. An introduction to simulated evolutionary optimization. IEEE Trans Neural Networks: Special Issue on Evolutionary Computation 1994;5(1):3–14.
[15] Baker JE. Reducing bias and inefficiency in the selection algorithm. In: Proceedings of the second international conference on genetic algorithms. New Jersey: Lawrence Erlbaum Hillsdale; 1987.
[16] Muhlenbein H, Schlierkamp-voosen D. Predictive models for the breeder genetic algorithm: I. Continuous parameter optimization. Evolut Comput 1993;1(1):25–49.
[17] MATLAB Reference Guide (Version 6.5 R13). The MathWorks Inc. 2002.
[18] Chipperfield A, Fleming PJ, Pohlheim H, Fonseca CM. Genetic algorithm toolbox for use with Matlab. Technical Report No. 512. Department of Automatic Control and Systems Engineering, University of Sheffield, 1994.
[19] Pohlheim H. Genetic and Evolutionary Algorithm Toolbox for use with Matlab version 3.5 RC1, http://www.geatbx.com/, Berlin, 2004.
[20] Richardson JT, Palmer MR, Leipins G, Hilliard M. Some guidelines for genetic algorithms with penalty functions. In: Proceedings of the third international conference in genetic algorithms. San Mateo, CA: Morgan Kaufmann; 1989.
[21] Steuer RE. Multiple criteria optimization: theory, computation, and application. New York: Wiley; 1986.
[22] Davern WA. A design criterion for sound-absorbent lining of an anechoic chamber. Appl Acoust 1972;5(1):69–71.
[23] Gardner GC, O'Leary ME, Hansen S, Sun JQ. Neural networks for prediction of acoustical properties of polyurethane foams. Appl Acoust 2003;64(2):229–242.
[24] Xu J, Nannariello J, Fricke FR. Predicting and optimising the airborne sound transmission of floor-ceiling constructions using computational intelligence. Appl Acoust 2004;65(7):693–704.

LETTERS TO THE EDITOR

This Letters section is for publishing (a) brief acoustical research or applied acoustical reports, (b) comments on articles or letters previously published in this Journal, and (c) a reply by the article author to criticism by the Letter author in (b). Extensive reports should be submitted as articles, not in a letter series. Letters are peer-reviewed on the same basis as articles, but usually require less review time before acceptance. Letters cannot exceed four printed pages (approximately 3000–4000 words) including figures, tables, references, and a required abstract of about 100 words.

An artificial neural network approach for predicting architectural speech security (L)

Jingfeng Xu
School of Architecture, Design Science and Planning, University of Sydney, NSW 2006, Australia

John S. Bradley and Bradford N. Gover
Institute for Research in Construction, National Research Council, 1200 Montreal Road, Ottawa, Ontario K1A 0R6, Canada

(Received 26 August 2004; revised 6 January 2005; accepted 6 January 2005)

Signal-to-noise type measures have been developed for predicting architectural speech privacy and speech security, which is required to accurately rate the probability of a listener outside a room being able to overhear conversations from within the room. However, these measures may not be ideal for speech security situations. In the present work, an approach that uses the artificial neural networks to directly represent the functional relationship between the octave band (250 Hz–8 kHz) S/N ratios and the speech intelligibility score and security thresholds has been investigated. The artificial neural network approach provides a direct and accurate method for predicting the speech intelligibility score and security thresholds. © *2005 Acoustical Society of America.*
[DOI: 10.1121/1.1862092]

PACS numbers: 43.55.Hy, 43.71.Gv, 43.60.Lq [NX] Pages: 1709–1712

I. INTRODUCTION

Speech security can be described on three different levels. The first level would be when only a very small percentage or none of the overheard words is intelligible. The second level is when no words are intelligible and it is often still possible to recognize the cadence or rhythm of the speech. Finally, the highest level of speech security would be when all speech sounds from the adjacent space are completely inaudible.[1] Speech privacy and speech security have been related to signal-to-noise (S/N) type measures, where the signal is the speech from the adjacent space. The simplest measure is the difference of A-weighted speech and noise levels. More sophisticated measures such as the Articulation Index (AI) (Ref. 2) and its more recent replacement, the Speech Intelligibility Index (SII),[3] are known to be better related to speech intelligibility within rooms. However, Gover and Bradley[3] have shown that SII and AI cannot be used to describe conditions for high levels of speech security which would correspond to acoustical conditions below SII=0, where SII is not defined. The difference in A-weighted levels is not limited in this way but it is much less accurately related to intelligibility scores. A more successful measure is the SII-weighted S/N ratio, which is a weighted sum of one-third-octave-band S/N ratios using the same frequency weightings as the SII measure. Although the SII-weighted S/N ratio predicts the intelligibility score and threshold reasonably well, the S/N loudness ratio provides a more accurate estimation of the thresholds of cadence and audibility.[1]

In the present work, an approach that uses the artificial neural networks (ANNs) to directly represent the functional relationship between the octave band (250 Hz–8 kHz) S/N ratios and the speech intelligibility score and security thresholds has been investigated. The objectives of the ANNs are to predict (a) the speech intelligibility score, namely the percentage of words correctly identified by each individual; (b) the intelligibility threshold, namely the percentage of listeners able to correctly identify at least one word; (c) the ca-

TABLE I. Ranges of input variables.

Input variables	Range of input variables for predicting the intelligibility scores and the intelligibility threshold		Range of input variables for predicting the cadence threshold and the audibility threshold	
	Minimum dB	Maximum dB	Minimum dB	Maximum dB
S/N Ratio at 250 Hz	−34.8	6.2	−34.8	−8.3
S/N Ratio at 500 Hz	−30.2	13.1	−30.2	−2.3
S/N Ratio at 1 kHz	−32.7	1.3	−32.7	−15.7
S/N Ratio at 2 kHz	−28.2	7.1	−28.2	−1.8
S/N Ratio at 4 kHz	−27.4	10.0	−21.8	0.5
S/N Ratio at 8 kHz	−23.2	8.7	−16.6	−6.3

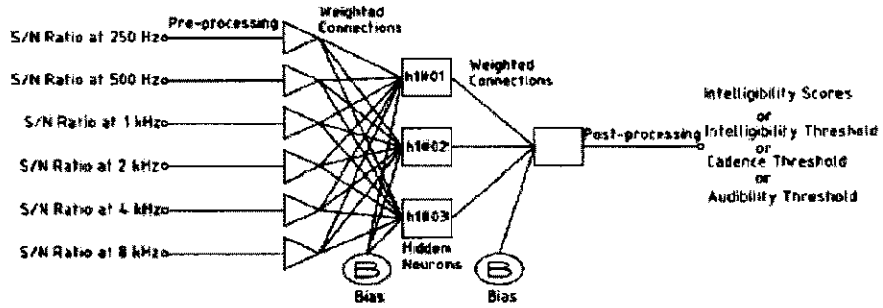

FIG. 1. Illustration of a three-layer feed-forward artificial neural network.

dence threshold, namely the percentage of listeners able to detect the cadence of the speech; and (d) the audibility threshold, namely the percentage of listeners able to hear the presence of the speech.

The ANN approach provides a direct and accurate method for predicting the speech intelligibility score and security thresholds. ANNs are inherently capable of representing nonlinear systems. They learn from historical data and model input–output functional relationships. The history and theory of ANNs, their advantages and shortcomings in applications, and their future utility have been presented elsewhere[4–6] and will not be presented here. A brief overview of how ANNs operate is presented by Nannariello *et al.*[7] and Li *et al.*[8]

II. DATABASE FOR ANN MODELS

Two speech intelligibility and security experiments were carried out by Gover and Bradley[1] at the Institute for Research in Construction (IRC), National Research Council Canada (CNRC). In the first intelligibility experiment (intelligibility scores and the intelligibility threshold), 36 subjects each listened to 340 test sentences. Subjects were then divided into two groups, 19 "better" subjects and 17 "worse" subjects, in accordance with their mean intelligibility scores across all 340 sentences. A follow-up experiment intended to determine not only the intelligibility score and the intelligibility threshold but also the thresholds of cadence of the speech and audibility of any speech sounds. In this second experiment the 19 better subjects from the first experiment each listened to 160 sentences. Details of these two experiments are presented by Gover and Bradley.[1]

The results of 19 better subjects in the above two experiments constitute the database for the ANN models in the present work. The 9500 [19×(340+160)] individual intelligibility score test cases were used as the database for predicting the intelligibility score. Of the 9500 cases, 7600 were used for training, 950 for verification, and 950 for testing. All the sentences in the first and second experiments, *viz.*, 500 (340+160) sentences (cases), were used as the database for predicting the intelligibility threshold. Of the 500 cases, 310 were used for training, 95 for verification, and 95 for testing. For predicting the cadence threshold and the audibility threshold, the 160 sentences (cases) in the second experiment were used as the database. Of the 160 cases, 128 were used for training, 16 for verification, and 16 for testing.

III. INPUTS AND OUTPUTS OF ANN MODELS

The inputs of the ANN models for all four prediction situations are the octave band (250 Hz–8 kHz) S/N ratios, that is to say, the difference in the transmitted speech level and the background noise level at each octave frequency band from 250 Hz to 8 kHz. The range of the input variables for predicting the intelligibility score and the intelligibility threshold when considering both experiments is different from that for predicting the audibility and the cadence thresholds when accounting for only the second experiment. Table I provides the range of each input variable of the four ANN models. The outputs of the ANN models are the intelligibility score, the intelligibility threshold, the cadence threshold, and the audibility threshold, and are within the range of 0%–100%.

TABLE II. Shift and scale factors to inputs of each ANN model.

	ANN model for predicting intelligibility scores		ANN model for predicting intelligibility threshold		ANN model for predicting cadence threshold		ANN model for predicting audibility threshold	
Input variables	Shift	Scale	Shift	Scale	Shift	Scale	Shift	Scale
S/N Ratio at 250 Hz	0.8478	0.0244	0.8561	0.0251	1.3117	0.0377	1.3117	0.0377
S/N Ratio at 500 Hz	0.6984	0.0231	0.6984	0.0231	1.0840	0.0363	1.0953	0.0362
S/N Ratio at 1 kHz	0.9629	0.0295	0.9748	0.0298	1.9676	0.0605	1.9299	0.0590
S/N Ratio at 2 kHz	0.7990	0.0284	0.7990	0.0284	1.1847	0.0421	1.0704	0.0382
S/N Ratio at 4 kHz	0.7333	0.0268	0.7333	0.0268	0.9791	0.0450	1.0969	0.0503
S/N Ratio at 8 kHz	0.7276	0.0314	0.7254	0.0316	1.6072	0.0968	1.6063	0.0966

TABLE III. Weights and biases to hidden neurons of each ANN model.

	ANN model for predicting intelligibility scores			ANN model for predicting intelligibility threshold			ANN model for predicting cadence threshold			ANN model for predicting audibility threshold		
	h1#01	h1#02	h1#03	h1#01	h1#02	h1#03	h1#01	h1#02	h1#03	h1#01	h1#02	h1#03
Bias	11.5184	3.4952	2.4780	4.7585	−1.0361	−3.6038	−1.3096	−3.4213	0.0453	1.6085	−0.0568	0.8694
S/N Ratio at 250 Hz	1.1366	1.4757	0.7391	2.3090	4.7684	−0.5849	−0.6167	−2.5940	0.9785	3.0270	4.2765	−1.6642
S/N Ratio at 500 Hz	10.5723	2.7610	4.5765	2.9866	−0.8594	−4.8108	−0.7203	−1.2851	0.3082	1.9515	2.4088	−1.6567
S/N Ratio at 1 kHz	−0.2854	4.9302	7.2539	3.1024	−2.6401	−9.3399	−1.8440	−0.1070	0.4341	−1.3097	0.1111	1.1948
S/N Ratio at 2 kHz	8.0602	1.3246	1.8921	2.1874	1.4327	−1.4269	1.0129	−4.0315	2.1161	4.1976	1.1180	−1.7192
S/N Ratio at 4 kHz	2.0982	2.0439	−0.0099	2.4986	0.7054	−0.0970	2.5294	−6.9358	2.9931	6.7447	1.3925	−3.6152
S/N Ratio at 8 kHz	1.1966	−1.0482	−2.9519	1.5709	2.3245	−0.1919	−1.8705	3.6446	−0.4777	−3.5032	−0.2028	2.2250

IV. ARCHITECTURE OF ANN MODELS AND PROCEDURES OF ANN ANALYSIS

Figure 1 illustrates the three-layer feed-forward ANN architecture applied in the present work. One hidden neuron layer, with three hidden neurons, was used. The ANN analysis was undertaken using STATISTICA Neural Networks.[9] The weights, which were initialized to uniformly distributed random values using the "uniform method," were adjusted by using "back propagation" and "conjugate gradient" algorithms to minimize the prediction error during the training. Conditions were set within the STATISTICA Neural Networks program by altering the model's parameters. "Early stopping" and "Weigend weight regularization" techniques were used to control overfitting. Training of ANNs was stopped when the rms error of the verification set could no longer be improved. The test set was used to independently check the performance of the network when an entire network design procedure was completed.

V. MODUS OPERANDI OF ANN MODELS

For the present work, the preprocessing of the inputs involves scaling input values to an appropriate range suitable for use in the ANN. Input values are multiplied by a scale factor, followed by the addition of a shift factor. Table II provides the shift and scale factors to input variables of each ANN model. These factors are automatically generated by the scaling algorithm of the STATISTICA Neural Networks.[9]

Each preprocessed neuron is multiplied by a scalar weight connecting the first-layer neurons to the hidden-layer neurons. At each neuron within the hidden layer, the weighted inputs are summed and bias value is subtracted from the summed weighted inputs. The resulting value is passed through a nonlinear activation function, in this work, sigmoidal logistic function $(1/(1+e^{-x}))$, where x is the resulting value). Table III provides the weights and biases linked to hidden neurons of each ANN model attained by training.

The output value of each hidden neuron is multiplied by the scalar weights for each connection between the hidden layer and the output neuron. The weighted outputs are summed and a bias value is subtracted from the sum to produce a single output value. Table IV provides the weights and biases linked to the output neuron of each ANN model attained by training.

The output is postprocessed by subtracting the shift factor, followed by division by the scale factor. In the present work, the shift factor and scale factor are 0 and 1, respectively, in all four situations as the range of outputs has already been normalized between 0 and 1 in the original database.

Work carried out by Nannariello *et al.*[10] and Xu *et al.*[11] presented a method of how to embed an ANN model into a standard spreadsheet. The same procedure can be adopted with those details provided in Table II–Table IV.

VI. RESULTS OF ANN ANALYSIS

Table V presents the statistical analysis results based on the ANN models specified in the above section. In a regression problem, the standard deviations (S.D.) of both the prediction error and original output data are important and they can be related by the S.D. ratio. The S.D. ratio in a regression problem is the ratio of the S.D. of the prediction error to

TABLE IV. Weights and biases to the output neuron of each ANN model.

	ANN model for predicting intelligibility scores	ANN model for predicting intelligibility threshold	ANN model for predicting cadence threshold	ANN model for predicting audibility threshold
	Output (intelligibility scores)	Output (intelligibility threshold)	Output (cadence threshold)	Output (audibility threshold)
Bias	0.0086	−0.6521	−1.5510	−0.9244
h1#01	0.5257	2.2279	−0.0603	2.8098
h1#02	1.5923	−1.8808	−1.2885	−2.7274
h1#03	−1.1333	1.0384	−0.4996	1.1762

TABLE V. Statistic data for ANN prediction results.

	ANN model for predicting intelligibility scores				ANN model for predicting intelligibility threshold				ANN model for predicting cadence threshold				ANN model for predicting audibility threshold			
	Tr[a]	Ve[b]	Te[c]	En[d]	Tr[a]	Ve[b]	Te[c]	En[d]	Tr[a]	Ve[b]	Te[c]	En[d]	Tr[a]	Ve[b]	Te[c]	En[d]
rms error	0.205	0.208	0.208	0.206	0.116	0.098	0.104	0.111	0.079	0.056	0.072	0.076	0.096	0.089	0.033	0.091
Error S.D.[e]	0.205	0.208	0.208	0.206	0.117	0.099	0.105	0.111	0.079	0.049	0.067	0.077	0.096	0.088	0.034	0.091
S.D. ratio[f]	0.477	0.476	0.475	0.476	0.280	0.246	0.244	0.267	0.192	0.115	0.139	0.183	0.254	0.211	0.096	0.240
R^2	0.773	0.773	0.774	0.773	0.921	0.940	0.941	0.929	0.963	0.987	0.982	0.967	0.936	0.958	0.992	0.942

[a]Tr=training set.
[b]Ve=verification set.
[c]Te=test set.
[d]En=entire set.
[e]Error S.D.=standard deviation of the prediction error.
[f]S.D. ratio=standard deviation ratio.

that of the original output data (an S.D. ratio of 0.1 is considered an excellent fit of the data, and an S.D. ratio of 1.0 is a poor fit).[9] The correlation coefficients R^2 (the "coefficient of determination") of the ANN predictions over the entire data sets for the intelligibility scores, intelligibility threshold, cadence threshold, and audibility threshold were 0.773, 0.929, 0.967, and 0.942, respectively. For comparison, in the work of Gover and Bradley,[1] the SII-weighted S/N measure has an R^2 of 0.762 for predicting the intelligibility scores and an R^2 of 0.919 for predicting the intelligibility threshold, and the S/N loudness ratio has an R^2 of 0.956 for predicting the cadence threshold and an R^2 of 0.899 for predicting the audibility threshold.

VII. DISCUSSIONS AND CONCLUSIONS

The present work indicates that the ANN approach provides a direct and accurate method for predicting speech intelligibility scores and security thresholds. The current method for predicting the speech intelligibility and privacy is first to develop a certain index and then relate the index to the subjective scores using a transfer function.[1–3] The ANN approach can use the S/N ratio information to directly predict the subjective speech intelligibility score and security thresholds. Compared with the previous work[1] that used one-third-octave-band S/N ratios, the ANN approach produced comparable, or better in terms of the audibility threshold, prediction results using only the "octave band" S/N ratios.

Specifics of the ANN models for predicting the speech security and intelligibility scores are also provided in the present work. With this information, ANN models can be embedded into standard spreadsheet applications, thus allowing predictions to be made in a transparent and direct fashion.

Similar investigations that use one-third-octave-band (160 Hz–8 kHz) S/N ratios have also been conducted in the present work. However, the results of the one-third-octave-band analysis were only slightly better than those of the octave-band analysis. This may be due to the information in adjacent one-third-octave bands being highly correlated and therefore not contributing any significant new information to the ANN.

The present work only takes into account the S/N ratios in predicting the architectural speech intelligibility score and security thresholds. Other factors, such as talker gender and voice characteristics, speech material, room characteristics, and so on could be included in the ANN models to investigate the possibility of further improving the prediction accuracy.

ACKNOWLEDGMENTS

The authors are grateful to Professor Fergus R. Fricke at the School of Architecture, Design Science and Planning, University of Sydney, Australia, and Dr. Joseph Nannariello at Renzo Tonin & Associates Pty Ltd, Australia for their valuable comments on the present work. The present research was conducted under an Australian Postgraduate Award and a School of Architecture Design Science and Planning Supplementary Scholarship.

[1] B. N. Gover and J. S. Bradley, "Measures for assessing architectural speech security (privacy) of closed offices and meeting rooms," J. Acoust. Soc. Am. **116**, 3480–3490 (2004).
[2] ANSI S3.5-1969, "American National Standard Methods for the Calculation of the Articulation Index" (American National Standards Institute, New York).
[3] ANSI S3.5-1997, "American National Standard Methods for Calculation of the Speech Intelligibility Index" (American National Standards Institute, New York).
[4] J. Hertz, A. Krogh, and R. G. Palmer, *Introduction to the Theory of Neural Computation* (Addison-Wesley, Redwood City, CA, 1991).
[5] A. Browne, *Neural Network Analysis, Architectures and Applications* (Institute of Physics, Philadelphia, 1997).
[6] J. Nannariello, M. R. Osman, and F. R. Fricke, "Recent developments in the application of neural network analysis to architectural and building acoustics," Acoust. Aust. **29**, 103–110 (2001).
[7] J. Nannariello and F. R. Fricke, "Introduction to neural network analysis and its application to building services engineering," Build. Services Eng. Res. Technol. **22**, 58–68 (2001).
[8] F. F. Li and T. J. Cox, "Speech transmission index from running speech: A neural network approach," J. Acoust. Soc. Am. **113**, 1999–2008 (2003).
[9] StatSoft, STATISTICA *Neural Networks version 4.0A manual* (StatSoft Inc, Tulsa, OK, 1999).
[10] J. Nannariello and F. R. Fricke, "A neural-computation method of predicting the early interaural cross-correlation coefficient ($IACC_{E3}$) for auditoria," Appl. Acoust. **64**, 627–641 (2002).
[11] J. Xu, J. Nannariello, and F. R. Fricke, "Predicting and optimising the airborne sound transmission of floor–ceiling constructions using computational intelligence," Appl. Acoust. **65**, 693–704 (2004).

Flat-walled multilayered anechoic linings: Optimization and application

Jingfeng Xu[a)]
School of Architecture, Design Science and Planning, University of Sydney, NSW 2006, Australia

Jörg M. Buchholz
MARCS Auditory Laboratories, University of Western Sydney, Locked Bag 1797, Penrith South DC, NSW 1797, Australia

Fergus R. Fricke
229 Rowntree Street, Balmain, NSW 2041, Australia

(Received 12 June 2005; revised 25 August 2005; accepted 25 August 2005)

The concept of flat-walled multilayered absorbent linings for anechoic rooms was proposed three decades ago. Flat-walled linings have the advantage of being less complicated and, hence, less costly to manufacture and install than the individual units such as wedges. However, there are difficulties in optimizing the design of such absorbent linings. In the present work, the design of a flat-walled multilayered anechoic lining that targeted a 250 Hz cut-off frequency and a 300 mm maximum lining thickness was first optimized using an evolutionary algorithm. Sixteen of the most commonly used commercial fibrous building insulation materials available in Australia were investigated and fourteen design options (i.e., material combinations) were found by the evolutionary algorithm. These options were then evaluated in accordance with their costs and measured acoustic absorption performances. Finally, the completed anechoic room, where the optimized design was applied, was qualified and the results showed that a large percentage (75%–85%) of the distance between the sound source and the room boundaries, on the traverses made, were anechoic. © *2005 Acoustical Society of America*. [DOI: 10.1121/1.2074907]

PACS number(s): 43.55.Pe, 43.55.Ev [NX] Pages: 3104–3109

I. INTRODUCTION

The MARCS Auditory Laboratories at the University of Western Sydney recently decided to construct an anechoic room for its research in the area of speech communication and auditory processes. The internal size of the room is 4500 mm long, 3600 mm wide, and 3500 mm high. The maximum anechoic lining thickness was limited to 300 mm due to the small size of the room and the desired cut-off frequency was 250 Hz. (The cut-off frequency is the frequency above which no pressure reflection factor exceeds 10%; this corresponds to an energy absorption exceeding 99%.) As the budget for the project was limited, the conventional anechoic lining system using individual units such as wedges was not affordable. An alternative anechoic lining system was therefore required.

The concept of flat-walled multilayered absorbent linings for anechoic rooms was proposed three decades ago. Flat-walled linings have the advantage of being less complicated and, hence, less costly to manufacture and install than the individual units such as wedges. Recently, flat-walled multilayered absorbent linings were also applied as the anechoic termination for other types of enclosures, such as the duct-type noise measurement enclosure,[2] which require anechoic conditions for their internal surfaces.

Davern[3] studied experimentally the design of flat-walled multilayered anechoic linings. The approach used was to design a flat-walled lining system by using conventional measurements in an impedance tube. However, the work proved to be tedious and time consuming because of the numerous trial and error measurements involved. The subsequent work undertaken by Dunn and Davern[4] proved that the overall impedance of a flat-walled multilayered system could be calculated by the repeated application of a single layer impedance equation. The inputs to the equation were simply the bulk acoustic properties (characteristic impedance and propagation constant) and the thickness of each layer of material. Xu, Nannariello, and Fricke[5] demonstrated that an evolutionary algorithm (EA) could be successfully employed as an optimizer to aid and speed up the design of flat-walled multilayered anechoic linings. The material investigated in the work was polyurethane open cell foams and the target cut-off frequency was 100 Hz. A further investigation[6] carried out by Xu, Buchholz, and Fricke on the application of multilayered polyurethane foams as the flat-walled anechoic lining indicated that for low (100 Hz) and mid (250 Hz) cut-off frequencies to achieve the minimum overall lining thickness the minimum number of layers of linings required is three. However, the materials used in the optimum designs of the above mentioned two works[5,6] might not be commercially available because the bulk acoustic properties of the materials were calculated using Delany and Bazley[7] type curve-fitting equations developed by Dunn and Davern[4] and Cummings[8] and it was assumed that any required thickness of the material was available. The MARCS Auditory Laboratories was also reluctant to use polyurethane foams for the

a)Electronic mail: jixu4247@mail.usyd.edu.au

anechoic lining material because of the fire hazard and mechanical durability problems related to this type of material so fibrous materials were required.

In the present work, the bulk acoustic properties of sixteen of the most commonly used commercial fibrous building insulation materials available in Australia were measured and on the basis of the measurement results the same evolutionary algorithm as that introduced in previous work[5] was used to optimize the design of the flat-walled multilayered anechoic lining to meet the design criteria, namely a 250 Hz cut-off frequency with a maximum lining thickness of 300 mm. The lining system for the anechoic room at the MARCS Auditory Laboratories was then selected from the design options provided by the EA on the basis of their costs and acoustic absorption performance measured using an impedance tube.[9] Finally, the completed anechoic room, where the optimized design was applied, was qualified and the results showed that a large percentage (75%–85%) of the distance between the sound source and the room boundaries, on the traverses made, were anechoic.

II. FUNDAMENTALS OF FLAT-WALLED MULTILAYERED ANECHOIC LININGS

An ideal acoustic absorbent material should have a low frontal acoustic reflection and a high internal acoustic attenuation. However, these two requirements for the same material are in conflict with each other. A method of partially overcoming this conflict is to use a multilayered lining system.[4] By selecting a front layer material with appropriate characteristic impedance, one can obtain a low primary reflection by encouraging the incoming acoustic wave train to enter the composite layer structure. Then, the inner layers of material can be selected to attenuate the wave energy within the material as much as possible without at the same time causing a substantial interlayer reflection.

Dunn and Davern[4] proved that the surface impedance, Z_i, at the front of a multilayered lining could be calculated by applying the single-layer equation to each material successively, i.e.,

$$Z_i = W_i \frac{Z_{i-1}\cosh(\gamma_i L_i) + W_i \sinh(\gamma_i L_i)}{Z_{i-1}\sinh(\gamma_i L_i) + W_i \cosh(\gamma_i L_i)}, \tag{1}$$

where the subscript i refers to the ith layer, starting from the layer closest to solid backing; L is the thickness of the layer; and W and γ are, respectively, the characteristic impedance and propagation constant of the layer. Both W and γ are complex numbers. When a material is backed by a solid surface ($Z_0=\infty$), the single layer equation can be written as

$$Z_1 = W_1 \coth(\gamma_1 L_1). \tag{2}$$

The pressure reflection factor at normal incidence, r, is the ratio of the pressure amplitude of the reflected wave to the incident wave in the reference plane for a plane wave at normal incidence and can be calculated by[9]

TABLE I. Materials investigated.

Type	Material ID	Fixed thickness (mm)	Density (kg/m^3)	Flow resistivity (Pas/m)
Low-density glasswool	1	50	10.4	3190
Mid-density glasswool	2	25	20.0	11180
	3	25	29.5	12378
	4	25	30.0	13915
High-density glasswool	5	25	108.0	47637
Mid-density polyester	6	25	33.0	6221
	7	25	40.0	7153
Low-density polyester	8	25	10.5	1410
	9	35	7.9	453
	10	65	8.8	535
	11	75	10.8	458
	12	85	10.8	594
	13	90	11.6	659
	14	30	9.6	562
	15	40	8.2	483
	16	50	9.3	663

$$r = \left| \frac{Z_i/\rho c - 1}{Z_i/\rho c + 1} \right|, \tag{3}$$

where ρ is the air density and c is the velocity of sound in air. The relationship between r and the normal incidence sound absorption coefficient α_n[9] is

$$\alpha_n = 1 - r^2. \tag{4}$$

III. MATERIALS INVESTIGATED

As indicated previously sixteen of the most commonly used commercial fibrous building insulation materials available in Australia were investigated in the present work. Measurements of thickness, density, and flow resistivity[10] of each material were made and results of these measurements are presented Table I. The bulk acoustic properties of each material were also measured using a two-thickness method.[11] Generally, the cost for the glasswool type material is higher than the polyester type material.

IV. OPTIMIZATION

Since the pressure reflection factor r of an anechoic lining at any frequency above the cut-off frequency shall not exceed 10%,[1] the design of an anechoic lining can be considered as a multiobjective optimization problem (MOP). The previous work[5] demonstrated that a Genetic and Evolutionary Algorithm Toolbox for use with Matlab (GEATbx)[12] could be successfully employed to tackle this MOP. In the present work, GEATbx was again applied.

A. Application of GEATbx

In the present work the sixteen materials investigated all have their own measured bulk properties and fixed thicknesses and the overall thickness of a material can only be multiples of its fixed thickness, i.e., variables in the present work all have a discrete nature. In order to apply GEATbx,

TABLE II. Optimization results.

Option ID	Material ID of each layer			Multiples of the fixed thickness of each layer's material			Overall thickness of the lining system (mm)	Pressure reflection factor at each midband frequency of one-third-octave bands ranging from 250 Hz to 1 kHz						
	Layer 1	Layer 2	Layer 3	Layer 1	Layer 2	Layer 3		250 Hz	315 Hz	400 Hz	500 Hz	630 Hz	800 Hz	1 kHz
1	4	1	16	4	2	1	250	9.6	7.7	1.7	4.5	0.8	4.6	6.3
2	7	1	15	3	2	2	255	1.3	2.6	6.2	8.4	4.5	1.3	11.6
3	5	2	15	2	4	3	270	8.6	8.4	3.7	1.5	0.7	6.1	8.6
4	2	1	16	5	2	1	275	10.2	10.3	5.1	7.4	4.9	2.6	4.7
5	7	1	16	3	3	1	275	8.1	11.6	8.2	9.1	4.4	3.9	3.2
6	3	1	15	2	3	2	280	7.6	2.6	8.6	10.1	7.5	2.5	10.2
7	4	1	15	2	3	2	280	7.0	3.3	9.1	10.4	7.1	2.3	9.8
8	2	1	15	4	2	2	280	4.2	6.5	6.2	7.0	5.0	0.9	11.8
9	2	1	15	2	3	2	280	8.0	0.8	8.5	10.3	7.9	3.2	10.1
10	7	1	15	2	3	2	280	5.6	5.0	10.3	11.3	6.9	2.1	11.2
11	5	1	15	2	3	2	280	9.9	8.1	4.4	8.1	5.3	6.6	5.3
12	7	1	15	3	2	3	295	5.9	11.7	9.6	2.7	3.6	7.2	11.3
13	5	1	16	2	4	1	300	8.4	10.3	7.8	10.5	6.0	5.2	1.4
14	7	1	16	4	3	1	300	11.0	11.1	6.9	6.5	3.0	5.6	3.3

the bulk properties and fixed thicknesses of the materials were organized into matrices with the index of each column of the matrix, ranging from one to sixteen, representing each material. Another variable required is the integer multiples of the fixed thickness of each material. During the EA searching process, the program would pick up the material of interest by pointing at the corresponding column of the matrix and vary the overall thickness of the material by assigning a certain integer multiple.

B. Optimization results

In the present work, a three-layered lining system was investigated because of its high efficacy compared with a two-layered lining system.[6] Taking into account the expected errors resulting from Eq. (1) and the measurements of the materials' bulk properties, it was considered that a reflection factor of no larger than 12 was acceptable during the EA search. It was also considered that frequencies below 1000 Hz were the most critical ones in the design of anechoic linings and thus the EA search was limited to one-third-octave band frequencies between 250 and 1000 Hz. Table II shows the optimization results provided by GEATbx.

Using the sixteen materials investigated, the program found fourteen options (i.e., material combinations) that could achieve a 250 Hz cut-off frequency with an overall thickness of the lining system no larger than 300 mm. Among the fourteen options, Options 2 and 12 are the cheapest because the least amount of glasswool material was required. The only difference between Options 2 and 12 was that Option 12 uses 40 mm more of Material 15 for Layer 3 than Option 2 does. The absorption performances of Options 2 and 12, in terms of the pressure reflection factor, were measured using an impedance tube.[9] The measurement results are plotted in Fig. 1. The difference between the measured pressure reflection factors presented in Fig. 1 and predicted ones shown in Table II appears to be due to the errors associated with Eq. (1) and the measurement of bulk properties of the single layer of materials. Since the measured pressure reflection factors of Option 2 at frequencies of 250 and 315 Hz are larger than 12, it was decided to apply Option 12 as the lining system for the anechoic room at the MARCS Auditory Laboratories.

V. INSTALLATION OF THE LINING

Layers of insulation materials were attached to each other and the internal surfaces of the room using spikes affixed to the internal surfaces of the room. Care was taken to eliminate air cavities between the layers of insulation materials and between the internal surfaces of the room and the most inner layer of insulation material.

At the joints where two sheets of the same layer of material meet each other large gaps were avoided by placing them tightly against each other. The joints at different layers were staggered to ensure that they did not overlap. Also, at corners of the room, multilayers of insulation materials were staggered to ensure that their edges overlapped. Figure 2 provides an illustration of the arrangement of multilayered

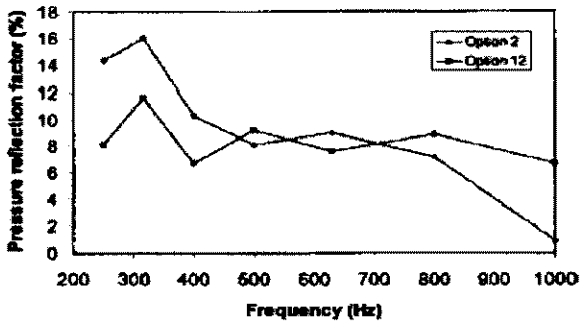

FIG. 1. Impedance tube measurement results of Option 2 and Option 12.

FIG. 2. Installation arrangements of multilayered materials.

materials. For the layer that is exposed to the air the adjoining sheets of material were loosely sewed together.

VI. QUALIFICATION OF THE ANECHOIC ROOM

The completed anechoic room was qualified in accordance with the procedure set out in ISO 3745:2003.[13] The sound source was located so that the assumed position of its acoustic center was at the geometric center of the room. Five straight microphone traverses were used. Four of the five traverses were from the geometric center of the room to the room corners (the lower Southeast, lower Southwest, upper Northeast, and upper Northwest corners) and lay in an imaginary plane that passed through the geometric center of the room. The fifth traverse was from the geometric center of the room to the West wall, which is one of the parallel walls closest to the geometric center of the room. One-third-octave band-filtered pink noise with the sequential mid-band frequencies from 250 Hz to 10 kHz was used as the test signal. The test signal was generated and digitally filtered[14] using Matlab.[15] For the five traverses, the measurement of the sound pressure level was carried out starting 0.5 m from the geometric center of the room and extending to the maximum distance that the measurement microphone could reach. The spacing between the measurement points was 0.1 m.

A. Sound sources

For the qualification of the room the directionality of the sound source must be uniform to within the allowable deviations as set out in ISO 3745:2003.[13] These limits are reproduced in Table III. For the mid-band frequencies below 800 Hz, a Bruel & Kjaer Type 4296 OmniPower Loudspeaker, which meets the requirements of ISO 140-3,[16,17] was used as the sound source.[13] For the higher frequency bands from 800 Hz to 10 kHz, a compression driver (TOA Electric TU-50) attached to a 1.5m-long and 6-mm-i.d. cylindrical tube was used as the sound source. The compression driver was acoustically shielded by a box wrapped with mass loaded vinyl material. As there was no directionality information for the custom-made high frequency sound source, its directionality was measured in accordance with the procedure set out in ISO 3745:2003.[13] The measurement was conducted in an anechoic room, with a 50 Hz cut-off frequency,[18] at the Australian National Acoustic Laboratories. Figure 3 shows the measured deviations in directionality of the custom-made high frequency sound source.

TABLE III. Maximum allowable deviation in directionality of the sound source for an anechoic room qualification as per ISO 3745:2003 (Ref. 13).

One-third-octave band frequency (Hz)	Allowable deviations in directionality (dB)
800–5000	±2.0
6300–10 000	±2.5

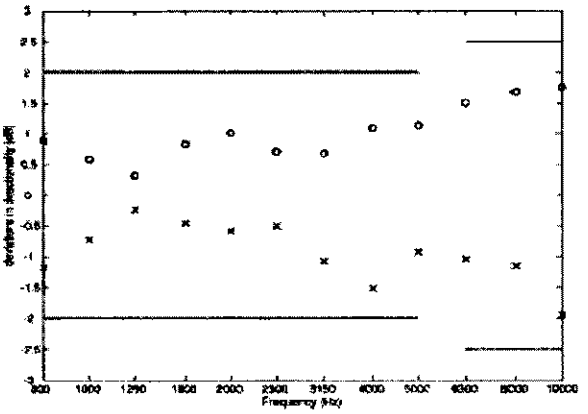

FIG. 3. Measured deviations in directionality for the custom-made high frequency sound source.

During the measurements a reference microphone was located at an arbitrary but fixed position in the room to check the variation of the sound source output. The drift of the sound power level of the sound sources (with the associated signal generation and amplification system) in any one-third-octave band, from 250 to 630 Hz for the low frequency sound source and from 800 Hz to 10 kHz for the high frequency sound source, was less than ±0.2 dB at any time during the measurement.

B. Qualification results

The maximum allowable deviation of the measured sound pressure levels from the theoretical levels, using the inverse square law as per ISO 3745:2003,[13] is reproduced in Table IV. Figure 4 shows the measured deviations for the traverse into the lower Southeast corner of the room. Similar results can be observed for the traverses into other corners. Figure 5 shows the measured deviations for the traverse into the West wall of the room.

VII. CONCLUSIONS

In the present work an EA was successfully applied to optimize the design of a flat-walled multilayered lining system for the anechoic room at MARCS Auditory Laboratories at the University of Western Sydney. Results of the EA search indicated that for the sixteen materials investigated

TABLE IV. Maximum allowable deviation of measured sound pressure levels from the theoretical level using the inverse square law in an anechoic room as per ISO 3745:2003 (Ref. 13).

One-third-octave band frequency (Hz)	Allowable deviations (dB)
≤630	±1.5
800–5000	±1.0
≥6300	±1.5

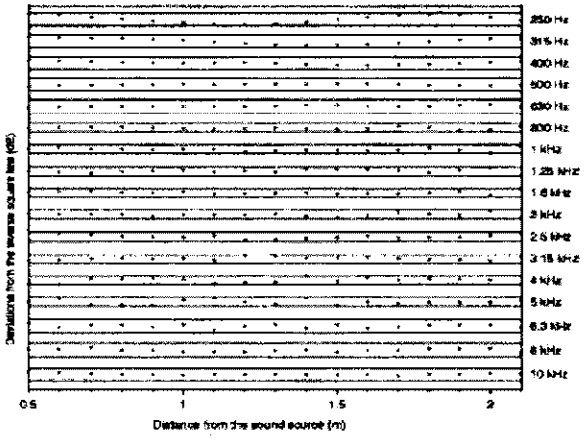

FIG. 4. Measured deviations for the traverse into the lower Southeast corner of the room. The frequency labels along the right vertical axis define the position of the 0-dB deviation for that frequency; the lines above and below the 0-dB position are the permissible variations from free-field performance in accordance with Table IV.

there were fourteen options that could achieve a cut-off frequency of 250 Hz with the overall lining thickness less than 300 mm. For all of the options the materials in the lining system exhibit a trend of a graduated increase of density and flow resistivity from the front layer (Layer 3) to the back layer (Layer 1).

The options found by EA were evaluated on the basis of their costs and two options were short listed. The acoustic absorption performances of the short-listed options were then measured in an impedance tube. Only slight differences were observed between the measured acoustic absorption performances and the predicted ones. The option that had the lower

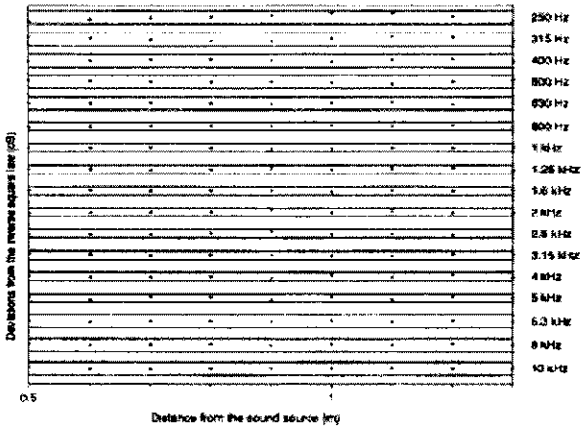

FIG. 5. Measured deviations for the traverse into the West wall of the room. The frequency labels along the right vertical axis define the position of the 0-dB deviation for that frequency; the lines above and below the 0-dB position are the permissible variations from free-field performance in accordance with Table IV.

pressure reflection factors at low frequencies was used as the lining system for the anechoic room at the MARCS Auditory Laboratories.

The lining system finally used in the anechoic room has an overall thickness of 295 mm, which is about 45 mm less than a quarter of a wavelength at the cut-off frequency of 250 Hz. The material cost of the applied lining system was about fifty Australian dollars per square meter. The qualification procedure carried out in the completed anechoic room indicates that

(1) A minimum anechoic distance of 2.1 m is achieved for the traverses to the four corners that are on an imaginary plane passing the geometric center of the room. This approximately corresponds to 75% of half of the diagonal distance (without taking into account the anechoic lining thickness) of the imaginary plane.
(2) A minimum anechoic distance of 1.3 m is achieved for the traverse to one of the walls closest to the geometric center of the room. This approximately corresponds to 85% of half of the distance (without taking into account the anechoic lining thickness) between the two parallel walls closest to the geometric center of the room.

ACKNOWLEDGMENTS

The authors are grateful to John Bassett, Rick Moss, and Ken Stewart at the University of Sydney for their technical support and assistance throughout the present work. The present research was conducted under an Australian Postgraduate Award and a School of Architecture Design Science and Planning Supplementary Scholarship.

[1]L. L. Beranek and H. P Sleeper, "The design and construction of anechoic sound chambers," J. Acoust. Soc. Am. 18, 140–150 (1946).
[2]A. Bracciali and G. Cascini, "Measurement of the lateral noise emission of an UIC 60 rail with a custom device," J. Sound Vib. 231, 653–665 (2000).
[3]W. A. Davern, "Flat-walled graded density anechoic lining," Tenth International Congress on Acoustics, Sydney, 1980.
[4]I. P. Dunn and W. A. Davern, "Calculation of acoustic impedance of multi-layer absorbers," Appl. Acoust. 19, 321–334 (1986).
[5]J. Xu, J. Nannariello, and F. R. Fricke, "Optimising flat-walled multilayered anechoic linings using evolutionary algorithms," Appl. Acoust. 165, 1009–1026 (2004).
[6]J. Xu, J. Buchholz, and F. R. Fricke, "Application of multi-layered polyurethane foams for flatwalled anechoic linings," Appl. Acoust. (in press).
[7]M. E. Delany and E. N. Bazley, "Acoustical properties of fibrous absorbent materials," Appl. Acoust. 3, 105–116 (1970).
[8]A. Cummings and S. P. Beadle, "Acoustic properties of reticulated plastic foams," J. Sound Vib. 175, 115–133(1993).
[9]ISO, ISO 10534-1:1996, "Acoustics—Determination of sound absorption coefficient and impedance in impedance tubes Part 1: Method using standing wave ratio," International Organization for Standardization, Geneva, 1996.
[10]ASTM, ASTM C522-03, "Standard test method for airflow resistance of acoustical materials," American Society for Testing and Materials, Philadelphia, 2003.
[11]C. D. Smith and T. L. Parrott, "Comparison of three methods for measuring acoustic properties of bulk materials," J. Acoust. Soc. Am. 74, 1577–1582 (1983).
[12]H. Pohlheim, "Genetic and evolutionary algorithm toolbox for use with matlab version 3.5," http://www.geatbx.com/, Berlin, 2004.
[13]ISO, ISO 3745:2003, "Acoustics—Determination of sound power levels of noise sources using sound pressure—Precision methods for anechoic and semi-anechoic rooms," International Organization for Standardization, Geneva, Switzerland, 2003.
[14]IEC, IEC 1260:1995, "Electroacoustics: Octave band and fractional-

octave band filters," International Electrotechnical Commission, Geneva, Switzerland, 1995.
[15]MathWorks, "MATLAB reference guide (Version 6.5 R13)," The MathWorks Inc, Natick, MA, 2002.
[16]ISO, ISO 140-3:1995(E), "Acoustics—Measurement of sound insulation in buildings and of building elements—Part 3: Laboratory measurements of airborne sound insulation of building elements," International Organization for Standardization, Geneva, Switzerland, 2003.
[17]Bruel & Kjaer, "Product data—Sound sources for building acoustics: Omnipower sound source-type 4269, Omnisource sound source—Type 4295, tapping machine—Type 3207, including power amplifier—Type 2716", http://www.bksv.com/, Nerum, Denmark, 2005.
[18]Australian National Acoustic Laboratories, "Research and development annual report 2002/2003," Australian National Acoustic Laboratories, Sydney, 2003, pp. 50–51.

Available online at www.sciencedirect.com
SCIENCE DIRECT®
Applied Acoustics 67 (2006) 476–485
applied acoustics
www.elsevier.com/locate/apacoust

Technical note

Application of multi-layered polyurethane foams for flat-walled anechoic linings

Jingfeng Xu [a,*], Jörg M. Buchholz [b], Fergus R. Fricke [a]

[a] *School of Architecture, Design Science and Planning, University of Sydney, NSW 2006, Australia*
[b] *MARCS Auditory Laboratories, University of Western Sydney, Locked Bag 1797, Penrith South DC, NSW 1797, Australia*

Received 9 May 2005; received in revised form 17 August 2005; accepted 18 August 2005
Available online 3 October 2005

Abstract

Previous work demonstrated that a multi-objective evolutionary algorithm could be successfully employed as an optimiser to make the design of flat-walled multi-layered anechoic linings more efficient. In the present work, such an algorithm is employed to investigate the practical aspects of the application of multi-layered polyurethane foams as the flat-walled anechoic lining. The investigation includes aspects such as the efficacy of a single layer of material, the minimum number of layers of linings to achieve the minimum overall thickness for low (100 Hz), mid (250 Hz) and high (500 Hz) cut-off frequencies, the use of the three-layered lining composite for low to mid cut-off frequencies and the effect of air gaps.

Keywords: Flat-walled multi-layered anechoic linings; Polyurethane foams; Evolutionary algorithms; Anechoic termination

1. Introduction

The concept of flat-walled multi-layered absorbent linings for anechoic rooms was proposed three decades ago. With the advantage of being less complicated and, hence, less costly to manufacture and install than the individual units such as wedges, it is an alter-

* Corresponding author. Tel.: +61 2 9351 5265; fax: +61 2 9351 3031.
E-mail address: jixu4247@mail.usyd.edu.au (J. Xu).

0003-682X/$ - see front matter © 2005 Elsevier Ltd. All rights reserved.
doi:10.1016/j.apacoust.2005.08.002

native to the more conventional wedge-type system. Davern [1] studied experimentally the design of flat-walled multi-layered anechoic linings. The approach used was to design a flat-walled lining composite by using conventional measurements in an impedance tube. However, the work proved to be tedious and time consuming because of the numerous trial and error measurements involved. The subsequent work undertaken by Dunn and Davern [2] proved that the overall impedance of a flat-walled multi-layered lining composite could be calculated by the repeated application of a single layer impedance equation.

On the basis of the above work [2], Xu et al. [3] demonstrated that a multi-objective evolutionary algorithm, Genetic and Evolutionary Algorithm Toolbox for use with Matlab (GEATbx) [4], could be successfully employed as an optimiser to make the design of flat-walled multi-layered anechoic linings more efficient. Their optimisation results showed that to achieve a 100 Hz cut-off frequency (cut-off frequency is the frequency above which no pressure reflection exceeds 10%; this corresponds to an energy absorption exceeding 99% [5].) a three-layered lining system composed of polyurethane foams only requires an overall thickness of 0.529 m, which is comparable to the thickness required for quality wedge-type anechoic linings to achieve the same cut-off frequency.

In the present work, such an algorithm is employed to investigate the practical aspects of the application of multi-layered polyurethane foams as the flat-walled anechoic lining. The investigation includes aspects such as the efficacy of a single layer of material, the minimum number of layers of linings to achieve the minimum overall thickness for low (100 Hz), mid (250 Hz) and high (500 Hz) cut-off frequencies, the use of the three-layered lining composite for low to mid cut-off frequencies and the effect of air gaps.

The fundamental theories and equations for calculating the impedance of a multi-layered lining composite have been covered in [2,3] and the advantages and basics of using a multi-objective evolutionary algorithm for the optimisation of flat-walled multi-layered anechoic linings, such as defining the objective functions, setting the design parameters and handling the constraints, and the application of GEATbx, such as setting the values of its parameters, have been discussed in detail in the previous work [3], therefore they are not repeated in the present work.

2. Material investigated

The material investigated in this work is fully reticulated (viz. open cell) polyurethane plastic foams. Cummings [6] studied 12 foams with steady flow resistivity σ in the range of 60–6229 MKS rayl/m and reported the curve-fitting equations for predicting the characteristic impedance W and the propagation constant γ of this type of material as follows:

$$W = \rho c\left[1 + 0.0953(\rho f/\sigma)^{-0.491} + \mathrm{j}\left(-0.0986(\rho f/\sigma)^{-0.665}\right)\right], \tag{1}$$

$$\gamma = (2\pi f/c)\left[0.167(\rho f/\sigma)^{-0.636} + \mathrm{j}\left(1 + 0.174(\rho f/\sigma)^{-0.372}\right)\right], \tag{2}$$

where ρ is the air density and c is the velocity of sound in air (throughout the present work a value of 1.2 kg/m^3 is used for air density and 340 m/s for sound velocity) and f is the frequency. The lowest valid frequency for Eqs. (1) and (2) is 100 Hz. Eqs. (1) and (2) indicate that a large flow resistivity value will result in large attenuation, but, at the same time, it will cause a high frontal reflection. A method of partially overcoming this conflict is to use a multi-layered lining composite. By selecting a front layer material with appropriate characteristic impedance, one can obtain a low primary reflection by encouraging the

incoming wave train to enter the composite layer structure. Then the inner layers of material can be selected to attenuate the wave energy within the material as much as possible without at the same time causing a substantial interlayer reflection.

3. Results

Since the pressure reflection factor of an anechoic lining at any frequency above the cut-off frequency shall not exceed 10% [5], the design of an anechoic lining can be considered as a multi-objective optimisation problem (MOP) [3]. In the present work, GEATbx is applied as the multi-objective optimisation tool to investigate the practical aspects of the application of multi-layered polyurethane foams as the flat-walled anechoic lining. Throughout the present study, pressure reflection factors are considered in one-third-octave bands at centre frequencies between 100 and 1000 Hz inclusive since the lowest valid frequency for Eqs. (1) and (2) is 100 Hz and it is assumed that frequencies below 1000 Hz are the most critical ones in the design of anechoic linings. During the search of the optimum result, the flow resistivity of each individual layer of material was varied freely between 60 and 6229 MKS rayl/m and it was assumed that any required thickness of each individual layer of material was available.

3.1. Single layer

First, the performance of a single layer of material for cut-off frequencies between 100 and 500 Hz is investigated. Fig. 1 shows the minimum thickness of a single layer of material as a function of the cut-off frequency. Fig. 2 shows the required flow resistivity of the single layer of material, which has the minimum overall thickness for the corresponding cut-off frequency. Fig. 2 indicates that with the decrease of the cut-off frequency from 500 to 100 Hz the required flow resistivity of a single layer of material is reduced from 1400 to 280 MKS rayl/m and there is a nearly linear relationship, between the cut-off frequency and required flow resistivity of the single layer of material, which can be approximately expressed as

$$\sigma = 2.82 \times f_c - 7.82, \tag{3}$$

where f_c is the cut-off frequency ranged from 100 to 500 Hz. Fig. 1 indicates that with the decrease of the cut-off frequency from 500 to 100 Hz the minimum thickness for a single

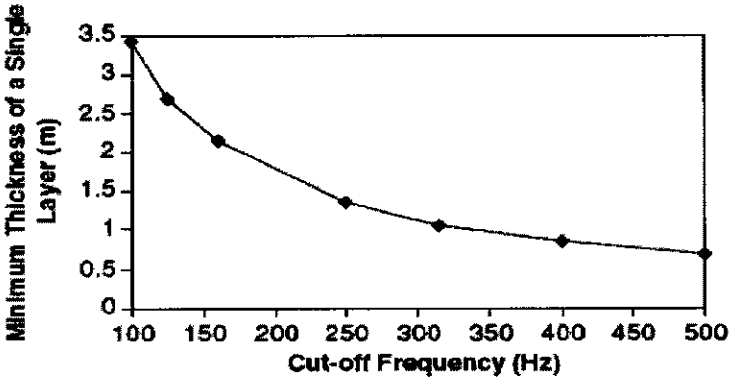

Fig. 1. The minimum thickness of a single layer of material as a function of the cut-off frequency.

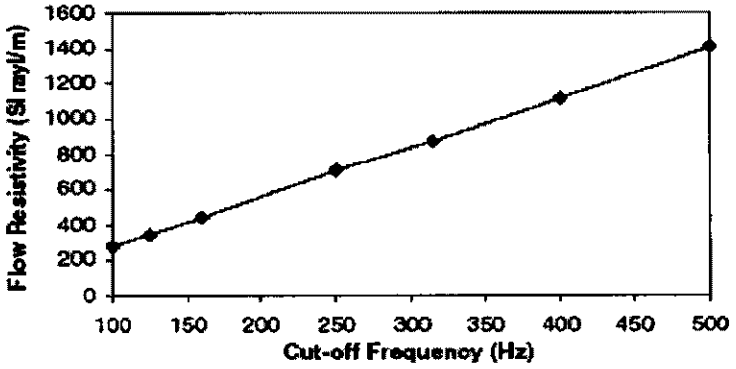

Fig. 2. The flow resistivity of the single layer of material, which has the minimum thickness for achieving the corresponding cut-off frequency, as a function of the cut-off frequency.

layer of material is substantially increased and to achieve the required cut-off frequency the minimum thickness of the single layer material needs to be equivalent to the wavelength at the corresponding cut-off frequency. Hence, it is not effective to use just a single layer of material as the flat-walled anechoic lining.

3.2. Number of layers

As discussed previously, employing multi-layers of material can partially overcome the reflection versus attenuation conflict and make the use of flat-walled anechoic linings more attractive. Thus, in the design of the flat-walled multi-layered anechoic lining it is important to determine for a certain cut-off frequency the minimum number of layers of linings to achieve the minimum overall thickness.

The dependency of the minimum overall thickness on the number of layers is investigated for three cut-off frequencies, 100, 250 and 500 Hz. The results of this investigation are shown in Fig. 3. These results indicate that

(a) For low (100 Hz) and mid (250 Hz) cut-off frequencies, a two-layered composite is still not effective to overcome the reflection versus attenuation conflict. However, the minimum overall thickness can be significantly reduced by employing a

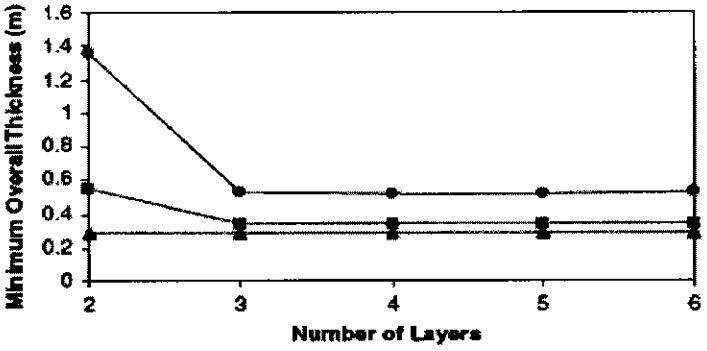

Fig. 3. The minimum overall thickness as a function of the number of layers. —●—, 100 Hz cut-off; —■—, 250 Hz cut-off; —▲—, 500 Hz cut-off.

three-layered composite in lieu of a two-layered one. The effect is more pronounced for the low cut-off frequency. An increase in the number of layers from three to six cannot further reduce the minimum overall thickness of the multi-layered lining composite. Therefore, for low and mid cut-off frequencies, the minimum number of layers of linings to achieve the minimum overall thickness is three.

(b) For high (500 Hz) cut-off frequency, the minimum number of layers of linings to achieve the minimum overall thickness is two as the minimum overall thickness cannot be further reduced by increasing the number of layers from two to six.

3.3. Three-layered lining composite

In most practical situations the cut-off frequency of an anechoic lining will be required to be no more than 250 Hz. Therefore, a three-layered lining composite will be of most interest. Fig. 4 shows the minimum overall thickness of a three-layered lining composite

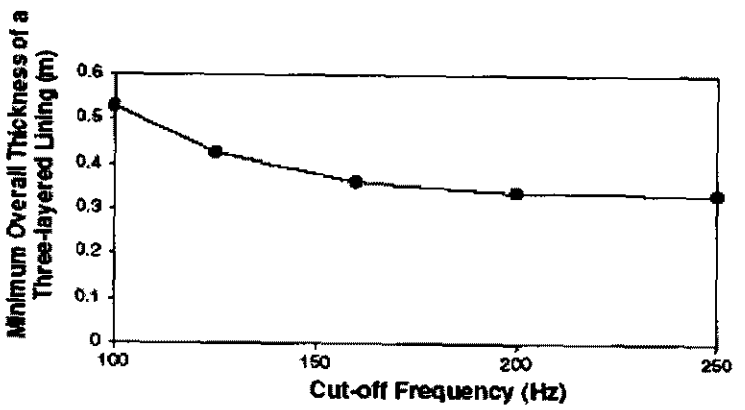

Fig. 4. The minimum overall thickness of a three-layered lining composite as a function of the cut-off frequency.

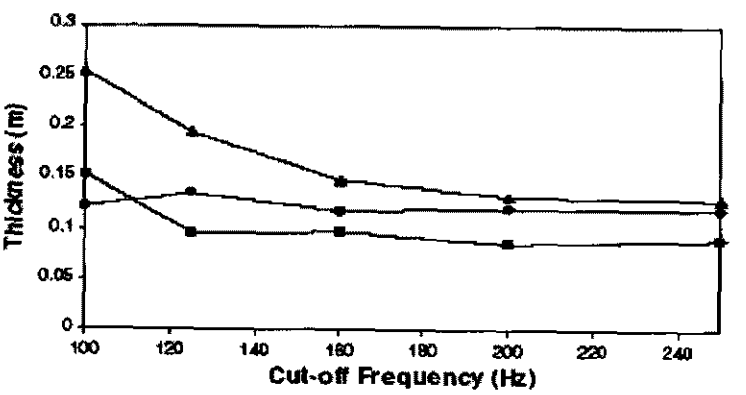

Fig. 5. The thickness of each individual layer of the three-layered lining composite, which has the minimum overall thickness for achieving the corresponding cut-off frequency, as a function of the cut-off frequency. Back layer is the layer that has the solid backing; front layer is the layer that faces the air; and mid layer is the layer in between the back layer and the front layer. —●—, back layer; —■—, mid layer; —▲—, front layer.

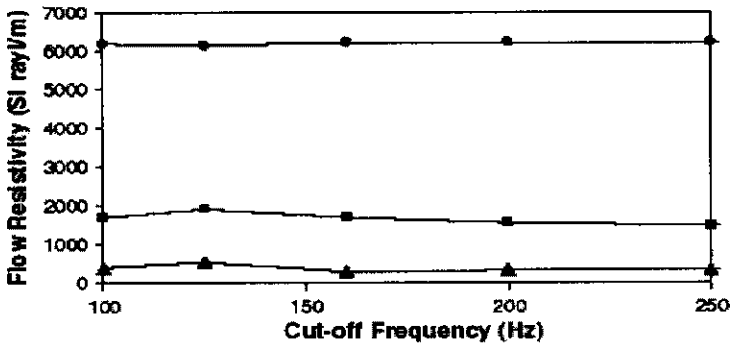

Fig. 6. The flow resistivity of each individual layer of the three-layered lining composite, which has the minimum overall thickness for achieving the corresponding cut-off frequency, as a function of the cut-off frequency. Back layer is the layer that has the solid backing; front layer is the layer that faces the air; and mid layer is the layer in between the back layer and the front layer. —●—, back layer; —■—, mid layer; —▲—, front layer.

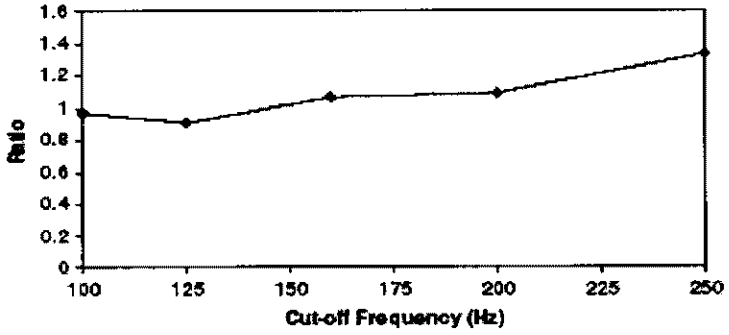

Fig. 7. Ratio of the minimum overall thickness of the three-layered lining composite to the average quarter wavelength in the composite as a function of the cut-off frequency.

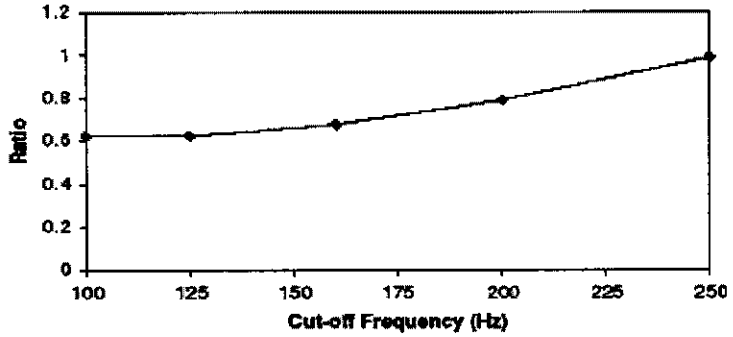

Fig. 8. Ratio of the minimum overall thickness of the three-layered lining composite to the quarter wavelength in the air as a function of the cut-off frequency.

as a function of the cut-off frequency. Figs. 5 and 6, respectively show the required thickness and flow resistivity of each individual layer of the three-layered lining composite, which has the minimum overall thickness for the corresponding cut-off frequency.

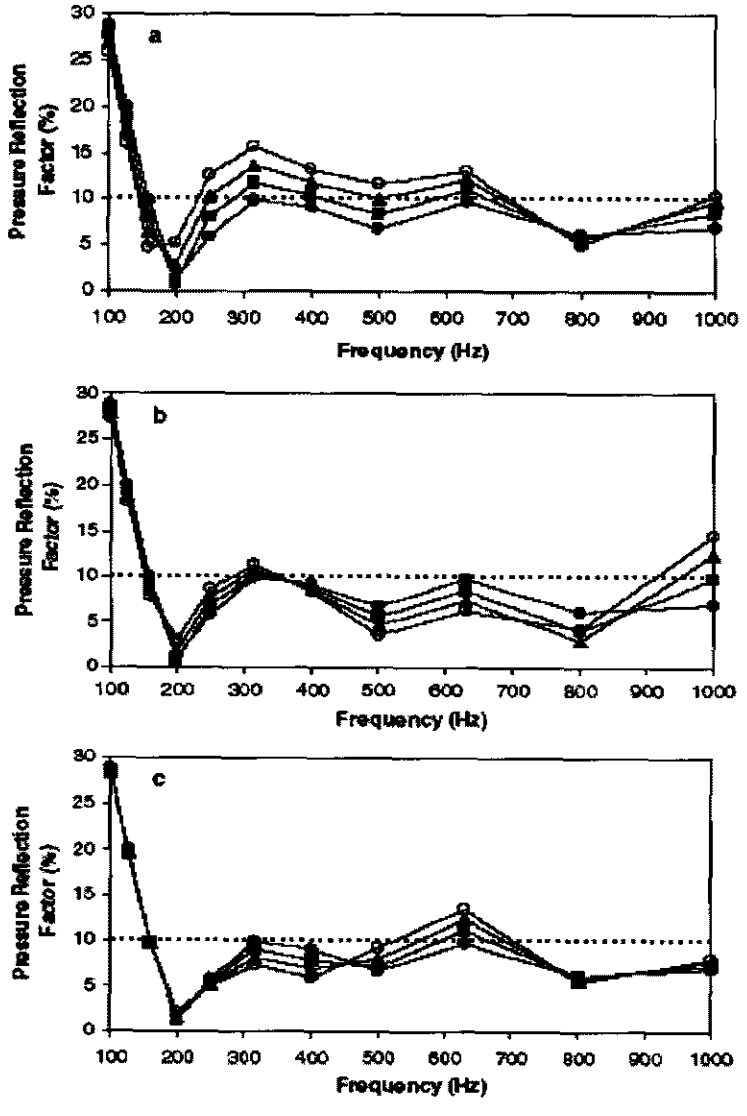

Fig. 9. Effect of air gaps, ranged from 0 to 0.03 m, on the pressure reflection factors of the three layered lining composite with the minimum overall thickness for achieving a cut-off frequency of 160 Hz. Back layer is the layer that has the solid backing; front layer is the layer that faces the air; and mid layer is the layer in between the back layer and the front layer. (a) If there is an air gap between the solid back wall and the lining composite. (b) If there is an air gap between the back layer and the mid layer of the lining composite. (c) If there is an air gap between the mid layer and the front layer of the lining composite. (d) If there are air gaps between the back layer and the mid layer and between the mid layer and the front layer of the lining composite. (e) If there are air gaps between the back solid wall and the back layer, between the back layer and the mid layer and between the mid layer and the front layer of the lining composite. —●—, 0 m for each air gap; —■—, 0.01 m for each air gap; —▲—, 0.02 m for each air gap; —○—, 0.03 m for each air gap; -------, 10% pressure reflection factor line.

Fig. 7 shows the ratio of the minimum overall thickness of the three-layered lining composite to the average quarter wavelength in the composite as a function of the cut-off frequency. Appendix A explains how the average quarter wavelength in the composite is calculated in the present work. Fig. 8 shows the ratio of the minimum overall thickness of the three-layered lining composite to the quarter wavelength in the air as a function of the cut-off frequency.

From Figs. 4–8 one can observe the following:

(a) The minimum overall thickness of the three-layered lining composite is close to the average quarter wavelength in the composite for cut-off frequencies between 100 and 200 Hz. It is getting closer to the quarter wavelength in the air with the increase of cut-off frequency from 200 to 250 Hz.
(b) For the three-layered lining composite the material with low flow resistivity should be placed in front of the material with high flow resistivity.
(c) For the material investigated to achieve a cut-off frequency between 100 and 250 Hz, the required flow resistivity for each layer of material in the three-layered lining composite basically do not vary with the cut-off frequency. The average flow resistivity for the front layer of material is 400 MKS rayl/m, which is close to the characteristic impedance of the air and the average flow resistivities for the mid layer and back layer are 1700 and 6200 MKS rayl/m, respectively.

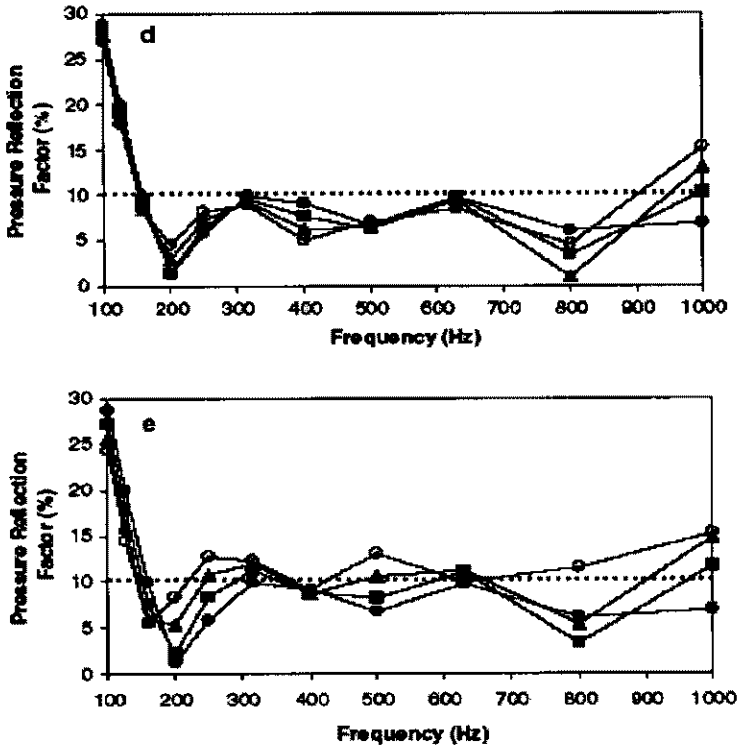

Fig. 9 (*continued*)

(d) The required thickness of the back layer basically does not vary with the cut-off frequency and is around 0.125 m. The thicknesses of the front layer and the mid layer have to be increased to achieve the decreased cut-off frequency.

3.4. Effect of air gaps

In a practical situation, when the flat-walled multi-layered lining is not installed properly there may exist air gaps between the lining and the solid back wall and between layers of lining material. Fig. 9 shows how the air gaps, ranged from 0 to 0.03 m, affect the pressure reflection factors of the three-layered lining composite with the minimum overall thickness for achieving a cut-off frequency of 160 Hz. It indicates that with the presence of the air gaps the pressure reflection factors at certain frequencies may exceed the requirement for an anechoic lining (10%) by up to 6% although they may also be reduced at some other frequencies especially at the frequencies lower than the cut-off frequencies. Similar effect of air gaps on the optimum lining composites for other cut-off frequencies can be observed.

4. Conclusions

The use of multi-layered polyurethane foams for flat-walled anechoic linings has been investigated in detail in the present study. The major findings of the investigation are: (1) a single layer of material is not as effective as a multi-layered lining composite; (2) for low (100 Hz) and mid (250 Hz) cut-off frequencies the minimum number of layers of linings to achieve the minimum overall thickness is three and for high (500 Hz) cut-off frequency the minimum number of layers of linings to achieve the minimum overall thickness is two; (3) for the material investigated in the present work and for cut-off frequencies between 100 and 250 Hz inclusive, using a three-layered anechoic lining composite the achievable minimum overall thickness is between a quarter wavelength in the lining composite and a quarter wavelength in the air for the corresponding cut-off frequency; (4) for the material investigated to achieve a cut-off frequency between 100 and 250 Hz, the required flow resistivity for each individual layer of material in the three-layered lining composite basically do not vary with the cut-off frequency. The average flow resistivity for the front layer of material is 400 MKS rayl/m, which is close to the characteristic impedance of the air and the average flow resistivities for the mid layer and back layer are 1700 and 6200 MKS rayl/m, respectively; (5) for the three-layered lining composite, the required thickness of the back layer basically does not vary with the cut-off frequency and is around 0.125 m. The thicknesses of the front layer and the mid layer have to be increased to achieve the decreased cut-off frequency; (6) to achieve the designed performance of the lining composite air gaps should be avoided.

The above findings are also applicable in the design of flat-walled multi-layered absorbent linings as the anechoic termination for other types of enclosures, such as the duct-type noise measurement enclosure [7], which require anechoic condition for their internal surfaces.

Similar work could be carried out for other types of materials or combinations of different types of materials provided that the bulk acoustic properties of the relevant materials can be measured or predicted. The empirical equations [6] applied in the present work

for predicting bulk acoustic properties take into account only the flow resistivity of the material. Future work needs to investigate the more elaborate models which make use of a combination of material parameters, such as flow resistivity, density, porosity and tortuosity.

Acknowledgements

Authors here are grateful to Professor Alan Cummings for providing the original laboratory measurement results in the work [6]. The present research was conducted under an Australian Postgraduate Award and a School of Architecture Design Science and Planning Supplementary Scholarship.

Appendix A. Average quarter wavelength in an *N*-layered lining composite

Assuming the material investigated in the present work is homogeneous, the average quarter wavelength λ_a at frequency f in an N-layered lining composite is calculated using the following equation:

$$\lambda_a = \frac{\sum_{i=1}^{N} L_i}{4f\sum_{i=1}^{N} \frac{L_i}{v_i}}, \tag{4}$$

where the subscript i refers to the ith layer; L is the thickness of each layer of material; and v is the acoustic wave velocity in each layer of material and can be calculated by the following equation [2]:

$$\beta = \frac{2\pi f}{v}, \tag{5}$$

where β is the wave number which is the imaginary component of the propagation constant γ. For the polyurethane foams investigated in the present work, β is equal to the imaginary part of Eq. (2).

References

[1] Davern WA. Flat-walled graded density anechoic lining. In: Proceedings of 10th international congress on acoustics, Sydney; 1980.
[2] Dunn IP, Davern WA. Calculation of acoustic impedance of multi-layer absorbers. Appl Acoust 1986;19(5):321–34.
[3] Xu J, Nannariello J, Fricke FR. Optimising flat-walled multi-layered anechoic linings using evolutionary algorithms. Appl Acoust 2004;165(11):1009–26.
[4] Pohlheim H. Genetic and evolutionary algorithm toolbox for use with matlab version 3.5. Berlin. Available from: http://www.geatbx.com/, 2005.
[5] Beranek LL, Sleeper HP. The design and construction of anechoic sound chambers. J Acoust Soc Am 1946;18(1):140–50.
[6] Cummings A, Beadle SP. Acoustic properties of reticulated plastic foams. J Sound Vib 1993;175(1):115–33.
[7] Bracciali A, Cascini G. Measurement of the lateral noise emission of an UIC 60 rail with a custom device. J Sound Vib 2000;231(3):653–65.

ALLBOOK BINDERY
91 RYEDALE ROAD
WEST RYDE 2114
PHONE: 9807 6026